UNIVERSITY OF SOUTHAMPTON

FACULTY OF ENGINEERING AND APPLIED SCIENCE

Department of Civil Engineering

THE HYDROLOGY OF THE DEGRADING SOIL CLIFFS AT NAISH FARM, HAMPSHIRE

by

Robert Ian Thomson

Thesis Submitted for the Degree of

Doctor of Philosophy

1987

UNIVERSITY OF SOUTHAMPTON

ABSTRACT

FACULTY OF ENGINEERING AND APPLIED SCIENCE

CIVIL ENGINEERING

Doctor of Philosophy

THE HYDROLOGY OF THE DEGRADING SOIL CLIFFS AT NAISH FARM, HAMPSHIRE

by Robert Ian Thomson

The purpose of the study was to increase understanding of the inter-relationship between hydrology and mass movements in an area of actively degrading soil cliffs. An undefended section of the Barton Clay cliffs of Christchurch Bay was used as the exemplar. Similar studies of such areas have been neglected in the past. It is considered that many of the difficulties encountered, techniques used, and ideas developed could usefully be employed in other similar areas.

The cliffs in the study area are composed of Plateau Gravel overlying the Barton Clay. The field studies included a survey of the gravel thickness, meteorological measurements, piezometric observations in the Plateau Gravel, Barton Clay and undercliff colluvium, and soil moisture measurements using a Neutron Probe in the undercliff colluvium. The inter-relationship between these measurements and the mass movements was investigated. Estimates were made of the seepage into the undercliff colluvium and its water balance.

A field monitoring programme was carried out over two years, from October 1982 to October 1984. During this time, the Plateau Gravel contributed a considerable amount of groundwater flow to the undercliff. An estimate was made of its temporal variation. It was shown that intercepting this flow would have a considerable effect on the undercliff water balance.

A model was developed which related meteorological conditions to groundwater levels. The model was used to determine the relative level of groundwater levels at the time of occurrence of a number of slumps. It was found that the timing of slumps was dependent on both the groundwater level fluctuation, as a result of meteorological conditions, and the gradual loss of lateral support afforded by the undercliff colluvium. The deeper the base of the slump, the less the groundwater level fluctuation, and the greater the influence of the variation in lateral support.

Groundwater flow in the undercliff colluvium is mainly via permeable tension cracks, shear surfaces and gravel seams. Thus, groundwater levels, and hence mass movement, respond rapidly to meteorological conditions. Mass movement is also considerably influenced by changes in the distribution of loading. The groundwater levels are themselves affected by mass movement due to the changing boundary conditions of the groundwater flow regime. The content of this thesis adds considerable understanding to the inter-relationship between the hydrology and mass movement of the soil cliffs at Naish Farm. The methodology of this work could usefully be used in similar studies of other areas.

ACKNOWLEDGEMENTS

I would like to thank Dr M.E. Barton for initiating the research, and providing advice and recommendations throughout the research and drafting of this thesis. Dr D.E. Clarke and Mr. P.F. Hillman have also provided useful advice.

I am grateful to Mr. C.W. Salter of Naish Estates (Hants) Ltd., for permission to work in the study area. I am also grateful to Mr. J. Coles of Seaview Road, Naish Farm for the daily measurement of wind and temperature instruments in the weather station.

I am grateful to all the people who have been involved with this research. I would especially like to thank Dr E.N. Bromhead of Kingston Polytechnic for the use of the drilling rig that made possible the installation of instrumentation on the cliff top. Dr Bromhead, together with Dr M.P. Chandler and Messrs B.J. Coles, M.R. Cooper, N. Dixon and R. Sandman, also gave invaluable assistance with the instrumentation. Technical assistance was also given throughout the research by Messrs A. Brookes and T. Pickett.

The Science and Engineering Research Council provided the financial support for this research.

Finally, I would like to thank my parents for their psychological and financial support in the production of this thesis.

CONTENTS

LIST OF TABLES

LIST OF FIGURES

LIST OF PLATES

LIST OF APPENDICES

ABBREVIATIONS

AE	actual evaporation
API	antecedent precipitation index
BC	Barton Clay
BS	Barton Sand
BS 1377	British Standard Number 1377
DBD	dry bulk density
E	east
EDM	electronic distance measurement
ENE	east north east
GMT	Greenwich meridian time
Hg	mercury
IOH	Institute of Hydrology
MAFF	Ministry of Agriculture, Fisheries and Food
MVF	moisture volume fraction
N	north
NE	north east
NGR	national grid reference
NNW	north north west
OD	ordnance datum
PE	potential evaporation
PG	Plateau Gravel
S	south
SMD	soil moisture deficit
SSE	south south east
SW	south west
W	west
WSW	west south west

CHAPTER 1

INTRODUCTION

1.1 Location and Purpose of the Study

Naish Farm is a holiday estate on the south coast of England. It is situated next to the county boundary with Dorset, approximately in the middle along the coastline of Christchurch Bay (see figure 1.1). The cliffs are unprotected and actively degrading in response to rapid toe erosion by the sea. Over the years, this has resulted in a considerable loss of land on the cliff top. Plates 1.1 to 1.12 show the nature of the area. Plate 1.1 shows the cliff top area, and plates 1.2 to 1.12 show the very wet and unstable nature of the undercliff. Plates 1.10 to 1.12 evidence the loss of the cliff top area that is taking place.

An initial general study of the degradation of the Barton Clay (BC) cliffs of Christchurch Bay was described by Barton (1973). Although a number of other studies have been made of the cliffs (see section 1.8), the largest and most significant is that of Barton and Coles (1984). This was into the characteristics and rates of the various slope degradation processes in the cliffs. The study described here is of the hydrology of the cliffs, the aim of which is to complement the work of Barton and Coles (op cit). It was, therefore, decided to locate the study area of this investigation within that of Barton and Coles. The study area also includes part of the cliff top in order to estimate its contribution of groundwater flow to the undercliff. The engineering application of such studies is in the design of effective slope stabilization works and greater understanding of slope processes.

1.2 Degradation of the Cliffs

Toe erosion causes the overall cliff slope angle to increase. This reduces stability and causes slope failure. This acts to reduce the cliff slope angle and increase stability. High rates of toe erosion necessarily result in high rates of slope degradation. If the toe erosion stops (as is the case for an inland slope, or an abandoned cliff, or one with toe protection), then slope degradation continues to occur until a stable slope angle is

achieved. This may be very much less than the angle existing during toe erosion, and therefore represents a considerable further loss of land.

1.3 Measures commonly used to arrest Cliff Degradation

Cliff stabilization works commonly include both toe and slope protection measures. To effectively design the latter, it is necessary to understand the degradation processes and how they are affected by such factors as the hydrology of the area. The hydrology of the area affects the stability of a slope mainly through the pore pressures and hydraulic gradient (i.e. seepage force) acting at potential or existing failure surfaces. To a smaller extent the soil moisture content also affects stability through the weight acting on the failure surface.

The aim of slope protection measures is to beneficially affect the factors influencing stability. Drainage is principally designed to reduce pore pressures, although it does also help to reduce the soil moisture content of the unsaturated part of the slope. The establishment of vegetation also helps to reduce the soil moisture content (due to the depth of rooting, vegetation allows more water to be evaporated from the soil than does bare ground), although its primary aim is to reduce erosion by wind and rain. Another measure which is normally undertaken, is regrading of the slope in order to redistribute the loading on the failure surface. However, degradation of a slope may involve the action of several processes. Because movement along one failure surface (potential or existing) may de-stabilize another failure surface, it is essential to stabilize the cliffs against all modes of failure. Great care has to be taken in re-grading a slope as stabilizing a slope against one mode of failure may de-stabilize it against another mode. Therefore, an understanding is required of the processes and causes of failure in order to ascertain the most effective set of remedial measures necessary to prevent their further occurrence.

1.4 Marine Erosion of the Cliff Toe

Although the toe erosion by the sea is not within the scope of this study, it is worth a short discussion in order to put the study area in the context of the evolving coastline.

The cliff toe is eroded by the energy imparted to it by the action of the sea. Cliff stabilization measures commonly dissipate this energy by means of a revetment seaward of the cliff toe. Groynes are also normally constructed to intercept sediment from the longshore drift. This causes a build up of beach material which also helps to dissipate the energy from the sea.

The coastline is inevitably made up of materials of varying erodibility. The more resistent materials form headlands between which bays are formed. The bays reduce the energy of the incoming waves, such that the rate of recession of the coastline is dependent on the erosion of the headlands. The shape of the coastline in the bay is dependent on the amount and direction of longshore drift. Figure 1.1 shows that the curvature of the coastline in Christchurch Bay is greatest on the west side of the bay. This is due to the west to east direction of longshore drift which is as a result of the predominantly south westerly direction of the waves. Man can affect coastline recession by interfering with the headlands, the longshore drift, and the offshore sediments.

Between 1848 and 1870 the Hengistbury Mining Company removed large quantities of material from Hengistbury Head. This enabled greater amounts of material to be moved from Poole Bay to Christchurch Bay by longshore drift. This lead to the development of an offshore bank extending from a spit at Christchurch Harbour to just below Highcliffe Castle (by 1880). This reduced the energy of the incoming waves and so afforded considerable protection for the cliffs west of Highcliffe against erosion by the sea. This state of affairs more or less continued until 1938, when a groyne was constructed on Hengistbury Head. This was so as to

reduce the loss of beach material from Poole Bay and allow a beach to build up at Bournemouth. The loss of material replenishing the offshore bank in Christchurch Bay lead to its rapid disappearance. This lead to the cliffs once again being subjected to rapid erosion by the sea. As a result, a number of engineering works have been constructed. The study area is in a 1.4 km length of undefended coastline between sea defences constructed at Highcliffe and at Barton-on-Sea. The strong point constructed at the Chewton Bunny outfall in 1967 greatly reduced longshore drift, and so increased the rate of erosion to the east, along the undefended coastline.

The rate of movement of undercliff material varies due to fluctuating groundwater pressures and the rate of removal of colluvium by the sea. To study the effect of the former, the latter should at least be constant. Unfortunately, in the past this has not been the case, due firstly to man's influence (as exampled above), and secondly, to variations in sea state and tide. It is beyond the scope of this study to delineate the effect of sea state from that of fluctuating groundwater pressures. Therefore, the rate of undercliff movement is complicated and may not exactly mirror the fluctuations in groundwater pressures.

1.5 Geology of the Region around Naish Farm

Figure 1.2 shows the drift and solid geology of the region around Naish Farm. The geological formations present in the study area are:

Recent	Colluvium
Pleistocene	Brickearth (about 0.3 m)
	Plateau Gravel (1.5 - 6m)
Eocene	Barton Clay (46.4 m)

The Barton Clay is mainly a stiff, fissured, over-consolidated

clay of marine origin. It has fairly frequent variations in lithology as shown by figure 1.3. The thickness of the Barton Clay given above is for the total sequence. Only zones A2 to F2 occur in the study area, the lower zones being below sea level. Figure 1.3 is based on evidence at Highcliffe, about 0.8 km west of the study area. However, with minor exceptions the lithology is consistent laterally along the outcrop in Christchurch Bay (Barton, 1973). The dip of the beds is approximately ¾ deg. ENE.

The Plateau Gravel (PG) is a high level terrace gravel spread over most of the coastal outcrop (Keen, 1980). In the study area, it rests on a slightly irregular erosion surface cut in zone F of the Barton Clay. It is mainly a coarse sandy gravel with approximately 30 per cent sand. There are also some thin lenses of gravelly sand. In places, the junction with the underlying clay has been periglacially disturbed, showing frost wedges, involutions and cryoturbation structures (Barton, 1984a).

Figure 1.2 shows that a part of the region around the study area is covered in a drift deposit of Brickearth. This lies on top of the PG and is up to 3 m thick (Keen, 1980). However, Keen describes the Brickearth as always occurring in close association with the gravel. Indeed, it has been observed in the study area that a thin deposit (about 0.3 m) does cover the PG. There is some mixing between the PG and Brickearth such that the exact contact is uncertain. Keen describes this mixing as taking place in the bottom 0.3 m of the Brickearth and top 0.3 m of the PG. He also describes the Brickearth (where no mixing occurs) as a structureless deposit consisting of 50 per cent fine sand, 30 per cent silt and 20 per cent clay with small flakes of flint up to 1 cm across.

The colluvium is derived from the other formations and exists mainly as sheets up to 13 m thick resting on three principle bench levels in the undercliff (see section 1.6). At the higher levels, it contains much sandy gravel but is progressively diluted with clay as it moves down the undercliff toward the sea.

Due to the dip of the beds, the solid geology gradually changes along the coastline. To the west, the Bracklesham Beds are exposed above sea level at about NGR 42004 09300 (see figure 1.2). At the study area, the top of the Bracklesham Beds (Mudeford Sands) is about 15 m below sea level. Halcrow (1971) gives particle size distributions of the Bracklesham Sands averaging 6 per cent clay, 14 per cent silt, and 80 per cent sand. To the east of the study area at about NGR 42204 09302, the Barton Sand is exposed at the top of the cliff. Figure 1.4 shows the lithology of the Barton Sand. Barton et al (1986) describe part of the K zone of the Barton Sand as containing 96 per cent fine sand. The change in geology causes the coastal landslips in Christchurch Bay to vary along the coastline. Despite this, the nature and extent of the landslips are fairly consistent, such that the results of the study area are considered to be applicable to the rest of the coastline. However, the changes in geology should be borne in mind when considering the cliffs other than at the study area.

1.6 Topography and Distribution of the Colluvium

The cliff height is generally about 31 m O.D. Just to the east of the study area is a dry valley (Barton, 1984a) where the cliff height falls to below 29 m O.D. before rising again. To the west of the study area, the cliff height gradually falls toward Chewton Bunny. The overall slope angle in the study area averages 17 deg. Figure 1.5 is a contoured plan of the study area.

In the study area the colluvium is principally distributed on three benches, where in each case it overlies a definite preferred bedding plane shear surface (see figure 1.6). These are the F, D, and A3 surfaces, named according to the geological zone in which they occur (see figure 1.3). In the centre of the study area they are at approximate elevations of 25, 9.5 and 2 m O.D. respectively. The easterly dip allows for about 1.2 m change in elevation per 100 m distance from west to east.

The F bench is relatively narrow but quite distinct. The dip of the beds is such that it disappears to the west and widens to the east (except below the dry valley where it is obscured by an accumulation of debris sloping steeply downwards from the cliff top scarp). The D bench is very wide, and shows a varied topography incorporating ponds and many breaks and changes of slope. To the east of the study area, the width of the A3 bench rapidly decreases until it finally disappears due to the dip of the beds taking the shear surface below the beach level.

Exposures of in situ strata occur only in the scarp faces. These are the cliff top scarp (exposing the PG), the F scarp at an elevation of 23-25 m O.D. (and thus named because it contains the F bedding plane shear surface) and the D scarp at 7-10 m O.D. (which contains the D surface). Occasionally, with appropriate beach conditions, in situ strata is exposed in a low A3 scarp. The position of this scarp is very close to that of the cliff toe. The D scarp is the most prominent, presenting a continuous exposure of in situ strata throughout the study area, which clearly separates the overlying D bench from the lower level A3 bench. The F scarp is largely covered by a thin mantle of colluvium and at certain periods of the year the F scarp may be entirely covered by slip debris.

1.7 Degradation Processes

The degradation processes affecting the BC cliffs of Christchurch Bay, and in particular at Naish Farm, are only briefly described here. A more detailed description together with a comparison of landslides from other areas is given by Barton and Coles (1984). Figure 1.7 shows the main processes and their associated forms.

1.7.1 Bench Sliding

This consists of colluvium sliding over in situ clay. The bounding

shear surface is of the compound type (Skempton and Hutchinson, 1969) with the translational (planar) part of the surface conforming to a preferred bedding plane within the BC. The position of the curved, rear portion of the shear surface is not known with certainty. However, from the evidence of boreholes and the upper, exposed part of the shear surface, it is thought to be very steep with a tight radius of curvature near the preferred bedding plane. This is in agreement with the evidence of Barton (1973) from trial pits at Highcliffe. At the front of the bench, either rubble is pushed over the scarp face by active bench sliding, or else a separate rotational edge failure develops (see figure 1.7) accompanied by numerous tension cracks. Bench slides may extend for very considerable distances measured along the outcrop. However, generally at any one time, different portions will have different rates of movement. This causes the development of arcuate (or sub-arcuate) lateral shear through the bench rubble.

1.7.2 Slumping

This involves the sliding of the in situ strata of a scarp slope: such sliding displaces the colluvium at the toe of the slump block and thus slumping must also involve bench sliding. The sliding shear surface forms a new rear part of the shear surface of the bench slide (section 1.7.1). Slumping is a commonly recognised process leading to scarp recession, and affects all the scarps within the BC undercliffs, but is most easily seen and recognised where it affects the top scarp.

Owing to the tight radius of curvature at the base of the slump block, the latter becomes a zone of intense shearing and the in situ material is completely remoulded into slip debris. The upper part of the back rotated slump block initially more or less retains its shape. However, as it slowly moves down the undercliff, it is progressively subject to increasing disruption due to both the action of its movement and weathering.

1.7.3 Spalling

The scarp slopes are subject to this process, which involves the detachment of small blocks of material, as a result of stress release, due mainly to the action of weathering (in particular, frost action, rainwash and shrinkage of clay). Spalling is a continuous process on all scarp faces but the rate is much faster on faces freshly exposed by recent slumping. This is related to the changes brought about by the relatively rapid release of stress. Unlike slumping, which involves the parallel retreat of a scarp face, spalling leads to a reduction in slope angle. However, fresh slumping generally intervenes before any considerable flattening of the profiles takes place.

1.7.4 Debris Slides

These involve the movements of loose accumulations of debris, generally starting off as scree, sliding on a steep (usually between 25 and 40 deg.) clay scarp slope, and over-running onto a bench (see figure 1.7). It is in the form of a thin tongue of debris, often less than 1 m but rarely more than 2 m thickness. At Naish Farm, the movement of the debris down the scarp slopes is arrested as the material accumulates onto the underlying bench. This is most prevalent on the F scarp, from whence the debris over-runs onto the D bench.

1.7.5 Mud Sliding

Two mud slides with discrete bounding lateral and basal shear surfaces having no direct relation to the preferred bedding planes (i.e. they may be entirely contained within the bench colluvium, or they may cut through the basal shear surface of the bench slide) are shown on figure 1.5 at locations A and B. Mud slides are commonly, but inappropriately, called 'mud flows'. The distinction between a slide and a flow is in the vertical

velocity distribution. For a slide, this is more or less constant with a sudden reduction at the shear surface. For a flow, the material behaves like a viscous fluid such that the velocity gradually decreases with depth.

In winter, the mud slides are extremely wet and treacherous with the matrix of the colluvium very much softer than that in the colluvium on the benches. In summer, however, the surface of the mud slides forms a dry hard crust. This dramatic change in moisture content and stiffness is a very characteristic and diagnostic feature. Barton and Coles (1984) attribute mud slide activity to an increase in groundwater outflow at their locations, although another influencing factor must be the reduced shear strength due to the complete loss of structure of the colluvium. The alarming feature of mud slides is that their velocity of movement is much greater than that of bench sliding. The mud slides shown on figure 1.5 are as noted by Barton and Coles (1984), except for the lower part of mud slide A (A_L). Mud slide A_L was activated during April 1983. Mud slide A_U feeds large amounts of soil and water to mud slide A_L. This is believed to be the cause of the lower mud slide activity.

1.7.6 Mud Runs

These are very superficial movements of fluid mud which occur after periods of prolonged, intense rainfall. The mechanism of movement is one of flow involving a suspension of mud in water. They are at most 2-3 cm in thickness. The total quantity of colluvium moved in this way is negligible.

1.7.7 Stream Erosion

No permanent streams exist in the study area, but ephemeral flows over clay slopes occur during, and just after, periods of rain. The amount of erosion is not significant, and even where more

permanent streams are present elsewhere in the undercliffs, the stream gullies (maximum of 1 m depth) tend to be small and insignificant features.

1.7.8 Man-Related Processes

These are as a result of pedestrian traffic (during summer), geologists collecting samples, and the tipping of refuse. However, they are not thought to have a significant effect on rates of cliff erosion.

1.8 Previous Work

1.8.1 Geology

The original classification of the Barton Beds was made by Burton (1933) and was based on palaeontology. Barton (1973) made slight changes to this classification based on lithology and a greater estimated thickness of the BC. The latter study was based on evidence at Highcliffe, and is, therefore, more relevant to this study.

Keen (1980) describes the composition and deposition of the PG and Brickearth. He described the PG at Naish Farm as a high level terrace gravel. He concluded that the gravels and brickearths of South Hampshire were deposited under a periglacial fluvial regime at the transition between interglacial and glacial conditions. They rest exclusively on surfaces cut during the course of their deposition. He noted that there were linear features in the underlying Tertiary rocks. From the evidence of inland pits to the east of the study area, these features have a broadly west to east trend. Although he recognised their existence at Barton, he could not determine their trend as the cliff face is only a 2-dimensional exposure. It is interesting to note that the

gravels were deposited at similar levels along a WSW to ENE line east of Naish Farm and a SSE to NNW line west of Naish Farm. Thus, Naish Farm is probably near to a change in direction in the linear trends. Booth (1974) estimated contours of the top of the BC at Highcliffe. They broadly show a North-South trend. Linear trends are important as groundwater flow will tend to concentrate in the channels.

Barton (1984a) describes several periglacial features found in the cliffs at Naish Farm. He noted the existence of involutions, cryoturbation structures, frost wedge casts, and a valley bulge. Involutions and cryoturbation structures cause rapid changes in the level of the PG/BC unconformity and may cause local variations in groundwater flow within the PG. Frost wedge casts can extend deeply into the BC and transfer groundwater rapidly from the PG to the deeper levels within the BC. It is considered here that they are not frequent, or large enough, to make a significant general effect on pore pressures in the BC. The valley bulge is a fold within zone F of the BC. It is situated beneath a dry valley in the cliff top. The drift deposit in the dry valley is of a very different grading from the rest of the PG, being a gravelly and clayey silty sand. This is of significance as it will affect the groundwater flow within the PG.

1.8.2 Coastal Erosion Problems in Christchurch Bay

Stopher and Wise (1966) describe Christchurch Bay and its coast erosion problems, particularly those at Mudeford, Highcliffe, Barton-on-Sea, and Hordle. Muir-Wood (1971) states the coastal landslips are caused by water bearing sands overlying clay, and that it is necessary to intercept these high flows. Stopher and Wise (op cit) state that the varied character of the BC makes it possible for groundwater to issue out of the cliffs at various levels, and that this causes stability problems. The BC also leads to instability in the overlying Barton Sand, since it creates an impermeable barrier to the flow of groundwater percolating through the sands.

Places like Herne Bay and Whitstable in Kent, have roads and houses close to the cliff top, such that high cost schemes have been installed. On the other hand, at Highcliffe, it is more a loss of amenity, such that only a low cost scheme was approved. Such schemes need to be more cost effective which requires a more detailed knowledge of the mechanisms and causes of failure. Such studies have been carried out at Highcliffe and Naish Farm (Halcrow (1971), Barton (1973, 1977, 1984b), Booth (1974), Barton and Coles (1983, 1984), Barton et al (1983), Barton and Thomson (1984, 1986a, b, c)).

1.8.3 Cliff Stabilization at Highcliffe

Mockridge (1983) gives an historical review of the erosion problems affecting the cliffs at Highcliffe and the methods used to protect them. As a result of the construction of the groyne off Hengistbury Head in 1939, the littoral drift from Poole Bay was virtually stopped. This lead to erosion of the beach that had previously built up in the eastern part of Christchurch Bay, until, by the late 1950's, the cliffs at Highcliffe were once again being threatened by marine erosion. To deal with the problem, a Mobbs and English permeable timber revetment was constructed in 1967/8. However, this was in danger from further slumping of the cliffs, such that advice was sought from Sir William Halcrow and Partners (Halcrow, 1971). They recognised the PG as making a major contribution of groundwater flow toward the undercliff and recommended that it should be intercepted. In comparison to the PG, the groundwater flow in the A3 sands was not large. However, it was a source of instability and therefore interception on the undercliff was recommended. The lower levels of the undercliff were particularly wet, which was supposedly due to the collection of rainfall, such that extra drainage was recommended.

In 1973/4 drainage and re-grading of the cliffs was carried out in order to stabilize the cliffs. A cut off in the form of a

concrete diaphragm wall was constructed. It was located at least 20 m from the cliff edge, except at the western end, where, owing to restricted access, the distance was reduced in part to about 12 m. Discharge to the beach takes place through sealed drainage outlet pipes provided at intervals along the line of the cut off. The base of the diaphragm was to be taken down into the BC for a distance of 0.6 m to 0.9 m. Barton and Thomson (1986c) report that in places the diaphragm did not reach the BC and that this was a contributing factor to a subsequent slump. A horizontal drain was constructed half way down the undercliff to pick up groundwater flow from the A3 zone. However, difficulty was experienced in tracing the sands during construction. The lower slopes were drained, and a gravel blanket added to aid surface drainage and to provide toe weight. It was later disturbed by movement and ceased to function as an aid to drainage.

In 1978/9 a second, maintenance phase was undertaken (Mockridge, 1983). The diaphragm wall was deepened in places where it did not reach the BC. Extra drainage was installed to deal with the water diverted around the western end of the diaphragm wall. The horizontal drain was steepened and left open (it had previously been gravel filled) as it had been choked with clay from runoff. Further drainage was installed in areas that were persistently wet. Grass was established on the lower, flatter slopes in order to reduce surface erosion. Mockridge (op cit) also recognised the need to build up a beach, and suggested adding beach material and extending and converting the eastern groynes to stone bastions.

1.8.4 Cliff Stabilization at Barton-on-Sea

Muir-Wood (1967, 1971) describes the defence works at Barton-on-Sea. The Barton Sand/BC junction falls from 18 m above O.D. in the west, to 1.5 m below O.D. in the east. The Barton Sand was recognised as a source of high flow to the undercliff needing to be intercepted. This was achieved by installing a deep drainage

trench in the undercliff landward of a diaphragm wall installed down into the in situ BC. Thus, although the groundwater flow was not stopped from reaching the undercliff, it was stopped from reaching the more unstable lower parts of the undercliff. (Note: the drainage trench was not necessary in the east of the defended section where the Barton Sand/BC junction fell below 3 m O.D.) This scheme caused some local controversy, such that only a small experimental section was installed in 1964, with its corresponding revetment work in 1966. In 1967 the rest of the drainage and cliff toe protection works were put in place. This included superficial drainage works, regrading and hydraulic seeding of the undercliff. Subsequently, movement occurred below the line of the deep drainage trench. This was dealt with by additional minor drainage works.

1.8.5 Cliff Stabilization at Naish Farm

It is probable that any future design of stabilization works for the undefended cliff section at Naish Farm, will be a mixture of the approaches used at Highcliffe and Barton-on-Sea. In the west, the groundwater flow to the undercliff from the PG will be cut off similar to that at Highcliffe. In the east, the groundwater flow to the undercliff from the Barton Sand will be cut off similar to that at Barton-on-Sea. From the preceding discussion it is clear that at both Highcliffe and Barton-on-Sea subsequent maintenance works have been necessary. This is a result of it being necessary to install a low cost scheme without sufficient knowledge of the mechanisms and causes of failure.

1.8.6 Mechanisms and Causes of Failure

The main studies at Highcliffe have been by Barton (1973) and Booth (1974). More detailed studies at Naish Farm have been carried out here, and by Barton and Coles (1984).

Barton (1973)

The topography of the undercliff was described as having a benched profile due to the shape of the basal shear surface (i.e. the surface of separation between disturbed and in situ material). For each bench, the seaward portion of the shear surface conforms to a bedding plane. The shape of the rear portion was identified in trial pits. It was steeply inclined with a small radius of curvature near the preferred bedding plane shear surface. Six bedding planes preferred as shear surfaces were identified in the BC and one just in the Barton Sand. These are shown on figures 1.3 and 1.4. The lower two were mostly obscured by slumped material after the construction of the revetment in 1967/8. However, the other preferred shear surfaces were identified as being present from where the bedding plane appeared above beach level up to within a few metres of where it disappeared at the PG/BC unconformity.

The A2 shear surface corresponds to a band of intensely fissured clay. The A3 shear surface was suggested as probably due to internal erosion of sand overlying clay (as described by Henkel, 1967). The D, F and G shear surfaces were suggested as possibly being connected with the nearby presence of nodules or other hard layers. Barton (1977) said that stress relief during the original formation, and continued retreat, of the cliffs is very probably contributory to the use of the D shear surface. Barton and Thomson (1986a) describe the A3 shear surface as probably due to a number of causes acting together, viz. pore pressure fluctuation; seepage erosion and piping; and equilibration response time. Barton (1984b) describes scarp slumping, and the accompanying bench sliding, as a compound landslide as classified by Skempton and Hutchinson (1969). Barton (1984b) also shows that they are ubiquitous in over-consolidated clays with flat lying bedding. Scarp slumping is controlled by the location of the preferred shear surface. Bench sliding is attributed to the undrained loading as a result of material being added to the rear of the bench (e.g. by scarp slumping), or to a rise in pore pressures.

The hydrogeology was described as complex. Although no permeability measurements were given, three permeable beds were identified, viz. the Mudeford Sands, the A3 zone of the BC, and the PG. Halcrow (1971) estimated the permeabilities from particle size analysis tests to be 5 x 10^{-7} m/s, 10^{-6} m/s and 0.1 m/s respectively. (Note: the PG sample was unusually gravelly, and so represents an upper permeability estimate.) This would appear to indicate that the flow of water out of the PG is probably much greater than that out of the other permeable horizons. Some groundwater level measurements were made showing the groundwater flow to be both lateral toward the undercliff and downward to the Mudeford Sands. Halcrow (1971) presents evidence of a hydraulic gradient in the downdip direction in the A3 zone parallel to the cliff edge. However, this would be expected with increasing depth. The PG was described as containing a reservoir of water up to 2 m in depth from which flow is both to the cliff face and Chewton Bunny via channels in the top of the BC. The response to rainfall of piezometric levels in the undercliff colluvium were described as rapid, especially at the front of the bench.

Stability calculations showed an increased likelihood of failure by bench sliding as the width of the bench decreased. It was suggested that wide benches probably fail by successive sliding of parts of the bench colluvium, the front moving first and the landward parts following due to loss of support. Two possible shear surfaces were considered for use during scarp slumping. One lead to movement of the whole of the bench colluvium, and the other to only part of it. Stability calculations showed the former to be more likely for narrow benches, and the latter for wide benches.

Booth (1974)

New shear surfaces preferentially use discontinuities such as bedding planes and fissures. The intensity of the development

of fissures was found to vary tremendously, both from zone to zone and laterally within zones. As the slump blocks move through the undercliff they gradually break down through a combination of the movement and weathering. The loss of structure makes the colluvium more susceptible to debris flows and mud slides due to the reduction in strength. The colluvial material was described as having lower slope angles than the in situ material due to lower cohesive and frictional strengths.

Difficulty was reported with particle size tests due to the aggregation of the clay content of the samples. This aggregation was less for samples taken nearer the cliff face. It was postulated that this was due to percolating water causing ion exchange, i.e. breakdown of interparticle bonds. Seepage was also reported as causing decalcification of the weakly cemented sand layers of the A3 zone. This causes a reduction in their cohesive strength.

Seepage was recognised as an important cause of instability. Seepage locations identified were:

i) the base of the PG;
ii) sand layers of the A3 zone;
iii) sand beds of zone H (i.e. the Barton Sand);
iv) interface between colluvium and in situ clay;
v) open fissures.

64 boreholes were sunk to investigate the regularity of the PG/BC unconformity and the groundwater levels in the PG. Measurements of the groundwater level were taken from the open boreholes 24 hours later. The results showed that there was a N-S trend in the contours of the contact, and that the contact sloped toward Chewton Bunny in its vicinity. The inferred slope of the groundwater table indicated that groundwater flow was either toward Chewton Bunny or to the cliff face via channels in the top of the BC.

It was noted that movement was not only related to rainfall (as is normally perceived), but also to evaporation and changes in soil moisture storage. By means of a crude water balance (rainfall minus potential evaporation on a monthly basis), it was shown that there was an excess of water to the groundwater store during winter and a deficit during summer. Limited measurements of groundwater level and soil moisture storage (using a gravimetric method) in the undercliff showed seasonal variations in response to the meteorological input. Groundwater level measurements were also made in the A3 zone and Bracklesham Beds. The former showed a slight seasonal variation (range = 0.2 m), and the latter showed a downward trend over a 2 year period. Spatial moisture content measurements showed a large increase just above a slip surface, and large changes near tension cracks and the ground surface.

Barton, Coles and Tiller (1983)

This was a statistical study of the size of cliff top slumps throughout the undefended section of cliffs at Naish Farm. They found that in the west, where the F shear surface was not used, the slumps were few and large as they were based on the D shear surface. Slumps were found to be more frequent in the east where the F shear surface is predominantly used. The mean and standard deviation of the length, maximum breadth, and area of each slump, increased going eastwards. This was probably due to the dip of the beds increasing the depth of the preferred shear surface and thus causing larger slumps.

Barton and Coles (1983, 1984)

A detailed investigation was made of the various degradational processes to determine their characteristics, rates of movement, and relative importance to the overall cliff degradation. Their study area included that used here, and extends slightly further

eastward. Therefore, their results are of relevance to this study.

Since 1947 the cliff top recession and overall slope angle have been increasing. Initially, this was due to the depletion of excess beach material previously present, but since about 1970 it has been due to the increased scour of beach material downdrift of the Highcliffe groynes. Spatially, both the D scarp and the cliff top scarp are receding at different and highly variable rates. For example, between 1976 and 1982 recession of the cliff top varied spatially between 0.4 and 5.1 m/year. Slip debris moving over the A3 scarp often obscures the position of the scarp and results in the cliff toe moving forward (i.e. negative recession). However, this is quickly removed by the sea such that on average the toe is receding. In the winter of 1977/8 a large slump (about 90 m long) occurred centred on NGR 4222 0932. This was based on the D shear surface as opposed to the F shear surface which is normally used. Evidence suggests that this slump is still moving along the D bench toward the sea and has a considerable influence on the topography of the study area.

The different degradational processes were described, and their rates of movement measured by periodically surveying a large number of surface pegs. The rate of movement to the sea varied both seasonally and between processes. For example, for bench sliding the movement rate in summer was virtually zero, whereas peak measured rates (averaged over two week periods during 1981/2) in winter were 25 mm/day for the F bench, 64 mm/day for the D bench, and 102 mm/day for the A3 bench. For shallower slides, at the same location within the undercliff, the relative movement rates were greater in winter and less in summer. This reflects the greater fluctuation in moisture content and pore pressures (and thus their stability) that occurs in shallower slides.

The most important process for transporting material down the undercliff was found to be bench sliding. There was a 6½ per cent net loss of colluvial material for the year 1981/2. This

indicated decreasing stability and that further slumps would take place in order to restore the losses of colluvial material. Thus, colluvial movement was described as a continuous process of redistribution of material which influences the discontinuous process of slumping. They state that a study of the full interaction between the two types of process can be regarded as an essential future step in the understanding of the fundamental mechanisms controlling degrading clay cliffs. It also requires a greater understanding of the role of hydrology which is the purpose of this study. An initial outline of this work was given in Barton and Thomson (1984). Some particular aspects are described in Barton and Thomson (1986 a, b, c).

1.9 Objectives of the Research

1.9.1 General

This study is intended to cover the important area of interaction between hydrology and slope degradation studies. Studies of slopes from a soil mechanics aspect demonstrate the outstanding influence of groundwater conditions on the overall stability. While predictions for transient and steady state seepage are made, and observations of in situ pore pressures undertaken, as part of slope stability investigations, it is very rare for such studies to be related to the basic hydrology of the slope being examined.

The soil slopes used as an exemplar are the BC cliffs in Christchurch Bay because of the intensive studies of the degradation processes already undertaken (see section 1.8). The study is aimed at complementing the work of Barton and Coles (1984). Such studies increase the knowledge of slope degradation such that more efficient slope stabilization works may be designed.

Previous work by Barton (1973) and Booth (1974) has identified the source of seepage to the undercliff and measured some groundwater

levels. This work is aimed to take this into much greater detail and to quantify the amount and distribution of seepage flows. It is also intended to increase understanding of the role hydrology plays in the degradation of the cliffs.

1.9.2 Correlation of Hydrological Variables with the Rate of Degradation

Meteorological conditions can affect slope stability by causing transient changes in groundwater conditions. In the past, researchers in other landslide areas have tried correlating various measures of meteorological conditions with the onset of movement. This is notoriously difficult due to the complicated interaction of many factors causing instability. It is an objective of this study to investigate these complications with a view to the possible development of relationships between meteorological conditions and landslide activity. It is also intended to investigate the interaction between groundwater levels and landslide activity by making observations in both the undercliff colluvium and the in situ strata.

These objectives would be simplified if the relationship between meteorological conditions and groundwater levels could be established and used to extend groundwater level records (using the longer meteorological record). This could be used to correlate with periods of instability (or even to extend such records).

1.9.3 Water Balance Studies on a Stretch of Degrading Undercliffs

Providing there is not a sudden change in loading of a soil element, a change in groundwater level (or pore water pressure) signifies a change in storage caused by an imbalance of input and output flows. The basic purpose of drainage in slope stabilization is to lower pore water pressures along critical surfaces to values which do not cause instability. It does this by intercepting and

diverting the input flows, and increasing the output flows, such that storage, and hence groundwater levels, are reduced to a level at which failure does not occur.

The purpose of the water balance is to identify the various components of storage and flow, and determine their relative size and importance.

1.9.4 Rate of Pore Pressure Equilibration

The delayed failure of slopes cut in overconsolidated fissured clays is due to the long time necessary for equilibration of pore pressures (Vaughan and Walbanke, 1973). The background to this problem lies in the response of a clay soil to unloading, which in this case is the natural slippage of material from the cliff slopes. As a result of unloading, there is a sudden decrease in total stress. This is accommodated by a sudden decrease in pore water pressure (the soil skeleton stays rigid). The depressed pore pressures lead to a net influx of water. This is accommodated by expansion of the soil skeleton. This leads to a drop in effective stress and rise in pore pressure. The time taken for pore pressures to equilibrate (i.e. for the soil skeleton to complete expansion) is dependent on the length of the drainage path and the coefficient of consolidation. The latter is dependent on the permeability of the clay. Failure of a slope will be delayed until the pore pressure rises sufficiently to cause instability. The equilibration rate is subject to minor perturbations due to fluctuating meteorological conditions. Thus, the actual time of failure is most likely to be related to the preceding weather conditions.

It was an objective of this study to examine the importance of the equilibration of pore pressures in the timing of cliff failures.

1.9.5 Design of Drainage Works in Relation to the Undercliff Hydrology

The ultimate application of this research is considered to be in terms of estimating the effectiveness of potential drainage works. The purpose of drainage is to

(a) reduce pore pressures (and hence improve slope stability),

(b) reduce soil moisture content (and hence improve "trafficability").

It is intended to relate the work to this objective.

1.10 Presentation of the Work

A programme of work has been undertaken in order to tackle the objectives given in section 1.9.

Previous work (see section 1.8) has recognised the importance of the PG as a source of seepage to the undercliff. Estimation of this seepage requires a knowledge of the groundwater flow in the PG. This will be affected by the continuity of the gravel and by the variation in level of the PG/BC unconformity. This has been investigated for the study area and the results are presented and discussed in chapter 2.

To solve the water balance for the undercliff, estimations need to be made of rainfall and evaporation for both the cliff top and the undercliff. The information is necessary on the cliff top as seepage from the PG onto the undercliff is controlled by the infiltration of rainfall. It is important to establish whether the undercliffs have a distinct micro climate, such that the rainfall and evaporation could be different to that experienced on the cliff top and further inland where meteorological stations are situated. Chapter 3 considers the measurement of rainfall and potential evaporation at Naish Farm. The statistical properties of the data are examined and compared with those of the surrounding region.

Chapter 4 gives a general introduction to the water balance. For convenience, the study area is sub-divided into three geohydrological domains each with its own water balance characteristics. The domains are the PG, the BC, and the undercliff colluvium. These are studied in more detail in chapters 6 to 9.

Chapter 5 presents a model relating measured groundwater levels to meteorological changes. Chapter 6 presents a detailed study of the PG domain. A number of groundwater level measurements were made. Some of these were used to study the application of the model described in chapter 5. The model also enabled estimations to be made of the groundwater flow in the PG. Chapter 7 presents a detailed study of the BC domain. Groundwater level and permeability measurements enabled estimations to be made of groundwater flow. Chapters 8 and 9 discuss the undercliff colluvial domain. Chapter 8 discusses the soil moisture measurements made using a neutron probe, and chapter 9 discusses the groundwater levels and seepage characteristics. The complete water balance for the undercliff is also presented and discussed in chapter 9.

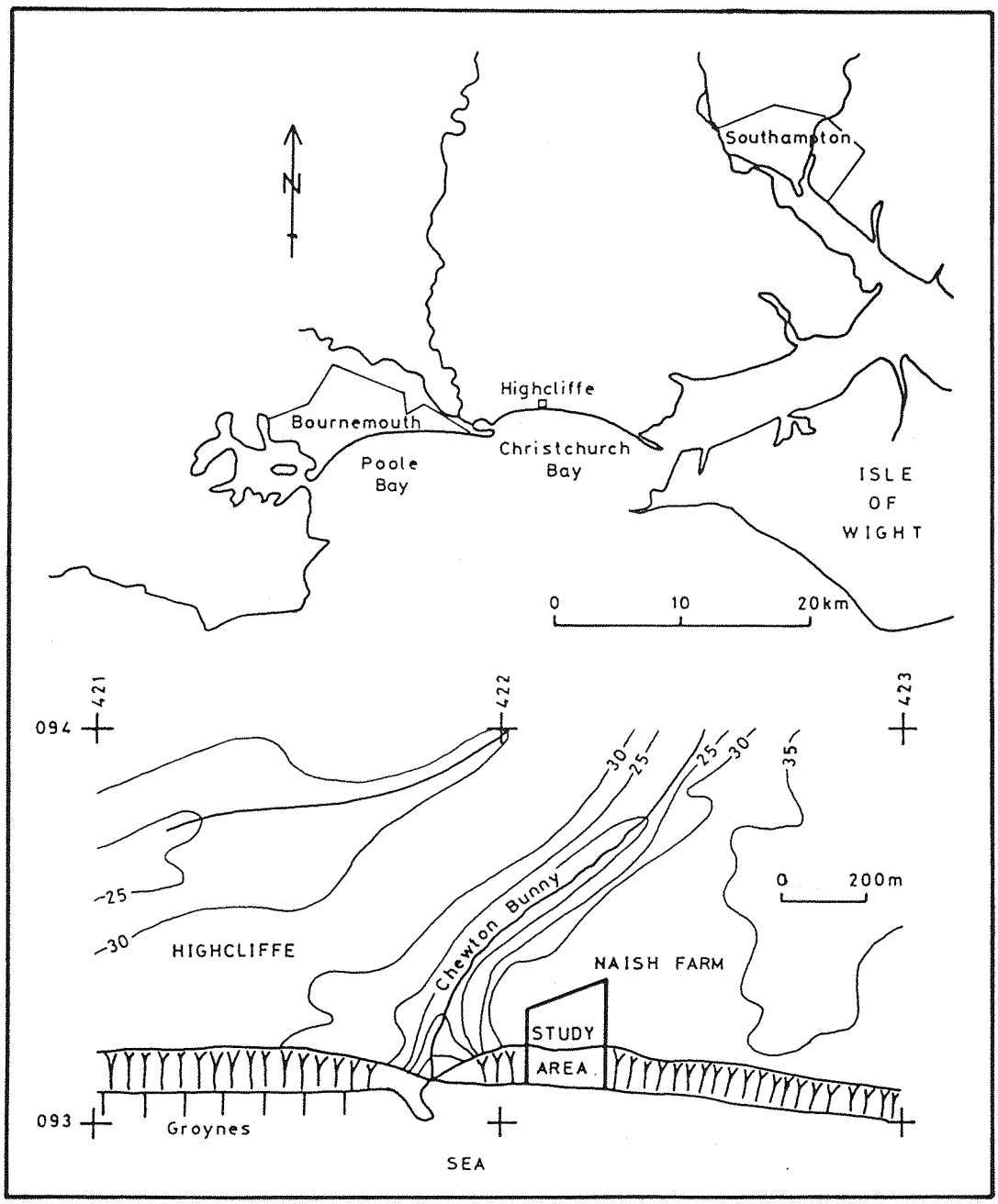

Figure 1.1 Location of the study area.

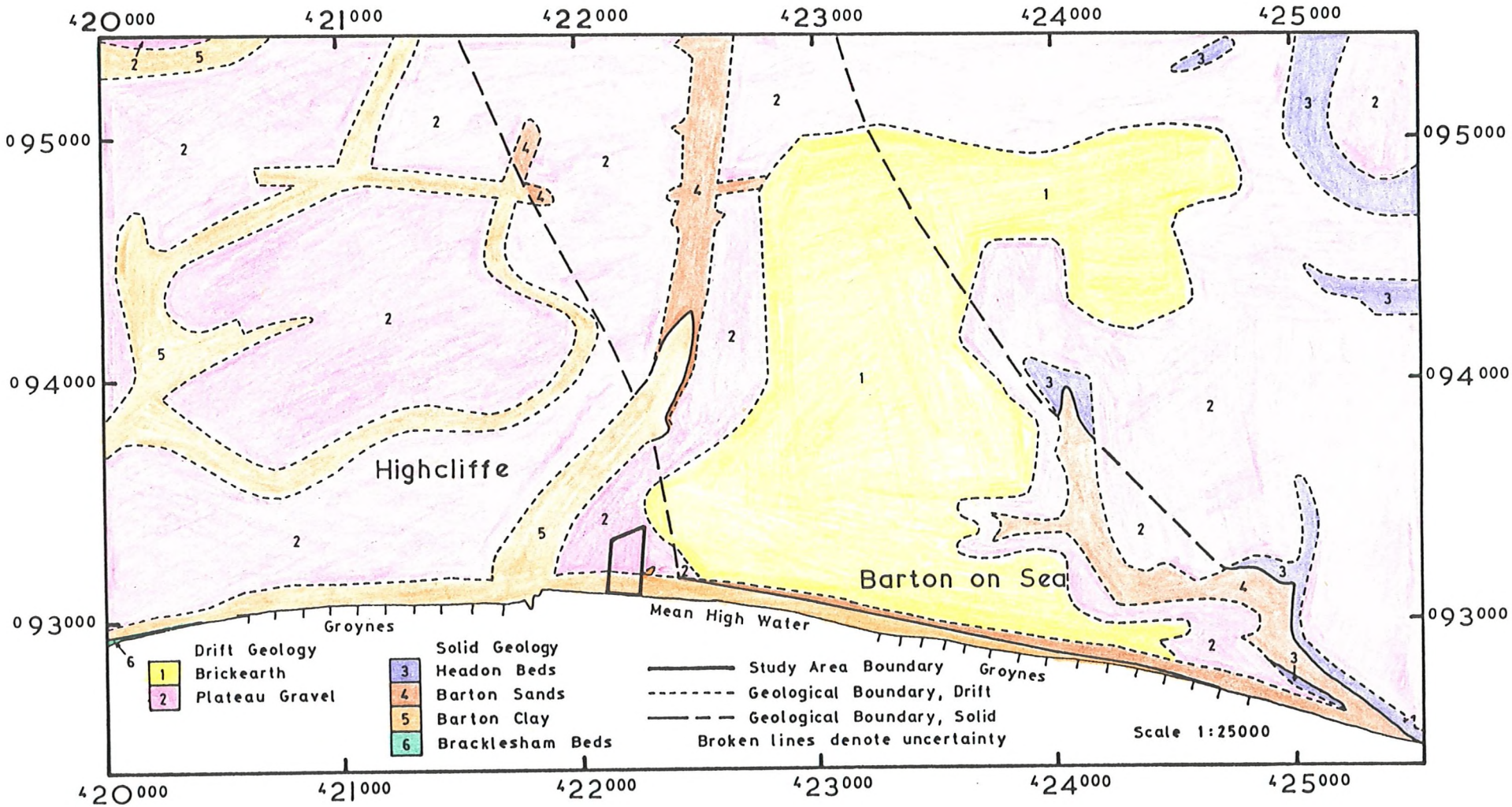

Figure 1.2 Geological map of the region around the study area.

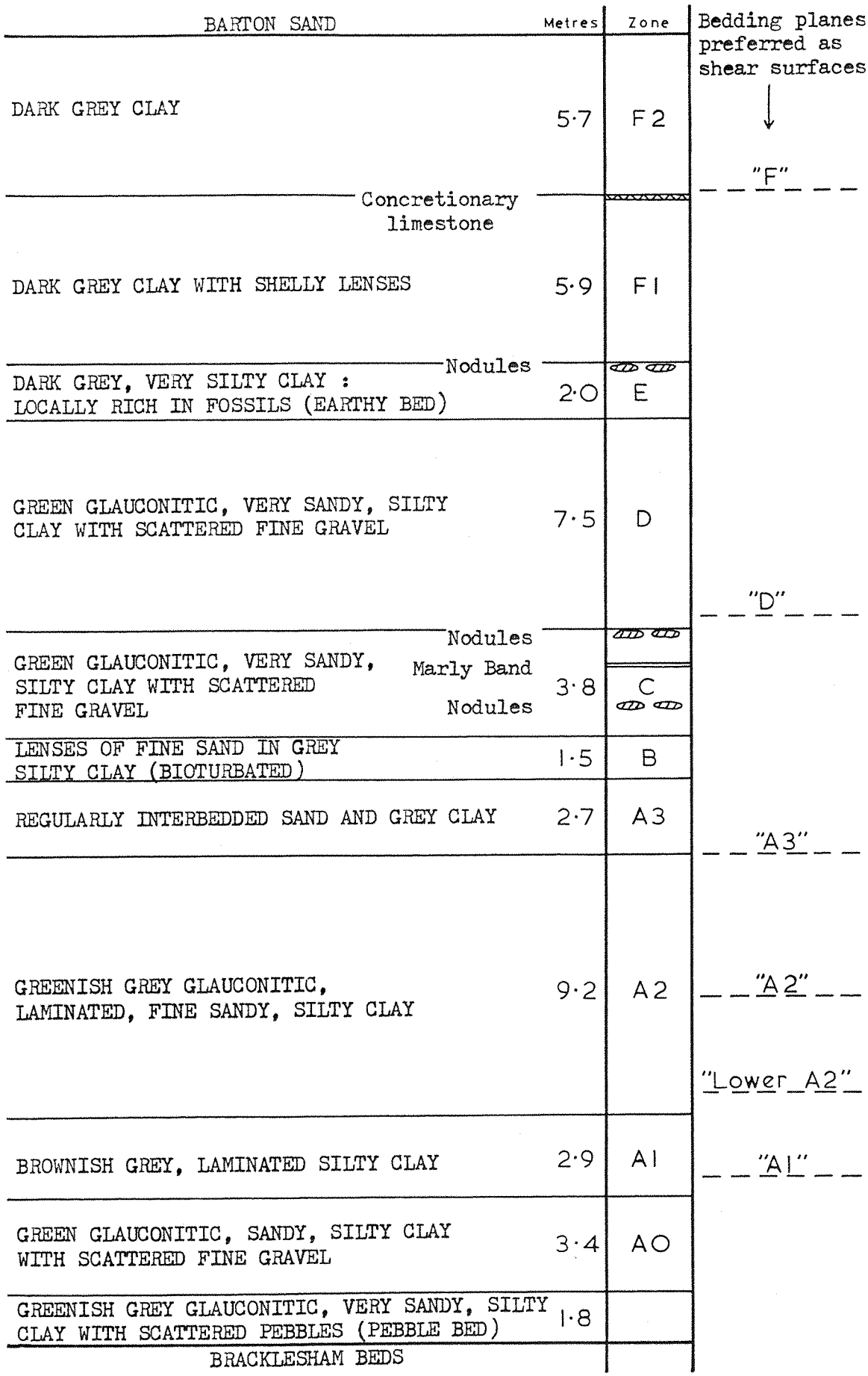

Figure 1.3 Lithological descriptions of the zones in the Barton Clay and the stratigraphic location of the preferred bedding plane shear surfaces. Based on Barton (1973).

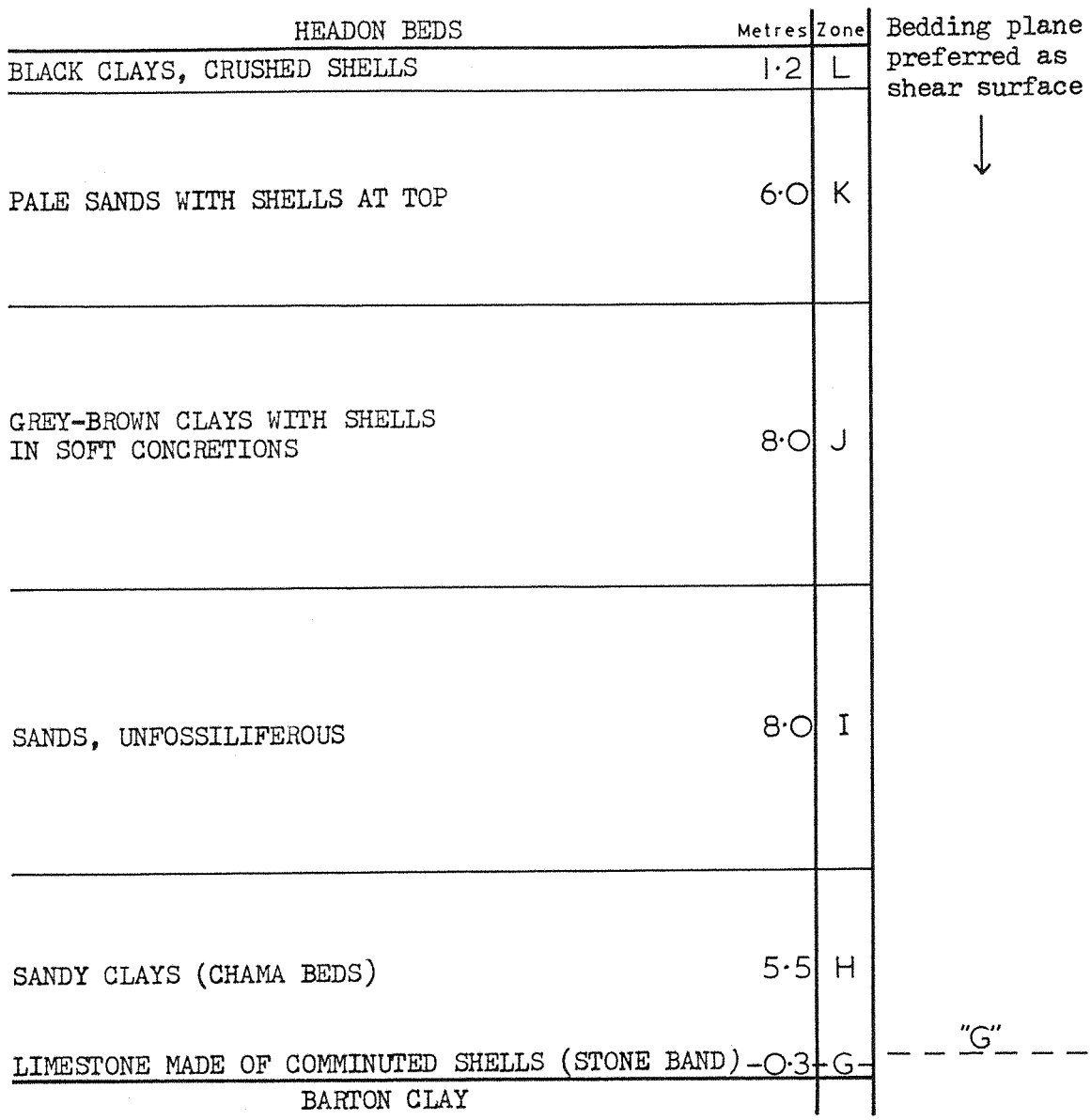

Figure 1.4 Lithological descriptions of the zones in the Barton Sand (based on Melville and Freshney, 1982) and the stratigraphic location of the preferred bedding plane shear surface (based on Barton, 1973).

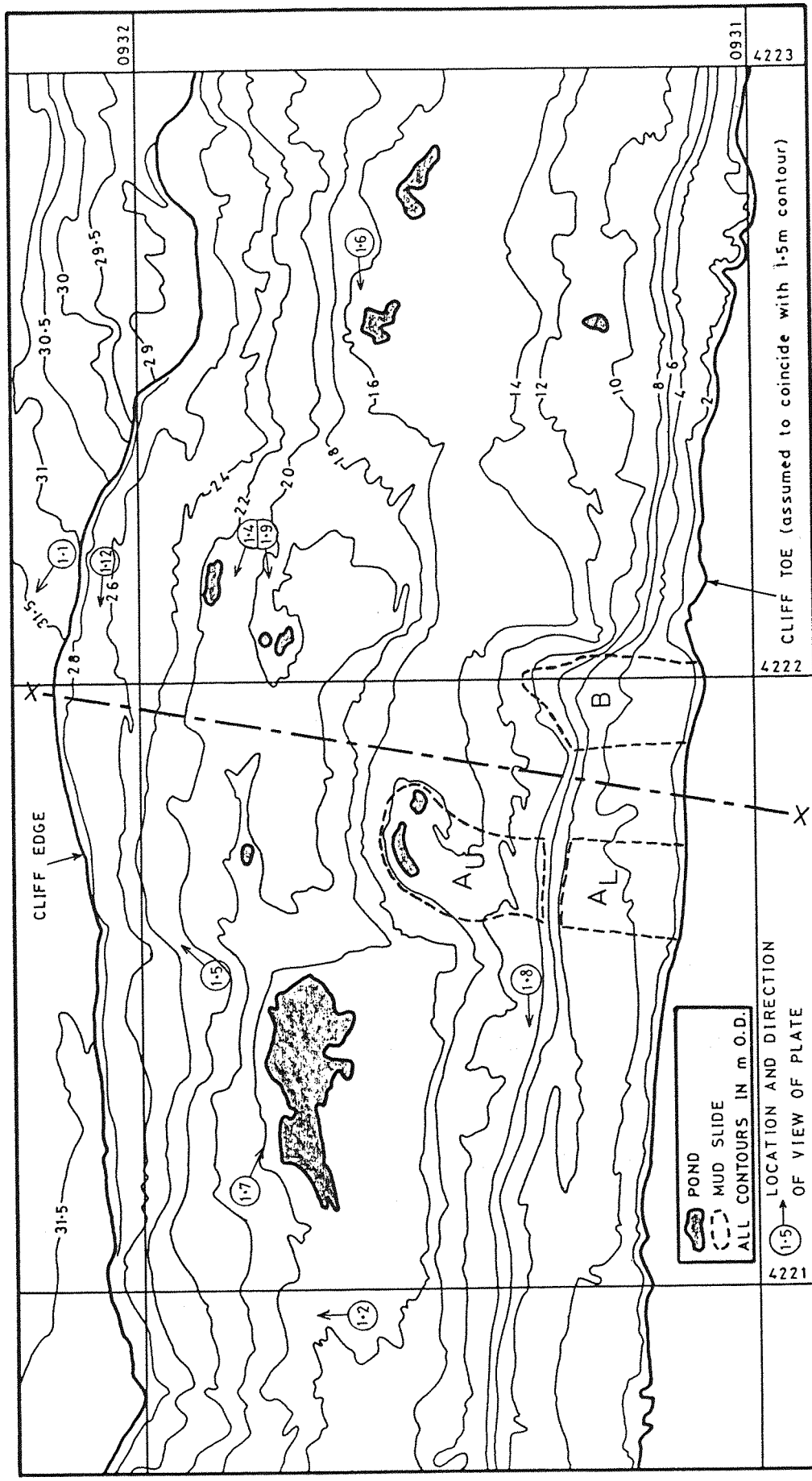

Figure 1.5 Contoured plan of the undercliffs showing the extent of mud slides A and B. Mud slide A is split into upper (A_U) and lower (A_L) parts. A geological section along line XX is given in figure 1.6. The figure also shows the location and direction of view of plates 1.1, 1.2, 1.4 to 1.9, and 1.12.

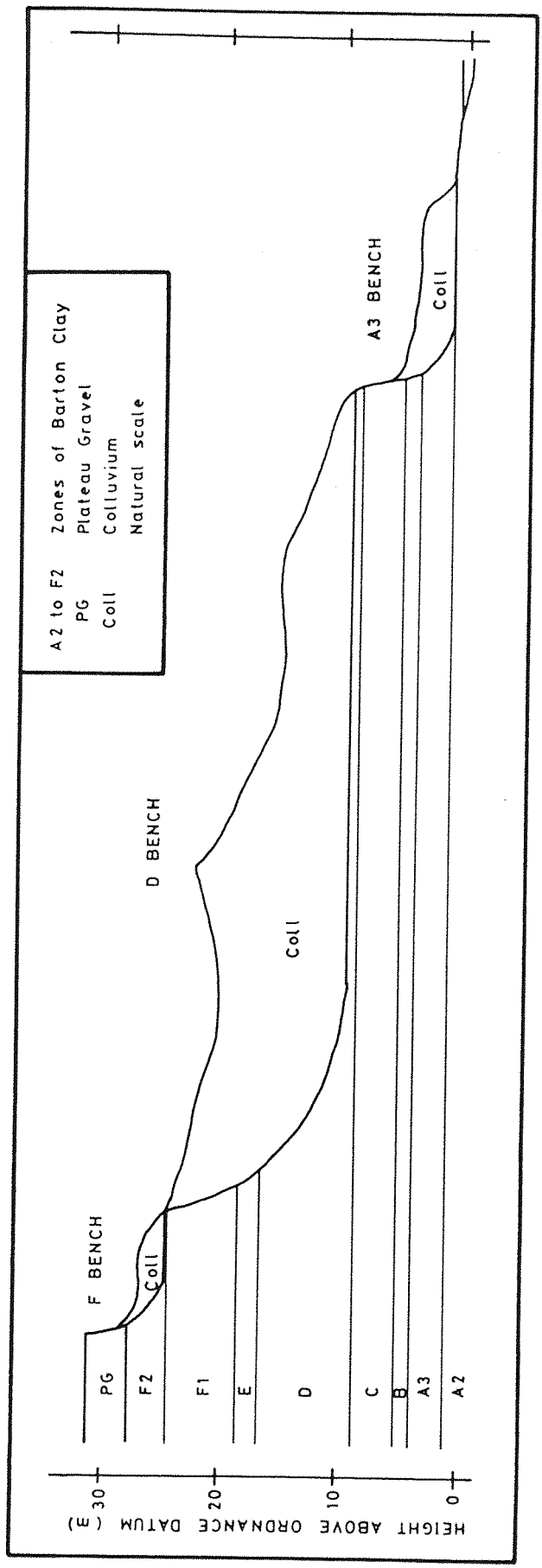

Figure 1.6 Geological section along line XX in figure 1.5.

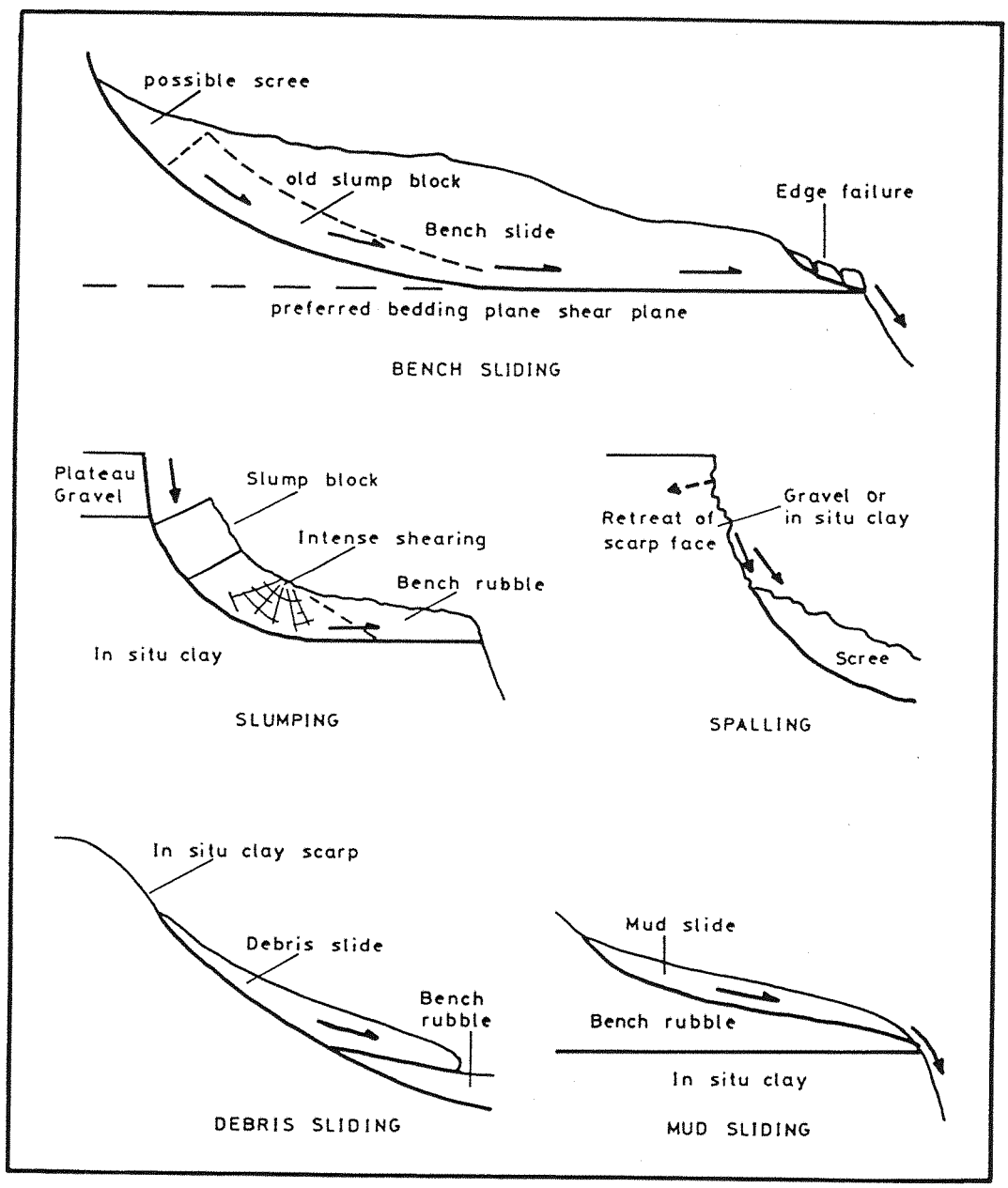

Figure 1.7 Examples of the main degradational processes.

Plate 1.1 View of the cliff top behind the study area. Naish Farm is a holiday estate and a number of chalets can be seen. The drilling rig in the foreground was used to install piezometers on the cliff top.

Plate 1.2 View of the cliff face at the western end of the study area. (See figure 1.5 for the location and direction of view.) The grass in the foreground is at about 16 m O.D. and the cliff top is at about 31 m O.D. Note the orange colour of the central portion of the cliff face in view. This is due to a precipitate of iron oxide staining the Plateau Gravel. Rainfall leaches out the iron oxide at the cliff face. The centre of view is a fresh face due to recent falls of material. Iron oxide is an important consideration in the design of any possible future drainage works to stabilize the cliffs. Drains may be blocked by bacteria which feed on the iron oxide unless they are given a sufficient gradient to be self cleansing.

Plate 1.3 View of the cliff face just west of the study area. The plate shows a dip in the Plateau Gravel/Barton Clay unconformity. The gravel thickness at this point (2.3 m) is shown on the plate. This is the cliff face exposure of the trough T1-T1 in figure 2.10.


2·3 m

Plate 1.4 General view of the upper part of the undercliff in the study area. (See figure 1.5 for the location and direction of view.) The cliff face, F bench, and F scarp can be seen. The F scarp is largely covered by a gravel scree except at A where the in situ Barton Clay is exposed. Just above this a dotted line highlights the exposed basal shear surface of the F bench. This is at about 25 m O.D. The cliff top is at about 31 m O.D. The position B is the location for the view of plate 1.5.

Plate 1.5 View of part of the upper part of the undercliff in the study area. (See figure 1.5 and plate 1.4 for the location and direction of view.) The direction of view is toward the north east of position B on plate 1.5. The in situ Barton Clay F scarp can be seen in the foreground (A). The Plateau Gravel/Barton Clay unconformity can be clearly seen and in the view is fairly horizontal at about 29 m O.D.

Plate 1.6 General view of the undercliff on the D bench. (See figure 1.5 for the location and direction of view.) The foreground is a very wet part of the undercliff. The EDM and theodolite can be seen set up at A. This was used to regularly survey the position of the instrumentation in the undercliff. Known survey points on the cliff top were used to fix the position of the EDM.


B
A


A


A

Plate 1.7 View of the large pond on the D bench of the study area. (See figure 1.5 for the location and direction of view.) The left hand side of the plate has been toned up to compensate for over-exposure of the photograph.

Plate 1.8 General view of the lower part of the undercliff. (See figure 1.5 for the location and direction of view.) The 4 cm on the right hand side of the plate is false colour. The plate shows the A3 bench and D scarp. The top of the scarp is at about 12 m O.D. whereas the A3 bench is at about 4 m O.D. The A3 bench can be seen to be very wet and difficult to traverse at the time the photograph was taken (winter). In the distance can be seen the cliffs at Highcliffe. These have been stabilized and are in stark contrast to the undefended cliffs of the study area.

Plate 1.9 General view of the D bench in the study area. (See figure 1.5 for the location and direction of view.) Note the greater presence of vegetation in comparison to the lower part of the undercliff (plate 1.8).

Plate 1.10 View from the undercliff of the large slump that occurred between 27th and 30th October 1985. The view is from the eastern end of the slump which is labelled H in figure 6.3.
The slump was based on the preferred bedding plane shear plane in the D zone.
(Photograph courtesy of Mr J M Bedford.)

Plate 1.11 View from the cliff top of the large slump that occurred between 27th and 30th October 1985. The view is from the western end of the slump which is labelled H in figure 6.3. The remains of the piezometer P91 (see figure 6.1) can be seen against the cliff face in the foreground (labelled A).
(Photograph courtesy of Mr J M Bedford.)


A

Plate 1.12 View from the undercliff of a small slump that occurred in the study area.
(See figure 1.5 for the location and direction of view.)
The slump was based on the preferred bedding plane shear plane in the F zone.
(Photograph courtesy of Dr M E Barton.)

CHAPTER 2

INVESTIGATIONS OF THE LEVEL OF THE PLATEAU GRAVEL/ BARTON CLAY UNCONFORMITY

2.1 Introduction

The Plateau Gravel (PG) on the cliff top provides a source of considerable seepage flow to the undercliff. Estimation of this seepage requires a knowledge of the groundwater flow in the PG. This will be affected by the continuity of the gravel, and by the variation in the level of the PG/Barton Clay (BC) unconformity. This chapter is concerned with the estimation of the level of the unconformity in the study area.

Drainage measures to protect the cliffs may well include a scheme to intercept the seepage in the gravels. Such a scheme would need to know the elevation of the unconformity along its line, and in particular the presence of any channels. Visual evidence at the cliff face is not always complete (in places, a scree masks the position of the unconformity), and the siting of the cut off (which would be in excess of 10-15 m back from the cliff edge) is such that the cliff face evidence may be inadequate.

A study of the PG thickness was, therefore, carried out to establish the continuity and identify any channels in the unconformity. The method used should be quick and cheap, consistent with obtaining enough data, of sufficient accuracy, for an adequate interpretation to be made.

The easiest, quickest, cheapest, and most accurate method is to survey existing exposures (in this case the cliff face). However, exposures are isolated, i.e. they do not adequately cover the area of interest. Borehole information is the next best source of data. It can cover the area of interest more evenly than a survey of existing exposures, but the amount of data possible is limited by cost and time. The unconformity at Highcliffe was investigated by the Local Authority and Booth (1974) using the information from 64 boreholes. A similar coverage at Naish Farm was not possible. However, the area of interest can be covered easily and cheaply using indirect geophysical

methods. Although it is the least accurate method, it can provide enough data to fill in the gaps left by borehole surveying.

For the survey at Naish Farm, all three basic methods were used, which are now described in turn. The exposure and borehole surveys were used as controls for the geophysical survey. The area surveyed is the cliff top part of the study area.

2.2 Cliff Face Exposure Survey

The gravel depth was measured at approximately 5 m intervals along the line of the cliff for the entire study area. A tape measure was used and measurements taken to the nearest 0.1m. A straight line was set up along the EDM survey base line B1-C1 (see figure 2.7). Offsets to the cliff edge were taken every 5 m, and the depth of gravel measured. The level of the unconformity was estimated using measurements of ground level and gravel depth. The results are presented in figure 2.1.

The section of cliff face measured was accessible at its base, and any scree covering the unconformity was generally light and easily cleared. To the west, the base of the gravels is not so accessible due to the high cliff face (caused by the absence of the F bench). However, visual evidence suggests that the level of the unconformity drops to the west as it approaches Chewton Bunny. A similar observation has also been noted on the other side of the Bunny at Highcliffe by Halcrow (1971). To the east, the unconformity is largely obscured by scree, and is not easily observed. The dry valley just to the east of the study area, is possibly also a site for a local drop in the level of the unconformity.

2.3 Borehole Survey

A total of 26 boreholes were sunk on the cliff top to install

piezometers. At the time of drilling, the gravel depth was noted. The boreholes do not evenly cover the survey area, as their main intention was to monitor groundwater levels, and not to measure gravel thickness. A description of the boreholes, including gravel depth, is given in Thomson (1986b). The accuracy of the measurement of the gravel thickness was at best $\pm$ 0.1 m. The change from gravel to clay was judged by "feel", so that it is possible that a sand lens at the base of the gravels would be thought to be clay. From visual evidence of the cliff face, the frequency of sand lenses at the base of the gravels is low, so that they are unlikely to cause any consistent error.

2.4 Geophysical Survey

2.4.1 Method

The method employed was that of electrical resistivity, with a Wenner electrode configuration and a constant electrode spacing of 6 m. The measurement of apparent resistivity was correlated with the depth of gravel, as found from both depth sounding and borehole measurements. A constant electrode spacing was used in preference to depth sounding, as it was quicker and able to cover the study area more completely (the positioning of chalets severely restricted depth sounding). A more detailed description of the method used, and the theory behind it, is given in appendix A.

2.4.2 Calibration of Results

The relationship used to estimate the gravel depth from a reading of apparent resistivity with an electrode spacing of 6 m was :

$$\text{Gravel Depth} = 0.0144 \times \text{Apparent Resistivity} + 1.53 \qquad (2.1)$$

This section describes how this relationship was evolved, the range of readings for which it is applicable, and the accuracy to which it predicts gravel depth.

2.4.2.1 Depth Sounding

To investigate a suitable electrode separation for the constant separation traverse, a number of depth soundings were made. It was decided that a separation of 6m was adequate. The depth sounding results showed that a smaller spacing would have been unable to detect the deepest gravels.

Depth sounding also yielded estimates of gravel depth and resistivity. The former were used to help estimate the calibration relationship (equation 2.1). The latter were used to investigate spatial homogeneity upon which equation 2.1 relies.

2.4.2.2 Deviations from the Theory of Depth Sounding

Analysis of the depth sounding results was by curve matching, assuming a laterally homogeneous horizontal two layered profile. Difficulty in obtaining accurate curve matching suggests that these assumptions are only approximate.

Firstly, the layers are not horizontal. The very purpose of this survey is to determine the deviation of the PG/BC unconformity from the horizontal. Slight variations should not seriously affect the theory. However, there is some evidence of abrupt changes in the unconformity due to periglacial features (Barton, 1984a).

Secondly, geological evidence suggests at least four layers of differing resistivity. A thin layer of topsoil (a brickearth-soil estimated up to 30 cm thick) covers the area, and from depth

sounding results it appears to have a lower resistivity than the gravel (probably due to its greater moisture holding capacity, even when dry). A permanent groundwater table exists over much of the area. The saturated gravel provides a layer of lower resistivity than the dry gravel above it. The saturated gravel layer thickness varies both spatially and temporally. At the time of the survey, it varied up to 1.9 m thick (the maximum figure is given by figure 6.30 for August 1982), being greater with increasing distance from the cliff face, and with the lower the elevation of the unconformity. The survey was carried out during a summer dry period (August 1982) when groundwater levels were low with minimal variation. Most of the depth sounding was carried out the following summer (August 1983) when groundwater levels were similar to those of the previous summer. To treat the PG as three separate layers (topsoil, dry gravel, and saturated gravel) would have greatly complicated the analysis. The thickness of the topsoil and saturated gravel was such that it was felt that a two layer model of PG and BC was adequate.

Thirdly, lateral inhomogeneities cause inaccuracies. Depth soundings for most locations were repeated with a different electrode orientation (where possible, the two orientations were perpendicular to each other). Differences in readings showed lateral variations of resistivity and layer depth. In such instances, separate estimates were made of gravel depth and resistivity, and the results averaged. From these results, it is calculated that a change in the orientation of the electrode spread, varies the estimate of the gravel depth by curve matching, by an expected amount of $\pm$ 0.25 m. As a comparison, the dependence of apparent resistivity on electrode orientation, leads to an estimated error in using equation 2.1 of $\pm$ 0.3 m.

The discussion has shown that the error in estimating the gravel thickness by depth sounding is variable, and may, in some instances, be quite large. If the expected error (for lateral inhomogeneity) derived from electrode orientation is arbitrarily

doubled to account for the error due to the use of only a two layer model, then the total error is $\pm$ 0.5 m.

2.4.2.3 Spatial Variation of Gravel Resistivity

The use of equation 2.1 relies upon the gravel resistivity being spatially homogeneous over the survey area, at least for any given gravel thickness. The numerous depth soundings provide a number of estimates of gravel resistivity. The variations in resistivity could be due to variations in the thickness of the topsoil (the topsoil and PG are effectively averaged as one layer). This can only be speculative, as no detailed survey of the topsoil has been made. However, Barton (1984a) observed a local thickening of the topsoil above involutions affecting the PG/BC unconformity. Figure 2.2 shows the relationship between gravel resistivity and depth estimated by depth sounding. The figure shows a definite relationship (at the 95 per cent level of confidence) with the resistivity decreasing with increasing gravel thickness. The reason for this is uncertain. However, the lower resistivity does suggest a higher moisture content. This could be due to the greater thickness of saturated gravel. The scatter about the regression line is a measure of the spatial inhomogeneity in gravel resistivity for a given gravel thickness. An important feature of this figure, is that the minimum estimated resistivity is 300 ohm.m. If, in the constant electrode separation survey, there are areas where readings of apparent resistivity approach this value, then either depth sounding or a greater electrode separation should be used to estimate the gravel thickness.

2.4.2.4 Verification of Depth Sounding Estimates

From the previous discussion, it can be seen that the interpretation of geophysical information is open to some doubt. The results were therefore compared with measurements of the gravel depth in boreholes. Depth soundings were made at the locations of eight

piezometers for which borehole information of the gravel depth exists. For these two different estimates, a two-tailed paired t-test (Chatfield, 1983) showed that for all depths there was no significant (at the 95 per cent level of confidence) difference between the two estimates ($t = 1.272$ with 7 degrees of freedom). Figure 2.3 is a scatter plot of the two estimations. Also shown is the regression line with its 95 per cent confidence band. From this it can be visually seen that for all depths there is no significant difference between the expected value for each of the two estimates. The large scatter of points is due to the various errors in both measurements. The expected errors have been estimated as, at best, $\pm$ 0.1 m for borehole measurement (see section 2.3), and $\pm$ 0.5 m for depth sounding (see section 2.4.2.2).

2.4.2.5 Calibration Equation

The previous section showed that there was no significant difference between the two types of estimate of gravel depth. Therefore, all depth estimates (by either depth sounding or borehole) were used to regress gravel depth on apparent resistivity for an electrode spacing of 6m. Figure 2.4 shows the scatter and the regression line with its 95 per cent confidence band. The equation of this line is given as equation 2.1. To gain an idea of the error in using equation 2.1, it is assumed that the calibration estimates of depth contain no error. What, then, is the error due to using equation 2.1 to estimate the gravel depth from an apparent resistivity reading? The average error between the true and predicted values is $\pm$ 0.45m ($\approx \pm$ 0.5 m). This compares equally with the estimated error for depth sounding (see section 2.4.2.2).

Figure 2.5 shows the location of the various depth estimates used for calibration. The non-uniform spatial distribution of estimates may cause some bias in the estimate of the regression line. It was difficult to achieve a more uniform distribution

due to the presence of chalets, and the siting of boreholes in positions dictated by other considerations.

As mentioned in section 2.4.2.3 there is an upper limit to the applicability of the calibration (300 ohm.m). Extrapolation of the line below the lowest calibration point (62 ohm.m) is also doubtful, especially at very low readings (a zero reading of apparent resistivity suggests a gravel depth of 1.5 m!). In calibration, it is assumed that the relationship between gravel thickness and apparent resistivity for a 6 m electrode spacing, is approximately linear. It is probable that at very high and very low readings the relationship is non-linear, and therefore prone to extrapolation errors. Theoretically, the true relationship will be of the form of figure 2.6.

2.4.2.6 Cliff Face Exposure Control

The gravel thickness was estimated at points along a line 3-10 m back from the cliff edge (see figure 2.7), using equation 2.1 and apparent resistivity readings. Readings along a line closer to the cliff edge are affected by the presence of the cliff edge. Figure 2.8 compares these resistivity estimates with the measurements at the cliff face. For this purpose, the line of the resistivity readings, and the line of the cliff face, were projected onto the B1-C1 survey base line. The gravel thickness not only varies along B1-C1, but also perpendicular to it. The evidence of figure 2.8 supports the use of equation 2.1 to estimate the gravel depths in the survey area.

2.5 Results and Discussion

2.5.1 Apparent Resistivity Results

The readings of apparent resistivity for an electrode separation of 6 m are plotted in figure 2.9. As can be seen, there are

considerable gaps in the coverage of the study area. This is due to the presence of holiday chalets and service roads. The scarcity of open ground is even greater outside the study area. Keeping rigidly to the same electrode orientation limited the coverage still further. A few readings in isolated places used different electrode orientations. The gaps in the coverage could have been further reduced by more variation in the electrode orientation. However, this would have greatly increased the time taken for the survey for relatively little increase in areal coverage.

The apparent resistivity readings vary from 15 ohm.m to 268 ohm.m. The extrapolation of the calibration equation for the high and low readings is open to some doubt (see section 2.4.2.5). However, the extreme readings still indicate variations in gravel thickness, and are therefore used in the analysis. However, ideally they should be verified with borehole information.

2.5.2 Contour Levels of the Unconformity

Figure 2.5 shows the ground level contours as drawn by Cartographical Services (Southampton) Limited from aerial photography. These were used with the apparent resistivity readings of figure 2.9 and equation 2.1 to obtain estimates of the O.D. level of the PG/BC unconformity. Contours of the unconformity were then drawn and are shown in figure 2.10. For this purpose, the 10 m grid was adequate. However, there was considerable ambiguity for areas where there were gaps in the survey, although they still show the general trends in the topography of the unconformity. The contours at the cliff face have used the information from the cliff face exposure survey. The expected error in the estimate of the gravel thickness, and therefore also in the level of the unconformity (assuming negligible error in interpolating ground level contours), is $\pm$ 0.5 m, which is 20 per cent of the contour variation (28 to 30.5 m O.D.).

Figure 2.10 shows the unconformity to have a fairly horizontal and gently undulating topography within the survey area. However, the contours show several interesting erosional features which may influence groundwater flow in the gravels. Groundwater flow is discussed in conjunction with groundwater levels in chapter 6. Some erosional features appear as a number of lines of ridges and troughs. Some of these lines are shown on the contour map. The general direction of these features is NE to SW. The trough T1-T1 was the site of a very large slump (no 2 in Barton et al, 1983) in February 1982, and for some time afterwards considerable water was seen to issue from the gravel at the cliff face at this point. High level features of the unconformity may obstruct groundwater flow in the gravel, whereas low level features will concentrate the flow, and be of engineering significance in the design of a cut off drain as part of cliff protection.

The geophysical method will only detect gradual changes in the level of the unconformity (see appendix A, section A.2.7). However, at NGR 422230 093225 (see figure 2.10) a change of 1.5 m was estimated over a distance of only 4 m. It may be that the true variation is much greater, and that the resistivity estimates are masking the change. At A, figure 2.5, borehole evidence shows a sharp drop in the unconformity (2.2 m drop over a distance of 2.1 m) which is not picked up by resistivity readings. Figure 2.9 shows how this small scale feature was not measured by the resistivity survey. It was just by chance that it was picked up by borehole. In general, however, the resistivity readings show only small undulations in the unconformity. This is further backed up by cliff face evidence (see figure 2.1 and plate 1.5).

2.5.3 Comparison with Results at Highcliffe

Booth (1974) drew contour lines of the unconformity for a similar size area to the west of Chewton Bunny, at Highcliffe. The two survey areas are 800 m apart. Data from 64 boreholes showed a

similar undulating surface. The level of the unconformity varied from 25.5 to 27 m O.D. (cf 28 to 30.5 m O.D. for the Naish Farm study area), except near to Chewton Bunny where it became much lower. The smaller variation may be due to a lower sample density. The lower level of the unconformity at Highcliffe relates to the original valley contours at the time of the deposition.

2.5.4 Unconformity Topography outside the Study Area

The ground level to the west and north west of the study area, slopes downward towards Chewton Bunny. It is anticipated that the unconformity level also slopes downward towards Chewton Bunny. This is based on the cliff face evidence from both sides of the Bunny. Conjecture as to the level of the unconformity to the east of the study area, is uncertain without further borehole and geophysical evidence. Just to the east of the study area is a dry valley. It may well be that the level of the unconformity is lower than that of the surrounding area. Barton (1984a) described the drift deposit in the dry valley as being only about 0.6 m thick. Further to the east, the cliff face evidence shows the PG to be a continuous and thick deposit. However, the unconformity is largely obscured by colluvial debris, such that no quantitative measurement has been possible. A geophysical survey in this area would be considerably complicated by the presence of Brickearth (up to 2m) on top of the PG.

2.6 Summary and Conclusions

A combination of methods were used to successfully survey the PG/BC unconformity for the area thought to contribute significant groundwater flow to the undercliff study area. These were :

A. a cliff face exposure survey,

B. a borehole survey,

C. a geophysical resistivity survey :

   i. by depth sounding ;

   ii. by a constant electrode separation traverse.

Method B was used to substantiate the validity of method Ci. Then both methods B and Ci were used to calibrate the results of method Cii. Method A was used to verify the suitability of the calibration. Methods A and Cii were then used to estimate levels of the unconformity. The expected error in estimating the unconformity level by method Cii was $\pm$ 0.5 m, which is 20 per cent of the contour variation (28 to 30.5 m). Thus, method Cii was accurate enough to show the variations in topography of the unconformity.

In the survey area, the top of the BC is a fairly horizontal and gently undulating surface. The variations in level may be interpretated in two ways. They may be either due to periglacial action (Barton, 1984a), or due to the erosional action of the moving gravel before it was deposited. Due to the scale of the features, the latter seems more likely to explain the NE-SW alignment of the linear trends noted in section 2.5.2. Thus, the trends that have been noted in the surveyed level of the unconformity, are considered to be palaeo-current indicators for the deposition of the gravels. The different alignment of the trends in the eroded surface of the BC at Highcliffe, could be due to the influence of the south flowing River Avon at the time of deposition.

The PG deposit is considered to be continuous to the west and north of the survey area, although the unconformity has a downward trend as it approaches Chewton Bunny. To the east, the level of the unconformity is less certain, and further work is necessary for its elucidation. However, it is expected to be a fairly horizontal, gently undulating surface.

The survey has confirmed the continuity of the PG deposit. The presence of channels in the unconformity has been confirmed, although no major ones have been detected which might seriously affect the design of a cut off drain. However, this does not preclude their possible presence, either in the surveyed area (small scale if this is the case), or further to the east.

Figure 2.1 Tape survey of the Plateau Gravel at the cliff face on 27th July 1982.

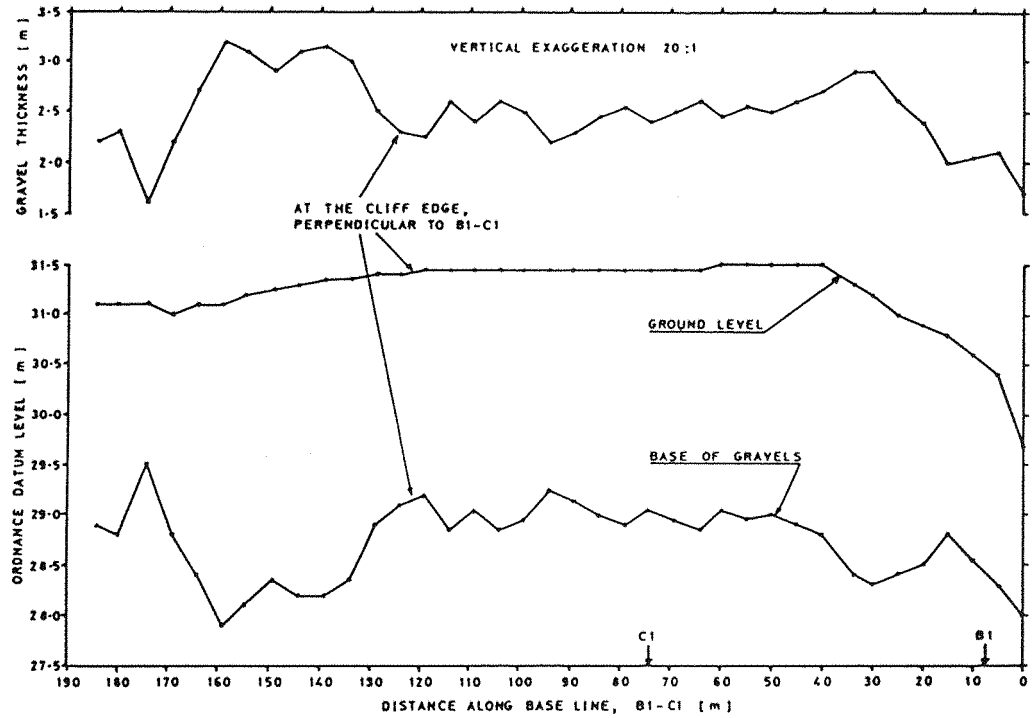

FIGURE 2.2
PLOT OF PLATEAU GRAVEL RESISTIVITY VERSUS GRAVEL DEPTH BY DEPTH SOUNDING

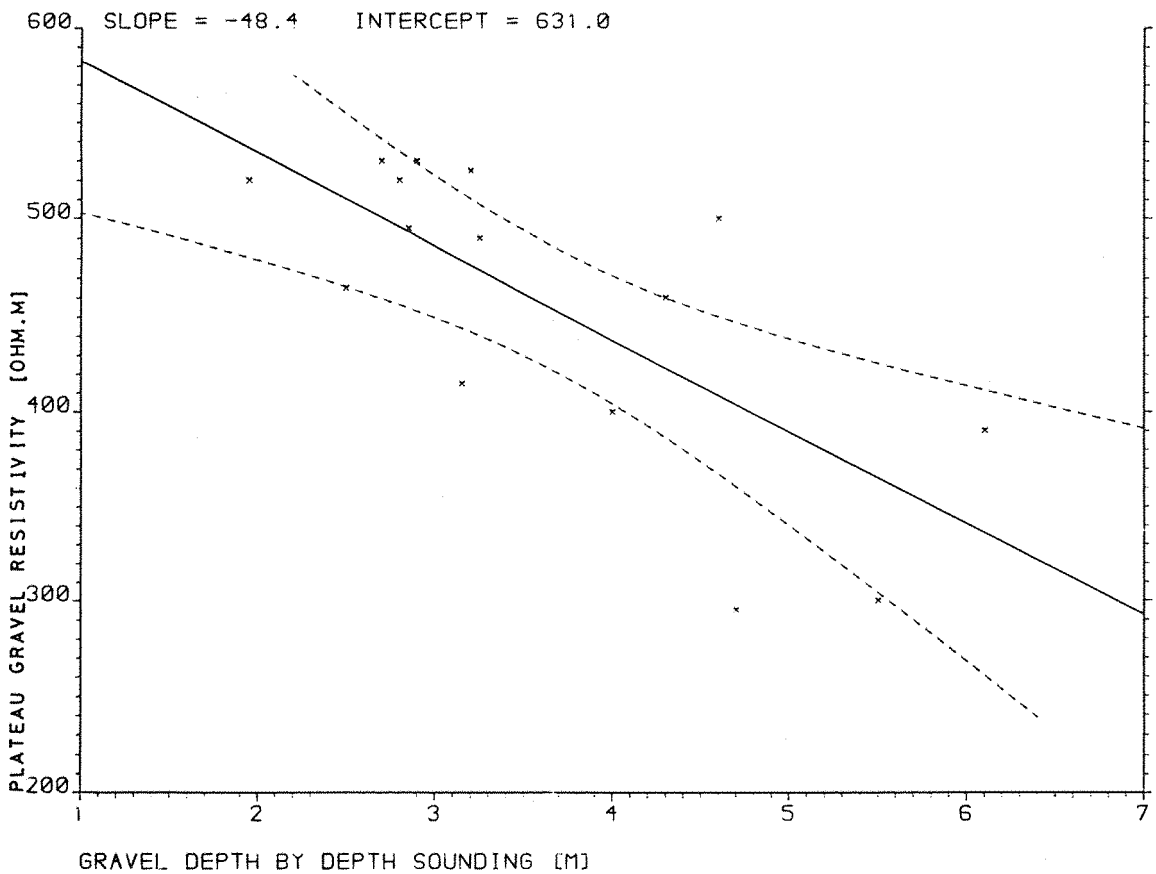

FIGURE 2.3

PLOT OF BOREHOLE GRAVEL DEPTH VERSUS
GRAVEL DEPTH BY DEPTH SOUNDING

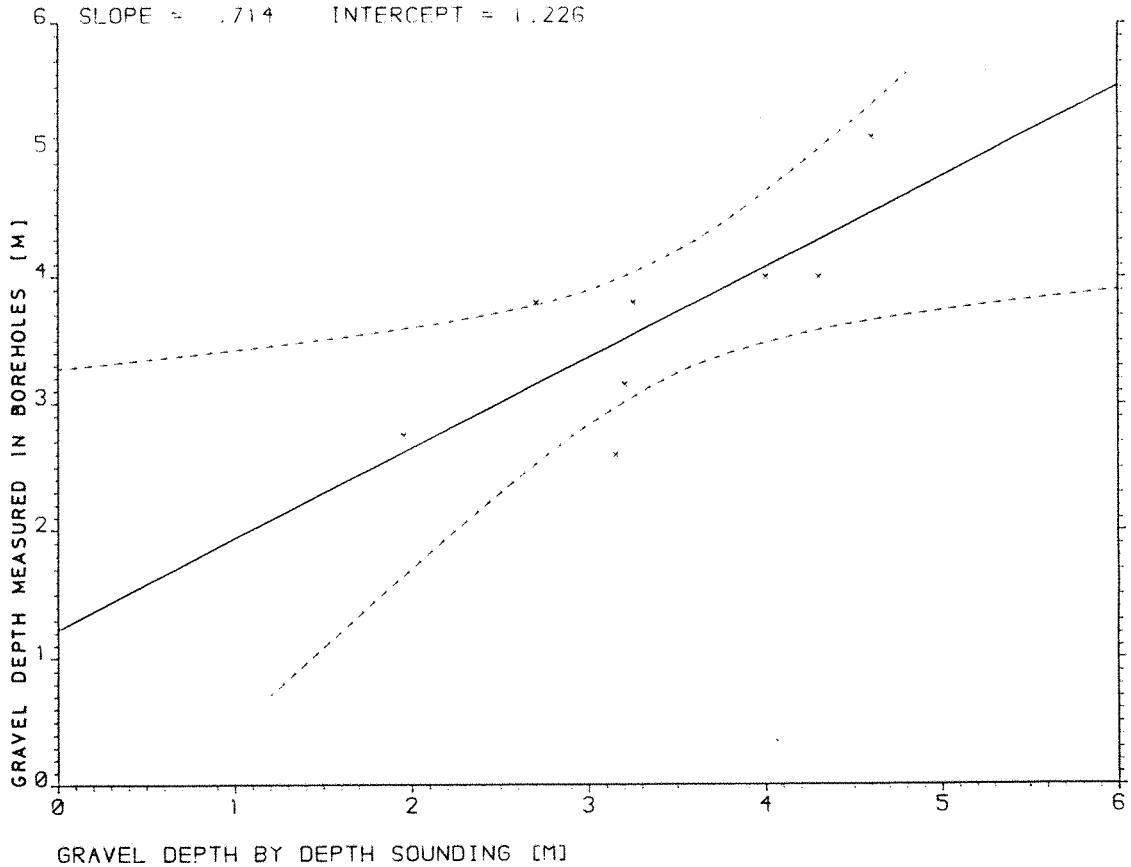

FIGURE 2.4

GRAVEL DEPTH BY BOREHOLE AND DEPTH SOUNDING VERSUS
APPARENT RESISTIVITY AT 6M SEPARATION

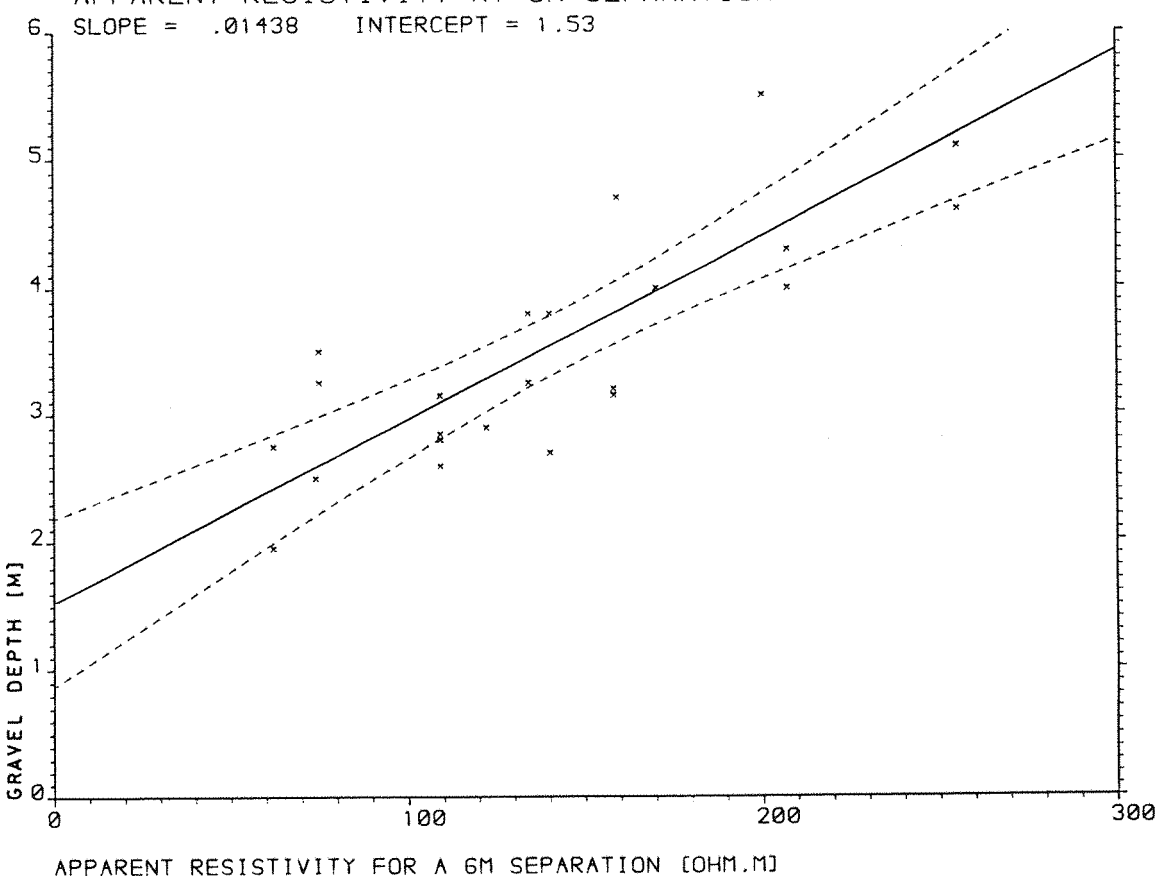

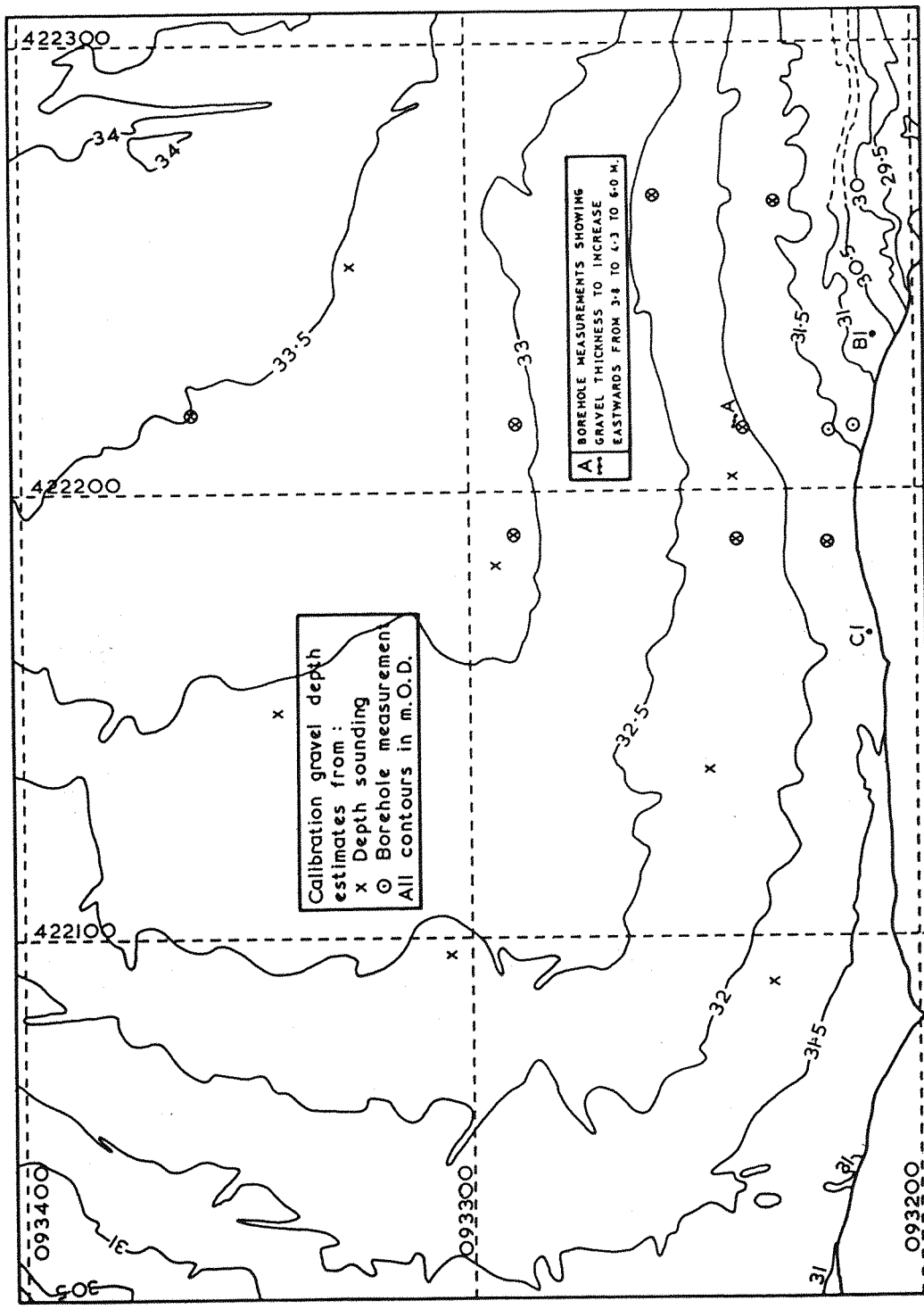

Figure 2.5 Ground level contours and location of the various gravel depth estimates used for calibration.

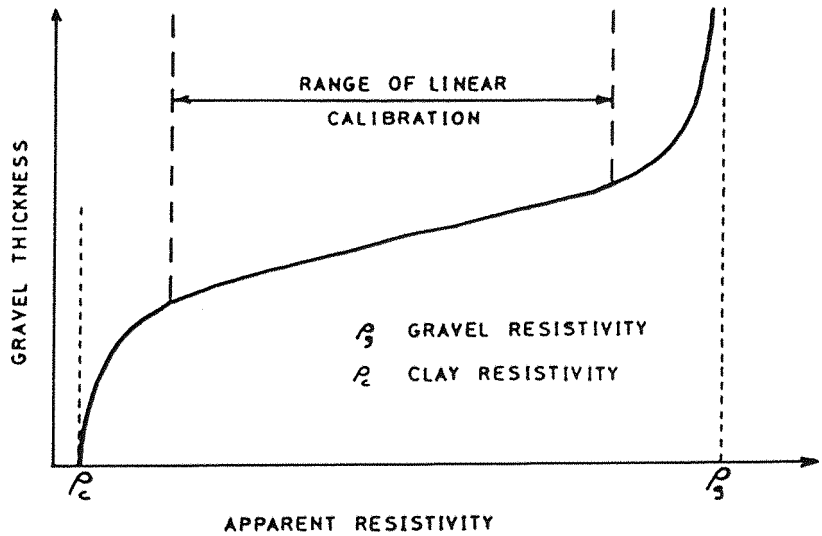

Figure 2.6 Theoretical form of the relationship between depth and apparent resistivity for a constant electrode spacing.

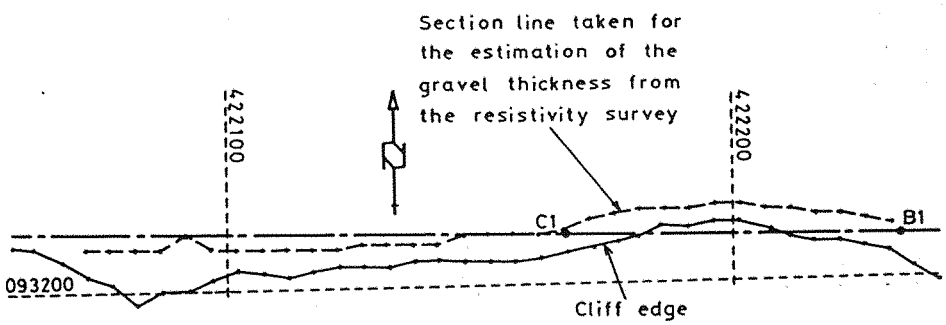

Figure 2.7 Position of the cliff face on the 27th July 1982.

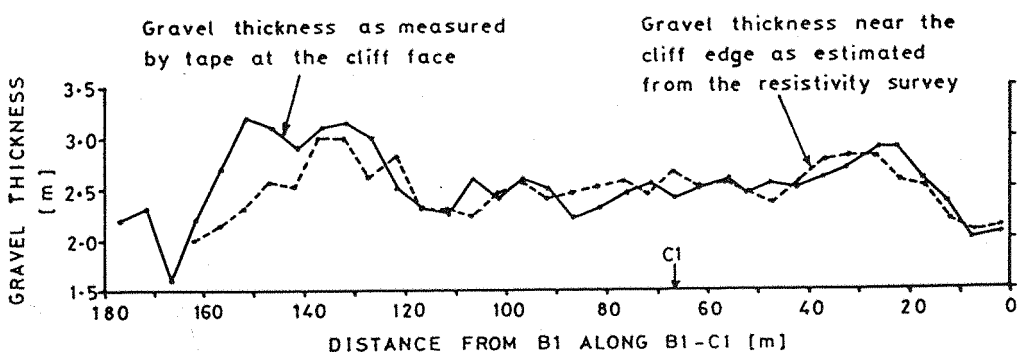

Figure 2.8 Comparison of resistivity and tape measure surveys for estimating the thickness of gravel.

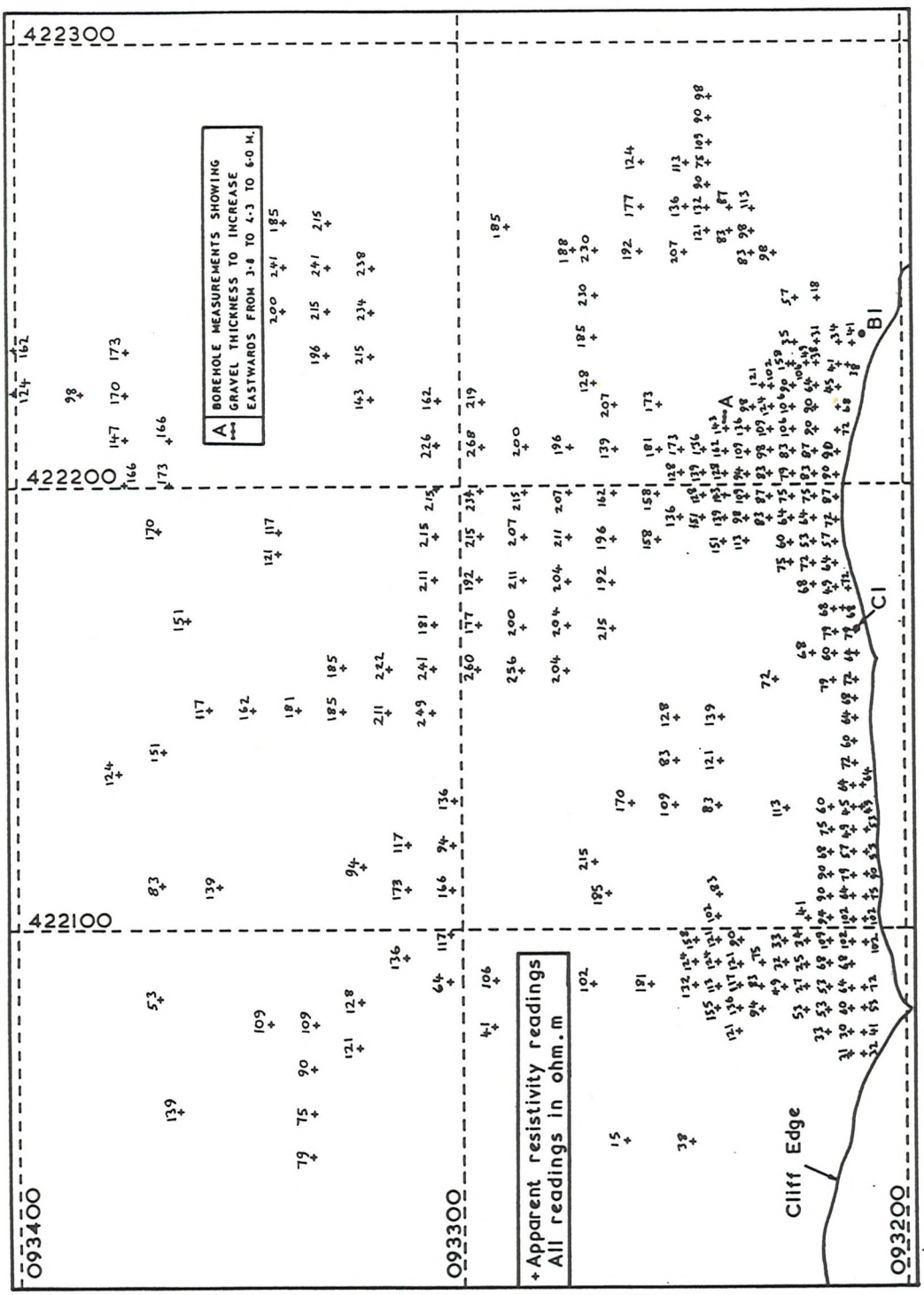

Figure 2.9 Apparent resistivity readings for an electrode separation of 6 m.

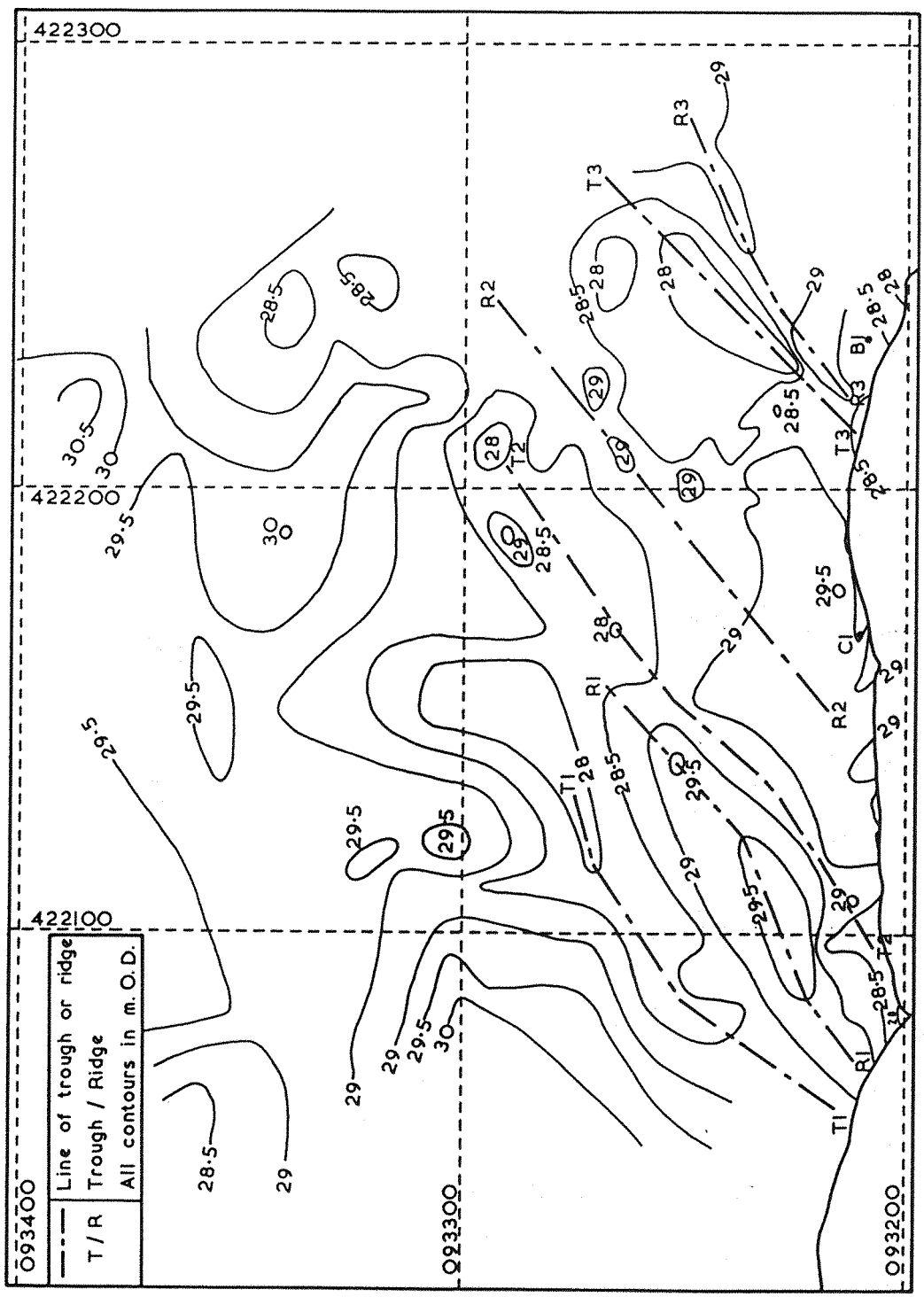

Figure 2.10 Contours of the Plateau Gravel/Barton Clay unconformity.

CHAPTER 3

METEOROLOGICAL INVESTIGATIONS IN THE NAISH FARM REGION

3.1 Introduction

The meteorological factors investigated centre on the measurement of rainfall and evaporation. For a given surface type, the maximum possible evaporation is dependent only on climatic conditions (the ability of the atmosphere to absorb moisture). This is termed the potential evaporation (PE) for a given surface (e.g. bare ground, open water, grass).

Meteorological data is available from a number of locations in the region around Naish Farm (see figure 3.1). However, the data is unlikely to accurately represent rainfall at the study site at Naish Farm. Therefore, a weather station was set up at Naish Farm (see figure 3.2 for its location). The data was collected over a 2 year period and compared with other nearby stations. The relationship between the weather at Naish Farm and that of the surrounding region was investigated, with a view to extending data records at Naish Farm using data from other stations. Meteorological data is also likely to vary spatially over much smaller distances. The effect of this on the study site has been considered.

This chapter considers the measurement of rainfall and potential evaporation at Naish Farm together with an appreciation of their respective possible errors. The data is examined for consistency and compared with data from the surrounding region. Statistical properties of the data distributions are considered at Naish Farm and Hurn Airport.

3.2 Rainfall Measurement at Naish Farm

Rainfall totals have been measured using a standard Snowden type rain gauge. The rim was levelled using a spirit level. Two such gauges (R1 and R8) were installed at 1 foot (0.305 m) above the ground and one was installed at ground level (R7). To minimise insplash and wind effects the latter was installed in the middle of a 1 m square pit 0.305 m deep. A 1 m square

cardboard grid with 0.2 m spacing was placed in the pit such that the top of the grid was flush with ground level. (Cardboard was satisfactory for the short measurement period but is not so for longer periods.) The purpose of the grid was to reduce insplash. Although the one used here was not to the exact specification of Shaw (1983, p 51), it is considered to be adequate. The purpose of installing a gauge at ground level was to investigate the aerodynamic loss effect which has been reported by numerous authors (e.g. Rodda, 1967a). The two gauges above ground level were used to investigate variation due to differences in adhesion.

A fourth rain gauge (R2) has been used to measure rainfall continuously. This was a Casella natural syphon rain gauge. It was 8 inches (0.203 m) in diameter and set 1 foot (0.305 m) above ground level. The chart was changed weekly.

Rainfall totals were measured at least once a week and always at the same time as the continuous rain gauge chart was changed. Daily rainfall is defined as the amount falling between 0900 GMT on the relevant day and 0900 GMT on the following day. This is consistent for comparison purposes with gauges at other sites. Rain gauge R1 was used as the standard for the site and daily amounts were apportioned using the continuous rain gauge chart. On a few occasions the continuous rain gauge failed to operate properly. The rainfall measured by R1 was then apportioned using the average of stations: Everton, New Milton, Christchurch, and Highcliffe or Stony Lane. (Bleasdale and Farrar, 1965, used up to six nearby stations less than 12 km distance from the gauge in question.) A total of 32 days rainfall were so apportioned.

All the above gauges were installed inside a compound as depicted by figure 3.3. Other rain gauges (R3, R4, R5, R6) were installed at various locations on the undercliff (figure 3.2). They were set 1 foot (0.305 m) above average ground level and with their rims levelled. Unfortunately, due to the high risk of vandalism (one gauge went missing), readings were only available for a

short period during the winter. R3 was also difficult to read due to the treacherous ground conditions on the A3 bench after wet periods.

3.3 Evaporation Measurement at Naish Farm

The rate of evaporation depends upon many factors. These include the prevailing meteorological conditions; the type of ground surface (characterised by its reflectivity and roughness); and the soil itself (or, rather, its unsaturated hydraulic conductivity). The latter is dependent upon soil moisture conditions. At high soil moisture content the hydraulic conductivity of the soil is also high, such that evaporation is limited by the atmospheric conditions. The usual approach to estimating evaporation is to first quantify the effect of the atmospheric conditions when water at the evaporating surface is non-limiting. This is termed the potential evaporation (PE). Actual evaporation (AE) is calculated by multiplying PE by a factor the value of which (between 0 and 1) is dependent upon the soil moisture conditions.

AE can be measured directly by lysimeter where rainfall and drainage are measured; the change in soil moisture storage is found either by weighing or neutron probe; and evaporation is found by solving the water balance. If the lysimeter is kept well irrigated then AE equals PE. Another method of measuring PE is to use a pan of open water. The Piché evaporimeter is similar but on a much smaller scale (30 cm^3 volume and 11 cm^2 evaporating surface compared with 1.8 m^3 and 3.35 m^2 respectively for a British Standard tank). The above are all direct measurements of PE from a specific evaporating surface. Empirical correction factors are applied to find the PE for other surfaces. A variety of indirect methods have been developed using weather data. They differ in the variables needed to be measured and the form of the empirical equations. One such method, the Penman method, has been used here. The calculation of AE from

PE is described later in chapter 5. The Penman method was originally developed in Penman (1948) and was based on a combination of sink strength (a mechanism for removing the vapour) and energy balance (energy is needed to convert water to vapour). This combination made the approach original and was useful in that it eliminated the need to measure the temperature and vapour pressure at the evaporating surface. The daily measured weather variables needed are "mean air temperature, mean dewpoint, mean wind velocity at a standard height and mean duration of sunshine". The empirical coefficients in the equations have differed over the years. The approach in Penman (1963) is used here because it is the same as that used by the Meteorological Office for their monthly estimates of PE for short grass. This enables comparison of results.

The equations used here (after Penman, 1963) to calculate the PE of three different surface types are now given.

i) Open water

$$E_o = \frac{\Delta / \gamma}{1 + \Delta / \gamma} \cdot R_A (1 - r) (a + b \cdot n/N)$$

$$- \frac{\Delta / \gamma}{1 + \Delta / \gamma} \cdot \sigma T_a^4 (0.56 - 0.09 \sqrt{e_d}) (0.10 + 0.90\, n/N)$$

$$+ \frac{1}{1 + \Delta / \gamma} \cdot 0.35 (0.5 + u_2/100) (e_a - e_d) \qquad (3.1)$$

where E_o is the open water evaporation (mm/day)

Δ is the slope of the saturation vapour pressure curve at mean air temperature (mb/^oC)

γ is the constant of the wet and dry bulb psychrometer equation (mb/^{o}C).

R_A is the theoretical incoming short wave radiation at the limits of the earth's outer atmosphere (mm of evaporation/day).

r is the albedo, or reflection coefficient, taken as .05 for water.

n is the actual number of hours of bright sunshine (hrs).

N is the theoretical duration of sunshine (hrs).

σT_a^4 is the black body radiation at mean air temperature $T_a(^{o}K)$ in mm of evaporation/day.

u_2 is the wind speed at 2 m above the ground (miles/day) .

e_d is the mean vapour pressure (mm Hg).

e_a is the saturation vapour pressure at mean air temperature (mm Hg).

The three terms in the equation represent, respectively, the incoming short wave radiation, the outgoing long wave radiation and a bulk aerodynamic term. The values of the coefficients a and b vary with geographical location. For Rothamstead, England, Penman (1948) found them to be 0.18 and 0.55 respectively. These values are taken to be representative of Southern England and have been used here.

ii) Short grass

$$E_T = \frac{\Delta / \gamma}{1 + \Delta / \gamma} \cdot R_A (1 - r) (0.18 + 0.55\ n/N)$$

$$- \frac{\Delta / \gamma}{1 + \Delta / \gamma} \cdot \sigma T_a^4 (0.56 - 0.09 \sqrt{e_d}) (0.10 + 0.90\ n/N)$$

$$+ \frac{1}{1 + \Delta / \gamma} \cdot 0.35 (1 + u_2/100) (e_a - e_d) \qquad (3.2)$$

where E_T is the evaporation from both soil and grass in mm/day, and r is .25

Equation 3.2 differs from equation 3.1 in two respects. Firstly, the reflectivity is increased, and secondly, the aerodynamic term is increased to allow for greater surface roughness.

iii) Bare soil

$$E_B = E_o \qquad (3.3)$$

where E_B is the evaporation in mm/day

The weather variables needed for the calculation of equations 3.1 to 3.3 which were measured at Naish Farm were wet and dry bulb temperatures and wind run. Readings were taken once a day at 0900 GMT. The readings of wet and dry bulb thermometers, which were installed in a Stevenson screen, were taken to be the average for that day. Wind run was measured using a three-cup anemometer set at a height of 2 m. The position of these instruments in the weather station compound is shown in figure 3.3. Daily sunshine data was obtained from Hurn Airport and assumed to be representative of Naish Farm as well. Temperature and wind run measurements were not taken on a total

of 15 days. Missing wind run data was filled in by using equal daily increments between successive readings. Missing temperature data was filled in by correlation with Hurn Airport. The data from Hurn Airport was daily values of maximum and minimum temperature and relative humidity. The average of the maximum and minimum temperatures (T_{HA}) was correlated with the dry bulb temperature at Naish Farm (T_a) to give the relationship:

$$T_a = 0.96903 \cdot T_{HA} + 1.191 \qquad (3.4)$$

For the days when wet and dry bulb temperature is available, the relative humidity ($RH_{NF} = e_d/e_a \times 100$) at Naish Farm is calculated using equations B.4 to B.8 in appendix B. These were correlated with Hurn Airport to give the relationship:

$$RH_{NF} = 0.80864 \cdot RH_{HA} + 13.705 \qquad (3.5)$$

Equations 3.4 and 3.5 were used to estimate dry bulb temperature and relative humidity at Naish Farm on days when data was missing. Using these estimates, and tables in Meteorological Office (1962), the wet bulb temperature at Naish Farm was estimated.

Appendix B gives the details of how equations 3.1 and 3.2 were solved using meteorological measurements.

3.4 Errors in Rainfall and Potential Evaporation Estimation

The climatological variables of rainfall and PE control the hydrologic water balance. Errors in these relatively large components introduce even larger percentage errors in the smaller effective rainfall component. Thus, an appreciation of these errors is necessary in the hydrologic study of the cliffs.

Errors may be of a number of different types. For the purpose of this discussion they are classified as representative, method,

or observational.

3.4.1 Errors due to Non-Representative Measurements

The measurements should be representative of the area of interest both in space and time. Not much can be done about the latter except to extend the study period long enough to be representative of random fluctuations and long term trends. This is rarely possible and certainly was not in this study. However, if sufficient data is collected and correlated with enough similar data from another weather station in the area, comparisons may be made to the average conditions and the data set extended to cover a representative period. The accuracy to which this can be done depends primarily on the lengths of available data. A more detailed discussion of the temporal variation of the data and its representativeness to other times is given later in this chapter.

Readings were not taken continuously during the study period. Rainfall and sunshine duration are daily totals; wind speed is a daily average; and temperatures are taken only once a day at a time (0900 GMT) that is assumed to approximate to the daily average. The latter can be in error, and also, averages and totals may not properly represent the effect of fluctuations.

The measurements should be representative of the area to which they apply. Variations in measurements away from the place where readings are taken (weather station) may be due to variations in shelter (or exposure), aspect, altitude or distance. The weather station should be representative of the average of these variations at all times. This may not be the case if the weather station is sited at some distance from the study area. Therefore, a local weather station was set up. Considerations taken in the siting of the weather station are given in appendix C. Measurement errors may be due to the site not properly representing either the spatial average or variation over the study area. Spatial variation is now

considered for PE and rainfall in turn.

3.4.1.1 Spatial Variation of Potential Evaporation

It was not possible to measure sunshine duration at Naish Farm. Data from Hurn Airport is used instead. There must be some error in assuming the data is representative of the study area. However, Howard and Lloyd (1979) have shown that PE estimates are relatively insensitive to errors in sunshine duration (+ 0.75 hours error gives + 0.6 per cent error in PE). Measurements of wind, temperature and humidity were made at only one location (weather station) and no attempt was made to measure the variation on the cliff top or the undercliff. Although the readings were believed to be representative of the cliff top, the same may not be true of the undercliff.

Air is more moist over sea than over land. Therefore, when winds are on-shore, there is likely to be a humidity gradient up the undercliff. Humidity will be higher (and therefore PE will tend to be less) on the undercliff than on the cliff top. Air temperature is greater in winter and less in summer over the sea than over land. Predominant on-shore winds will create a temperature gradient up the undercliff. This would tend to make PE on the undercliff less in summer and greater in winter. Overnight mist often lingers on the undercliff. PE is then decreased due to lower temperature, less sunshine, and increased humidity. Wind speed is highly variable, and is greater on the undercliff and very near the cliff edge. This is due to increased exposure and the degree of variation depends upon the general wind direction and magnitude. However, in general, wind speeds are greater on the undercliff than on the cliff top. Increased wind speeds increase the PE estimate.

It would be very difficult to measure the net effect of these factors, especially over an extended period. Whilst recognising the possibility of a spatial variation in PE between the undercliff and cliff top, the two are assumed in this analysis to be equal and represented by the cliff top weather station.

3.4.1.2 Spatial Variation of Rainfall

A study of the spatial variation of rainfall is difficult due to the high risk of vandalism. The risk is least on the undercliff in winter. Limited readings were taken at various positions (see figure 3.2) and results are shown in table 3.1. The considerable differences are in part due to the aerodynamic effect of the gauges not being at ground level (see section 3.4.2.1.4). However, the differences are too great for this to be the sole reason. A much more significant reason is the effect that the undercliff topography has on altering wind, and thus, rainfall distribution. The gauge R5 was considerably affected by the close proximity of the cliff face, which afforded it a large degree of shelter. Similarly, gauge R3 is protected by the D scarp. However, readings for this gauge are complicated by sea spray during stormy weather (note in particular the period 26th January to 1st February, 1983). Other gauges are not considered to have been significantly affected by sea spray. Gauges R4 and R6 were sited in the middle of the undercliff and were not so affected by nearby scarps or sea spray. However, the readings are still reduced and it is difficult to assess whether this is solely due to the gauge being above ground level.

With so few gauges in a very rough topography it is difficult to draw any reliable conclusions from these results. However, a theoretical study has been made by Poreh and Mechrez (1984) of the effect of wind and small scale topography on rainfall. They termed rainfall as hydrological point rainfall per unit projected area (see figure 3.4 for definition), HPR, and relative rainfall intensity, I as HPR/R_{REF}, where R_{REF} is the rainfall in the absence of any topographic disturbance. For on-shore winds and rainfall consisting of large drops, I is increased (decreased for off-shore winds) on the undercliff and is equal to unity on the cliff top. For small drops I is unity for both undercliff and cliff top. The difference between rainfall on the undercliff and cliff top depends upon the rain drop size, and wind direction and magnitude. The net effect is unknown but with rainfall

predominantly due to south westerly winds, the rainfall might be expected to be slightly greater on the undercliff than on the cliff top. However, this theory does not predict the aerodynamic effect of standard rain gauges. This could be due to the assumptions made in the theory. Robinson and Rodda (1969) using a wind tunnel found that the leading edge of a gauge sets up a surface of separation which curves backwards and over the gauge. Above the surface wind speeds are increased by as much as 30 per cent, whereas below it a turbulent zone is set up and the wind speed is decreased. The increased wind speed carries some of the rain past the gauge orifice to be deposited downwind of the gauge. The sharpness of the gauge rim was also found to have an effect. It is contended here that the sharp changes in topography act in a similar way so that small scale rainfall distribution on the undercliff is highly variable. This aerodynamic effect is also noticeable on the cliff top where the cliff edge appears to act as the leading edge of a surface of separation. Thus, the rainfall near the cliff edge will be less than that further away from it.

The above discussion shows that there is likely to be a spatial variation of rainfall due to the presence of the undercliff. The amount of variation will vary from storm to storm. To account for this variation, several rainfall measurements should be made on both the undercliff and the cliff top. However, the above results and discussion show that it is difficult to be representative with such measurements on the undercliff; also the scope for measurements on either the undercliff, or the cliff top, is severely limited by the risk of vandalism. In the absence of any other information, this study assumes that the rainfall at the cliff top weather station applies uniformly over the study area. The above discussion shows that errors may ensue from this assumption.

3.4.2 Errors due to Method of Measurement

Rainfall is estimated using a standard rain gauge and PE is

estimated using the empirical Penman equation. Both estimates are subject to errors due to their method of measurement.

3.4.2.1. Rainfall

Errors in rain gauge measurement are due to adhesion, condensation, evaporation, splashing, and the aerodynamic effect. Rain gauges are designed to limit these errors. However, small errors do still occur.

3.4.2.1.1 Adhesion

Adhesion is that part of the rainfall that adheres to the inner parts of the rain gauge before entering the measuring cylinder. After rainfall stops, the adhesion evaporates and therefore creates a negative bias. The magnitude of the error is dependent on season and frequency of wetting. Rasmussen and Halgreen (1978) found the average annual error to be 2 per cent with a summer maximum of 5 per cent. Allerup and Madsen (1980) found the error to vary from 2.5 to 5.8 per cent with an annual average of 4 per cent. Both these studies were made in Denmark. The error will also depend upon the type of surface of the gauge. At Naish Farm gauges R1 (copper) and R8 (galvanised iron) differ only in material. R8 caught 2.5 per cent less than R1 from 18th April to 17th October 1984. If spatial variation of rainfall is ignored (which seems reasonable considering the close proximity of the gauges to one another) this difference must be due to the difference in adhesion.

3.4.2.1.2 Evaporation and Condensation

Evaporation from the collecting container is negligible even under strong drying conditions (Rasmussen and Halgreen, 1978). Condensation errors occur when more dew collects in the rain gauge

than on the ground below. Rasmussen and Halgreen (1978) and Allerup and Madsen (1980) found these errors to be negligible.

3.4.2.1.3 Splashing

Rain gauge design eliminates splashing out errors; and setting the rim 0.305 m above ground level eliminates splashing in errors. The rain gauge set at ground level is in a pit 0.305 m deep. However, splashing on bare ground is greater than on grass. Therefore, partly to eliminate splashing in errors a grid was put in the pit as previously described.

3.4.2.1.4 Aerodynamic Effect

Rain gauges set above ground level are exposed to the wind. Robinson and Rodda (1969) found that wind speeds increase over the rain gauge opening. This carries some rain drops past the gauge so that rainfall is underestimated. This error is called the aerodynamic effect. The magnitude of the error depends on rain drop size and wind speed during rainfall. This will vary from site to site. However, for a site at Wallingford, England, Rodda (1967a) found that over a five year period the error was 6.6 per cent and varied seasonally between 4 and 9 per cent. Robinson and Rodda (1969) found that the wind speed at 1 foot (0.305m) above ground level is considerably reduced inside a turf wall surround. A turf wall is commonly used for exposed sites. The wind speed under the grid of a ground level gauge was reduced still further to a negligible amount, so that the aerodynamic effect can be considered eliminated. At Naish Farm,the ground level gauge R7 (galvanised iron) was found to catch 1.5 per cent more than the standard rain gauge R1 (copper) for the period 18th April to 17th October, 1984. Allowing for the difference in adhesion, the aerodynamic effect results in a 4 per cent underestimate.

Rasmussen and Halgreen (1978) analysed the differences in weekly readings for rain gauges at ground level and 1.5 m above

ground level. They found their readings to be represented by the relationship:

$$\sqrt{R_o} = \sqrt{R_{1.5}} + \varepsilon \qquad (3.6)$$

where R is weekly rainfall, the suffix denoting the height of the gauge, and ε is normally distributed with constant mean and variance independent of rainfall total. Allerup and Madsen (1980) analysed daily readings greater than 1 mm and found the relationship:

$$\frac{R_0}{R_{1.5}} = \exp (\alpha \ln I_{1.5} + \beta V \ln I_{1.5} + \gamma V + \delta) \qquad (3.7)$$

where α , β , γ , δ are regression parameters; V is wind speed at 10 m above ground level; I is average rainfall intensity during rainfall; and R is daily rainfall, the suffix denoting the gauge height. The purpose of such relationships is to convert the standard gauge rainfall to that at ground level so as to eliminate bias errors due to the aerodynamic effect. Whilst the value of this type of analysis is recognised no such relationship has been developed at Naish Farm due to the limited amount of ground level rainfall data. This study uses uncorrected rainfall data for gauge R1. However, in a consideration of errors the aerodynamic effect is represented by a constant percentage of measured rainfall.

3.4.2.2 Potential Evaporation

The errors due to the method of estimating PE lie in the choice of equation, its parameters, the measurements used to solve the equation, and the period over which the estimate is made.

There are a number of equations based on weather variables, each one of which will give a different estimate of PE. For example, Smith (1964) found that the average annual value of PE for grass for a 26 year period, calculated by the Penman (1948)

method, was only 68 per cent of the Thornthwaite (1948) method. The difference varied seasonally, being least in spring and greatest in autumn. It is probable that variations would also occur at Naish Farm, although no such analysis has been made.

The Penman formula itself has undergone a number of variations. The wind function in the bulk aerodynamic term in particular has been a source of confusion (Stigter, 1980). The formula as given in Penman (1963) does not account for altitude. Although this is not significant at Naish Farm, as it is only at 35 m O.D., altitude has been accounted for as given by Chidley and Pike (1970).

For open water the wind function given in Penman (1948) was revised in Penman (1963). Stigter (1980) reports that this revision is "good enough to be preferred over any attempt for more adaptations".

For short grass Penman (1948) uses a seasonally dependent correction factor to convert from the PE for open water. Equation 3.2 from Penman (1963) used the same wind function as Penman (1948) for open water. Stigter (1980) reports that there have been more recent revisions of the wind function and suggests that these may be better, although Penman (1963) is used in this study. Shaw (1983) reports that MAFF (1967) used different coefficients for the outgoing long wave radiation term. The suggested values of a and b were also different. Shaw (1983) also reports a different version of equation 3.2 where the outgoing long wave radiation term is multiplied by 0.95 to allow for the fact that vegetation does not radiate as a perfect black body.

The Penman equation has not been adapted for bare soil. Instead, estimations have been made based on open water evaporation and using correction factors. Penman (1948) suggests that PE for bare soil is 90 per cent that of open water. Later, Penman (1963) said that they were of the same order (i.e. PE for bare soil equals PE for open water) when evaporation conditions are not excessive (which may not be the case in summer).

Needless to say these variations can be significant. Table 3.2 summarises the differences in calculated values of PE due to these variations.

Whichever form of the equation is used, a number of parameters have to be estimated, the values of which will vary with season and latitude. The parameters a and b relate the solar radiation arriving at the earth's outer atmosphere, to the incoming short wave radiation before reflection at the earth's surface. Chidley and Pike (1970) give a wide range of values for various locations around the world. MAFF (1967) accounts for latitude. However, apart from recognising the fact, no account seems to be made of seasonal variation. Howard and Lloyd (1979) found "substantial errors" in the calculated value of PE arising from errors in these parameters. They also found that errors in the assumed value of albedo cause significant errors in calculated PE. The use of a constant value of albedo will cause seasonal errors. For bare soil the errors are even worse, as the albedo also varies with soil type and wetness (Thompson et al, 1981). For example, PE for bare soil is overestimated when the soil is not saturated.

Smith (1964) found that the coefficient of variation of the annual estimate of PE was about half that for tank measurements. This is because the use of regression equations in the formula result in a weighting of the estimates towards the mean (Penman, 1948). Concentrating on the wind function, Penman (1948) says

> "it is doubtful whether a measurement [of wind velocity] at a single height and the assumption of zero velocity at ground level are sufficient to define the wind velocity profile even over a smooth surface, they cannot be expected to take account of the local turbulence introduced by many obstructions and surface irregularities. These will vary with wind direction....."

Instruments can be used to measure radiation directly. If the incoming short wave radiation is measured, the need for the regression

parameters a and b is eliminated. If net radiation is measured, the need for the regression parameters in the first two terms of equations 3.1 and 3.2 is eliminated.

The Penman formula does not take into account the heat capacity effect of the ground (i.e. no allowance is made of previous weather conditions). Thus, Smith (1964) found seasonal over (summer) and under (winter) estimates.

Temperature readings are only taken once a day, the value of which is assumed to approximate the average. This will cause considerable error to daily estimates of PE. However, if the readings are averaged over several days the error is reduced. Thus, daily estimates of PE are generally not recommended. Instead, daily average values of the measured meteorological variables are averaged over several days and the average PE estimated for this longer period. Penman (1948) suggests periods of a month or more if the radiation is not directly measurable (i.e. sunshine duration data is used). However, shorter periods are commonly used. Howard and Lloyd (1979) say

> "a number of assumptions made in the Penman equations may become invalid over periods less than five days but.... the method may still be considered to provide adequate daily potential evaporation estimates if the sum of 30 one-day estimates is in good agreement with a single thirty-day estimate over the same period".

This obviously depends upon the use of the computed shorter period values. This study uses seven-day estimates. Table 3.2 compares seven-day estimates totalled monthly with monthly estimates for the period of observation.

3.4.3 Observational Errors in Rainfall and Potential Evaporation Estimates

The rainfall totals in the gauges were measured weekly with a standard measuring cylinder calibrated in .1 mm intervals up to

10 mm. A reading was taken from the bottom of the meniscus. Some errors may occur due to the inability to place the cylinder on a flat surface, and due to dirt, etc. obscuring the meniscus. Thus, errors may be greater than the expected $\pm$ .1 mm (assuming the cylinder is only filled once). As a result, the error will be at least $\pm$ 1 per cent. Errors in reading the continuous rain gauge chart are variable depending on rainfall amount and whether the storm goes through 0900 GMT. Normally, they are not significant ($\pm$ .2 mm) and cancel out over the week.

The temperatures are read to $\pm$ .25°C. This introduces a significant error for daily estimations of PE. However, random errors cancel out when readings are averaged over several days. Good wet bulb temperature readings are dependent upon the wick being kept clean and moist. If not, readings will be over-estimated, thus introducing a bias to the readings. Errors in wet bulb readings are the most significant of the measured variables (Howard and Lloyd, 1979). Wind run is measured to $\pm$ .1 km/day and sunshine duration is given to $\pm$.1 hrs/day. Table 3.3 analyses the induced error in PE as a result of bias readings.

3.4.4 Summary of Possible Errors

The data period at Naish Farm is too small to be representative of a longer period of time. Therefore, errors will occur when making conclusions about other times based on the results of the data period. These errors can be reduced by comparing data with other longer period sites. Both rainfall and PE are spatially variable over the study area. It has not been possible to enumerate this variation. As a result, there may be some error in assuming a spatially constant value of rainfall and PE as derived from the local weather station.

The rainfall measurement itself is subject to a number of errors. The observational error is a relatively small (less than 1 per cent) random error varying from week to week. More serious bias

errors result from adhesion and the aerodynamic effect. The former is least in winter when the readings are of most interest, whereas the latter is least in summer. One should be wary of putting figures to such errors from the available data. However, it is considered that rainfall is underestimated by, at most, 10 per cent.

It is not possible to enumerate the absolute error in PE by using the Penman (1963) method. However, relative errors can be derived by comparing the results with other methods and assuming the absolute error to be of the same magnitude. These errors are large and show a seasonal variation. The effect of arbitrarily large bias errors will be considered in later analysis. Observational errors are most serious with wet bulb temperature especially as only one reading is taken per day. The Penman formula does not model evaporation very successfully for short periods, such that individual seven-day estimates may be somewhat in error.

Errors in both rainfall and PE may be quite large. Later analysis will include a consideration of errors as a result of using these input variables.

3.5 Data Homogeneity

The rainfall and PE data record at Naish Farm will be inconsistent (or non-homogeneous) if the observations are affected by a change in exposure due to either chalets being moved or cliff recession. Neither is thought to have been significant during the study period. However, the possibility of inconsistency has been investigated. The data record is too short to use the split record statistical tests of mean and variance as used by Sharma (1985). Instead double-mass analysis is used.

> "Double-mass analysis tests the consistency of the record at a station by comparing its accumulated annual or seasonal

> precipitation with the concurrent accumulated values of mean precipitation for a group of surrounding stations". (Linsley et al, 1975).

Double-mass analysis may also be used for PE data. The data record for Naish Farm is too short to use accumulated annual values. Instead monthly values are used. Figures 3.5 and 3.6 show the double-mass curves for the Naish Farm data. PE and, from June 1984, rainfall data are only available from Hurn Airport. In figure 3.5, the curve using the regional mean of rainfall for the independent axis shows no apparent inconsistency, whereas the curve using Hurn Airport rainfall shows a possible break in consistency. The changes are small, and may not be significant. An objective analysis of significance is therefore necessary.

Singh (1968) put double-mass analysis on the computer by comparing the fit of a single straight line to that of a fourth degree polynomial. The criteria used is arbitrary and, because the use of monthly data causes seasonal changes of the slope,it was decided that the method was not appropriate. Instead of using Singh's analysis, it was decided to use the statistical tests given in Buishand (1982). Appendix D describes the tests and gives the results. Only one test statistic for PE and none for rainfall is significant at the 95 per cent level. The results for rainfall show a considerable improvement when four stations are used instead of one. It is probable that the test statistics for PE would also improve if more than one weather station were used. Also, the test assumptions are to some extent violated due to seasonal variation in the mean of the Y_i's (Y_i = difference between the value at Naish Farm and the mean of the surrounding stations for month i). This is especially true for PE, as at Naish Farm it is greater in autumn and winter, and less in spring and summer, than it is at Hurn Airport. It is therefore concluded that the test results are not, as a whole, significant. Added to this, no large slumps or movement of chalets/caravans occurred in the area during the study period. It is assumed that the rainfall and PE at Naish Farm are homogeneous.

3.6 Comparison of the Study Period with Historic Data

Monthly and annual meteorological data from a long period station (Hurn Airport) was analysed in order to find out how the study period compared with historic data. It is assumed that the deviation from the norm is similar at Naish Farm. The period used was 1952 to 1984 for rainfall and 1954 to 1984 for PE.

A number of studies, e.g. Ashmore (1944) for Wrexham data, and Rodda and Sheckley (1978) for England and Wales data, have shown the presence of trends in annual and seasonal rainfall. The same may be true for PE. Various tests (for details see, for example, Kottegoda, 1980, pp 31-34) for trend, viz. turning point test, Kendall's rank correlation test, and linear regression, were carried out on annual and monthly data. It was concluded that no significant trend exists in any of the data. Rodda and Sheckley (1978) also found a weak 10 year periodicity. A study of the serial correlation coefficients shows no apparent periodicity or persistence.

A study of the frequency distribution of meteorological data will show how significantly different from the norm the study period has been. In the UK, the normal distribution is usually fitted to annual data and the log-normal distribution to monthly data (Shaw, 1983). For normality, the skew of the data should be approximately zero. The longer the duration of totals, the smaller is the skew of the data. Ashmore (1944) found that skew was absent from three year totals. Both normal and 3-parameter log-normal distributions were fitted to the data and the results are shown in table 3.4. The negative values of the location parameter for the log-normal distribution of PE indicates a net condensation. Although the Penman formula is able to give a negative result, the Meteorological Office represent this as a zero value of PE. Table 3.4 shows that in most cases the normal distribution seems to be adequate, and that little extra fit is achieved by using the log-normal distribution. For PE the normal distribution does not fit February, March, or annual data. The log-normal distribution gives an adequately improved fit to

February and annual data, but not for March. It is somewhat surprising that the normal distribution fits monthly, but not annual data. This is the reverse of what was expected. For rainfall, the normal distribution fits all data except June for which the log-normal distribution gives an adequate fit. Table 3.5 shows the probability of non-exceedance for each month during the study period. This assumed the normal distribution for all data, except February and annual PE, and June rainfall, for which the log-normal distribution was used. The main study period is from October 1982 to October 1984. Data prior to this period has been included in the table, as it is relevant to a parallel study (Barton and Coles, 1984) which started a year earlier. The table, and the comments below, compare individual months with historic data of the same month. A comparison of different months of the year is given in a later section.

The annual PE has been high and has increased between 1981 and 1984. For individual months, the difference between a high and a low PE is not as significant as it is for rainfall, due to the much smaller standard deviations (see table 3.4). To some extent, high/low PE's are associated with low/high rainfall (e.g. see April to August 1983). Annual rainfall has varied : 1981 was a wet year; 1982 was a very wet year; 1983 was a dry year; 1984 was average. For the year starting on 1st October, 1982/3 was a wet year and 1983/4 was a dry year. The summer of 1982 was wet; the dry summer of 1983 continued through the autumn to November; the summer of 1984 was as dry as 1983 but started and finished a month earlier. The wet months of the 1982/3 winter were October to December; for the 1983/4 winter they were December and January; and for 1984/5 winter they were November and December. The spring of 1983 (April to June) was continuously wet, whereas in 1984 the spring had two distinct wet months (March and May). 1981 was characterised by the very wet months of March, May and September. The winter of 1981/2 had three distinct wet periods, viz. September/October, December, and March.

The hydrologic significance of a wet month as described above should be considered with care. The expectation of rainfall varies throughout the year; the interaction with PE varies seasonally; the significance will be dependent on previous rainfall. An attempt to show how hydrologically significant the probabilities in table 3.5 are is given in the next section. The seasonal terms, e.g. winter, in the above discussion are used loosely as distinct from the exact definitions used in appendix E.

3.7 Comparison of the Hydrologic Significance of Individual Months of the Year

Broadly speaking, winter months are more significant than summer months due to the seasonal variation of PE, assuming rainfall to be approximately uniformly distributed throughout the year. A more detailed consideration for the region using Hurn Airport data is given below. The figures have not been adjusted for differences in the number of days in the month. Slight, but not significant (to the discussion), differences would occur if the data were so adjusted. The term hydrologic significance refers to the likely occurrence of mass movement due to the frequency distribution of weather for that particular month.

Table 3.4 shows the variation of the monthly mean and standard deviation for both rainfall and PE. The mean of PE is approximately sinusoidal with the maximum in summer (103.5 mm) and minimum in winter (4.8 mm). The monthly mean rainfall is variable but can be divided into two groups: February to August which has low rainfall (43.2 to 62.2 mm); and September to January which has high rainfall (77.9 to 91.7 mm). The standard deviation of PE is small, and fairly constant for the winter period of September to March (3.1 to 4.9 mm), whereas in the summer it rises to a maximum of 13.6 mm. The standard deviation of rainfall is much higher than that for PE. It is at its lowest and most constant during March to August (28 to 33.3 mm). It is higher during

September to February, when it rises rapidly to a maximum in October, after which it gradually reduces in value.

The mean value of PE is greater than the mean value of rainfall for the period April to August. If effective rainfall is defined as rainfall minus PE, then the hydrologically effective period is September to March. The greatest effective rainfall is December (86.9 mm) followed by November (78.5 mm), January (78.3 mm), October (61 mm), February (42.3 mm), March (28 mm) and September (26.9 mm). If other than mean conditions are considered, then an allowance needs to be made for the standard deviation. For example, if an arbitrary monthly rainfall amount is taken as being hydrologically significant, what is the probability of it being, or not being, exceeded? Table 3.6 shows the probability of non-exceedance for two different rainfall amounts (100 and 125 mm). The relative significance between months varies only slightly between these rainfall amounts (e.g. October is most significant for 125 mm and December the most significant for 100 mm rainfall). However, the most likely period for significant rainfall is September to January. To consider the effectiveness of each month in terms of effective rainfall, an allowance needs to be made for PE. To simplify analysis, the mean PE for each month is used. This is reasonable as the standard deviation is small, especially in the most relevant winter period. Table 3.6 shows the probability of not exceeding 100mm effective rainfall for each month. The most significant period is October to January with December being the most significant month. Comparison of tables 3.5 and 3.6 identifies those months with more than 100 mm of effective rainfall (assuming PE to be the mean and not the true value) as December in the 1981/2 winter; October and November in the 1982/3 winter; December and January in the 1983/4 winter; November in the 1984/5 winter; and December 1985 (data for 1985, although used here, has not been included in the tables).

The hydrological significance of any month also depends upon the significance of previous months, i.e. upon the likely existing

groundwater conditions. It is not possible to quantify this effect here, except to say that later winter months (e.g. January and February) are likely to be more significant, and earlier winter months (e.g. October and November) less significant, than table 3.6 suggests.

3.8 Comparison of the Weather at Naish Farm and other Weather Stations in the Region

The previous discussion has relied upon data from Hurn Airport. However, the temporal distributions of rainfall and PE at Naish Farm will not be exactly the same as that at Hurn Airport. The differences are assumed not great enough to affect the previous discussion applying to Naish Farm. However, some comparison of data for the region has been made. There is insufficient data to estimate the regional variation of standard deviations of the data. Therefore, no estimates of standard deviations at Naish Farm are possible. Data is available to make a regional comparison of the annual and monthly means. A rough estimation of the annual and monthly means at Naish Farm has been made based on the Meteorological Office (1963) method of estimating the average annual rainfall as described by Shaw (1983, pp 189-191). The method is also applicable for monthly averages. The method used is:

i) An index map of the area was drawn showing stations where an average rainfall is available. These averages are based on the standard period 1941-1970.

ii) A second map was drawn on tracing paper showing the stations in i and also the Naish Farm weather station. This map is layed over the map in i.

iii) For each month/year that there is data for Naish Farm, the data from the stations in i are expressed as percentages of their respective average values. Isopercental lines are then drawn on the tracing paper.

iv) The percentage, p, for Naish Farm is interpolated and the average value, R, estimated from

$$R = \frac{100\ r}{p}$$, where r is the value at Naish Farm in mm.

With several years of data there are several estimates of R, and the mean gives the estimate of the average value for the standard period. However, for the data at Naish Farm only one or two estimates of each average was possible. Therefore, the error is likely to be large. Although it is not possible to estimate the size of this error, it is considered to be unacceptably large in some cases. This was due to either low rainfall, or the predominance of convective rainfall (thunderstorms). When rainfall is low, small spatial variations of the amount will cause large changes in the position (and value) of the isopercentals, and therefore the estimated percentages for Naish Farm. Also, because of the low values of p, small variations in rainfall amount at Naish Farm will cause large changes in the estimated average value. The rainfall for June 1983 was due mainly to two separate days of convective rainfall. These weather phenomena are very localised such that the spacing of the stations in i is too great to draw reliable isopercentals. Because of these reasons, this method could not be used to estimate the averages for June, July, and August. Instead the following procedure was used.

i) Monthly averages for the period September to May were estimated using the previous method.

ii) The averages in i were summed to give the nine month average for Naish Farm (NINEMNF).

iii) For other stations in the region, where the data is available, the monthly averages were summed to give the average rainfall for the period September to May ($NINEMR_j$ where j denotes the station).

iv) For each of the stations in iii the ratio, $a_j = \frac{MONTHR_j}{NINEMR}$ was calculated where $MONTHR_j$ is the average monthly rainfall for June, July, or August for station j

v) Using the maps of the previous method, lines of equal values of the ratio, a, were drawn, and the value for Naish Farm interpolated (a_{NF}).

vi) The average monthly rainfall was calculated by multiplying together the results of ii and v:

$$MONTHNF = a_{NF} \cdot NINEMNF$$

Rainfall averages have been calculated for Naish Farm using five other weather stations in the region (see figure 3.1 for their location) Table 3.7 gives the rainfall averages based on two different periods. For the standard period (1941-70), the averages were obtained from the Meteorological Office, except for Naish Farm which were calculated by the above methods. For the period 1952-84 the Hurn Airport averages are obtained from table 3.4, and the Naish Farm averages by the formula:

$$NF_2 = NF_1 \cdot \frac{HA_2}{HA_1} \qquad (3.8)$$

where NF and HA are the averages for Naish Farm and Hurn Airport respectively; and the suffixes 1 and 2 refer to the periods 1941-70 and 1952-84 respectively.

Examination of the monthly averages for Hurn Airport shows some variations between the two periods. However, variations for adjacent months cancel one another, so that the discussion of the previous sections is basically unaffected. The pattern of monthly averages for Naish Farm is similar to Hurn Airport. However, for months October to December the rainfall is

considerably less (by greater than 10 mm); for months January, February, and April the rainfall is moderately less (by 5 to 10 mm);and for months March, and May to September the rainfall is about the same (the difference is less than 5 mm). These seasonal differences are probably due to the seasonal variability of weather types, which are affected differently by the proximity to the coast. However, the pattern is still the same such that it is reasonable to apply the comments regarding the last section (using Hurn Airport data) to Naish Farm. In fact, all the other stations in the region show the same pattern of seasonal variation of rainfall averages as Hurn Airport. There are two estimates of average annual rainfall for the study period at Naish Farm in table 3.7. There is a considerable difference between the two estimates, which reflects the large possible errors in the method when so little data is available. One value is the sum of monthly estimates, and the other is the Meteorological Office (1963) method using annual data. The latter method uses only one estimate and could, therefore, be considerably in error. Also, comparison with other regional values suggests that the higher value (the sum of monthly estimates) is more reasonable. The average annual rainfalls for the different stations in figure 3.1 shows that there is a spatial variation in rainfall. The rainfall is greater to the North and away from the coast. Thus, the low value of average annual rainfall at Naish Farm could be due to its closeness to the sea. Figure 3.1 also shows annual rainfall figures for 1983 at a number of other stations. The rainfall was greatest to the North and West in the region. The figures show that rainfall decreased rapidly towards the coast, as indicated by the difference in the rainfalls at Highcliffe and New Milton with that at Naish Farm. This shows clearly the need to measure rainfall at Naish Farm.

Average values of PE in the region are only available for Hurn Airport for the period 1954-84. The percentage, p, for Naish Farm for any month is taken to be equal to that at Hurn Airport. The average values for Naish Farm are shown in table 3.7. The

average annual PE at Naish Farm is slightly less than that at Hurn Airport. This difference is not spread evenly through the year. In the Autumn (September to November) PE is greater at Naish Farm, and in the Winter (December to February) it is about the same for both stations, whereas in the Spring and Summer the the PE is greater at Hurn Airport. This could be due to the temperature measurements being read four times a day at Hurn Airport, but only once a day at Naish Farm. The accuracy of representing the daily average by a single measurement may vary with season. This will lead to a seasonally varying bias error. Alternatively, the seasonal difference in PE could be due to coastal effects, similar to that discussed in the section on measurement errors. In the next section it is this second cause that is assumed to be the case.

3.9 Extension and Modelling of Rainfall and Potential Evaporation at Naish Farm

The data collected at Naish Farm is of only a limited duration. More meaningful interpretation of the effect of meteorological conditions could be inferred if the data were extended or modelled. Data extension is the prediction of historic data, whereas modelling is the generation of new data. Extension and modelling differ in that the latter relies upon random probability to generate data, whereas the former relies upon existing data from other weather stations. The generation of new data is not limited, whereas the extension of data is limited, by the amount of data from the other weather stations. However, extended data can be used to predict the actual groundwater conditions at a given time. Modelled data can be used to estimate the probabilities of occurrence of relevant groundwater conditions (once the relationship between the weather and groundwater conditions has been established). This section discusses the extension and modelling of Naish Farm data. The data at Naish Farm is extended to cover the period August 1980 to December 1985. The generation of modelled data is suggested as a topic for further research.

3.9.1 Modelling of Meteorological Data

Rainfall and PE are modelled using frequency distributions fitted to the observed data. Srikanthan and McMahon (1983) present several models of PE, some of which generate values independently, and the others dependently, of rainfall. In section 3.6 it was noted that there appears to be some correlation between monthly PE and rainfall. Although no analysis has been made, the correlation is not thought to be strong, and therefore, the error in not allowing for it is not considered to be great. Consequently, rainfall and PE are assumed to be independent.

The frequency distributions of both monthly and annual data for Hurn Airport was discussed in section 3.6. The distribution parameters are shown in table 3.4. There is insufficient data to do a similar analysis for Naish Farm. However, the means were estimated in section 3.8. The standard deviation and skewness cannot be estimated from the data. The skewness and coefficient of variation (ratio of standard deviation over mean) are assumed to be the same as for Hurn Airport. The latter is the same as assuming a normal distribution and an equal percentage of the averages at the two sites (as for Meteorological Office, 1963, but with no spatial variation of the percentage). The type of frequency distribution is assumed to be the same for the two locations. Using these assumptions, it is possible to estimate the distribution parameters for Naish Farm. If the data is assumed not to be serially correlated, values may be generated by the equation:

$$Y = \mu_Y + \sigma_Y \cdot Z \qquad (3.9)$$

where μ_Y and σ_Y are respectively the mean and standard deviation of the variable Y; and Z is a normal deviate with zero mean and unit variance. This is called a white noise model. A more sophisticated model incorporating serial and cross correlation, and skewness in the random component, Z, is not warranted due to the lack of data on which it is based.

Such a model for PE is described in Srikanthan and McMahon (1983) although it could equally be applied to rainfall generation. Let the variable X denote rainfall/PE. Depending on whether the data is described by a normal or log-normal distribution, the value of X is related to Y by one of the following relationships:

$$X = Y \quad \text{for a normal distribution} \tag{3.10}$$

$$X = \exp(Y) + \alpha \quad \text{for a log-normal distribution} \tag{3.11}$$

where α is a location parameter.

The modelling of daily PE values has been done by Srikanthan and McMahon (1983) using pan evaporation data. However, the Penman formula is inappropriate for obtaining daily values of PE (see section 3.4.2.2). Therefore, it is not possible to model daily PE. Modelling daily PE is not as important as daily rainfall. Rainfall is larger and more variable. Because groundwater conditions can vary greatly over periods of only a few days, it is important to know the variation of daily rainfall. Therefore, daily rainfall totals need to be modelled, whereas the modelling of monthly (and 7-day) PE values should be sufficient. Due to the slower response of groundwater, as compared to surface water, the modelling of daily rainfall here does not need to be quite so sophisticated as for surface water. However, the slower response does mean that the monthly rainfall distribution is important. A problem of modelling daily rainfall, is that aggregation to produce monthly rainfall totals, does not preserve the statistics of the actual monthly rainfall. Therefore, monthly values should be generated as previously described, and the daily rainfall model used to apportion the daily values. The modelling of daily rainfall is discussed in appendix E.

Rainfall values are generated using a random number between 0 and and 1 from a uniform distribution (Kottegoda, 1980, pp 98-102). This number is then used as a probability of non-exceedance with the fitted frequency distribution to generate a rainfall value.

For large random numbers it is better to use an alternative procedure to generate rainfall (see appendix E). The generated daily rainfall amounts have to be adjusted to give the same aggregated monthly totals as generated by the monthly rainfall model. This is done month by month, for example, by a constant proportional increase or decrease for all wet days. Alternatively, the rainfall values could each be reduced, or increased by an equal probability of non-exceedance.

The Naish Farm data is too short to both accurately estimate the necessary model parameters and to be temporally representative. Because the Hurn Airport data is much longer, Naish Farm data could be modelled by first generating data for Hurn Airport, and then converting this to Naish Farm data by using a suitable relationship. The use of a relationship is the same as data extension which is described next.

3.9.2 Extension of Meteorological Data

This is the prediction of data for Naish Farm using historical data from other nearby weather stations. Suitable historical data has been obtained for Hurn Airport. This can be correlated with Naish Farm using two approaches. The first is a regression analysis. Figures 3.7, 3.8 and 3.9 show linear regression of monthly rainfall and PE and daily rainfall. All the relationships are influenced by the spatial variations of the isopercentals of the data with respect to the long term average. Relative to the long term average, Hurn Airport (101.2/100.2 per cent) has been wetter than Naish Farm (96.4/96.6 per cent) for the regression period (daily/monthly). This will be reflected by the relationships in figures 3.8 and 3.9. The slope for daily rainfall is flatter, as the difference in relative wetness of the regression periods (daily regression period is 23rd September 1982 to 9th October 1984; monthly regression period is October 1982 to October 1984), is greater for daily than for monthly rainfall.

The slope of the long term average relationships will be steeper, and equal to .923, the ratio of the average annual rainfalls at Naish Farm and Hurn Airport (taking the intercept as zero). The variability in the pattern of areal rainfall is greater for daily than it is for monthly totals. This is reflected by the increased scatter. Hendrick and Comer (1970) found that inter-station correlation (scatter) also depended upon inter-station distance and azimuth, daily rainfall amount, and the season of the year. The latter two are due to variations in weather type. Thus, scatter could be reduced by analysing the data seasonally, and by using several weather stations to obtain an areal average. However, there is insufficient data to analyse seasonally, and with several weather stations data extension is limited by the station with the shortest data length.

The second correlation approach is to equate probabilities of non-exceedance for Naish Farm and Hurn Airport. A given value at Hurn Airport will have a probability of non-exceedance which may be calculated from the fitted distributions already described (normal or lognormal for monthly values, and Johnson S_B for daily rainfall). If the same probability of non-exceedance is assumed for Naish Farm, then the value can be calculated from its fitted frequency distribution. For daily rainfall, this results in seasonal correlation curves as depicted in figure 3.10. The curves have upper and lower limits. The curves are very sensitive to the upper limit, which can vary quite considerably and still achieve an adequate value of the goodness-of-fit criterion for the frequency distributions. In the absence of any alternative information on the difference in extreme values for the two sites, the upper limit was set equal for both sites for each season. However, this still caused the relationship to curve markedly for Autumn and Winter. A straighter relationship was achieved by adjusting the upper limits to the values given in appendix E and shown by figure 3.10. The curves are based on frequency distributions fitted to the same two year period 23rd September 1982 to 9th October 1984 for both Naish Farm and Hurn Airport.

As the first approach is based on a period when Hurn Airport was wetter (relative to the average) than Naish Farm, its use for data extension will, on average, under-predict rainfall for Naish Farm. On the other hand, for monthly values, the second approach will be more representative of the long term average, and will also allow for seasonal variations. Using the monthly averages in table 3.7, the slopes of the long term average seasonal linear relationship are calculated as .951, .963, .902, .898 for Spring, Summer, Autumn, and Winter respectively. The average slopes for the curves of figure 3.10 are 1, 1, .941, .88 for the same respective seasons. This shows that the use of figure 3.10 will more closely reflect the long term average rainfall than does figure 3.9, and is therefore preferred for extending data. The daily values should be adjusted, so that the aggregated monthly value, is equal to the value obtained using a monthly rainfall relationship. An alternative third approach to estimating daily rainfall from the monthly prediction is to multiply each day's amount at Hurn Airport by the ratio of the monthly totals for Naish Farm and Hurn Airport.

None of these approaches includes scatter due to the irregularities in the areal rainfall pattern. This is a serious limitation if the precise "true" value is required for any given time. In this case, more weather stations are required, although this will reduce the maximum possible length of extended data. However, if the precise "true" value is not necessary, or the relationships are being used with modelled Hurn Airport data, then the irregularities in the areal rainfall pattern can be ignored (assuming the irregularities are random). This is only the case because the study area is small so that the areal rainfall pattern in the region can be neglected.

3.9.3 Extension of the Data Record for Naish Farm

The meteorological data record for Naish Farm has been extended to cover the period August 1980 to December 1985. Monthly values were derived from those at Hurn Airport by using the equal

probabilities of non-exceedance approach outlined in section 3.9.2. The distribution parameters were those calculated for the period 1952-1984 for rainfall and 1954 - 1984 for PE.

Daily rainfall outside the period 23rd September 1982 to 9th October 1984 can be calculated by any of the approaches described in section 3.9.2, and the values adjusted so that the monthly aggregated total equals the monthly rainfall derived in the previous paragraph. The adjustment allows a seasonal variation in the relationship between the two sites. Figure 3.10 allows for the differences in the distribution properties between the two sites. The third approach described is the simplest, i.e.

$$R_{NF} = R_{HA} \cdot \frac{\bar{M}_{NF}}{\bar{M}_{HA}} \qquad (3.12)$$

where R and $\bar{M}$ denote daily and monthly average rainfall; and the suffixes NF and HA denote Naish Farm and Hurn Airport. This is a linear relationship through the origin with the adjustment already included when the monthly frequency distribution is normal. The relationships in figure 3.10 are nearly linear, so that the difference between using them, and equation 3.12, is relatively small. Equation 3.12 was considered satisfactory for this study, and was therefore used to derive daily rainfall at Naish Farm.

Weekly PE was calculated from the monthly generated values. The monthly PE is converted into daily average values. These are assigned to the middle of the month. Daily rates are assigned between the middle of one month and the next, by linear interpolation. A week's PE is then the sum of seven consecutive daily rates. This will have the tendency to slightly underestimate monthly PE in the summer, and slightly overestimate monthly PE in the winter.

3.9.4 Suggested Further Work

Further investigation of the spatial variation of monthly rainfall

and PE is necessary. This would facilitate improved estimates of the means and standard deviations of rainfall and PE at Naish Farm. At the moment there is little or no indication of the accuracy of the present estimates.

Further work could extend the data record from the present 5 years up to 30 years. This would require the daily rainfall record at Hurn Airport for this period. The data could also be used to improve the estimates of the model parameters for daily rainfall at Hurn Airport.

A very long data record (greater than 30 years) could be produced by generating data for Hurn Airport using the fitted frequency distributions. Such a data record could be used to produce a long record of predicted groundwater levels for a statistical analysis. In this case, it would probably be more appropriate to use figure 3.10, instead of equation 3.12, to derive daily rainfall. The use of a model to generate data, requires further investigation of the frequency and seasonal variation of extreme values, of both daily and monthly rainfall.

3.10 Summary

Rainfall and PE have been measured at Naish Farm over a two year period. Discussion is given to the possible errors in estimating these quantities. The data collected is considered to be homogeneous. Measurements at other sites have been investigated. In particular, the data for Hurn Airport has been examined in detail. Results indicate that no significant trend or periodicity exists in the data. Frequency distributions have been fitted to the data, and the significance of the study period examined. The most hydrologically significant period of the year is October to January. Average annual and monthly rainfall and PE at Naish Farm have been estimated, and comparison made with other weather stations. The PE at Naish Farm is similar to that at Hurn Airport with values slightly higher in winter and lower in Summer.

Greater regional variation is found with rainfall. The amount increases northwards due to the influence of the coast. The averages also show that the study period has been relatively wetter at Hurn Airport than it has at Naish Farm. The extension and modelling of data for Naish Farm is discussed. The data record has been extended to cover the period August 1980 to December 1985 using Hurn Airport data. The generation of modelled data is suggested as a topic of further research.

Table 3.1 Rainfall Measurements on the Undercliff

Date		Rain Gauge				
From	To	R1	R3	R4	R5	R6
29.12.82	02.01.83	3.6	2.0	3.1	1.5	
03.01.83	04.01.83	26.4	16.5	24.0	12.0	
05.01.83	11.01.83	8.8	6.7	8.8	8.1	
12.01.83	18.01.83	3.8	1.3	2.9	1.5	
19.01.83	25.01.83	7.8	5.1	7.7	5.5	
26.01.83	01.02.83	21.8	21.6	18.3	14.7	
02.02.83	08.02.83	4.5		3.9	2.4	
09.02.83	15.02.83	1.8		1.9		2.4
16.02.83	22.02.83	-		NIL		NIL
23.02.83	01.03.83	17.8		16.3		15.9
02.03.83	08.03.83	1.2		.9		1.1
09.03.83	15.03.83	9.8		9.7		9.0
16.03.83	22.03.83	9.4		12.3		11.8
23.03.83	29.03.83	13.8		9.5		9.0
Total catch relative to R1		100	73.7	91.4	59.6	91.4

Note: For the location of rain gauges see figures 3.2 and 3.3.

Table 3.2 Analysis of Different Versions of the Penman Formula

Month	Open Water		Short Grass				
	I	II	I	II	III	IV	V
January	13.3	10.2	8.0	9.6	8.6	10.8	10.8
February	23.5	20.3	14.1	18.0	16.5	19.1	18.9
March	38.4	35.0	26.9	29.6	30.1	30.7	29.8
April	76.8	71.6	53.8	58.2	58.4	60.0	64.4
May	94.2	88.7	75.4	74.2	74.3	75.8	76.7
June	125.4	118.8	100.3	96.9	97.4	99.0	104.4
July	146.2	137.6	117.0	113.3	112.1	115.6	123.1
August	115.8	108.3	92.6	89.9	91.0	91.8	97.2
September	67.5	62.4	47.3	54.3	54.6	55.5	55.2
October	41.5	37.2	29.1	31.9	30.9	33.5	34.1
November	15.3	12.3	9.2	11.4	10.9	12.3	10.8
December	9.3	6.5	5.6	6.2	9.0	7.4	7.1
Total	767.2	708.9	579.3	593.5	593.8	611.5	632.5
D%	+ 8.2	-	- 2.4	-	+ 0.1	+ 3.0	+ 6.6

Notes: D is the deviation from the value calculated using Penman (1963). The figures in the table are in mm of water and are based on data from Naish Farm for the period March 1983 to August 1984.

The months March to August are the averages for the years 1983 and 1984.

The estimates are based on monthly period averages of the meteorological variables except as indicated below. The references where the relevant equations can be found are:

Open Water	I	is Penman (1948)
	II	is Penman (1963)
Short Grass	I	is Penman (1948)
	II	is Penman (1963)
	III	is Penman (1963), using 7 day period averages
	IV	is Shaw (1983)
	V	is MAFF (1967)

Table 3.3 Analysis of Bias Errors in Measured Meteorological Variables

Month	PE (mm)	Perturbation (mm) in PE due to indicated bias error			
		Dry Bulb + .25°C	Wet Bulb + .25°C	Sunshine + 0.5 hr	Wind Speed + 10 km/day
January	9.6	+ 4.4	- 4.3	- 2.2	+ 0.3
February	18.0	+ 3.8	- 3.2	- 0.9	+ 0.6
March	29.6	+ 3.4	- 3.3	0.0	+ 0.3
April	58.2	+ 3.2	- 2.7	+ 0.8	+ 0.6
May	74.2	+ 3.5	- 2.9	+ 1.8	+ 0.8
June	96.9	+ 2.9	- 2.3	+ 2.0	+ 0.9
July	113.3	+ 2.5	- 1.9	+ 2.3	+ 1.1
August	89.9	+ 2.6	- 2.3	+ 1.6	+ 0.8
September	54.3	+ 3.6	- 3.3	+ 0.6	+ 0.6
October	31.9	+ 4.1	- 3.7	- 0.6	+ 0.7
November	11.4	+ 3.0	- 3.0	- 1.8	+ 0.3
December	6.2	+ 4.0	- 4.0	- 2.5	+ 0.3
Annual	593.5	+ 41.0	- 36.9	+ 1.1	+ 7.3
% error	0	+ 6.9	- 6.2	+ 0.2	+ 1.2

Dry Bulb		Wet Bulb		Sunshine		Wind Speed	
B.E. (°C)	P. (%)	B.E. (°C)	P. (%)	B.E. (hr)	P. (%)	B.E. (km/day)	P. (%)
+ .5	+ 13.9	+ .5	- 12.2	+ 1	+ 0.4	+ 20	+ 2.4
+ .25	+ 6.9	+ .25	- 6.2	+ .5	+ 0.2	+ 10	+ 1.2
- .25	- 6.7	- .25	+ 6.7	- .5	- 0.2	- 10	- 1.2
- .5	- 13.2	- .5	+ 13.1	- 1	- 0.5	- 20	- 2.4

Notes: B.E. is the bias error
P is the perturbation in the value of PE

The figures are based on data for Naish Farm for the period March 1983 to August 1984. The months March to August are averages of the years 1983 and 1984.

PE is calculated for short grass due to Penman (1963).

Table 3.4A Normal and Log-Normal Frequency Distributions fitted to Monthly and Annual Rainfall Data for Hurn Airport

	Normal Distribution				3-Parameter Log-Normal Distribution			
Month	μ_X	σ_X	Data Skew	Test stat	α	μ_Y	σ_Y	test stat
January	85.1	41.4	- 0.286	1.00				
February	56.1	38.3	0.523	1.73	- 146.8	5.295	0.187	1.73
March	62.2	32.5	- 0.093	3.18				
April	43.2	28.3	0.635	0.64	- 81.1	4.798	0.225	2.09
May	58.0	30.8	0.548	5.36	- 98.3	5.033	0.195	3.18
June	56.0	32.1	0.397	8.64	- 167.7	5.400	0.143	2.09
July	44.2	28.0	0.652	6.45	- 75.2	4.756	0.231	2.09
August	58.6	33.3	0.333	3.91	- 217.8	5.615	0.120	4.64
September	77.9	45.9	0.308	2.82	- 334.0	6.015	0.111	1.73
October	84.9	62.0	1.108	1.36	- 76.0	5.012	0.372	0.27
November	87.4	50.3	0.720	6.09	- 108.2	5.244	0.253	2.45
December	91.7	46.7	0.555	0.27	- 141.7	5.433	0.198	3.18
Annual	805.5	140.5	0.518	5.73	52.3	6.607	0.185	6.09

Table notes on page 101

Table 3.4B Normal and Log-Normal Frequency Distributions fitted to Monthly and Annual PE Data for Hurn Airport

	Normal Distribution				3 Parameter Log-Normal Distribution			
Month	μ_X	σ_X	Data Skew	test stat	α	μ_Y	σ_Y	test stat
January	6.8	4.5	0.746	2.48	- 10.0	2.784	0.263	1.32
February	13.8	3.1	0.526	9.84	- 2.4	2.768	0.189	5.19
March	34.2	3.2	0.725	9.06	22.0	2.463	0.256	7.52
April	59.9	7.0	0.125	5.19				
May	85.7	8.8	- 0.057	1.32				
June	100.5	13.6	0.608	2.10	38.4	4.105	0.217	2.87
July	103.5	13.5	0.813	5.58	57.1	3.797	0.285	3.26
August	84.3	9.9	1.018	2.10	56.6	3.261	0.348	2.87
September	51.0	4.7	0.472	1.32	23.8	3.291	0.170	0.55
October	23.9	3.2	0.369	3.65	0.0	3.165	0.134	1.32
November	8.9	3.1	0.123	2.10				
December	4.8	4.9	1.433	1.71	- 5.2	2.202	0.462	1.32
Annual	577.3	38.9	0.959	10.61	462.6	4.688	0.330	4.42

Table notes on page 101

Notes on table 3.4

1. The log-normal distribution was not fitted to data with skew less than 0.3.

2. Rainfall/PE is denoted by the variable X which has a mean μ_X and a standard deviation σ_X. The variable Y is related to X by the relationship:

$$Y = \ln (X - \alpha)$$

where α is a location parameter. Let Z be normally distributed with zero mean and unit variance. If X is log-normally distributed then the variable Y is related to Z by:

$$Z = \frac{Y - \mu_Y}{\sigma_Y}$$

where μ_Y and σ_Y are the mean and standard deviation of Y. The parameters of a log-normal distribution (α , μ_Y and σ_Y) were fitted by the method of moments (Kottegoda, 1980, pp 229-230).

3. The test statistic is χ^2 distributed. Six equal classes were used for the test. The 95 per cent confidence level values of χ^2 are:

Normal distribution (3 degrees-of-freedom) equals 7.81
Log-normal distribution (2 degrees-of-freedom) equals 5.99

4. The units of α , μ and σ are mm of water.

Table 3.5 Probabilities of Non-Exceedance for Monthly and Annual Rainfall and PE Data for Hurn Airport during the Study Period

	Rainfall				PE			
	1981	1982	1983	1984	1981	1982	1983	1984
January	.090	.183	.423	.951	.680	.596	.954	.754
February	.483	.418	.166	.306	.680*	.549*	.935*	.870*
March	.964	.884	.294	.635	.646	.933	.209	.112
April	.553	.185	.934	.067	.382	.546	.192	.966
May	.928	.224	.899	.758	.023	.715	.071	.182
June	.668*	.858*	.878*	.184*	.191	.630	.285	.873
July	.463	.943	.104	.138	.236	.406	.916	.882
August	.061	.736	.090	.095	.580	.350	.942	.700
September	.941	.404	.395	.313	.895	.343	.500	.820
October	.524	.945	.468	.541	.562	.287	.744	.954
November	.155	.749	.208	.882	.849	.935	.373	.697
December	.726	.562	.704	.569	.484	.419	.533	.163
Year	.667	.891	.345	.466	.258*	.656*	.735*	.899*

	Year from 1st October		
	1981/2	1982/3	1983/4
Rainfall	.539	.772	.223
PE	.610*	.738*	.896*

Note * denotes figures based on log-normal distribution.
All other figures based on normal distribution.

Table 3.6 Probabilities of Non-Exceedance for Extreme Rainfall

	Rainfall = 100 mm		Rainfall = 125 mm		Rainfall = 100+ $\overline{PE}_i$ (mm)	
	Pr	obs	Pr	obs	Pr	obs
January	.641	13	.833	5	.700	11
February	.874	6	.964	2	.934	3
March	.878	5	.973	0	.987	0
April	.978	2	.998	0	*	0
May	.914	4	.985	0	*	0
June	.908	4	.975	1	*	0
July	.977	2	.998	0	*	0
August	.893	4	.977	1	*	0
September	.685	10	.848	6	.944	1
October	.596	10	.741	5 (2)	.735	6
November	.599	12	.773	8 (1)	.665	11
December	.571	14	.762	7 (2)	.611	13

Notes: $\overline{PE}_i$ is the average PE for month i, where i = January,...., December.
P_r is the probability of non-exceedance. *probability greater than .999.
obs is the number of times the given rainfall has been exceeded during the period 1952 to 1984. The figures in brackets denotes the number of times a rainfall of 200 mm has been exceeded.

Table 3.7 Monthly and Annual Averages for Rainfall and PE for the Highcliffe Region

	Rainfall averages for 1941-1970						Rainfall averages for 1952-1984		PE averages for 1954-1984	
Location	B	C	E	F	HA	NF	HA	NF	HA	NF
January	93	83	81	82	85	78	85.1	78	6.8	6.6
February	60	52	53	52	55	50	56.1	51	13.8	14.4
March	60	54	53	52	56	54	62.2	60	34.2	32.7
April	53	47	47	45	49	43	43.2	38	59.9	55.1
May	62	56	53	52	58	58	58.0	58	85.7	84.6
June	51	48	48	49	47	46	56.0	55	100.5	93.3
July	54	48	53	55	49	48	44.2	43	103.5	97.1
August	73	65	67	71	67	63	58.6	55	84.3	80.0
September	80	73	73	76	75	77	77.9	80	51.0	54.3
October	91	83	80	75	85	72	84.9	72	23.9	29.3
November	103	92	92	92	95	81	87.4	74	8.9	12.8
December	92	83	82	83	85	74	91.7	80	4.8	5.7
Year	872	784	782	784	806	744	805.3	744	577.3	565.9
Annual	872[a]	784[a]	782[a]	784[a]	806[a]	715[b]	805.5[c]	715[d]	577.3[c]	565.9[a]

Notes: The location notation is: B, Bisterne; C, Christchurch; E, Everton; F, Freshwater; HA, Hurn Airport; NF, Naish Farm

Figures of the "year" are summed monthly values.

Figures for "annual" are:

a. The same as for "year"
b. Estimated using the Meteorological Office (1963) method for annual data.
c. Average of annual data. Differs from "year" due to rounding off error.
d. This is calculated by multiplying the figure for Hurn Airport by the ratio of the 1941-1970 figures for Naish Farm and Hurn Airport.

Figure 3.1 Location map for weather stations in the Naish Farm region.

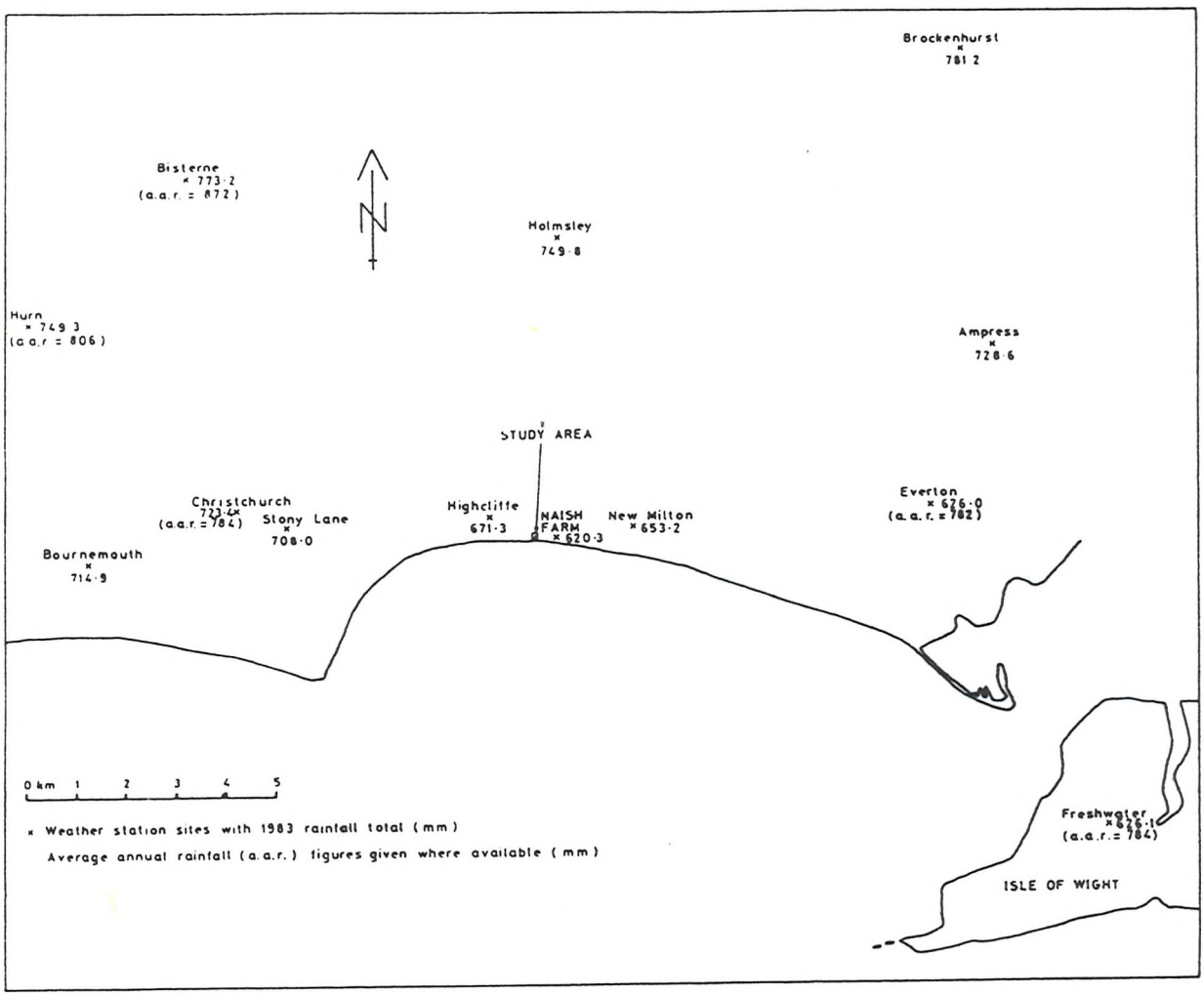

Figure 3.2 Location map for the weather station and undercliff rain gauges at Naish Farm.

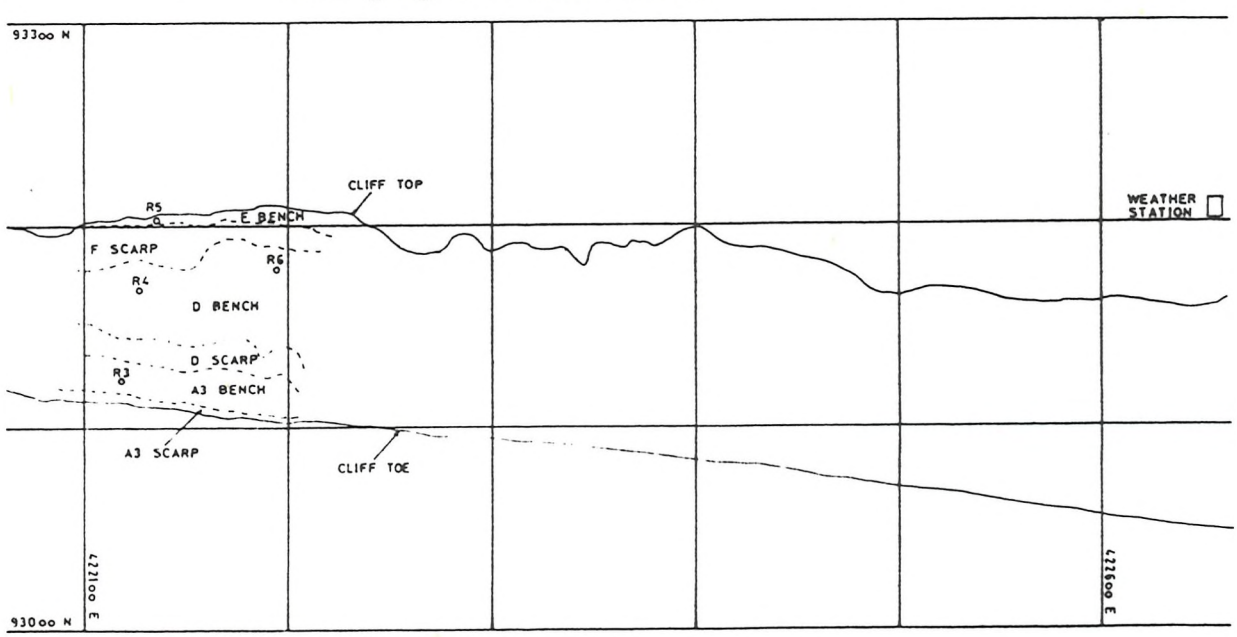

Figure 3.3 Location of the instruments in the weather station at Naish Farm.

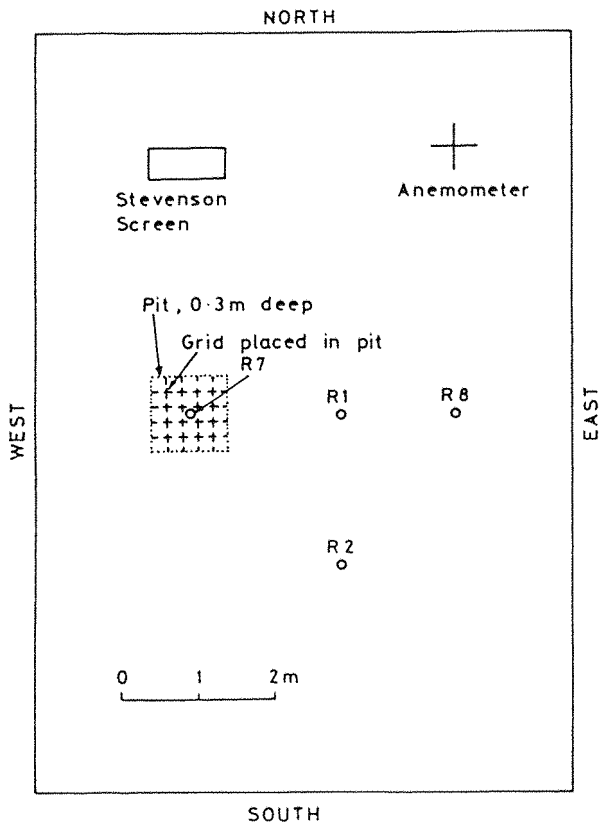

Figure 3.4 Definitions for rainfall measurements on sloping surfaces.

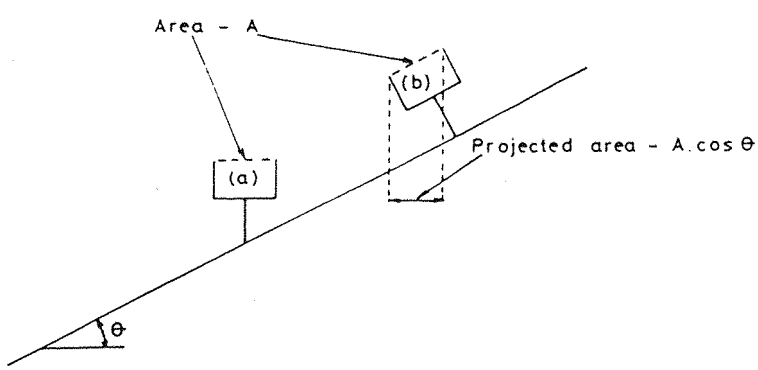

MR - Rainfall in (a) per unit orifice area

HR - Rainfall in (b) per unit orifice area

HPR - Rainfall in (b) per unit projected area

R_{REF} - Rainfall in absence of topographic disturbance

$HR / MR = \cos\theta + \sin\theta . \tan\phi . \cos(z_a - z_b)$ (From Sharon, 1980)

ϕ - Rainfall inclination from the vertical

z_a - Azimuth toward which the plane of the orifice is inclined

z_b - Azimuth toward which rain is falling

$HPR = HR / \cos\theta$ $\quad I = HPR / R_{REF}$

FIGURE 3.5

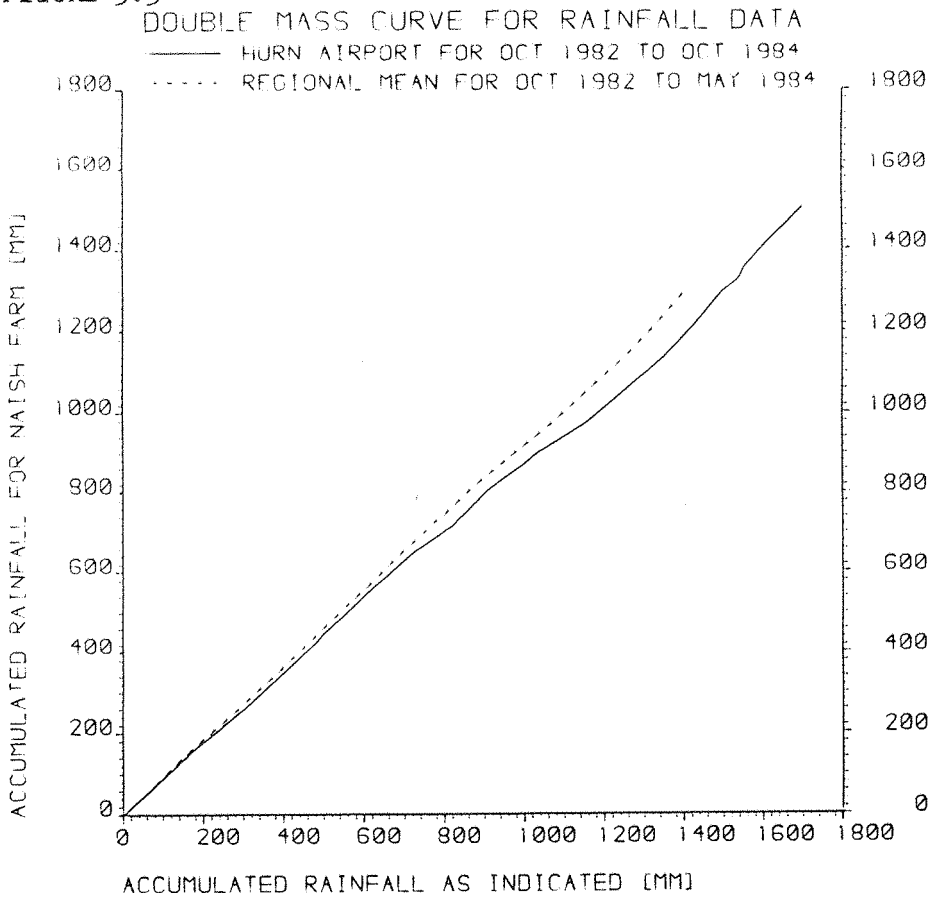

FIGURE 3.6

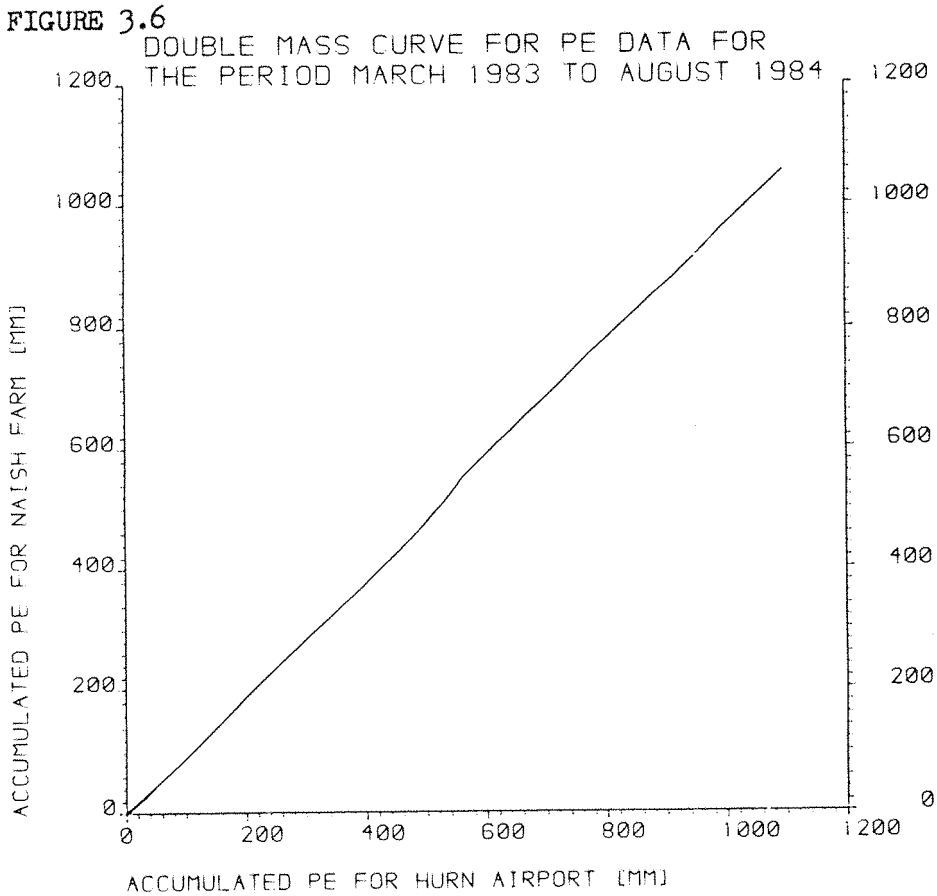

FIGURE 3.7

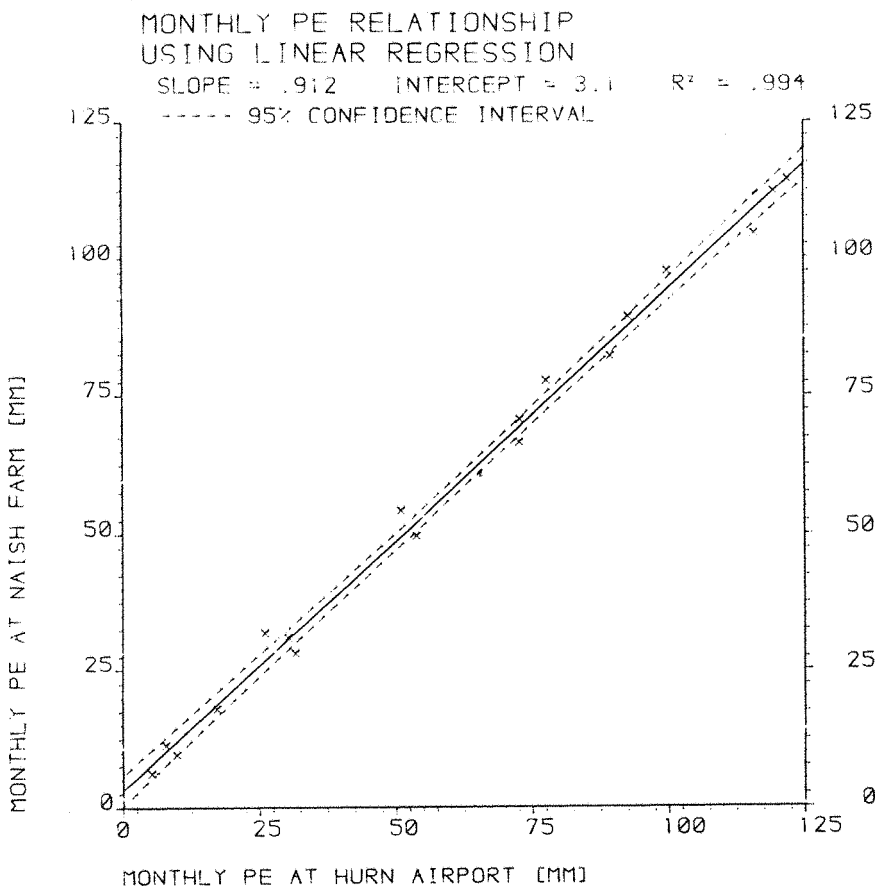

FIGURE 3.8

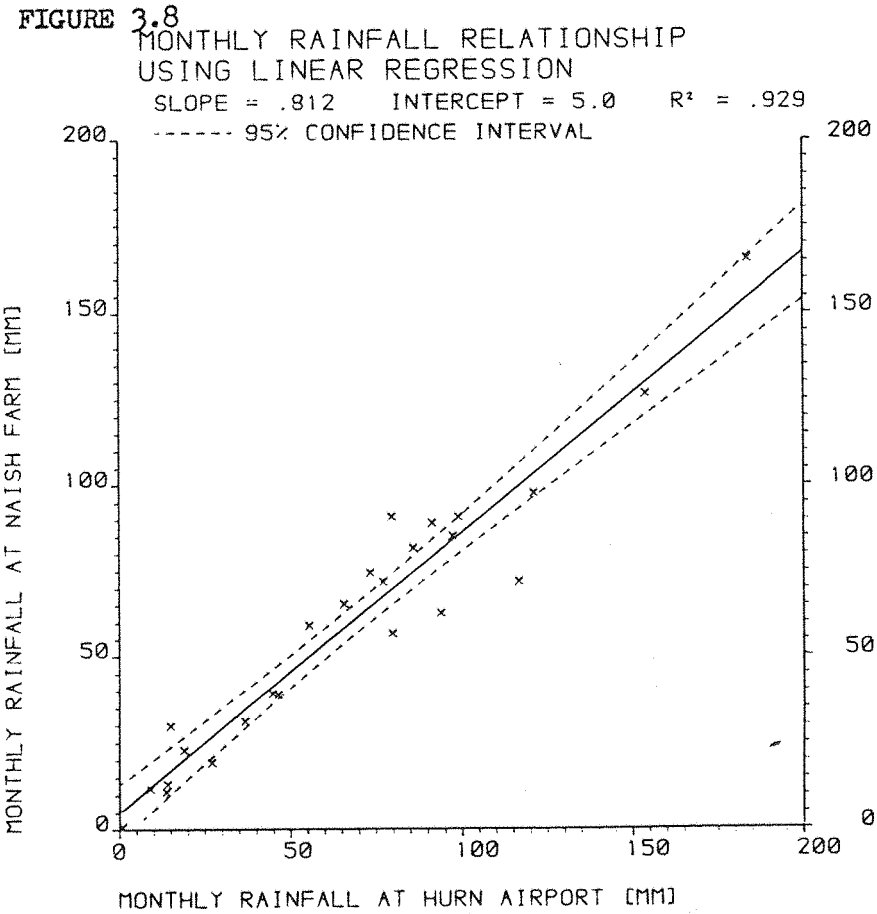

FIGURE 3.9

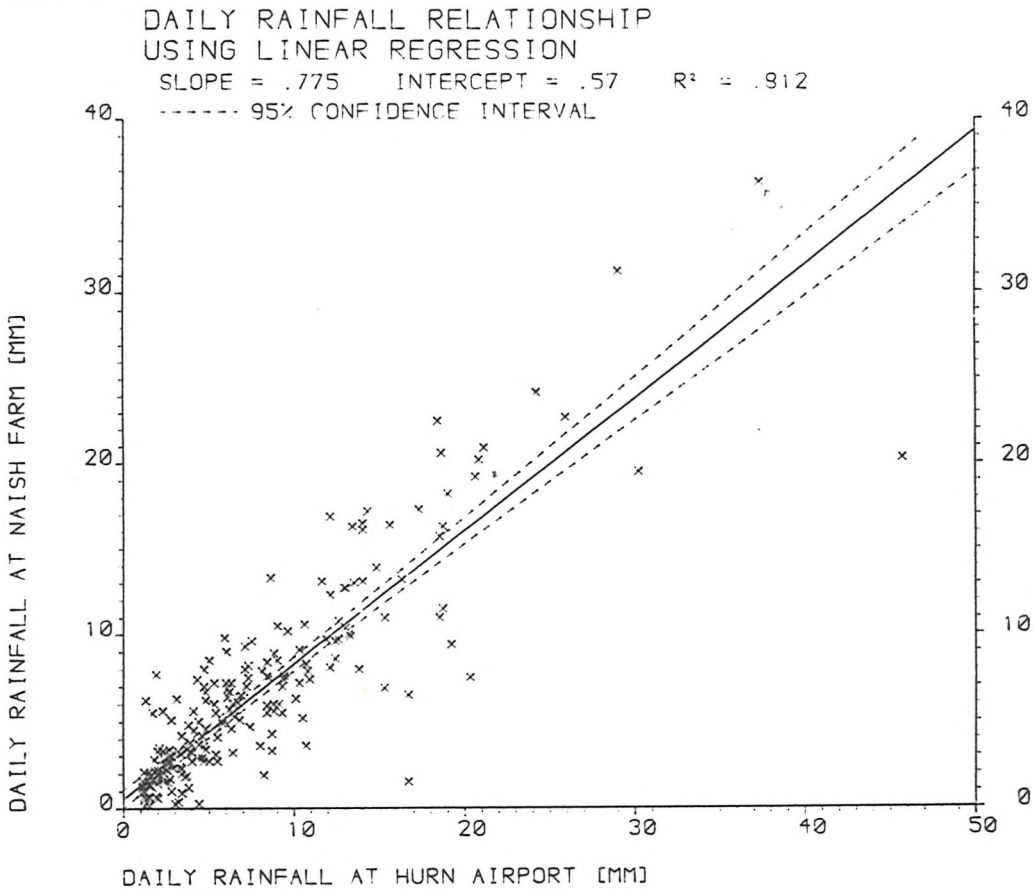

FIGURE 3.10

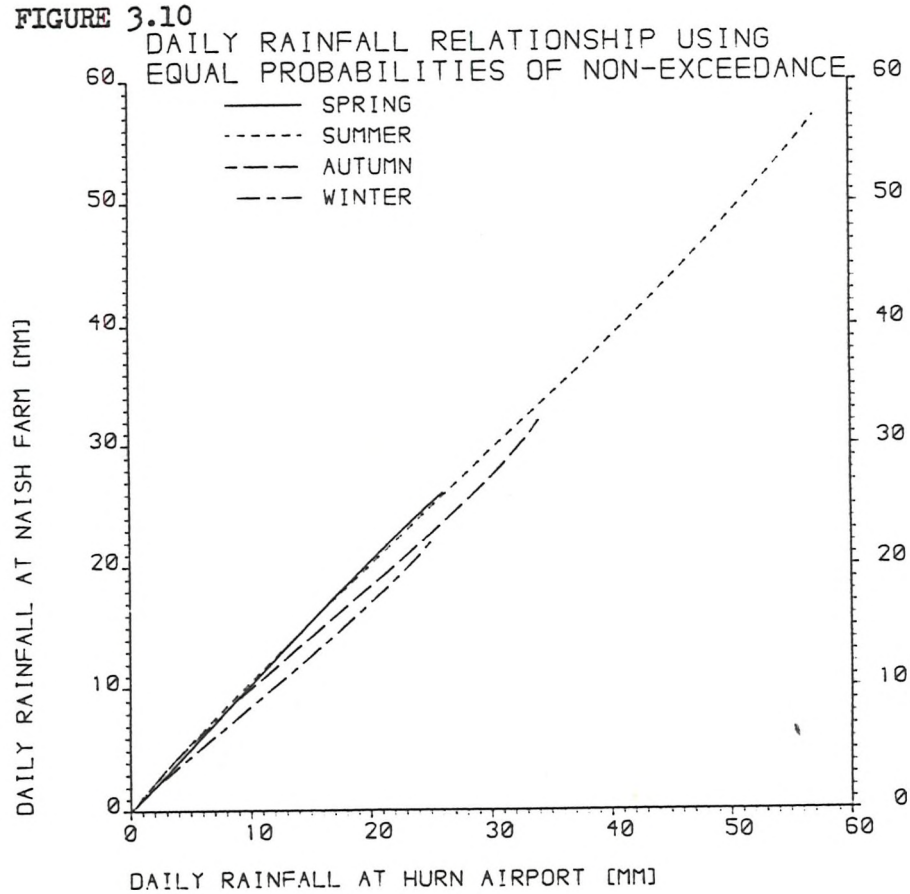

CHAPTER 4

WATER BALANCE : GENERAL CONSIDERATIONS

The study area can be sub-divided into three component geohydrologic domains (see figure 4.1). Each domain acts both as a store and as a medium through which seepage takes place.

4.1 Plateau Gravel Domain

This includes the grassed surface and topsoil, and some built over ground (small chalets and access roads), as well as the Plateau Gravel (PG) itself. The topsoil is developed on a thin layer of Brickearth up to 0.3 m thick. There is some mixing with the PG. The Brickearth thickens (up to 2 m) about 250m east of the study area. Keen (1980) describes the Brickearth as being 50 per cent fine sand, 30 per cent silt, and 20 per cent clay. The PG provides a good drainage such that the Brickearth does not get waterlogged. The ground surface slopes gently toward the cliff edge or Chewton Bunny (see figures 1.1 and 2.5). No surface runoff has been observed from the grassed surface. The lack of streams or ponds in the Brickearth or PG, suggests that any runoff that does occur, infiltrates after rainfall has stopped. The amount of surface runoff could be estimated if the rainfall rate and infiltration capacity were known. However, the measurement of rainfall was such that the estimation of rainfall rate is not accurate enough, and the presence of gravel makes the installation of ring infiltrometers difficult. The PG is used as a soakaway for runoff from chalets and roads. Waste water is lead away to Chewton Bunny. There may be some leakage from service pipes, but this is unknown.

The hydraulic properties of materials like PG are difficult to determine. In situ measurement of soil moisture content and tension would enable the estimation of groundwater recharge and changes in soil moisture storage in the unsaturated zone. However, the necessary instrumentation is difficult to install

and the results could be of dubious value.

The estimation of changes in groundwater storage necessitates the measurement of the water table level and the specific yield of the PG. The former is estimated from piezometric measurements and assuming the equipotentials in the PG to be vertical. The latter can be estimated from estimations of drainable porosity. This is estimated from the difference between the total porosity (as determined from in situ bulk and particle densities) and the drained moisture content. Plumb (1984) determined the particle density to be 2.67 Mg/m^3. (PG is predominantly quartz which has a specific gravity of 2.65 Mg/m^3. The slightly higher value is probably due to iron cement.) Bailey (1983) determined the in situ density, from tests on an intact slump block, to be 2.06, 2.01, and 2.00 Mg/m^3. This gave total porosity values of .23, .25, and .25 with moisture contents (by volume) of .12, .11, and .16 respectively. These results give drainable porosity values of .11, .14, and .09. However, the slump block had been subjected to drying by the influence of evaporation, and it is therefore probable that the true value of drainable porosity (and therefore specific yield) will be lower. However, the values give an indication of the probable upper limit to the true value.

The saturated permeability has been estimated from laboratory tests to be 1.5×10^{-5} m/s (1.3m/day) for a sand lens, and 1.2×10^{-4} m/s (10.4 m/day) for a very sandy gravel sample of the PG (see appendix F). The sand lenses also have a higher total porosity. Plumb (1984) determined the bulk density of a sand lens to be 1.71 Mg/m^3, giving a total porosity of 0.36. The lower bulk density is probably due to the fact that the particle size distribution covers a much narrower range of particle sizes than the rest of the PG. The moisture content was not determined, but it is probable that the specific yield was also different from that of the very sandy gravel deposits sampled by Bailey (1983).

Particle size distributions of the PG from various sources are given in table 4.1. The proportion of sand and gravel are spatially variable. This will cause the hydraulic properties to also vary. However, the PG is still very much more permeable than the underlying Barton Clay (BC) (see section 4.2). This will cause the downward percolation of water (from rainfall recharge) to be held up in the PG. The direction and velocity of groundwater flow has not been investigated with tracer techniques. Such tests are apt to fail due to the wrong choice of tracer, or a lack of understanding of the hydrogeologic system (Davis et al, 1980). It is estimated that, due to the low hydraulic gradient (slope of water table) in the PG and the above permeabilities, it would take several months for the tracer to move only a few metres. For example, for the water table slope between P60 and P63 (see figure 6.11B), it would take about 32 days to travel 5 m. Thus, only localised movements of groundwater could be measured. It was therefore considered that such tests would give no more information than water table level measurements. The groundwater in the PG flows both downwards into the BC, and laterally to either the cliff face or Chewton Bunny. The vertical flow is permanent, whereas the seepage at the cliff face is markedly seasonal. The flow pattern within the PG is further complicated by the irregular level of the PG/BC unconformity (see chapter 2). The presence of paved areas creates a non-uniform recharge to groundwater which may significantly affect the flow pattern. Zucker et al (1973), using a finite difference model, showed that for alternating paved and non-paved areas, where the runoff from the paved areas was additional recharge to the non-paved areas (as is the case at Naish Farm), there was no significant difference to the groundwater flow pattern (when compared with uniform recharge).

A rough estimate of the area contributing groundwater flow to the undercliff is shown in figure 4.2. The estimation assumes

that the PG/BC unconformity is horizontal, and at a level of 26 m O.D. to the west of Chewton Bunny (Booth, 1974), and 28.5 m O.D. to the east of Chewton Bunny (see figure 2.1). It is assumed that the direction of groundwater flow is perpendicular to the relevant contour, and that the groundwater divide is equidistant (along the direction of groundwater flow) between the 26 m and 28.5 m O.D. contours respectively to the west and east of Chewton Bunny. The dip of the Barton Beds causes the Barton Sand (BS) to outcrop 170 m east of the study area (see figure 1.2). It is estimated that underneath the cliff edge, at the eastern edge of the undefended length of cliff, the bottom of the BS is at about 14.2 m O.D. The position of the water table will be affected by the contrast in permeability between the BS and the PG. Figure 1.4 gives the stratigraphy of the BS. Barton et al (1986) found zone K to be a fine sand with only 2 or 3 per cent fines. This infers a permeability (using Hazen's formula) similar to that of PG (see appendix F). However, the BS is variable, such that other zones may be less permeable, and so inhibit the downward flow of water. This could be a useful topic of further research. Figure 4.2 assumes that where the BS occurs, the groundwater divide is equidistant between the cliff face and the water course (Becton Bunny), which is the intersection of the water table with the ground surface.

Figure 4.2 shows that a considerable area contributes groundwater flow to the undercliff. For much of the undefended section, the contributing area is greater than that for the study area. The maximum contributing area is about 4.5 times greater than the average for the study area. This should be borne in mind when extrapolating the results of the water balance for the study area to the rest of the undefended length of cliffs.

4.2 Barton Clay Domain

The stratigraphy of the BC is given in figure 1.3. Only zones A2 to F2 occur above beach level in the study area (see figure 1.6). The undefended cliff section also inlcudes zones G to I of the BS (see figure 1.4 for the stratigraphy of BS). Table 4.2 shows some results of particle size distribution analyses on the BC. Owing to the fairly frequent vertical variations in lithology, the BC is markedly anisotropic in permeability. The permeability should be greatest parallel to the bedding. However, this is complicated by the presence of fissures. Fissuring will be affected by stress relief, and will therefore vary with depth and distance from the cliff edge.

Groundwater flow will be mainly along fissures and permeable layers of sand or fossils. In particular, in the study area, the sand beds of the A3 zone are believed to provide a significant flow to the undercliff. This was even allowed for in the design of the cliff slope stabilization works to the west at Highcliffe (Halcrow, 1971). East of the study area (but still in the undefended section of cliff), the more permeable BS will provide significant seepage to the undercliff. It may also be subject to seepage erosion and subsequent back-sapping causing destabilization of the in situ material. (Barton and Thomson, 1986a, discuss this with respect to the A3 zone as a possible cause of the preferred shear surface at the A3/A2 boundary.) Seepage holes have been observed in the weathered zone at the top of the Barton Clay (Thomson, 1983). West (1985), using pinhole tests, found no evidence that the weathered zone was dispersive. However, it may be that the seepage hollows follow old shrinkage cracks formed when the BC was being weathered and before the PG was deposited. (It should be noted that such hollows can also be formed by tiny burrowing animals such as molluscs. This has not been investigated, and could be the subject of further study.)

Seepage erosion in the top of the BC would be of significance if a cut off drain were to be installed in the PG. Such a scheme might include a diaphragm wall. This would need to be of sufficient depth in the BC to decrease the hydraulic gradient and hence, to decrease the forces tending to dislodge soil particles.

Seepage into the BC domain takes place from groundwater flow from the undercliff colluvium and inland areas as well as the input from the PG. Discharge from the BC domain takes place into the undercliff colluvium, the underlying Bracklesham Beds, and the sea.

4.3 Undercliff Colluvial Domain

The local permeability of the clay colluvium can be quite low, as indicated by the permeability of the BC (section 4.2). However, the presence of much PG derived material, together with numerous deep tension cracks, promotes a relatively high mass permeability. The active slope movements, by opening new tension cracks and widening old ones, induce changes in the mass permeability. The surface of the undercliff is highly irregular, and allows the formation of ponds, some of which are perennial. The presence of ponds and tension cracks enables large changes in storage to take place in the undercliff. Vegetation is mainly confined to the upper parts of the undercliff where the topsoil has not been broken up and buried. The vegetation is mainly composed of grasses and early colonising plants such as plantains, thistles, nettles, and aquatic plants such as marsh reeds and mare's-tail. There are also some gorse and bramble bushes and sallow scrub. The surface layers undergo considerable changes in moisture state, from a very soft, in places impassable, clay in winter, to a hard, dry crust in summer.

Apart from direct rainfall, other inputs to the undercliff colluvial

domain are seepages from the PG and BC, and sea spray and waves. The latter mainly only affects the A3 bench in stormy weather. The colluvium is usually already saturated, such that this input immediately runs back to the sea. Output from the colluvium is via evaporation (from ponds, vegetation and bare ground), seepage into the BC (some of which re-enters the colluvium lower down the undercliff), and surface runoff and groundwater seepage to the sea.

4.4 Water Balance Equations

The general water balance equation may be expressed as:

$$\Delta S = \sum_{i=1}^{n} I_i - \sum_{i=1}^{m} O_i \qquad (4.1)$$

where ΔS is the increase in storage,
I is the set of inputs,
O is the set of outputs,
n and m are the numbers of inputs and outputs respectively.

The water balance equation may be applied to each of the geohydrological domains as follows:

4.4.1 Plateau Gravel Domain

$$\Delta S_1 = P_1 \pm G_1 - E_1 - L_1 - D_1 - R_1 \qquad (4.2)$$

where ΔS_1 is the increase in storage in the PG domain,
P_1 is the precipitation over the cliff top area,
G_1 is the lateral groundwater flow into the area from inland,
L_1 is the percolation into the BC domain,
D_1 is the discharge at the cliff face boundary of the PG domain,
R_1 is the surface runoff across the boundaries of the PG domain,
E_1 is the evaporation over the cliff top area.

Surface runoff is negligible (section 4.1), and the boundaries are chosen such that G_1 is zero. Thus:

$$\Delta S_1 = P_1 - E_1 - L_1 - D_1 \qquad (4.3)$$

4.4.2 Barton Clay Domain

$$\Delta S_2 = P_2 + L_1 + L_3 \pm G_2 - E_2 - L_2 - D_2 - R_2 - Q_2 \qquad (4.4)$$

where ΔS_2 is the increase in storage in the BC domain,

P_2, E_2, R_2 are the precipitation, evaporation and runoff respectively for the exposed scarp faces of the in situ BC,

L_3 is the percolation from the undercliff colluvium,

G_2 is the lateral groundwater flow into the area from inland,

L_2 is the percolation into the underlying Bracklesham Beds,

D_2 is the percolation into the undercliff colluvium,

Q_2 is the groundwater flow across the boundary below the cliff toe.

The area of exposed scarp face is small such that P_2, E_2, and R_2 can be neglected. Thus:

$$\Delta S_2 = L_1 + L_3 \pm G_2 - L_2 - D_2 - Q_2 \qquad (4.5)$$

4.4.3 Undercliff Colluvial Domain

$$\Delta S_3 = P_3 + D_1 + D_2 + W_3 \pm G_3 - E_3 - L_3 - D_3 - R_3 \qquad (4.6)$$

where ΔS_3 is the increase in storage in the undercliff colluvium,

P_3 is the precipitation on the undercliff,

W_3 is the input from waves and spray,

G_3 is the lateral groundwater flow into the area from the colluvium outside the area,

E_3 is the evaporation from the undercliff,

D_3 is the groundwater seepage at the cliff toe from the colluvium onto the beach,

R_3 is the surface runoff from the colluvium onto the beach.

The catchment boundaries are chosen such that G_3 is negligible. The contributions from sea spray and waves (W_3) is largely lost as immediate runoff. The remainder is considered to be negligible. Thus:

$$\Delta S_3 = P_3 + D_1 + D_2 - E_3 - L_3 - D_3 - R_3 \qquad (4.7)$$

D_1 and D_2 are obtained from equations 4.3 and 4.5 respectively. Substituting in equation 4.7 and rearranging gives:

$$(Q_2 + D_3 + R_3) = (P_1 + P_3) - (E_1 + E_3) - (\Delta S_1 + \Delta S_2 + \Delta S_3) - L_2 \pm G_2 \qquad (4.8)$$

This is the same as the water balance for all three domains lumped together, i.e.

$$Q = P - E - \Delta S - L \pm G \qquad (4.9)$$

where Q is the total outflow across the boundary under the cliff toe,

P is the rainfall,

E is the evaporation,

ΔS is the increase in storage,

L is the leakage to the underlying Bracklesham Beds,

G is the lateral groundwater flow across all vertical boundaries other than under the cliff toe.

Chapter 5 discusses a groundwater level prediction model, which is used in chapter 6 to solve the water balance for the PG domain. This calculates (D_1 + L_1). Chapter 7 calculates L_1 and G_2, and L_2 for the BC inland of the cliff face. The water balance is then solved to calculate the outflow across the vertical boundary under the cliff face. This is assumed to enter the undercliff colluvium. Chapter 8 discusses the estimation of ΔS_3. Chapter 9 applies the water balance to the undercliff colluvium. This in effect solves equation 4.9, except that the outflow includes the leakage to the Bracklesham Beds for the area under the colluvium. Also, the change in storage in the BC under the colluvium, is assumed to be negligible.

The water balance considerations above, ignore the contributions due to a loss, or gain, of material (which contains water). Both the PG and BC domains lose material through slumping and spalling. The colluvial domain gains material from the other domains and loses it to the sea. These contributions are significant when a large slump occurs, with material being pushed onto the beach and lost from the system. However, no such slump occurred during the study period, such that the effect of a loss of material from the system on the water balance, is assumed to be negligible.

Table 4.1 Particle Size Distribution of the Plateau Gravel

Source	Particle Size %							
	Silt & Clay	Sand			Gravel			Cobble
		Fine	Medium	Coarse	Fine	Medium	Coarse	
1a	6	6	20	9	10	32	17	-
1b	2.5	5.5	25	6	10	39	12	-
1c	2	2.5	16	9.5	9	39	22	-
1d	-	3	47	7	6	27	10	-
1e	-	10	86	4	-	-	-	-
1f	20	8	25	5	4	32	6.5	1.5
2	0.5	1.5	14	11	11	39	22	-
3	-	2	93	3	2	-	-	-
4a	2.5	4	21.5	10	14.5	35	12.5	-
4b	7.5	6	79	2.5	2	2	1	-

Source: 1 Booth (1974)
2 Bailey (1983)
3 Plumb (1984)
4 West (1985)

Notes: Samples 1e, 3, and 4b were purposefully taken from sand lenses. With the exception of 4f, the other samples are more representative of the PG. Sample 4f was taken from near the base of the exposure. This author suspects that the sample may have been contaminated with underlying BC.

Table 4.2 Particle Size Distribution of the Barton Clay

Source	Horizon	Particle Size %		
		Clay	Silt	Sand
2	F	30	46	24
1	F upper	65	34	1
1	F lower	59	36	5
2	E	41	51	8
1	E	34	59	7
2	D upper	15	50	35
2	D lower	22	50	28
1	D upper	28	57	15
1	D middle	25	35	40
1	D lower	50	37	13
2	C upper	17	57	26
2	C lower	32	39	29
1	C	37	25	38
2	B	13	49	38
1	B (clay lens)	39	57	4
2	A3 (clay)	23	60	17
1	A3 (clay)	52	46	2
2	A3 (sand)	7	30	63
2	A2	24	59	17
1	A2	38	52	10
2	A1	32	40	28
1	A1	41	58	1
2	A0	23	18	59
1	A0	35	18	47

Source: 1 Kilbourn (1971)
2 Booth (1974)

Booth gives grading limits for a number of samples. The above figures represent the average.

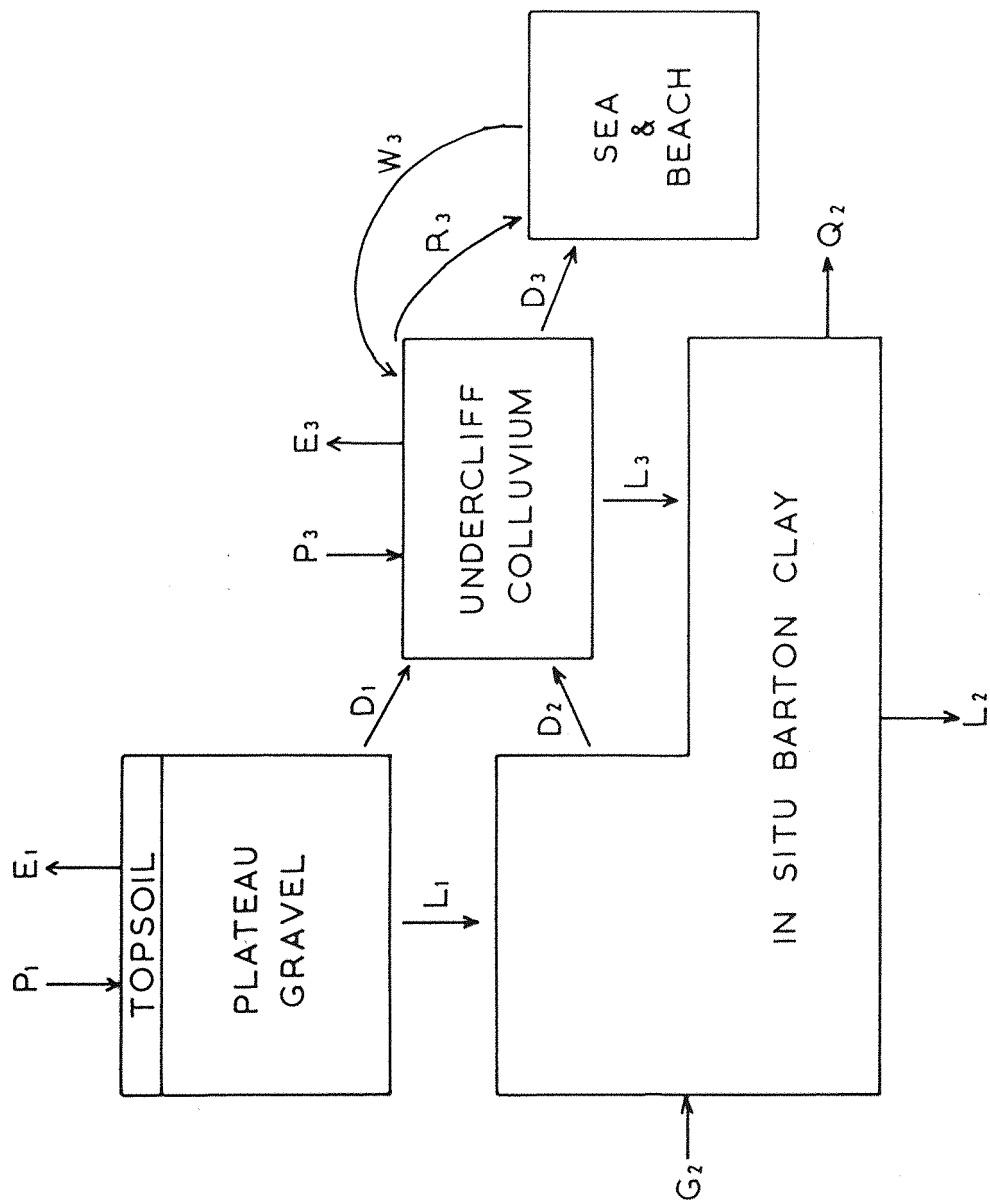

Figure 4.1 Diagrammatic representation of the water balance showing the three geohydrological domains. The symbols are defined in section 4.4.

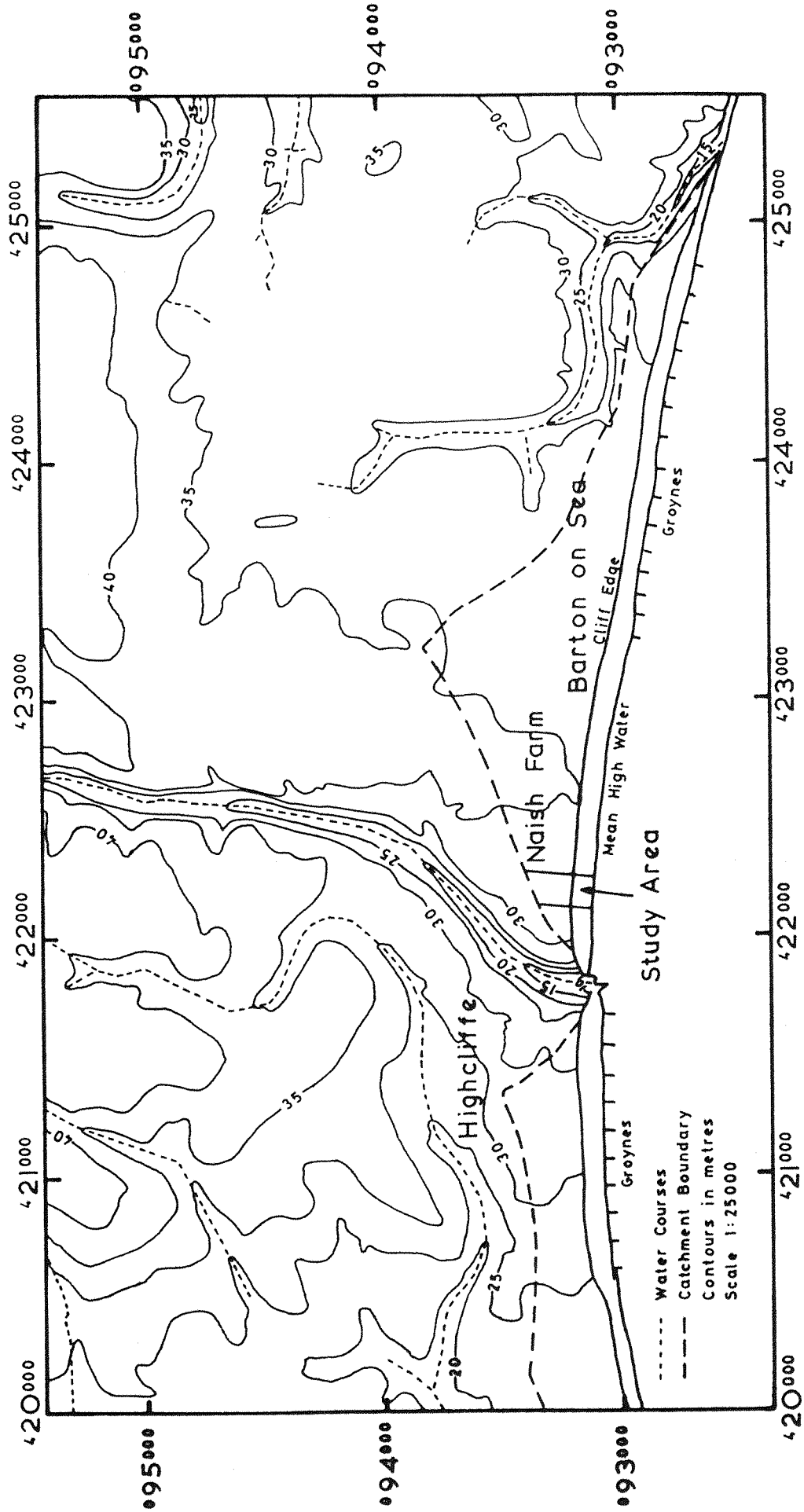

Figure 4.2 Estimated cliff top catchment areas for seepage to the undercliff.

CHAPTER 5

A MODEL FOR PREDICTING GROUNDWATER LEVEL RESPONSE TO METEOROLOGICAL CHANGES

5.1 Introduction

The aim of the model is to predict groundwater level fluctuations caused by meteorological variations. Application of the model to groundwater level measurements in the Plateau Gravel is given in chapter 6. The relationship between meteorological conditions and groundwater level is complex. It has been simplified in this model by using a water balance approach. The model is as in Barton and Thomson (1986b).

5.2 Theory of the Model

The model consists of two separate water balances. The first is for the upper part of the profile, and calculates the effective rainfall percolating down below the influence of evaporation. It is:

$$ER = P - RUNOFF - AE - \Delta S \qquad (5.1)$$

where P is rainfall; RUNOFF is surface runoff; AE is actual evaporation; ER is effective rainfall; ΔS is the increase in soil moisture storage.

The effective rainfall percolates down the profile to become recharge to the groundwater table where a second water balance is applied:

$$RECHARGE = DRAINAGE + \Delta W \qquad (5.2)$$

where DRAINAGE is the loss of water to groundwater flow; and ΔW is the change in water storage which is achieved by a change in the water table level.

As the water balances involve volumes of water, they need to be solved over a set period of time. This is called the time step of calculations.

5.2.1 Calculation of Effective Rainfall

Effective rainfall is calculated by solving equation 5.1. RUNOFF is approximated as a constant percentage of rainfall.

AE and ΔS are estimated by using a soil moisture deficit (SMD) model. This model assumes that when the SMD is satisfied, there is no further change in soil moisture storage ($\Delta S = 0$). It has been assumed by some authors (e.g. Penman, 1949) that no effective rainfall occurs while there is an SMD, although a number of researchers have reported this not to be the case (e.g. Kitching et al, 1977). Smith et al (1970) introduced a direct effective rainfall component, where a proportion of the infiltrated rainfall bypasses the SMD model to go directly as effective rainfall. Rushton and Ward (1979) examined a number of different possible direct effective rainfall models. The need for a direct effective rainfall component may be due to the presence of a system of cracks (e.g. tension cracks), or a reflection on the limitation of the SMD concept for representing the soil moisture fluxes within the soil matrix. The model here includes a direct effective rainfall component (ER_1) in addition to the component available when SMD = 0 (ER_2). The value of ER_1 is taken as a proportion (A) of the infiltration.

When water is plentiful, it is freely evaporated to the atmosphere at a rate which is determined by meteorological factors. Under these conditions, the evaporation is flux controlled, and its rate is referred to as the potential evaporation (PE). When water is not plentiful, i.e. as the soil dries out, the evaporation rate may fall below PE and is profile controlled, i.e. control is by the maximum rate at which moisture is transferred to the evaporation surface. The two conditions may be defined as:-

Flux Control	:	$PE \leqslant P - RUNOFF$; $AE = PE$
Profile Control	:	$PE > P - RUNOFF$; $AE \leqslant PE$

The evaporation rate, AE, is a function of PE and SMD. The function used here is the same as that used by Lloyd et al (1966) and is shown by figure 5.1.

The calculation of effective rainfall is summarised in figure 5.2. The term DETENTION is a model concept introduced for the rainfall less the surface runoff. Physically, DETENTION may be considered to consist of interception storage on vegetation, and ponded storage at the soil surface. When the evaporation rate under flux control has been satisfied, any excess water infiltrates the soil surface. INSTORE is the amount by which SMD is reduced, and ER_2 is the excess after SMD has been reduced to zero. A mathemetical summary of the model to calculate effective rainfall is given in appendix G.

5.2.2 Calculation of Recharge

Effective rainfall entering the top of the unsaturated zone eventually displaces a similar quantity at the bottom as recharge, although the two distributions will not be the same.

Headworth (1972) noted there was a delay between an effective rainfall and a groundwater response (and therefore recharge), which he termed the "response interval", and Harper (1975) termed as the "time lag". In the model, it is termed the DELAY time, and is taken to be a whole number of time steps.

The unsaturated zone is considered to act like a leaky reservoir, with input ER (displaced in time by DELAY), and output recharge. The concept of representing hydrological processes by reservoirs has been used by others (e.g. Nash, 1960). The outflow response from a single reservoir, having received an instantaneous unit input, is to decay exponentially as described by:

$$q = \frac{1}{K} \cdot e^{-t/K} \qquad (5.3)$$

where t is the time since the input, and K is the decay constant with units of time. The unit of time is equal to the length of one time step. The model uses this equation and assumes the effective rainfall to occur instantaneously at the start of the time step to which it refers. Assuming proportionality and superposition, and including the delay time, equation 5.3 gives the total recharge for the n^{th} step (see appendix H) as:-

$$RECHARGE_n = e^{-1/K}.\ RECHARGE_{n-1} + (1-e^{-1/K}).ER_{n-DELAY} \qquad (5.4)$$

This is an iterative equation which must be started by assuming an initial value of recharge well before the start of the calibration period, so that there are enough iterations to make the error due to the estimation of the initial recharge negligible. The number of iterations necessary before the start of groundwater level prediction, depends upon the effective rainfall distribution and the value of K. A value in excess of 5K iterations should be more than adequate.

5.2.3 Calculation of a Change in Groundwater Level

A change in groundwater level is calculated by solving equation 5.2. However, to do this, two other relationships are needed. The first relates a change in storage to a change in groundwater level. This is termed the specific yield, SY, which may vary with groundwater level, but is assumed to be constant for a given time step. Equation 5.2 is re-written as:

$$RECHARGE = DRAINAGE + (h_1 - h_0).SY \qquad (5.5)$$

where h_0 and h_1 are the groundwater levels at the start and end of the time step.

The second relationship relates the drainage to the storage. If drainage and storage are transformed by dividing by SY, they become the instantaneous rate of fall of groundwater level due to drainage

only, and groundwater level respectively. This relationship was derived by Thomson (1921 and 1931) and Headworth (1972) for locations in chalk. The drainage relationship was derived by the method used by Headworth (1972), and is described below.

The groundwater level record is examined for periods of falling groundwater levels. The mean fall in groundwater level per time step between readings is determined for the entire range of recorded groundwater levels. Each value of the rate of fall in groundwater level (groundwater recession) is then plotted against the mean groundwater level between readings. Ignoring the experimental errors, the plot must inevitably give a wide scatter of points due to the continued recharge lessening the recession rate. However, for any given groundwater level, the groundwater recession rate due to drainage alone, is the maximum rate at which the groundwater level will fall. An envelope curve drawn through the highest values of groundwater recession rate, gives the required relationship between groundwater level and groundwater recession due to drainage alone. The curve is approximated by a series of straight lines (Headworth, 1972) each of the form:

$$h = h_m - \frac{1}{RECESS} \cdot \frac{dh}{dt} \qquad (5.6)$$

where h is the groundwater level, h_m is the "minimum" groundwater level, and RECESS is a recession constant with units of 1/time.

The instantaneous drainage flow is:

$$q = -SY.\frac{dh}{dt} \qquad (5.7)$$

Rearranging equation 5.6 in terms of dh/dt and inserting in equation 5.7 gives:

$$q = SY.RECESS.(h-h_m) \qquad (5.8)$$

This shows that if the groundwater level varies linearly over the time step, then so does the instantaneous drainage flow. The total drainage for the time step is:

$$\text{DRAINAGE} = \left[\frac{q_1 + q_0}{2}\right] \cdot T \qquad (5.9)$$

where q_0 and q_1 are the instantaneous drainage flows for the start and end of the time step; and T is the length of the time step and equals one by definition. Substituting equation 5.8 in equation 5.9 gives:

$$\text{DRAINAGE} = \frac{1}{2} \cdot SY \cdot RECESS \cdot (h_1 + h_0 - 2.h_m) \qquad (5.10)$$

Substituting equation 5.10 in equation 5.5 and rearranging gives:

$$h_1 = \frac{\frac{RECHARGE}{SY} + h_0\left[1 - \frac{RECESS}{2}\right] + RECESS \cdot h_m}{\left[1 + \frac{RECESS}{2}\right]} \qquad (5.11)$$

This is an iterative equation which requires h_0 to be initialised. The values of SY, RECESS and h_m for each iteration are taken to apply to the groundwater level h_0. The time step may be of any length, provided the assumptions of a linear variation in groundwater level and a constant SY hold. The units of h_1, h_0, h_m and RECHARGE should be the same. A schematic view of the whole model is given in figure 5.2.

5.3 Use of the Model

The results of the application of the model to piezometric observations at Highcliffe are given in chapter 6. Some aspects of the application of the model are now discussed.

5.3.1 Time Step for Calculations

The groundwater level data (Thomson, 1986b) indicate that a time step of one day is necessary to satisfy the assumption of a linear variation in groundwater level. Howard and Lloyd (1979) presented evidence that the length of the time step also affects the calculation of effective rainfall. They found a significant difference between one day and ten day time steps. A one day time step has been used in this study.

5.3.2 Split Record Test

At least one year's data is needed to calibrate the model. It is not always possible to obtain unique estimates for the parameters (Gupta and Sorooshian, 1983). Therefore, a second year's data is used to test the calibrated solution, to ensure that the fit is still adequate. This is called a split record test, and has been used in this study with two years' data (October 1982 to October 1984).

5.3.3 Performance Criterion

Model performance was assessed objectively using a performance criterion (objective function). The one used here (CORREL) is the same as that proposed by Nash and Sutcliffe (1970), and is similar to one (U_7) used by Diskin and Simon (1977) in their comparison study of a number of objective functions.

$$\text{CORREL} = \frac{C1 - C2}{C1} = 1 - U_7 \qquad (5.12)$$

where $C1 = \Sigma(obs_i - \overline{obs})^2$; and $C2 = \Sigma(obs_i - pred_i)^2$

obs_i are the observed groundwater level data with mean $\overline{obs}$.
$pred_i$ are the predicted groundwater levels corresponding to the observed groundwater levels.

5.3.4 Model Calibration

Model calibration is made easier by some prior estimation of parameter values. The parameter D (figure 5.1) was set at a large fixed value and not optimised. The value of SY was assumed to be constant for all groundwater levels. An initial estimate of the drainage relationship was made using the method in Headworth (1972), as previously described in section 5.2.3. The parameters SY, K, DELAY, A, C, RUNOFF were optimised using an automatic procedure similar to the univariate method described in Beard (1967). A subjective graphical comparison of the observed and predicted recessions for the optimised parameter set was made. The drainage relationship was adjusted, and the optimisation procedure repeated until a satisfactory fit was obtained.

5.4 Discussion

5.4.1 Precision

There will always be some discrepancy between the observed and predicted outputs. These will be due to a combination of errors in the input and observed output data, approximations and assumptions made in the model, the size of the time step, and the choice of objective function. These sources are discussed below.

Ambiguity (in the pattern of groundwater level fluctuation between readings) and errors in the output data can be reduced by more frequent observations. In good conditions, groundwater level readings are repeatable to within $\pm$ 1 cm. However, sometimes the error may be greater due to adverse weather conditions and the use of two alternating observers. Errors in the input data may be observational, due to the method of measurement, or due to non-representativeness of the measurement. These were discussed in chapter 3. For

example, it is estimated that rainfall may be underestimated by as much as 10 per cent due to the method of measurement.

The runoff proportion can vary with rainfall intensity and surface moisture conditions. The assumption of runoff being a constant percentage of rainfall is an approximation. This should not lead to a significant error when runoff is small, such as on the cliff top. Rushton and Ward (1979) used a constant proportion of rainfall for a chalk catchment from which runoff was small (1½ per cent). Houston (1982) also used a constant proportion, but only for rainfall above a certain amount for the day. This reflected the dependence of runoff on rainfall intensity. Pirt and Bramley (1985) used an exponential function, where the runoff proportion increased with decreasing SMD. Increasing sophistication of runoff estimation inevitably leads to an increase in the number of parameters. This increases the difficulty of optimisation.

A number of alternative direct effective rainfall models are possible (Rushton and Ward, 1979). It is probable that the direct effective rainfall parameter A is not a constant, and varies with SMD and rainfall intensity. Therefore, direct effective rainfall could be estimated with increasing sophistication using similar functions as have been used for runoff. For example, Bergström and Sandberg (1983) used a power function where the direct effective rainfall component increased with decreasing SMD. Wellings (1984), for a chalk catchment, found that direct effective rainfall only occurred above a certain value of SMD. The parameter A has been held constant in this study so as to ease optimisation.

Many different SMD models have been used in the past. Calder et al (1983) and Alley (1984) compare different SMD models. Also, the shape of the function in figure 5.1 (or any other SMD model) will vary with soil type (due to different hydraulic properties of the soil) and evaporative demand (PE) (Thompson et al, 1981). This is

not normally taken into account, probably due to the necessity of increasing the number of parameters.

The method of estimating runoff and direct effective rainfall in the model can easily be altered, if desired, as can the choice of the SMD model. Alternatively, effective rainfall (and recharge) could be measured directly by lysimeter (e.g. Kitching et al, 1977, and Keating, 1984), or from profile moisture content and potential measurements (Freeze and Banner, 1970; Sophocleous and Perry, 1985; Steenhuis et al, 1985; Wellings, 1984), although this would require a large amount of field work.

The unsaturated zone is assumed to act like a single leaky linear reservoir. For deep groundwater tables, it may be better represented by a number of such reservoirs in series, as in the more general Nash (1957) model. Increasing the number of reservoirs has the effect of delaying the peak recharge. Thus, a specific DELAY parameter might not be needed in this instance. The effective rainfall is assumed to be instantaneous at the start of the time step, both for this study, and in the Nash model. Dooge (1960), for a single linear reservoir, assumed the input (effective rainfall) to be a constant rate throughout the time step. Using this assumption, the recharge is then a function of three terms: the (n-1)th recharge; the (n-DELAY)th effective rainfall; and the (n-DELAY-1)th effective rainfall. This involves slightly more calculation than using equation 5.4, as in this study. It is assumed that water movement in the unsaturated zone is downward, i.e. recharge is zero or positive. For shallow groundwater tables, recharge may also be negative (i.e. upward flow), as evaporation may occur directly from the groundwater table. The model does not allow for this situation.

The assumption of a constant specific yield, SY, with depth may be in error, especially in variable formations. Also, for shallow groundwater tables, Gillham (1984) found that the specific yield decreased as the groundwater table approached the soil surface. The inclusion of a variable SY would greatly complicate optimisation, unless there was a prior knowledge of the relative changes in SY with depth.

It is assumed that all the model parameters have constant values, i.e. they do not vary in time. This is unlikely to be true, but it is assumed that parameter variation is not great. The parameters K and DELAY are likely to vary seasonally. In summer, when the groundwater table is low, there is a greater depth of soil through which effective rainfall is transmitted to the groundwater table. This has the effect of increasing the parameter values. Also, in summer (when the groundwater table is low) the unsaturated profile is likely to be drier than in winter. This decreases the unsaturated permeability, and therefore increases the parameter values. The drainage relationship is optimised subjectively by comparing predicted and observed recession periods. The model assumes the same drainage relationship applies to rising groundwater levels as it does to falling groundwater levels. No independent method has been used to check the accuracy of the drainage relationship. Rehm et al (1982) measured the drainage from a groundwater table using nested piezometers and assuming vertical flow. Piezometers at other sites could measure lateral flow if present. However, large errors are likely where there are low hydraulic gradients in the direction of flow.

The longer the time step the greater the departure of the model from reality, e.g. that groundwater levels vary linearly, or that effective rainfall occurs instantaneously at the start of the time step. Also, Howard and Lloyd (1979) showed that the length of the time step affects the total amount of calculated effective rainfall. A shorter time step requires more input data and computer resources. A compromise has to be made, which inevitably introduces some error.

A number of different objective functions have been used by different researchers. "The form of the objective criterion (function) chosen will affect the values of the fitted parameters because each criterion of fit places a different emphasis on the

differences between measured and calculated values" (Ibbitt and O'Donnell, 1971). The choice of the objective function is subjective in itself. Diskin and Simon (1977) suggest, and used, a procedure for the selection of an objective function. This is beyond the scope of this study. The choice of automatic optimisation technique will also affect the fitted parameter values (Ibbitt and O'Donnell, 1971). The choice of calibration period will also affect the sensitivity of model parameters. Some parameters are only sensitive at certain times, or at certain groundwater levels. If these form only a small portion of the calibration period, the objective function will be relatively insensitive to parameter changes, which will affect the search for optimum values.

5.4.2 Other Models

A number of other models for simulating groundwater level fluctuations have been produced. Leach and Herbert(1982), Rushton and Rathod (1979), and Zucker et al (1973) solved the general groundwater flow equation using numerical methods. These require a knowledge of boundary conditions. Numerical methods also have stability and convergence problems, especially in thin unconfined aquifers (Faust and Mercer, 1980). Where this approach is not appropriate, others have been made.

Belmans et al (1983) solved the unsaturated groundwater flow equation using a one-dimensional numerical model. This was used to redistribute the moisture in the unsaturated zone (c.f. the transfer function used in this study). Then a water balance of the unsaturated zone (including rainfall and evaporation) gave the recharge term. The drainage term was calculated as a function of water level (as in this study, although a different type of function was used). The change in water level was calculated using a relationship similar to equation 5.5. Anderson and Pope (1984) also solved the unsaturated groundwater flow equation using a numerical method. They modelled the storm/groundwater response in a two-dimensional slope.

Rennolls et al (1980) and Viswanathan (1983) use time series models to relate rainfall to groundwater levels. Houston (1983) also used time series models, but also included other factors affecting the groundwater levels, such as pumping rates.

Bergström and Sandberg (1983) use a model that is a water balance approach to simulating groundwater levels. Their drainage relationship is mathematically equivalent to the one used in this study, but their calculation of effective rainfall is different, and they do not use a transfer function for recharge (except for one application where it is not stated mathematically). Hurley (1986) formulates two models using different approaches. One is a time series model, and the other is a water balance approach. The latter relates drainage to groundwater level, although the form of the relationship is different from that used in this study. Also, it does not use a transfer function, and the exact method of calculating effective rainfall is not specified.

The model of Sangrey et al (1984) is of particular interest in being developed for general landslide studies. It differs from the model presented here. Sangrey et al calculated effective rainfall as the value of rainfall minus potential evaporation, when positive (else zero), using a time step of one month. They did not include surface runoff or surface soil moisture storage effects. Their equation for the calculation of recharge was the same as here, (equation 5.4) except that they did not allow for a delay in groundwater response. They used a simple linear relationship between groundwater level and recharge, whereas here, a water balance has been used, so that equation 5.11 is a function of the groundwater level at the start of the time step as well as the recharge.

Canuti et al (1984) also use a linear correlation of groundwater level, but with the logarithm of a term they call the antecedent precipitation index (API) which is analogous to recharge. It is a measure of past rainfall. However, the API did not account for evaporation, and so gave high summer readings.

5.4.3 Groundwater Pressures

The model has been developed to simulate fluctuations in the level of the groundwater table. The model may also be used to predict groundwater pressures below the water table, which are influenced by the position of the water table. The specific yield, SY, would have to be redefined as a relationship between the recharge (or drainage) and the resultant increase (or decrease) in piezometric level if there was no drainage (or recharge). This is evidenced (see chapter 7) by data for some piezometric pressures in the Barton Clay at the test site which show a similar, but more damped, response to meteorological influences than does the water table in the Plateau Gravel. Harper (1975) presented evidence that suggested that piezometric pressures in confined aquifers may also be predicted from records of rainfall (although observations need to be adjusted to account for the effect of fluctuations in atmospheric pressure). He found that the plot of piezometric pressure versus recession rate was non-linear, but this could be approximated by a series of straight lines as suggested in section 5.2.3. The data Harper presents would need a time step of considerably less than one day. This would require the use of a continuously recording rainfall gauge. The diurnal variation of PE should be estimated, although a daily average could be sufficiently accurate.

Thus, the model can be used to simulate the piezometric pressure of any point below the water table, provided it is only influenced by meteorological and stable drainage conditions, other effects, such as tidal changes, atmospheric pressure changes, piezometric time lag, or land movement, have not been included. Due consideration for these effects would have to be made before applying the model.

5.4.4 Application of the Model to Landslide Studies

While the model has some general similarity with models used in the field of hydrology, such as the regional water balance models

(discussed by Alley, 1984) and recharge calculations for aquifers (discussed by Freeze and Banner, 1970; Howard and Lloyd, 1979; Keating, 1984 and Rushton and Ward, 1979 and others), it has been formulated particularly for use in landslide studies such as at Naish Farm. Sangrey (1982) and Sällfors and Svensson (1984) have drawn attention to the comparative neglect of studies of the temporal variations of water tables and pore pressures, despite their crucial role in slope stability. To remedy this deficiency, work has been done by Bertini et al (1984a and b), Canuti et al (1984), Hurley (1986), Sangrey et al (1984), Anderson and Pope (1984), and Anderson and Howes (1985). All but the first include modelling techniques (see section 5.4.2). Reasons for the lack of this type of study are the often complex hydrogeology; the short life expectancy of piezometers in areas of landslide activity; and the difficulty in relating groundwater levels to landslide activity, due to the latter subsequently affecting the former (a feedback effect). Therefore, many studies simply relate rainfall to landslide activity (e.g. Brand et al, 1984; and Canuti et al, 1985).

Three particular applications of the model presented here can be summarised as follows.

1. Prediction of groundwater levels resulting from meteorological changes. Owing to the delayed response of groundwater levels to rainfall events, the advance warning given by the meteorological observations could prove an advantage over direct piezometric readings (Harper, 1975; Barton and Thomson, 1984). If piezometric readings were being taken, they could be used to update the model. For example, (see figure 5.3) in a slope where the piezometric level goes above a certain level (hazard warning level), failure may occur. A model of the groundwater response will give a more objective prediction of the hazard. Rushton and Tomlinson (1980) showed the importance of accurately forecasting rainfall and evaporation.

2. Prediction of maximum likely, future groundwater levels. Given the continuity of the recharge/drainage conditions, then the meteorological records could be used to find the return period of any given groundwater level. However, care should be exercised when the groundwater level is outside the range used in calibration.

3. Prediction of groundwater levels at a particular time in history when an event occurred, for example, a slope failure (see figure 5.4). Back analysis is an important means of determining soil parameters in stability studies (Chandler and Skempton, 1974), and the accuracy of the result could be improved if the recharge/drainage conditions of the calibrated site were analogous to those that existed at the position of the failure plane prior to the failure.

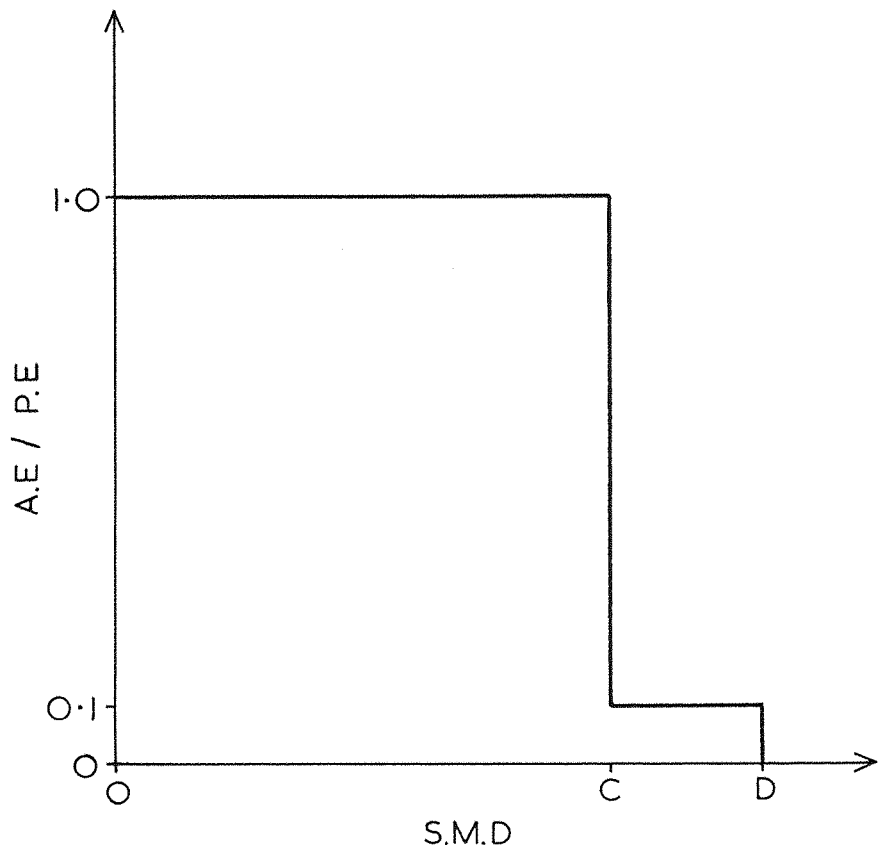

Figure 5.1 Relationship between AE and PE and SMD used in the model.

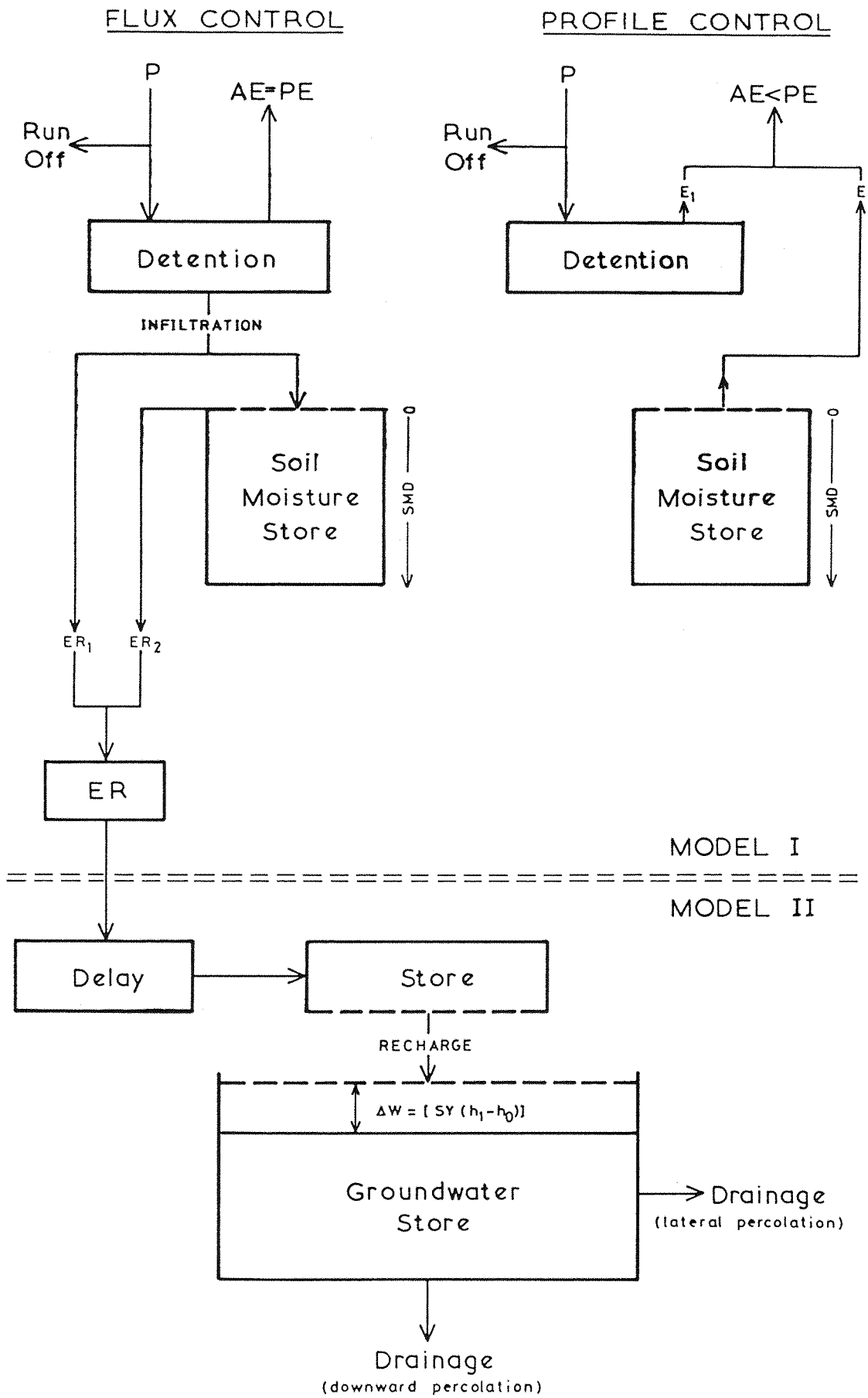

Figure 5.2 Schematic view of two-part model for predicting groundwater level response to meteorological changes.

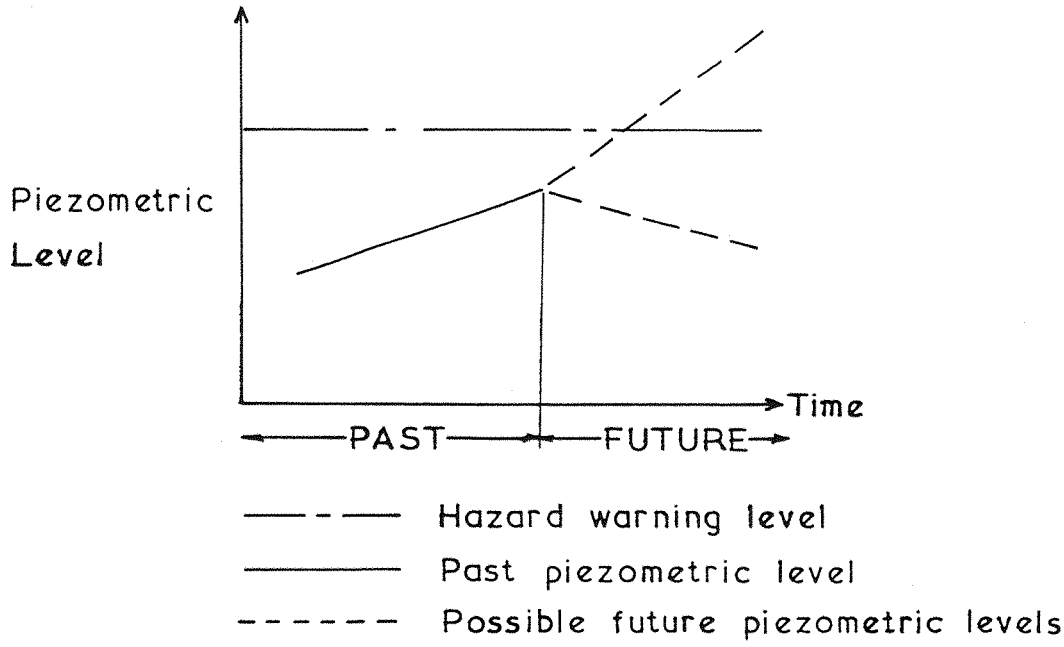

Figure 5.3 Model application for the warning of an impending slope failure.

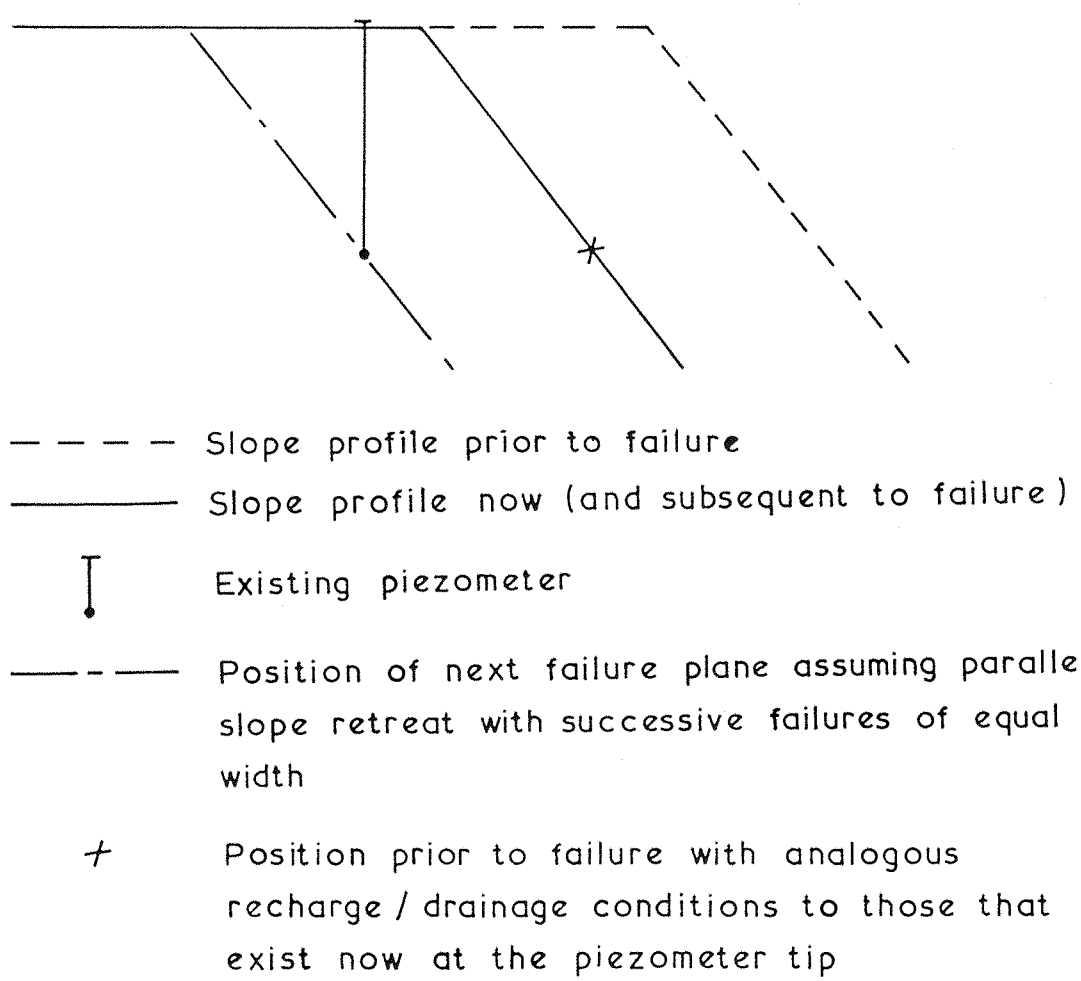

Figure 5.4 Model application for use in the back analysis of slope failure.

CHAPTER 6

PLATEAU GRAVEL DOMAIN

6.1 Introduction

A study of the areal variation of the base of the gravel was described in chapter 2. A discussion of the hydrological role of the Plateau Gravel (PG) domain in the undercliff water balance was given in chapter 4. Surface runoff is minimal and rainfall infiltrates to the groundwater table in the gravel. The groundwater in the gravel drains either to the Barton Clay (BC), to the undercliff colluvium, or to Chewton Bunny. In order to investigate this drainage, a number of groundwater level measurements have been made. This chapter describes these measurements and how they have been used to estimate the combined seepage to the undercliff colluvium and the underlying BC.

6.2 Groundwater Level Observations

The locations where groundwater level measurements have been made in the PG are shown in figure 6.1. Standpipe piezometers were used to monitor groundwater level and were generally installed to the base of the PG. Those installed below the base of the PG were backfilled with gravel so as to ensure that the groundwater level being measured was that of the PG. Borehole measurements, piezometer response tests, and groundwater level observations are all given in detail in Thomson (1986b).

As indicated by the observation period given in table 6.1 some piezometers were installed in October 1982 and some in January 1984. Readings were taken weekly up to 1st November 1984. For some isolated (never two in succession) weeks readings were not taken due to holidays or inclement weather. Sometimes, readings were taken more often, e.g. 28th December 1982 to 12th January 1983 and 18th March 1984 to 14th April 1984 when they were taken once or twice every two days. Readings were also taken on 5th December 1984 and 29th January 1985, but the groundwater table rose considerably after 1st November 1984 and, because these readings were infrequent, no certainty can be attached to their

reliability. This highlights the need to take frequent readings so that if a reading is in error it can be easily detected.

6.3 Fluctuations in Groundwater Observations

Groundwater level observations can be affected by a number of factors. It may be that more than one factor is operating at a given time. Fluctuation in observed groundwater level is caused by the influence of these factors varying in time. It is important to recognise these influencing factors in order to properly understand groundwater fluctuations.

It is considered that the only recharge is from rainfall. There are no streams, ponds, irrigation systems, or pumping of groundwater. Leakage from service pipes is possible although there is no evidence for the study area. Tidal variations are not considered to affect groundwater levels. Evaporation from groundwater is negligible unless the water table is near the ground surface (Todd, 1959,p 155). Todd presents data from White (1932) which would indicate that the depth of the groundwater table in the PG is sufficient not to be affected by evaporation.

Todd (1959, p 158) states that changes in atmospheric pressure have no effect on groundwater tables (unconfined aquifers). However, others have found that it does have a small effect. Turk (1975), working with fine grained aquifers, explained the effect as due to the presence of entrapped air in the capillary fringe. As the capillary fringe in gravel is very much smaller, Turk states that the fluctuation due to atmospheric pressure changes is probably smaller than field measurements would detect. Therefore, this is not considered a problem.

De Zanger (1981) observed exceptionally large rises in measured groundwater levels during heavy rainfall. This was due to a wetting front (surface layer of saturated soil) causing air

entrapment in the unsaturated zone. The ground air pressure is then greater than the standpipe (atmospheric) air pressure. To compensate for this difference in air pressure, the water level in the standpipe rises to a higher level than that of the groundwater table. The effect is short lived as the excess soil air pressure is soon released after rainfall stops (due to redistribution of moisture in the saturated surface layer). As it has not been possible to take measurements during heavy rainfall, this is not considered a problem. Also, the presence of the cliff face would speed the dissipation of excess soil air pressure.

When the volume of water needed to cause a change in the piezometer water level (in response to a change in groundwater level) is large in comparison to the rate of entry at the piezometer tip, there will be a time lag between the observed and true groundwater levels. To investigate this, falling head tests were conducted. The piezometers all gave fairly immediate responses (basic time lag, T (as defined by Hvorslev, 1951), less than 75 sec) except for P62 (T = 7 hrs) and P64 (T = 1 hr). Although every care was taken during piezometer installation, it is considered that the slow response for these two piezometers is due to clogging of the filter tip with fines. However, the response is still rapid enough for the readings not to need adjustment. The results of the response tests were not used to make any estimations of the gravel permeability as both the filter sand and the porous plastic piezometer tip are probably less permeable than PG.

The effect of meteorological variations on the groundwater levels in the PG can be seen from an examination of the water level record for P73 (figure 6.2). Other water level records (Thomson, 1986b) for piezometers installed in the PG show a similar pattern of groundwater level fluctuation. There are slight variations in the magnitude of the groundwater level rises; the timing of the peaks; and the steepness of the groundwater level recessions. The variation in magnitude of the groundwater level rises is indicated by the variation in range given in table 6.1. The timing of the peaks varies between piezometers by only a few days. To see the effect

of meteorological variations on groundwater levels, compare figure 6.2 with table 3.5 (which gives a measure of the wetness of individual months in the study period). October to December 1982 were wet* months and correspond to high groundwater levels. April to June 1983 were wet months and correspond to raised groundwater levels compared with before and after this period. December 1983 and January 1984 were wet months during which groundwater levels rose to a peak. The groundwater level peaks at the beginning of April 1984 and the end of May 1984 follow the wet months of March and May 1984. The wet months of October to December 1984 correspond to a rise in groundwater levels. It is clear from this discussion that rising and high groundwater levels occur during wet periods when rainfall is recharging the PG aquifer. Groundwater flow in the saturated zone (below the groundwater table) causes groundwater to discharge out of the PG. This is evidenced by the periods of falling groundwater levels. These occur during dry periods when rainfall recharge is minimal. Thus "groundwater level fluctuations can be conceived of as the cumulative effect of the net groundwater recharge - discharge processes" (Adamowski and Hamory, 1983).

The discharge process is influenced by the boundary conditions. Changes in the boundary conditions will affect the discharge and therefore the groundwater level. At Naish Farm changes in the boundary conditions of the PG occur when there is a cliff top slump. Therefore, inevitably groundwater levels will be intermittently affected by intermittent slumping. Figure 6.3 shows the size and position of slumps that have occurred in the study area between July 1982 and October 1985. Slumps A, B, D, E, F and G were relatively small slumps based on the F shear plane. The large slumps C and H were based on the D shear plane. The size of the slumps may be compared to those in the study of Barton et al (1983). The study area is within their zone B in which the average breadth and length of slumps was 2.3m and 8.5m respectively. This compares well with the smaller slumps but not

*For this discussion, a "wet" month is defined as one for which the probability of rainfall not exceeding the measured total is greater than 0.5, i.e. the measured total is greater than the monthly mean.

the larger slumps C and H which are larger than any in zone B of the Barton et al study. Thus, large slumps like C and H are unusual.

Slumps A and B occurred between 1st and 8th December 1982 which was just after the start of the observation period. They do not appear to have affected any groundwater level readings. Slump C started in January 1984 but only slowly moved down the cliff face until the July when a sudden large drop occurred. The only PG groundwater level record to be affected by the slump was P51 (see figure 6.4). However, it was not until the July that the groundwater level suddenly dropped. This was due to the gravel not being sufficiently exposed to affect the groundwater flow until the large drop in the July. All other slumps quickly moved down the cliff face (between site visits) to fully expose the PG. Slumps D and E occurred between 5th December 1984 and 29th January 1985. Their breadth is uncertain due to their being obscured by gravel debris (from subsequent spalling). It is not possible to say whether groundwater level readings were affected by these slumps as readings were only subsequently taken once (29th January 1985). Slumps F and G were obviously not fresh when observed on 31st October 1985. It is considered probable that they occurred soon after the previous site visit on 29th January 1985. Slump H occurred from 27-30th October 1985. As no readings were taken subsequent to the occurrence of slumps F,G and H, it is not possible to say whether groundwater levels were affected.

From the foregoing discussion it appears that groundwater level measurements in the PG have been relatively unaffected by cliff top slumping. Although the occurrence of slumps in the study area during the study period is limited, it appears that small slumps have had no significant effect on groundwater levels and that the large slump C has had only a limited effect (only P51). Thus, the affected groundwater levels are limited to those only a short distance (depending on the size of the slump) inland of the slump.

From this discussion it is clear that groundwater fluctuations in the PG are a result of variations in both meteorological and landslide influences. The latter is intermittent and has only significantly affected one groundwater level record during the study period.

6.4 Areal Variation of Groundwater Level Observations

Table 6.1 gives the observed range and the maximum and minimum recorded groundwater levels at a number of locations. They show that water was always present in most of the PG. Only near the cliff edge do groundwater levels fall below the base of the PG. This is evidenced by P61, P71 and P81 which were all about 10m from the cliff edge (see figure 6.1). The groundwater level at P61 falls below the base of the PG less often than at P71 and P81 because the base of the gravel is about 1m lower at P61 (see table 6.1). There does not appear to be any areal correlation of the range in groundwater level (see figure 6.1 and compare with the values in table 6.1). The variation in range is probably due to variation in specific yield which reflects the heterogeneity of the PG. Heterogeneity is further evidenced by the difference in range between P60 (range = 1.27m) and P62 (range = .97m) which are only 1m apart. On the other hand, maximum and minimum groundwater levels are areally correlated. They decrease toward the cliff edge. Parallel to the cliff edge, there is little variation (compare P63 with P73, and P60 and P62 with P72) except near the cliff edge (compare P61 with P71) where the level of the base of the PG greatly influences groundwater levels. Figures 6.5 and 6.6 show that on average groundwater levels are equal parallel to the cliff edge. However, there is a large amount of scatter which increases towards the cliff edge. Figures 6.7 to 6.10 show increasing groundwater level and decreasing scatter away from the cliff edge. The relationship between groundwater levels at different sites is hysteretic due to the difference in timing of a rise in groundwater

level. These differences can occur even over a very short distance as evidenced by figure 6.8.

Figure 6.11 shows various cross sections (see figure 6.1 for their location) through the PG domain. The PG/BC unconformity has been plotted from measurement at the cliff face (see figure 2.1) and in boreholes (figures given in table 6.1), and from the results of a resistivity survey (figure 2.10). The resistivity and borehole evidence tend to agree fairly well except in one or two instances, i.e. P52 and P73. These may be due to either the accuracy of the methods of estimating the level of the unconformity, or sharp local variations in level (e.g. due to involutions). This was discussed in Chapter 2. The groundwater level results (where available) are shown for three different dates, at high and low groundwater levels. When groundwater levels are low, they may fall below the base of the PG, especially near the cliff edge and where the gravel base is high. The slope of the groundwater table indicates groundwater flow toward the cliff face. However, on 1st February the slope was near horizontal for P71 to P72 and P81 to P82, and away from the cliff edge for P92 to P93. This may be due to the areally variable response to rainfall recharge (as evidenced by the difference in range between P60 and P62). This also explains the step in figure 6.11(B) in the groundwater table between P60 and P62 on the 1st February. On later dates (after the groundwater table had been falling for some time due to negligible recharge) the step between P60 and P62 is not evident. The groundwater level at P71 was approximately the same as that for P72 whilst the groundwater table was above the base of the PG. When the groundwater level at P71 fell below the base of the PG, the rate of fall of groundwater level was greater than that at P72 (i.e. the slope of the groundwater table increased). The results for P82 and P93 are limited so that comparison on other dates is not possible.

P93 is in a channel cut into the BC running NE-SW to the cliff face. The channel may be affecting the direction of groundwater

flow. Undulations in the unconformity may also be the cause of the near horizontal groundwater table slopes of P71 to P72 and P81 to P82. Any effect of undulation in the unconformity is likely to be greatest near the cliff edge where the thickness of saturated gravel is least. However, there are insufficient groundwater level measurements to establish the true effect of unconformity undulation on groundwater flow. Also, it was subsequently found that P93 contained an appreciable amount of sediment. The results for P93 should therefore be treated with caution (unfortunately, it was not possible to determine the basic time lag which is thought to be large). However, on 1st February the observed groundwater level was at a maximum. Therefore, the reading should equal the true groundwater level for that date (Hvorslev, 1951).

The low ground level near the cliff edge on figure 6.11(A) is part of a dry valley which runs NE-SW on the cliff top. The area of the dry valley near the cliff edge is covered in gorse bushes indicating the area to be wet, i.e. a high groundwater table. Barton (1984a) observed the drift deposit in this valley to be "a gravelly and clayey silty sand, up to 0.6m thick and very different in grading from the PG". This would affect the drainage of the PG. The drainage was improved after July 1984 by the large slump C (figure 6.3) which was part of this dry valley (see section 6.3). The improved drainage affected the groundwater level at P51 (which is shown on figure 6.4 to fall to the base of the gravel) but not significantly at P52. This shows that a slump has only a limited areal effect on groundwater levels.

Figures 6.12 to 6.14 show the groundwater contours on 1st February, 11th July and 12th September 1984 respectively. On the first date groundwater levels were high; whereas on the latter two dates they were low, and were before and after slump C affected gravel drainage. Estimates are shown on the figures of the areas where the groundwater level was below the base of the gravel. These are based on groundwater contours and unconformity level contours

(figure 2.10). There are insufficient groundwater level measurements to estimate contours over the whole of the study area. The contours are based on linear interpolation between piezometers. Some extrapolation to the cliff face has also been made. With so few measurement sites the exact location of the contours is unlikely to be accurate (especially those extrapolated to the cliff face). However, a rough indication of groundwater flow direction can be made. On all three dates groundwater flow is mostly perpendicular to the cliff edge except where it is affected by undulation in the PG/BC unconformity.

6.5 Modelling of Groundwater Level Records

The groundwater level response of piezometers in the PG is effectively immediate and is due mainly to variations in vertical recharge caused by meteorological changes (see section 6.3). Therefore, the model described in chapter 5 has been used to simulate groundwater levels. The groundwater level records that have been modelled are P61, P62, P63, P64.

6.5.1 Problems in Parameter Estimation

Optimisation was complicated by the presence of more than one optimal solution; interdependence of parameters; persistence; and the dependence of the solution on the initial parameter values, the order of parameters in optimisation, and the calibration period. This section discusses these problems. The comments are generally applicable to locations elsewhere, and not to just those in the PG.

6.5.1.1 Persistence

The objective function used is a form of least squares (of the difference between observed and predicted values) criterion. Clarke (1973) states the assumptions which should be met for the

application of a least squares criterion. He also states that "virtually all (hydrological) models give sequences of residuals (predicted minus observed output) which necessitate rejection of the assumption that they are mutually uncorrelated" (i.e. meaning that persistence occurs). Persistence exists in this model because the groundwater level is calculated as a function of the previous groundwater level (see equation 5.11). Thus, a part of the error in a predicted groundwater level is due to the error in the previously predicted groundwater level. Because of this, a performance criterion based on the minimisation of the squares of the errors is "not the most sensible objective function" and the interpretation of model parameters may be "fallacious" (Clarke, 1973). To overcome this problem, the optimised model is checked visually by comparing the predicted and observed recessions. The drainage relationship is then adjusted and the model re-optimised until the recessions are parallel. Alternatively, a different objective function could have been used. Sorooshian and Dracup (1980) present an objective function that allows for correlated errors (persistence). This procedure would require greater computation and therefore computer time. Whether the parameter estimation would be significantly altered would need further investigation.

6.5.1.2 Calibration Period

Some parameters may only affect the output at certain groundwater levels or at certain times of the year. Also, some parameter values may vary with time. Therefore, different calibration periods will place a different emphasis on the values of the individual parameters. Thus, each calibration period will produce a different set of optimal parameter values. Ideally, as the length of the calibration period increases, the optimum parameter values will converge to the same (consistent) "true" values. A long calibration period is not possible. However, the use of a split record test (see section 5.3.2) does increase the likelihood that a consistent solution is obtained. (A consistent solution is one that gives a good (optimal) prediction for all calibration periods.)

6.5.1.3 Parameter Interdependence

Mein and Brown (1978) found that parameter estimates were strongly dependent on each other. This dependency increased with increasing model complexity (number of parameters). Ibbitt and O'Donnell (1971) state that interdependence of parameters is a major weakness of the univariate method of optimisation (the one used in this study). Optimisation is slow and may not reach the true optimum. The method of optimisation used found a solution for which the objective function hardly varied (the last complete search of all parameters yielded an improvement in the objective function of less than 0.0005) in the parameter space. This is not necessarily the optimum and results showed clusters of solutions (depending on initial order and starting values of parameters in optimisation) around either optimums (global or local) or ridges (indicating parameter interdependence) in the objective function surface. Johnston and Pilgrim (1976) point out that local and global optima may be part of the same curved ridge. Clusters of solutions around what appears to be the same optimum indicate indifference of the objective function to the parameter values near the optimum. This indifference may be due to the form of the objective function or the model structure (the ability of the model to give the same simulated output when one parameter is perturbated by adjustment of the other parameters, i.e. interdependence). A different objective function may not only alter the indifference around the optimum solution, but also the optimum parameter values (section 6.5.1.1).

Parameter interdependence is not surprising considering the interconnected structure of the model (see figure 5.2). For example, if SY were increased, for the water balance to equate, it would be necessary to decrease runoff (RUNOFF) or evaporation (affecting parameters A and C). Because of the effect of interdependence, it has been found that the optimal solution depends

upon the initial parameter values and their order of optimisation. Johnston and Pilgrim (1976) and Mein and Brown (1978) also found that the initial parameter values affected the optimal parameter solution. The problem of parameter interdependency may be reduced by either reducing the number of model parameters (by prior estimation or measurement, or by simplifying the model structure so as to use fewer parameters); or by using other hydrologic time series data (e.g. effective rainfall or recharge data by using lysimeters). The latter was shown by Kuczera (1982) to improve the reliability of parameter estimates.

The effect of interdependency of parameters on optimisation was reduced by not optimising the parameter D (it was set at 100mm) and by estimating the drainage relationship from the observed recession curve. (The drainage relationship and SY are strongly interdependent.) This left 6 parameters to be optimised by the univariate search method. One of these (DELAY) gave consistent optimal values due to it only taking integer values. Thus, effectively there were 5 parameters which were interdependent in optimisation. Different initial parameter values and order of optimisation were used in order to ensure as far as possible that the global optimum was found. Also, the physical relevance of the parameter values and the comparison of values between sites was considered.

6.5.2 Parameter Estimation

Estimation needs to be made of the physically possible parameter values (bounding values) as well as the expected values for the sites being modelled (to provide initial estimates of parameters and to ensure realistic final solutions). The procedure of obtaining the parameter estimates is given together with a discussion of the optimised parameter values and their accuracy.

6.5.2.1 Bounding Values

Table 6.2 gives the maximum and minimum values of parameters and step sizes used in the automatic optimisation procedure. The maximum step size ensures that the optimum is rapidly located. The optimum is accurately located by reducing the step size progressively by half until it reaches the minimum value. This is small enough to ensure that changes in the objective function are negligible. The minimum step size is the accuracy to which parameters are estimated.

By definition the parameter SY must be between 0 and 1 and for computational reasons (see equation 5.11) it must not equal 0. Therefore, the minimum value of SY is equal to the minimum step size. By definition the parameter C must be between 0 and the value of the parameter D (100 mm); and the value of the parameter A must be between 0 and 1. The upper values of the parameters K and DELAY are arbitrary and may be greater for other groundwater level data. The lower value of K is arbitrary although for values as low as .5 it would probably be appropriate to use a time step smaller than one day. The minimum possible value of true runoff is zero. Negative values have been allowed so as to investigate bias errors in the rainfall. The minimum value of RUNOFF given in table 6.2 is arbitrary. Ibbitt (1972) showed that random errors in input and/or output data can affect parameter estimates. Dawdy and Bergmann (1969) found that both bias and time distribution errors in rainfall can affect parameter estimates. The latter occurs if the time step is too large and/or the rain gauge is too far from the site of interest. The rain gauge is considered to be close enough to the piezometers for this not to be a problem. Although the time step of one day was considered to be short enough, further work would be necessary to establish if a shorter time step would significantly alter parameter estimates. However, bias may well exist due to both the method of measurement (up to 10 per cent underestimation) and the spatial variation of rainfall (unknown) due to small scale topographic features (cliff edge, chalets, etc.) Errors in rainfall measurement were discussed in section 3.4. Runoff is calculated as a constant proportion of true rainfall.

Any bias (constant proportion) error in rainfall would be accommodated by the model as "runoff". As this bias may be negative, the parameter RUNOFF may also be negative.

6.5.2.2 Expected Parameter Values

To ensure that realistic parameter values are obtained from the optimisation process, some initial estimate has to be made of the parameters. Runoff has not been observed. Therefore, the value of the parameter RUNOFF is expected to be zero, or negative to allow for underestimation of rainfall. The groundwater response to rainfall is fairly immediate. Therefore, the value of the parameter DELAY is expected to be about 1 or 2 days. Because the peak groundwater response to rainfall occurs within about a week, the value of the parameter K is expected to be less than 7 days. By observation of the groundwater response in summer, the parameter A is expected to have some value greater than zero. The work of other researchers (Smith et al, 1970; Rushton and Ward, 1979) seems to suggest values of about 0.15 to 0.3 although their soils were different to those on the cliff top. The value of A is expected to be fairly consistent between piezometers. The value of the parameter C is given by Penman (1949) to be 100 mm for grass and 25 mm for bare ground. Thompson et al (1981) reduce the "available water" by an arbitrary 25 per cent for permeable soil. The soil on the cliff top in the study area is permeable and the grass cover variable, being very good in places and almost bare in others. The parameter C is a measure of the available water so that its value is expected to vary spatially between 20 and 75 mm depending on the grass cover. As discussed in chapter 4, the value of the parameter SY is expected to be at most between 0.09 and 0.14. This is based on measured drainable porosities which are considered to have been affected by evaporation and therefore to be greater than the true values. Other researchers (e.g. Nwankwor et al, 1984) have found that field values of SY may be very much lower than laboratory measured

values. Values should be obtained under the conditions for which they are to be used. In this study, it is from the natural groundwater table fluctuations as a result of meteorological changes.

6.5.2.3 Calibration Procedure

The data used for calibration was for the period from 1st November 1982 to 12th January 1984. A number of different initial values of parameters and their order of optimisation were used to obtain a number of solutions. The optimised solution was used to see if the drainage relationship was satisfactory (by comparing the plot of predicted and observed recession curves). If it was, then the solution was used to predict groundwater levels for the test period (12th January to 1st November 1984). These were compared with observed groundwater levels to check that the model was still giving a good prediction. This was also useful where there was more than one optimal solution with similar values of the objective for the calibration period. Finally, the solution was used as the initial values for re-optimisation using the calibration period 18th October 1982 to 1st November 1984 (all the data). This was done to check that the re-optimised parameter values were consistent with those of the shorter calibration period (see section 6.5.1.2). It may be noticed that data collected on 5th December 1984 and 29th January 1985 has not been used for parameter optimisation or verification. This is because they could not be checked for errors due to their being so infrequent.

6.5.2.4 Results and Discussion

The finally accepted parameter values describing the drainage relationships for each of the four piezometers are given in table 6.3. For the other parameters, the global optimal values for the calibration period, together with values of the objective function (CORREL) for the calibration period, test period, and for the whole data period, are given in table 6.4. Due to parameter interdependence (see section 6.5.1.3), some difficulty was encountered in

deciding on these optimum solutions.

6.5.2.4.1 Parameter Interdependence between SY and RUNOFF

The most significant interdependence was found to be between SY and RUNOFF. The value of SY multiplied by the drainage relationship gives the drainage component in equation 5.2. When the value of SY differs from the optimum the model tries to balance equation 5.2 by varying recharge. Over a long enough period of time, the change in soil moisture storage (Δ S in equation 5.1) is approximately zero and effective rainfall (ER) is equal to recharge. Rainfall (P) and PE cannot be changed by the model and during the winter AE equals PE. Therefore, the only component that can change (with the exception of A and C when an SMD is present) the amount of recharge is runoff. In fact, the optimum value of RUNOFF varies inversely with the value of SY. However, the greater the parameters differ from their "true" values the more rapidly the objective function diminishes in value. For short periods of time changes in the runoff component of equation 5.1 produce changes in the AE and Δ S components. This affects the amount and distribution of effective rainfall, and therefore recharge affecting the groundwater level. As the parameter values become more erroneous the prediction fit is increasingly affected and the value of the objective function is reduced.

The interdependence between SY and RUNOFF causes a ridge in the objective function surface. Figure 6.15 shows values of the objective function along the ridge for each piezometer. The optimisation method used quickly finds the ridge but then only slowly moves up it toward the global optimum. There is a limit to the increase in the value of the objective function at which the optimisation procedure stops. Therefore, the global optimum is not found. Instead, a number of solutions are found with similar parameter values except for SY and RUNOFF. The final values of SY and RUNOFF depend on the initial parameter values and order of

optimisation. Figure 6.15 was drawn by holding A, C, K, and DELAY constant and optimising SY for different values of RUNOFF. The global optimum was then found to be the maximum value of objective function in figure 6.15.

6.5.2.4.2 Parameter Interdependence between A and C

The parameters A and C were also interdependent. The parameter C exists to determine when the SMD is zero when there is an increase in the proportion of rainfall affecting the groundwater level. The parameter A exists so as to allow rainfall to affect groundwater level when an SMD is present. To some extent, the effect of the parameter A can be simulated by reducing the value of C (hence the interdependence). However, this would significantly affect the distribution of effective rainfall, such that the interdependence is not strong.

The interdependence between parameters A and C leads to two different sets of optimal solutions. Within each set, the parameter values were similar except for SY and RUNOFF. The two sets differed from each other by the values of A and C. During optimisation this was only a problem for P62. However, the solutions for P61 and P62 were found to be inconsistent (see section 6.5.2.4.4) due to different optimal values of A and C being found. Thus, the effect of inter-dependence depends upon the piezometer and the calibration period (if not long enough). P62 is discussed in more detail in section 6.5.2.4.3 and the inconsistency in both P61 and P62 is discussed in section 6.5.2.4.4.

6.5.2.4.3 Objective Function Surface for P62

As an example, the objective function surface for P62 is examined in detail. Although not the same, it is similar for the other piezometers.

Figure 6.16 is a contour map of the objective function in A and C parameter space (other parameters equal to the optimal values in tables 6.3 and 6.4). The loci of the optimal values of each parameter (whilst the other is held constant) cross at optimal solutions. Ideally, these lines should cross once at right angles. On figure 6.16 they cross twice: at the global optimum (A = .245, C = 53); and at a local optimum (A = .175, C = 34). Both pairs of values seem reasonable. The presence of two optima shows the interdependence of these parameters. Which optimum the optimisation procedure found depended upon the initial parameter values and order of optimisation.

Figure 6.17 shows the objective function contours for different values of SY and RUNOFF (other parameters equal to the optimal values in tables 6.3 and 6.4). The ridge in the contours shows that there is a strong linear relationship between these parameters. The model performs almost equally as well with any pair of parameter values along this ridge (see also figure 6.15). The locus of the optimal values of SY, whilst holding RUNOFF constant, is shown on the figure. Figure 6.15 shows the variation of the objective function value along this locus. The locus of the optimal values of RUNOFF for constant SY is virtually along the same path. Thus, once one parameter has been optimised, subsequent optimisations of both SY and RUNOFF produce only slight changes in parameter values, and hence objective function value. Thus, progress up the ridge is slow and is stopped short of the global optimum. This is a major problem of the univariate method of optimisation and why diagrams such as figures 6.15 and 6.17 should be drawn to investigate the presence of a ridge and locate the global optimum.

Figure 6.18 shows the change in the value of the objective function when parameters are individually perturbed about the optimal solution. The relationship at the local optimum is shown dotted for A and C. It is more peaked for C and flatter for A at the local than at the global optimum. This is because the value of C takes over some of the effect of the parameter A (see section 6.5.2.4.2). As more

data is influenced by a parameter, the relationship of figure 6.18 becomes more peaked. The contours of figure 6.17 show that the relationship of figure 6.18 for SY and RUNOFF along the ridge varies little in peakness. However, if interdependence were taken into account (as in figure 6.15) the relationship would be a great deal flatter.

Appendix I gives the results of a sensitivity (measure of peakness) analysis and enables comparison to be made with other piezometers. Comparison of values of S_1 (see appendix I for definitions of S_1 and S_2) gives a measure of the variation in peakness between different piezometers for each parameter. Comparison of values of S_2 gives a measure of the difference in peakness (or sensitivity) between different parameters. This is further discussed in section 6.5.2.4.5.

6.5.2.4.4 Consistency of the Parameter Solutions

A parameter solution is consistent if it is the same (or similar) for different calibration periods. The optimal solutions of table 6.4 were used as the initial parameter values for re-optimisation using all the data (18th October 1982 to 1st November 1984) for calibration. The new parameter values are given in table 6.5. The purpose of this is to investigate whether the shorter period from 1st November 1982 to 12th January 1984 is long enough for calibration, i.e. that it produces a parameter solution that is consistent with other calibration periods. If it is long enough, the parameter values should be similar and the values of CORREL(1) decreased slightly and CORREL(2) and CORREL(3) increased slightly between tables 6.4 and 6.5. For P61, however, this is not the case. Large changes in the value of CORREL have been caused by a change in the value of C. The slight decrease in SY and increase in RUNOFF (decrease in underestimation of rainfall) is due to a movement of the global optimum along the relationship between SY and RUNOFF.

For P62, parameter and CORREL values are similar. The increase in the value of C is due to the insensitivity of this parameter (see figure 6.18) at this solution. This indicates that the calibration period is long enough to define this optimal solution. However, there is no guarantee that the global optimum of the calibration period has not changed to a local optimum for the whole data period. This was investigated by using the local optimum for the initial parameter values in re-optimisation using the whole data period. It was found that it marginally became the global optimum (CORREL = .9509 as opposed to .9470).

Therefore, there is still some ambiguity as to the true solution. The optimum described by the solutions given in tables 6.4 and 6.5 is preferred because the value of A compares more favourably with the other piezometers.

The large changes in the values of CORREL for P63 are caused by a large change in the value of K. The true value of K varies with time. Therefore, the use of a constant value for the whole calibration period is only an approximate assumption. The fact that the optimal solution has changed shows that the calibration period is not long enough to estimate the long term average value of K.

For P64, a change in the optimal solution is signified by changes in the values of K, A and C and a shift in the relationship between SY and RUNOFF.

Some variation of optimal parameter values between different calibration periods is inevitable. This is due to the sensitivity of the parameters (see appendix I) and the fact that the model is only an approximation of nature. The longer the calibration period, the smaller this variation should be (i.e. parameter estimates should be consistent) for the "true" optimal solution. From this brief investigation, it appears that the calibration period is not long enough to give "reliable" estimates of the

long term average parameter values; or to resolve the ambiguity over the different optimal solutions of A and C. The effect of errors in the parameter estimates will be considered later in the application of the parameter solution to estimating the groundwater seepage from the PG.

6.5.2.4.5 Sensitivity and Values of the Parameter Estimates

Table 6.4 gives the values of the parameter estimates and appendix I summarises the results of a sensitivity analysis. Comparison of S_2 values (in appendix I) gives a measure of the difference in sensitivity between different parameters.

The most sensitive parameter is SY. However, this sensitivity is considerably reduced if the interdependence with RUNOFF is taken into consideration (compare SY and SY*). The value of SY varies widely between .043 and .092 indicating the heterogeneous nature of the PG. The value of C varies between 25 (or 17 if the whole of the data period is considered) and 64mm and is the expected reflection of the differing grass cover at the four sites (the grass cover becomes poorer toward the cliff edge, probably due to greater pedestrian traffic). It is of about the same sensitivity as A except for P62 for which it is considerably less sensitive. The value of A is fairly constant although it appears to have some spatial correlation with the value of C. At P63 and P64 where there is better grass cover (higher C value) the value of A is about .33; whereas where the grass cover is poorer (at P61 and P62) the value of A is slightly less at about .25. The value of K varies spatially between 1.5 and 4.7. This may be partly due to temporal variation of the parameter value (see section 6.5.2.4.4, paragraph 3) such that a much longer calibration period would yield less spatial variation. The parameter DELAY takes values of 1 or 2 days indicating the rapid groundwater response to rainfall. The relatively large change in the value of the objective function as a result of the minimum possible parameter perturbation seems to indicate the need to reduce the length of

the time step, at least for the routing of effective rainfall to recharge.

The combination of surface runoff and under/overestimation of rainfall determines the true value of RUNOFF. Surface runoff has not been observed and is thought not to occur except perhaps during intense rainfall near the cliff edge where the ground is barer and has a greater slope (see figure 6.11(B)). It is therefore considered that the value of RUNOFF is due to the under/overestimation of rainfall. The RUNOFF values vary between -0.1 and 0.01. These represent not unexpected errors in rainfall measurement (see section 3.4) although they do represent a large spatial variation. RUNOFF is one of the least sensitive parameters (along with K and DELAY). This is made worse by the interdependence with SY (compare RUNOFF and RUNOFF* in appendix I). Figure 6.15 shows that for large changes in RUNOFF there is little variation in the value of the objective function. Due to this indifference, it is by no means certain that the optimum along the ridge represents the "true" value of RUNOFF. A different objective function or calibration period, or even slight data errors, could easily result in a different global optimum along the ridge. Therefore, no firm conclusion can be made about the spatial variation or amount of under/overestimation of rainfall. However, figure 6.15 does suggest that rainfall is probably slightly overestimated at P63 and underestimated at P61, P62 and P64. Further inspection of figure 6.15 also shows that it is by no means certain that RUNOFF does not take a value of zero. The reduction in the value of the objective function (as compared to the global optimum) in doing so is .0033, .0015, .0001, .0045 for P61, P62, P63 and P64 respectively. These are relatively small differences when compared to those between tables 6.4 and 6.5 as a result of parameter optimisation using different calibration periods.

Now, if the hypothesis is that rainfall is neither underestimated nor overestimated and that surface runoff is zero (i.e. RUNOFF is areally constant and equal to zero), what is the significance of the RUNOFF estimates for the four piezometers? The hypothesis

of spatially constant value cannot be tested. It is assumed that any variation is random and not spatially correlated. However, the mean of the sample (-.0475) can be tested to see if it is significantly different from the zero population mean of the hypothesis. The unbiased sample estimate (s) of the population standard deviation is .045. Assuming the test statistic t (= $\overline{\text{RUNOFF}}$. $\sqrt{n}$ /s, where $\overline{\text{RUNOFF}}$ is the mean of the sample size n) to be t-distributed with n-1 degrees-of-freedom, there is a greater than 5 per cent probability of the mean of any sample being less than -.0475 given that the population mean is zero. Thus, the sample mean of -.0475 is not significantly different from zero. Subsequent use of the model in this thesis will assume RUNOFF to be zero but will consider the possible error in the results due to this assumption. Due to interdependence, the value of SY also needs to be changed (from the values given in table 6.4). The parameter values for subsequent use are given in table 6.6. The new values of SY do not change the large spatial variation that exists in the PG as remarked in the second paragraph of this section.

6.5.2.4.6 Spatial Variation of the Objective Function Value

The value of the objective function decreases toward the cliff edge. This is probably due to the assumptions of the model being less valid near the cliff edge. The most likely cause is that the drainage relationship is not constant in time. A constant drainage relationship means that the net groundwater flow out of a vertical element of the PG aquifer (excluding recharge) is uniquely given by the groundwater table level. But the groundwater flow into and out of the element depends upon the hydraulic gradient and therefore the surrounding groundwater levels. Therefore, for the drainage relationship to be constant in time the groundwater level must be uniquely related to the surrounding groundwater levels. Figures 6.5 to 6.10 (also see section 6.4) show that the scatter of the groundwater level with the surrounding groundwater levels increases toward the cliff edge. Therefore, the drainage relationship nearer

the cliff edge will be less constant in time and any prediction subject to a greater error, which explains the decrease in the value of the objective function toward the cliff edge.

6.5.2.4.7 Drainage Relationship

Figures 6.19 to 6.22 show the drainage relationships described by the parameter values given in table 6.3 for each of the modelled piezometers. The error bars assume a possible reading error of water level of $\pm$ 1cm. The relationship does not form a complete envelope as theoretically it should (see section 5.2.3). This is a further indication that the relationship is variable in time. It is probably hysteretic, varying for different periods of rising and falling groundwater levels. The relationship the model uses is the average rate of recession of the groundwater table during the data period. The average relationship for rising groundwater levels is probably different. To ensure that the groundwater level is still adequately predicted, the model will tend to adjust the other parameters, e.g. SY so as to balance the water balance equation, and K so as to alter the distribution of recharge (and therefore drainage). Although this may give a good prediction of groundwater level, it will not necessarily give an accurate prediction of the distribution of the drainage component of the water balance. This is relevant in respect to the accuracy of using the model to predict seepage from the PG.

6.5.2.4.8 Model Results for the Data Period

Figures 6.23 to 6.26 show the observed and predicted groundwater levels for each of the four piezometers using the parameter values in tables 6.3 and 6.6. The differences between the observed and predicted groundwater levels result not only from the difficulty in finding the optimal solution, but also from data errors, and the fact that the model uses assumptions and approximations in order to simplify the representation of nature (see section 5.4.1).

However, the general pattern of groundwater level fluctuation is still predicted. The range, peaks, and recessions in groundwater levels are generally well predicted. Therefore, the model is considered to be a good simulation of the groundwater response to meteorological fluctuations. Also shown on the figures are the distributions of rainfall, effective rainfall, recharge, and drainage. The large increase in drainage flow at high groundwater levels is due to seepage at the cliff face. The fairly constant drainage flow throughout the year is due to leakage into the Barton Clay (between the piezometer section and the cliff edge).

Due to the uncertainty of the parameter estimates (see section 6.5.2.4.4), the "true" parameter values may not have been found. In particular, the assumption of zero RUNOFF may be in error (see section 6.5.2.4.5, paragraph 3). This produces little change in the error in groundwater level prediction due to the interdependence of RUNOFF with SY. However, if there is a shift in the relationship between RUNOFF and SY then errors in groundwater level prediction will occur. There is evidence of this for P64 (see section 6.5.2.4.4). The shift was equivalent to an increase in RUNOFF by .03 (for any given value of SY). The effect of this sort of change for the whole data period is shown in figure 6.27 for P62. Also shown is the effect of using the different optimal values of A and C (see section 6.5.2.4.3).

Figure 6.27 shows that a shift in the SY/RUNOFF relationship causes a slight underestimation (or overestimation depending on the direction of the shift) of groundwater level throughout the data period. The predicted groundwater levels using the lower values of A and C only differ from those using the higher values during late summer and early winter. The lower value of A reduces the groundwater level recovery whilst an SMD is present. The large rise in groundwater level at the start of winter occurs sooner using the lower value of C because the SMD is more rapidly reduced to zero.

6.5.3 Application of the Model for the Prediction of Groundwater Levels

Figures 6.28 to 6.31 show the predicted groundwater levels for the period August 1980 to December 1985 for all four piezometers. The groundwater level prediction assumes that the position of the cliff edge remains static. From figure 6.3 it can be seen that this is not the case. This may cause considerable error in the prediction of the groundwater level at the various locations (especially in the vicinity of a slump). However, the figures do represent the relative response and height of the general groundwater table at different periods. It should be noted that the model is only really applicable to the groundwater level range for which it was calibrated. Groundwater levels outside this range should be treated with caution as extrapolation of the drainage relationship may well be in error. However, for the period in the figures the predicted groundwater levels were inside the calibration range except for the maximum groundwater level at P61 (see figure 6.28).The initial groundwater level was estimated as the average for the time of year. The initial SMD was estimated as equal to the value of the parameter C. Any error due to these estimates should rapidly become minimal and certainly by the first winter (when SMD equals zero). Further investigation would be needed to establish how long these estimates significantly affect the predicted groundwater level. The predicted period of the figures is too short to calculate the return period of groundwater levels as suggested in section 5.4.4. Further investigation using much longer data periods would be necessary to perform this sort of analysis.

6.6 Calculation of Seepage from the Plateau Gravel

Water drains from the PG both downwards into the BC and laterally at the cliff face and Chewton Bunny. In this study, it is the seepage to the undercliff that is of interest. Leakage to the BC may still reach the undercliff and is discussed in the next chapter. Therefore, it is the combined seepage to both the cliff face (in the study area) and the BC that is calculated in this section.

Seepage to the undercliff is part of the water balance of the undercliff. In consideration of measures to drain and improve the stability of the cliffs, it is important to establish the sources of seepage and to quantify their amounts (i.e. establish their significance). Seepage from the PG to the undercliff could be reduced by the installation of a cut-off drain (Barton and Thomson, 1986c). The significance of the leakage to the BC which might bypass such a scheme is considered in the next chapter. The significance of a cut-off drain in reducing seepage to the undercliff is considered in chapter 9.

6.6.1 Estimating Groundwater Flow

Direct measurement of groundwater flow would require it to be intercepted throughout the thickness of saturated flow. This would be impractical for anywhere other than at the cliff face. A suitable apparatus would be similar to one shown in figure 3.5 in Atkinson (1978) which was taken from Whipkey (1965). However, there is a limitation on the length of the cliff face used such that the measurement may not be very representative. Also, the apparatus would be highly susceptible to vandalism which is a major problem at the site.

Due to the problem of measuring seepage flow directly, it is usually estimated indirectly by relating it to other measured physical quantities (in this case groundwater levels and the temporal pattern of rainfall and potential evaporation). The parameters of this relation need to be estimated either by direct measurement or modelling. A model is used to simulate groundwater level and the parameters adjusted until the simulated groundwater levels compare favourably to the observed ones. The seepage flow is related to the pattern of groundwater levels. Using the measured or modelled parameters the seepage flow can be estimated from the groundwater levels.

Rushton and Redshaw (1979) give a number of techniques available for the study of groundwater flow. However, only the mathematical

models technique is appropriate to problems involving moving groundwater tables (such as in this study). Mathematical models use either digital or analog computers. The former is more commonly used as it is more flexible and does not require the knowledge of specialised electronic equipment. Digital mathematical models, with appropriate initial and boundary conditions, simultaneously solve the equation of groundwater flow at a number of distinct positions (nodes) in time and space. The problem is normally simplified by making various assumptions which inevitably limits the accuracy of the solution. However, with fewer assumptions it is necessary to have more geohydrologic input data. The accuracy of the solution is then dependent on the accuracy of the input data. Thus, the level of sophistication (lack of assumptions) of the method chosen depends upon the specific problem and the accuracy and availability of geohydrologic input data (Prickett, 1979).

The groundwater flow equation is a differential equation (e.g. see Mercer and Faust, 1980) which is commonly solved using either finite difference or element methods (e.g. see Faust and Mercer, 1980). This requires a discretised grid with a large number of nodes in space and (for time variant problems such as in this study) time. Groundwater levels are simulated at each node. The problem in this study is complicated by the fact that it is a thin unconfined aquifer (saturated gravel). The undulating unconformity and the large fluctuation in groundwater level (relative to the aquifer thickness) cause severe non-linearity in the differential equations which leads to solution convergence problems (Faust and Mercer, 1980). Even if this problem is overcome, a considerable amount of input data is required. Initial groundwater levels and boundary (including their movement) conditions are needed. The position of the groundwater divide is believed to be a function of the groundwater level (see section 6.6.2). The cliff face does not always represent a groundwater boundary. This is due to significant leakage to the BC during dry periods. Figures 6.11 to 6.14 show that the groundwater table intersects the base of the gravel at different distances from the cliff face both areally (for the same

date) and temporally (for the same section line). The areal variation is due to undulations in the PG/BC unconformity. The recharge, gravel permeability and specific yield, and the leakage to and level of the PG/BC unconformity need to be specified at each node. Much of this input data could be approximated or simplified without serious error (e.g. recharge, permeability, and specific yield could be considered constant over large areas of the aquifer). However, a considerable amount of input data (upon which the accuracy of the model is dependent) is still needed. Also, the accuracy of the model can only be checked by the limited groundwater level data available. Thus, it was felt that a sophisticated model which solves the differential equation of groundwater flow for a large number of points is not warranted. An alternative procedure was adopted and is now described and then compared to the more rigorous differential equation of groundwater flow.

Equation 5.2 is the water balance at the groundwater table: RECHARGE is the flow of water to the groundwater table from the unsaturated zone; DRAINAGE is the flow of water from the groundwater table to the saturated zone; ΔW is the net flow to the groundwater table and is assumed proportional to the change in groundwater table level. The model described in chapter 5 calculates the DRAINAGE component as a unique function of the groundwater table level. Assuming the aquifer to be incompressible, an equal quantity of water must flow out of the vertical aquifer element at the location where equation 5.2 is applied. This flow is either lateral or as leakage to the BC. If this DRAINAGE flow is assumed to be representative of an area of the aquifer the total seepage out of the gravel can be estimated. The drainage relationship at each of four locations has been established (see figures 6.19 to 6.22) and used to estimate groundwater flow out of the PG. More details of the method and results are given in the next three sections. Before that, however, a comparison is now made with the more rigorous general groundwater flow equation.

Equation 6.1 is the groundwater flow equation for an unconfined

aquifer assuming that the slope of the groundwater table is small; vertical components of flow are negligible; the average potential (in the vertical) is equal to the potential at the groundwater table; DRAINAGE (i.e. flow into the aquifer) is immediately distributed throughout the depth of the aquifer; the confined storage coefficient is very much smaller than the specific yield.

$$\frac{\delta}{\delta x}\left(m.K_x.\frac{\delta h}{\delta x}\right) + \frac{\delta}{\delta y}\left(m.K_y.\frac{\delta h}{\delta y}\right) = SY.\frac{\delta h}{\delta t} - RECHARGE(x,y,t) \qquad (6.1)$$

where x and y are the horizontal space coordinates; t is time; SY is specific yield; K_x and K_y are the permeabilities in the x and y directions; m is the aquifer thickness; h is the potential or groundwater table level.

Equations 5.2 and 6.1 are comparable in that the spatial differential part (left hand side) of equation 6.1 is equivalent to the DRAINAGE term of equation 5.2. The model in chapter 5 calculates the DRAINAGE as a unique function of the groundwater table level, whereas equation 6.1 calculates the equivalent component as a function of the water level (as m) and the spatial rate of change in slope of the groundwater table (in effect the surrounding groundwater levels). This is because the derivation of equation 6.1 uses the slope of the groundwater table (Darcy's Law) to describe the groundwater flow into and out of an aquifer element. Equation 6.1 is therefore a more rigorous and proper method of describing the groundwater flow. However, as already mentioned, equation 6.1 is probably too difficult to apply to the PG due to non-linearity problems (due to the variation in the value of m both in space and time). It is also considered that the necessary input data (such as permeability and the positions of the unconformity and the groundwater divide) is either lacking or not accurate enough to justify such a sophisticated model.

6.6.2 Estimation of the Groundwater Catchment

The cliff top groundwater catchment area for the PG was discussed in chapter 4. It was assumed that groundwater flow in the PG was perpendicular to the discharging surface (cliff face or Chewton Bunny). Figures 6.12 to 6.14 show that this is approximately so, although there are some slight variations due to undulations in the PG/BC unconformity. The geohydrologic information is insufficient to include these variations in the estimation of the groundwater catchment. For simplicity, it is assumed that the flow lines are toward the cliff face and are parallel to the line through P61 and P64. The east and west boundaries of the groundwater catchment are given by two such flow lines (figure 6.1). These define the length of the cliff face (and therefore catchment area) contributing seepage to the undercliff. This length of the cliff face is defined by the area of the undercliff to which the water balance in chapter 9 is applied.

In chapter 4, the groundwater divide was estimated as being equidistant (along the flow lines) between the average line of the cliff face and the 28.5m contour along Chewton Bunny. This assumed that the PG/BC unconformity was horizontal and at a level of 28.5m O.D. However, it was discussed in chapter 2 that the unconformity slopes downwards as it nears Chewton Bunny. This makes it difficult to determine the position of the outflow boundary along Chewton Bunny. This results in error in the estimation of the position of the groundwater divide.

To improve on this estimate, it was decided to fit a suitable curve to the groundwater level data and so find the position of the groundwater divide along a line through P61 and P64. The method used is described in appendix J. Figures 6.32 to 6.35 give the results. Complications arise in making a reliable estimate when recharge is taking place. This causes a wide scatter in the results although on average they do agree fairly well with the position given in figure 6.1 (177m from the cliff face). The figures appear to show a clear relationship between groundwater level and the position of the groundwater divide. This might be

due to the Chewton Bunny boundary moving toward the Bunny as the groundwater levels rise. Thus, the midway position between the two boundaries (groundwater divide) will also move toward the Bunny. It might also be because as groundwater levels rise the drainage conditions at the cliff face become increasingly better than those at Chewton Bunny. This is due to more of the cliff face being used as a drainage outlet at higher groundwater levels (see figures 6.12 to 6.14). As water will flow toward the easiest outlet, a much greater gravel area will drain toward the cliff face at higher groundwater levels. Thus, probably due to a combination of the above reasons, the distance of the groundwater divide from the cliff face increases with groundwater level. The form of the relationship is unknown and the scatter in figures 6.32 to 6.35 too great to suggest anything other than a straight line. Therefore, as an approximation a straight line relationship has been assumed. The figures give the 95 per cent confidence limits which show that the regression line is significant.

The straight line relationship is used to estimate (for each time step of the calculations) the position of the groundwater divide along the line through P61 and P64. The proportional increase or decrease in the position of the groundwater divide with respect to that shown in figure 6.1 is assumed constant for all flow lines (lines parallel to the one through P61 and P64). Thus, the proportional increase in the catchment area is equal to the proportional increase in the position of the groundwater divide.

6.6.3 Estimation of Gravel Drainage

Using the parameters given in tables 6.3 and 6.6, the model described in chapter 5 was used to calculate the groundwater level and DRAINAGE component for each day at the locations P61, P62, P63 and P64. The former is used to calculate the position of the groundwater divide; the latter is used to calculate the drainage from the line extending (through P61 and P64) from the cliff face

to the groundwater divide. This is then used to calculate the total drainage from the catchment area for each day.

The model in chapter 5 calculates the groundwater level at the end of each time step (day) whereas the DRAINAGE is calculated as a volume for the whole time step. As the groundwater level varies linearly through the time step (assumption made in section 5.2.3), the position of the groundwater divide does the same (due to the assumption of a linear relationship between groundwater level and the position of the groundwater divide). Thus, the average position of the groundwater divide is calculated from the average groundwater level using the appropriate relationship (figures 6.32 to 6.35). This gives four estimates of the position of the groundwater divide from which the weighted average (GWDPOSITION) is calculated. The weighting is calculated from the relative values of the coefficient of determination of figures 6.32 to 6.35 (.547, .496, .476, .585 respectively).

It is assumed that the catchment area represented by each piezometer is proportional to its representative length along the line through P61 and P64. Therefore, the drainage from the total catchment area (CATCHMENTDRAINAGE) is proportional to the drainage from the line through P61 and P64 (LINEDRAINAGE). Representative lengths along the line through P61 and P64 are assigned to each piezometer. They are based upon the catchment boundaries (cliff face and groundwater divide) and the mid positions between piezometers and are given in table 6.7. The DRAINAGE from each piezometer is multiplied by its representative length and summed to give LINEDRAINAGE. Let AREA be the catchment area; REFERENCEAREA be the area of the catchment in figure 6.1 (19119m^2); GWDREFERENCEPOSITION be the reference position in figure 6.1 of the groundwater divide along the line through P61 and P64 (177m). Each piezometer represents the same proportional length of a flow line for all flow lines. This means that the total drainage from a flow line is proportional to its length. Thus, the total gravel drainage is given by:

$$\text{CATCHMENTDRAINAGE} = \text{AREA} \times \frac{\text{LINEDRAINAGE}}{\text{GWDPOSITION}} \qquad (6.2)$$

It was stated in section 6.6.2 that the proportional increase in the catchment area is equal to the proportional increase in the position of the groundwater divide. Therefore, the catchment area is given by :

$$\text{AREA} = \frac{\text{GWDPOSITION}}{\text{GWDREFERENCEPOSITION}} \times \text{REFERENCEAREA} \qquad (6.3)$$

Substitution of equation 6.3 in equation 6.2 gives :

$$\text{CATCHMENTDRAINAGE} = \text{LINEDRAINAGE} \times \frac{\text{REFERENCEAREA}}{\text{GWDREFERENCEPOSITION}} \qquad (6.4)$$

Equation 6.4 is used to calculate the total gravel drainage for each day.

Figures 6.13 and 6.14 show that at low groundwater levels large areas of the PG become dry. Where the PG is dry, it is necessary to allow the rainfall recharge to become drainage. The model described above allows drainage to occur even when the PG is dry and no recharge is taking place. This is done to simplify model calculation (i.e. the need to calculate the area of dry gravel as a function of groundwater level). This means that at low groundwater levels the distribution of CATCHMENTDRAINAGE is slightly different from that of the "true" total gravel drainage. However, the CATCHMENTDRAINAGE distribution is more relevant to the calculation of the distribution of seepage to the cliff edge. This is because it allows for change in storage in the BC. The values of SY and the drainage relationship for the BC will be different from those in the PG. However, any errors will be in distribution, and as the relevant values of drainage are small anyway, this is not considered to be significant.

6.6.4 Discussion of Results

The estimated groundwater seepage out of the PG (gravel drainage) from August 1980 to December 1985 is given in figure 6.36. Gravel drainage can be split into two components : leakage into the BC; and seepage at the cliff face. Gravel drainage occurs throughout the year due to the continual presence of leakage. Thus, the smaller values of gravel drainage in figure 6.36 (predominantly during summer) are due to leakage into the BC. The larger values (predominantly during winter) are due to both leakage and seepage at the cliff face. The summer of 1981 was unusually wet (see table 3.5) which explains the exceptionally high gravel drainage at that time. The large and rapid fluctuations at high values of gravel drainage shows the great sensitivity of seepage at the cliff face to groundwater levels in the PG. The partitioning of gravel drainage into leakage into the BC and cliff face seepage is considered in chapter 7. The effectiveness of a possible cut-off drain installed on the cliff top will then be discussed. However, it can be seen from figure 6.36 that such a drain would intercept considerable quantities of water which would otherwise reach the undercliff.

When considering values of gravel drainage such as those given in figure 6.36, it is important to consider the possible errors in their estimation. The most important errors are those in the size of the peaks and in their timing. Unfortunately, it is not possible to measure gravel drainage directly. Therefore, no direct comparison can be made. However, errors can be investigated by looking at the effect of possible errors in the model itself or the input data. Sources of possible error are : the estimation of the catchment area; the estimation of the input variables (meteorological data); the ability of the model in chapter 5 to accurately estimate drainage from a vertical element of the aquifer; the representativeness of the four piezometers used in the calculations. These are now discussed in turn.

Estimating the catchment area involves the positioning of three boundaries. The fourth boundary (the cliff face) may also lead to error but this is small (see section 6.6.3). Two of the boundaries are assumed to be flow lines and parallel to the line through P61 and P64. The flow line assumption is made so that flow across the boundary can be assumed to be zero. As discussed in section 6.4, figures 6.12 to 6.14 show this to be only an approximation. The possible errors are not estimated here but are recognised. The third boundary (the groundwater divide) is examined and may be used as a guide to the effect of errors in the other boundaries. Figure 6.36 shows the effect of assuming the position of the groundwater divide to be constant and as shown in figure 6.1. Only the amount of gravel drainage is affected and not the pattern of fluctuation. The use of a constant position of groundwater divide overestimates the catchment area at low groundwater levels and underestimates it at high groundwater levels (see figures 6.32 to 6.35 and compare with the constant boundary distance shown in figure 6.1 of 177m). This leads to a corresponding overestimate (at low groundwater levels) and underestimate (at high groundwater levels) of gravel drainage. Figure 6.36 shows that the errors are only large at high groundwater levels (up to 20 per cent). The scatter in figures 6.32 to 6.35 shows that there may be considerable error in the positioning of the regression line especially for high groundwater levels. At the highest groundwater levels, the possible error (due to the positioning of the regression line) in the position of the groundwater divide is approximately 25 per cent of that by assuming a constant position (i.e. up to 5 per cent error in the gravel drainage). However, the error at high groundwater levels may be considerably worse if the true form of the relationship is not a straight line. Sensibly, there should be a maximum boundary distance. The straight line relationship will be in greater error when this maximum boundary distance is reached within the range of observed groundwater levels. From figures 6.32 to 6.35 it would appear that the maximum boundary distance is at least 185m. Thus, any errors incurred by using the relationships shown in figures 6.32 to 6.35 are likely to be less than that shown in figure 6.36 for a constant groundwater divide.

The value of PE is only significant during the summer (see table 3.4) when the gravel drainage is relatively small. Errors in peak winter values of gravel drainage caused by errors in PE are not significant and have, therefore, not been plotted.

In chapter 3, rainfall measurements were considered to be underestimated by up to 10 per cent. In section 6.5.2.4.5 an attempt was made to estimate the magnitude of this error by using the groundwater level prediction model (chapter 5). However, little success was found except to say that the error appeared to vary spatially such that the true rainfall varied between 99 and 110 per cent of the measured value. The groundwater level prediction model (chapter 5) compensated for an underestimation in rainfall by adjusting the other parameter values (principally SY). However, the gravel drainage model (section 6.6.3) cannot make any similar compensation. Figure 6.37 shows the error due to a 10 per cent underestimation of rainfall constant both spatially and temporally. Discussions in chapter 3 and section 6.5 suggest this to be the maximum likely error. Underestimation of rainfall leads to an underestimation of gravel drainage (although the pattern of fluctuation is unaltered). The magnitude of the underestimation varies but is greatest for peak values. As an example, the peak value of December 1982 is underestimated by $16m^3$/day (12 per cent). Figures 6.36 and 6.37 show that if there are errors in the position of the groundwater divide and in rainfall estimation, then the resulting errors in gravel drainage will tend to cancel each other out.

The estimation of gravel drainage relies upon the validity of the groundwater level prediction model (chapter 5) and the accuracy of its calibrated parameter values. The validity of using the groundwater level prediction model for estimating DRAINAGE relies on the assumption of a constant value of SY with depth and a drainage relationship uniquely related to groundwater level. Because of the interrelation of SY and the drainage relationship, only the latter is discussed here. Consideration of the more proper general groundwater flow equation (section 6.6.1) suggests that the drainage

relationship is not just a function of groundwater level and section 6.5.2.4.6 suggests that the consequent error in this assumption increases toward the cliff face. The calculation of gravel drainage weights the four piezometers according to the area of the aquifer they each represent. The weighting is greatest (see table 6.7) for those piezometers (P63 and P64) for which the assumption of a unique drainage relationship is believed to be least in error (i.e. furthest from the cliff face). Even if the drainage relationship is a unique function of groundwater level, some error may exist in its determination. This is especially so at low and high groundwater levels where the observed groundwater level data used for calibration is insufficient to accurately estimate the parameters of the relationship.

Figure 6.36 shows that at low groundwater levels there can be a sudden and rapid decrease in gravel drainage. This is due to the form of the drainage relationship shown in figures 6.19 to 6.22. The true form of the drainage relationship should be as for P62 (figure 6.20). But for P61, P63 and P64 the drainage relationship flattens out at very low groundwater levels. This causes a sudden drop in the rate of groundwater level recession (and, therefore, DRAINAGE) at low groundwater levels. The groundwater levels are never really low enough for this to be significant at P61 but it is significant at P63 and P64. The underestimation of DRAINAGE at very low groundwater levels is counterbalanced by an over-estimation at slightly higher groundwater levels, i.e. DRAINAGE is redistributed, not lost. These errors are small and occur at times (low water levels) not significant to this study.

The estimation of the drainage relationship at high groundwater levels relies upon the fitting of the groundwater level prediction model to only one or two observed groundwater levels. Examination of figures 6.23 to 6.26 shows that high groundwater levels are not always fitted perfectly. Examination of figures 6.19 to 6.22 shows that even a small error in groundwater level prediction will lead to a considerable error in the estimated value of DRAINAGE. Thus, there may be errors in the drainage relationship which lead to significant errors in the estimated peak values of gravel drainage.

In order to examine the representativeness of the four piezometers used in the calculation of gravel drainage, a much larger number of piezometers is needed. Unfortunately, the groundwater level prediction model has only been calibrated for the four piezometers. However, some idea may be gained by comparing the four individual piezometers. Figure 6.38 shows the estimated gravel drainage when using only one, instead of four, piezometers, i.e. the DRAINAGE at an individual piezometer is considered representative of the whole catchment area. It can be seen that there is considerable variation. Some of this variation may be accounted for by spatial variation of the model parameter C. This increases with distance from the cliff edge and is considered to be adequately sampled by the four piezometers. However, figure 6.38 shows that there is still considerable variation caused by spatial variation of other parameters which may not be adequately sampled by the four piezometers.

It is, therefore, probable that a significant error exists in using only four piezometers. This error will be in the distribution and size of the peaks. The gravel drainage totalled over longer periods of time (say 7 days) will have less error. This will be the case when the values are used with the undercliff water balance (chapter 9). However, the values given in figure 6.36 are still considered to be a useful guide as to the likely distribution and peak values of gravel drainage.

6.7 Summary

Weekly, and some daily, groundwater level measurements were taken in the PG over a 2 year period. They were affected by meteorological variations, and to a limited extent, by cliff top slumping. The effect of cliff top slumping is intermittent and over periods much longer than 2 years may be very significant. I.e. the average groundwater level at a location will be very different to what it was 10 or 20 years previously due to the much greater cumulative losses of cliff top material than those encountered during the study period.

Groundwater was present in the PG at all times except near the cliff face when groundwater levels were low. The direction of groundwater flow is considered to be locally complicated by undulations in the PG/BC unconformity. However, in the area studied, groundwater flow was generally found to be approximately perpendicular to the cliff face.

The model described in chapter 5 was used to simulate the groundwater level at four different locations in the PG. There was some difficulty in obtaining reliable parameter estimates. This was principally due to parameter interdependence between SY and RUNOFF, and A and C. The latter was only a problem at P61 and P62; the former was a problem at all four locations. The model fit deteriorated toward the cliff face. This was ascribed to the assumption that the drainage relationship was a unique function of groundwater level being increasingly violated toward the cliff face.

An attempt was made to estimate the amount of rainfall under-estimation. This was done by assuming zero surface runoff and allowing negative values of the parameter RUNOFF. However, due to the strong interdependence with SY, and there being only four estimates, no reliable estimate could be made, such that a value of zero was assumed.

In describing groundwater flow it is appropriate to use the general groundwater flow equation. However, it was considered that there would be some difficulty in its application. Also, the accuracy of the solution would be dependent on geohydrological input data much of which was either not available or of insufficient accuracy. Therefore, a much simpler method was adopted.

The calibrated groundwater level prediction models of the four piezometers were used to estimate the gravel drainage. Considerable errors were found to be possible by not accurately determining the rainfall and catchment area. These errors affected the amounts of gravel drainage. The use of only four calibrated locations

was considered to cause errors in the distribution of gravel drainage. These errors should be reduced when the values are totalled over longer periods (about 7 days for the undercliff water balance). Despite these errors, the estimates of gravel drainage are still considered useful.

Table 6.1 Summary of Plateau Gravel Groundwater Level Records

Location	Observation Period		Maximum	Minimum	Range	PG Base	P1	P2
	From	To	(m O.D.)	(m O.D.)	(m)	(m O.D.)		
P51	13.10.82	29.1.85	29.90	29.04	0.86	29.04	0	0
P52	13.10.82	29.1.85	30.62	29.42	1.20	29.24	0	0
P60	28.10.82	29.1.85	30.16	28.89	1.27	28.40	0	0
P61	18.10.82	29.1.85	29.72	28.12	1.60	28.17	3.7	0
P62	28.10.82	29.1.85	29.81	28.84	0.97	28.37	0	0
P63	3.11.82	29.1.85	30.74	29.76	0.98	28.09	0	0
P64	28.10.82	29.1.85	31.42	30.21	1.21	29.49	0	0
P71 [a]	13.10.82	29.1.85	30.24	<28.81	>1.43	29.11	64.6	51.7
P72	13.10.82	29.1.85	29.96	28.89	1.07	28.55	0	0
P73	13.10.82	29.1.85	30.72	29.77	0.95	29.18	0	0
P81	25.1.84	29.1.85	29.85	28.46	1.39	29.07	60.1	0
P82 [b]	25.1.84	9.5.84	29.72	<29.63	>0.09	29.26	<80.0	80.0
P91	25.1.84	29.1.85	29.39	28.84	0.55	28.54	0	0
P92	25.1.84	29.1.85	30.11	29.35	0.76	29.06	0	0
P93	25.1.84	16.5.84	29.75	29.43	0.32	27.90	0	0

Notes:
a. The bottom of the piezometer is at 28.81 m O.D.
b. The bottom of the piezometer is at 29.63 m O.D.
P1. is the percentage of the observation period that the groundwater level is below the base of the PG.
P2. is the percentage of the observation period that the groundwater level is below the bottom of the piezometer.

Table 6.2 Maximum and Minimum Allowable Optimisation Step Sizes and Parameter Values

Parameter	Value		Step Size	
	Maximum	Minimum	Maximum	Minimum
RUNOFF	1.0	-0.2	0.008	0.001
A	1.0	0.0	0.04	0.005
C(mm)	100	0	8	1
K(days)	20.0	0.5	0.8	0.1
DELAY(days)	10	0	1	1
SY	1.0	0.001	0.008	0.001

Table 6.3 Parameter Values of the Optimal Drainage Relationship

Parameter	P61	P62	P63	P64
$h_m(1)$	28.1	28.2	29.75	30.2
RECESS(1)	.05	.0055	.2	.075
$h_m(2)$	27.85	29.0	29.45	29.8
RECESS(2)	.015	.069	.0123	.0125
$h_m(3)$	28.4	29.3	30.06	30.3
RECESS(3)	.032	.19	.2	.0278
$h_m(4)$	29.0	30.0	29.8	31.05
RECESS(4)	.28	.8	.0482	.29

Note: The drainage relationship is described by four straight lines of the form given by equation 5.6. Each line is described by a pair of parameter values, viz. h_m and RECESS. Their units are m O.D. and $days^{-1}$ respectively. The number in brackets identifies each line, the ascending order being for progressively higher groundwater levels.

Table 6.4 Optimal Parameter Solution for the Calibration Period

Parameter	P61	P62	P63	P64
RUNOFF	-0.05	-0.05	0.01	-0.1
A	0.27	0.245	0.325	0.32
C(mm)	25	53	64	64
DELAY(days)	1	2	1	1
K(days)	2.3	4.7	3.9	1.5
SY	0.0485	0.057	0.091	0.077
CORREL(1)	0.9212	0.9569	0.9866	0.9817
CORREL(2)	0.8900	0.9269	0.9302	0.9716
CORREL(3)	0.9079	0.9460	0.9672	0.9778

Note: CORREL is the objective function value. The number in brackets refers to:

1. The calibration period, 1st November 1982 to 12th January 1984.

2. The test period, 12th January 1984 to 1st November 1984.

3. The total period, 18th October 1982 to 1st November 1984.

Table 6.5 Optimal Parameter Solution for the Complete Data Period

The parameter values given in table 6.4 were used as initial values for re-optimisation using all the data (18th October 1982 to 1st November 1984) for calibration.

Parameter	P61	P62	P63	P64
RUNOFF	-0.035	-0.046	0.007	-0.105
A	0.27	0.255	0.325	0.345
C(mm)	17	60	63	61
DELAY(days)	1	2	1	1
K(days)	2.5	5.0	2.6	2.0
SY	0.0475	0.057	0.0905	0.081
CORREL(1)	0.9122	0.9560	0.9826	0.9801
CORREL(2)	0.9260	0.9300	0.9521	0.9839
CORREL(3)	0.9205	0.9470	0.9731	0.9816

Note: CORREL is the objective function value. The number in brackets refers to:

1. The period, 1st November 1982 to 12th January 1984.
2. The period, 12th January 1984 to 1st November 1984.
3. The period, 18th October 1982 to 1st November 1984.

Table 6.6 Parameter Solution for Model Application

Parameter	P61	P62	P63	P64
RUNOFF	0	0	0	0
A	0.27	0.245	0.325	0.32
C(mm)	25	53	64	64
DELAY(days)	1	2	1	1
K(days)	2.3	4.7	3.9	1.5
SY	0.0425	0.0525	0.0925	0.061
CORREL(1)	0.9179	0.9553	0.9865	0.9772
CORREL(2)	0.8923	0.9299	0.9297	0.9569
CORREL(3)	0.9078	0.9463	0.9671	0.9702

Note: CORREL is the objective function value. The number in brackets refers to :

1. The period, 1st November 1982 to 12th January 1984.
2. The period, 12th January 1984 to 1st November 1984.
3. The period, 18th October 1982 to 1st November 1984.

Table 6.7 Plateau Gravel Drainage : Lengths of the Line through P61 and P64 represented by each Piezometer

Piezometer	Position[a] (m)	Representative Length (m)		
		From [a]	To [a]	Length
P61	9	0	18.55	18.55
P62	28.1	18.55	53.5	34.95
P63	78.9	53.5	115.05	61.55
P64	151.2	115.05	165-205[b]	49.95-89.95

Notes:

a. These measurements are the distances from the cliff edge along the line through P61 and P64.

b. This is the position of the groundwater divide which varies with groundwater level according to the relationships in figures 6.32 to 6.35.

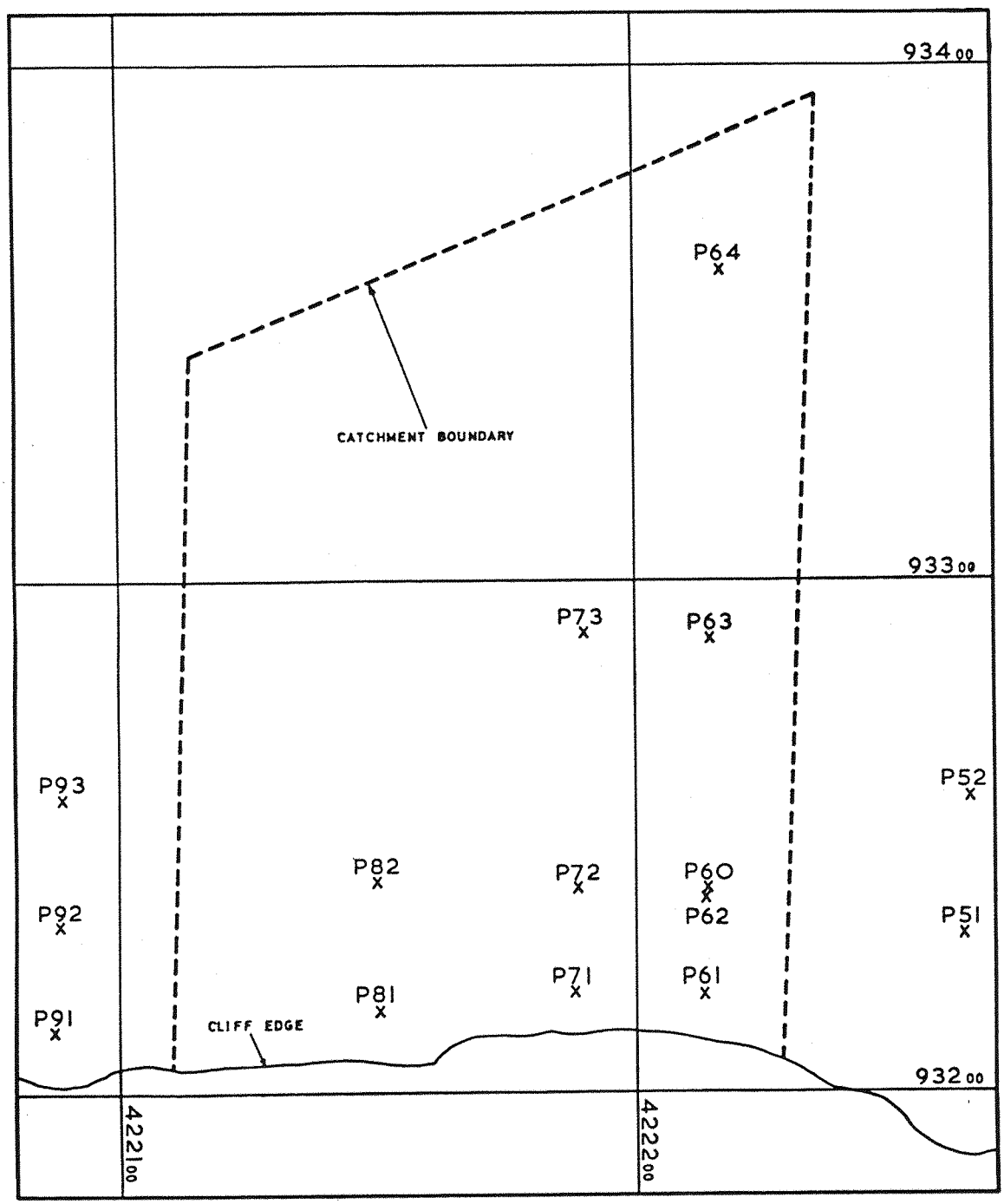

Figure 6.1 Location map for piezometers in the Plateau Gravel.

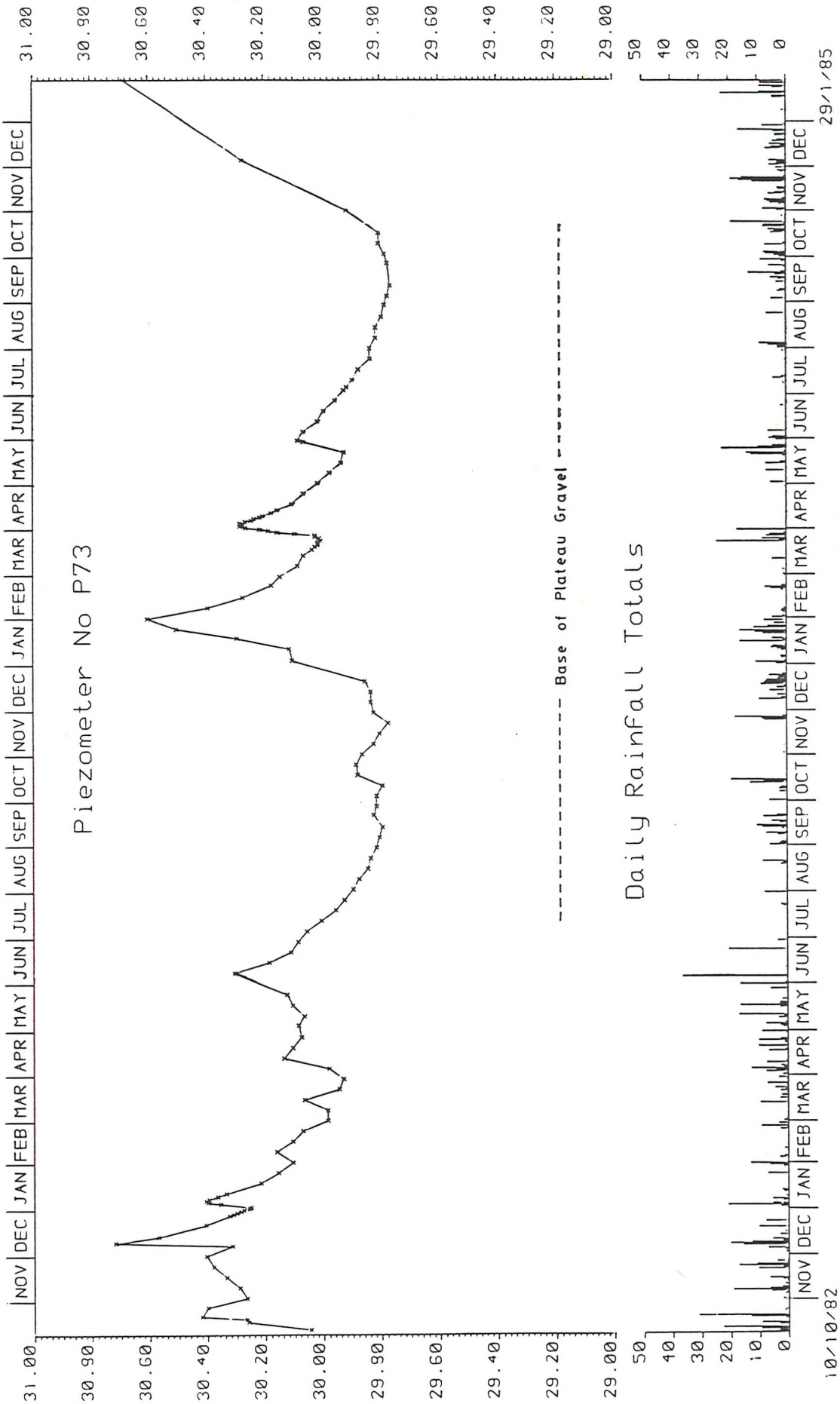

Figure 6.2 Groundwater level record for the Plateau Gravel at P73.

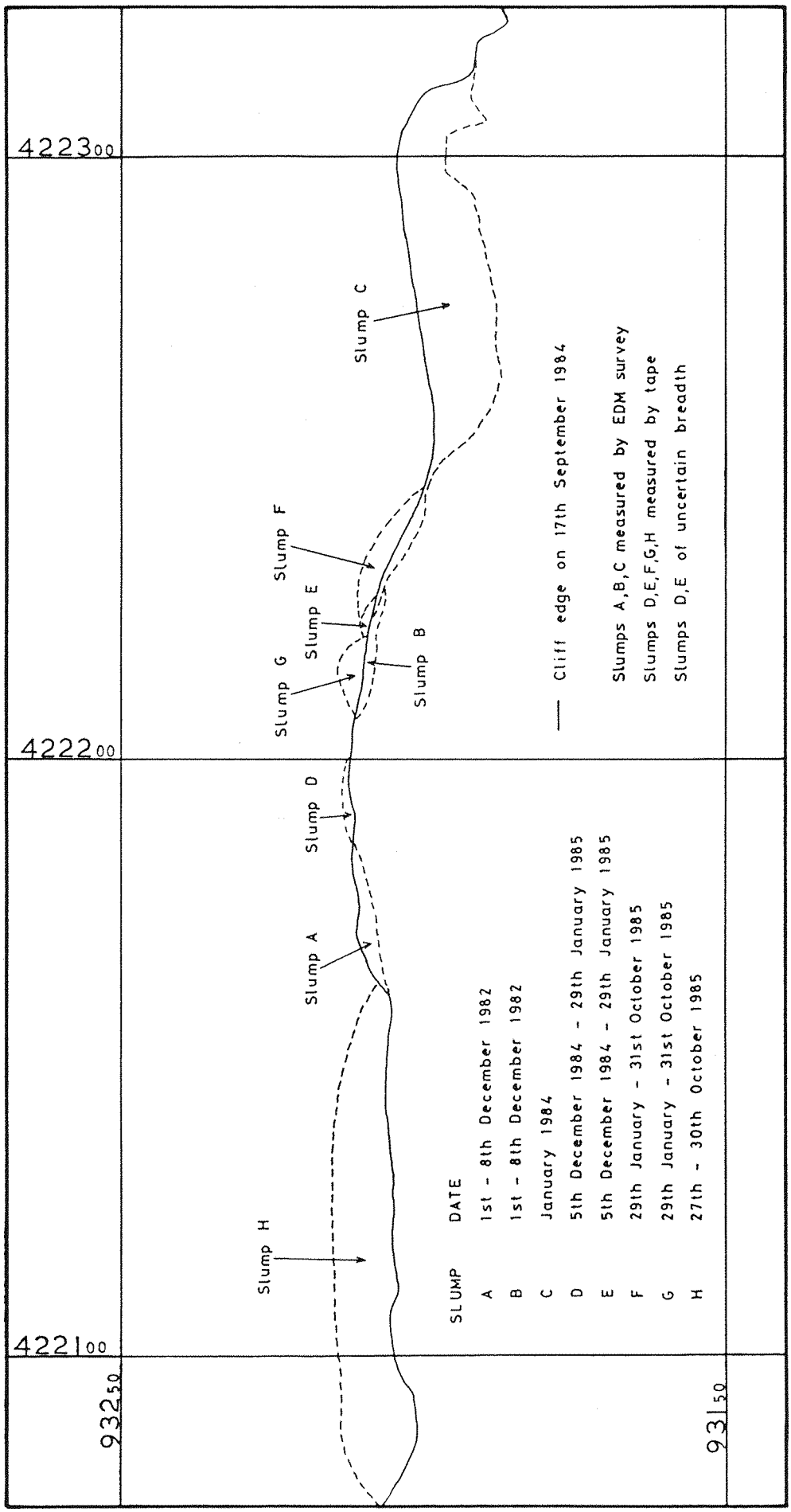

Figure 6.3 Cliff top slumps affecting the study area between July 1982 and October 1985.

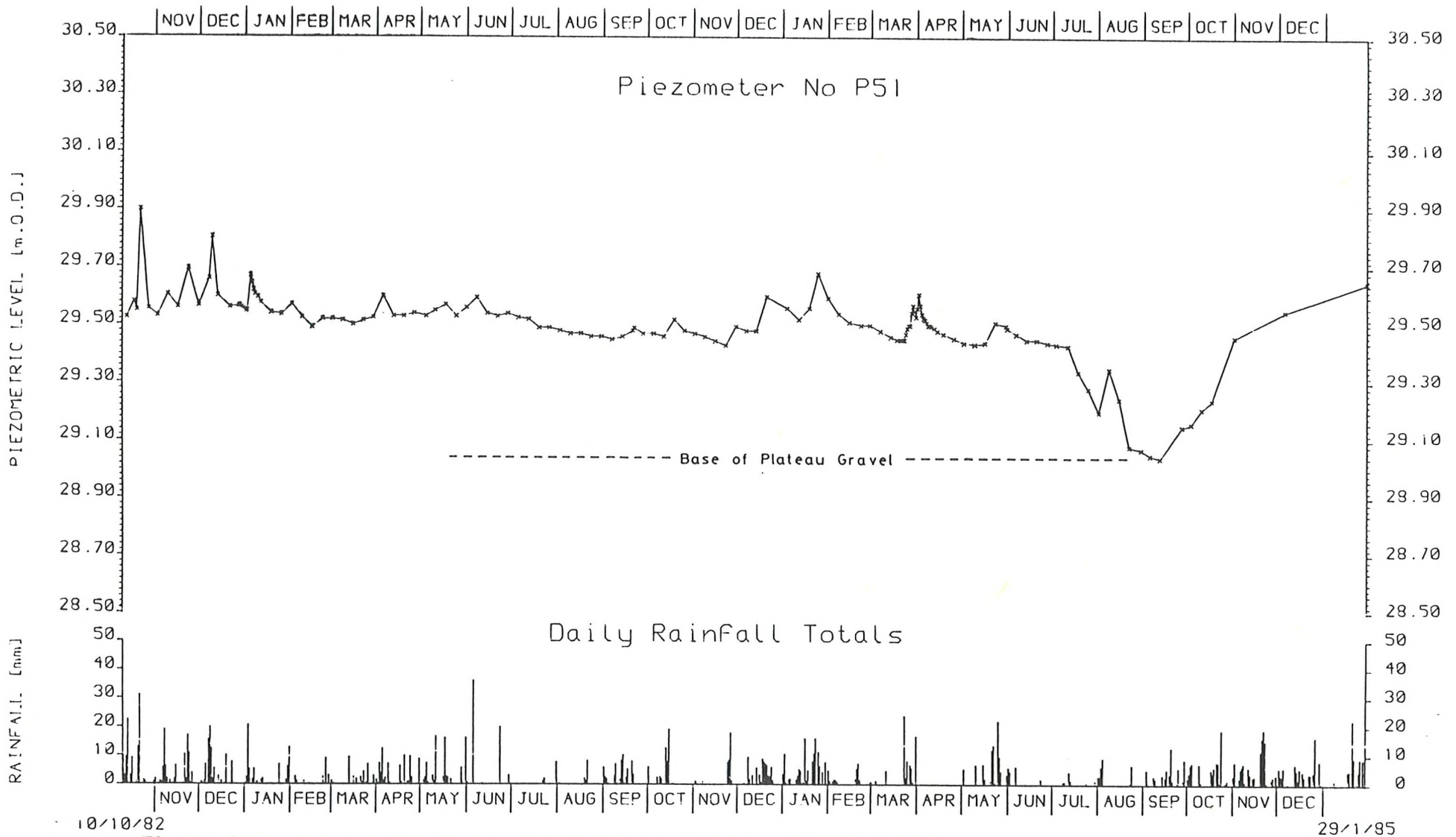

Figure 6.4 **Groundwater level record for the Plateau Gravel at P51.**

FIGURE 6.5 GRAVEL WATER LEVELS AT P72 AND P62

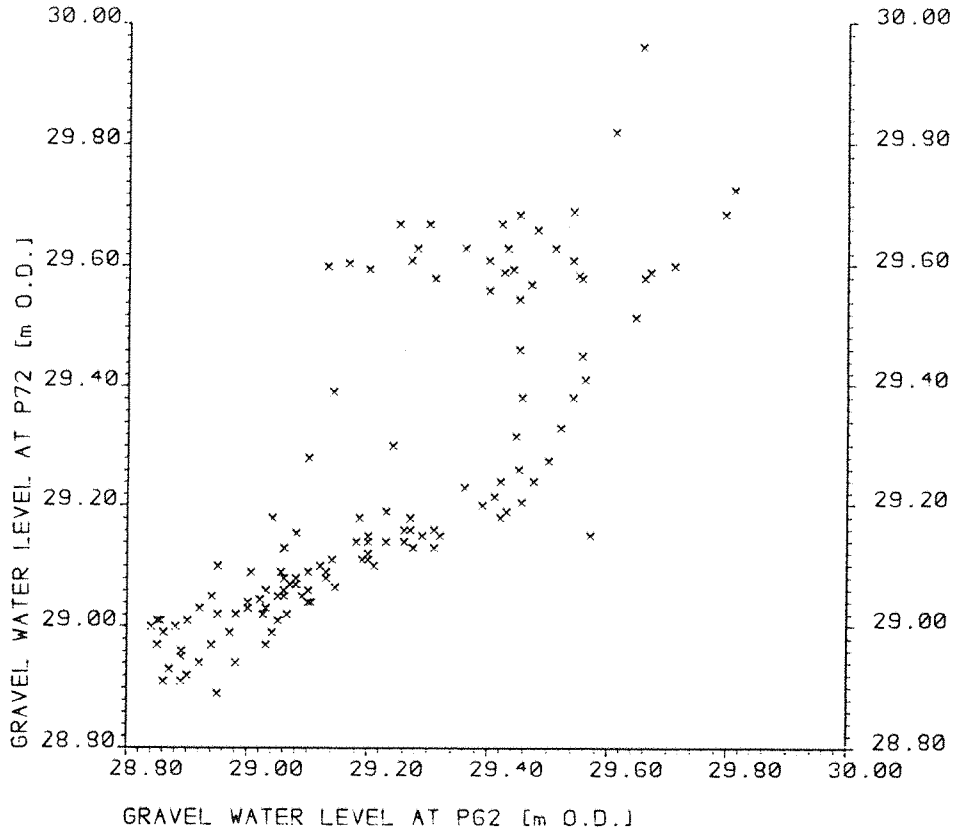

FIGURE 6.6 GRAVEL WATER LEVELS AT P73 AND P63

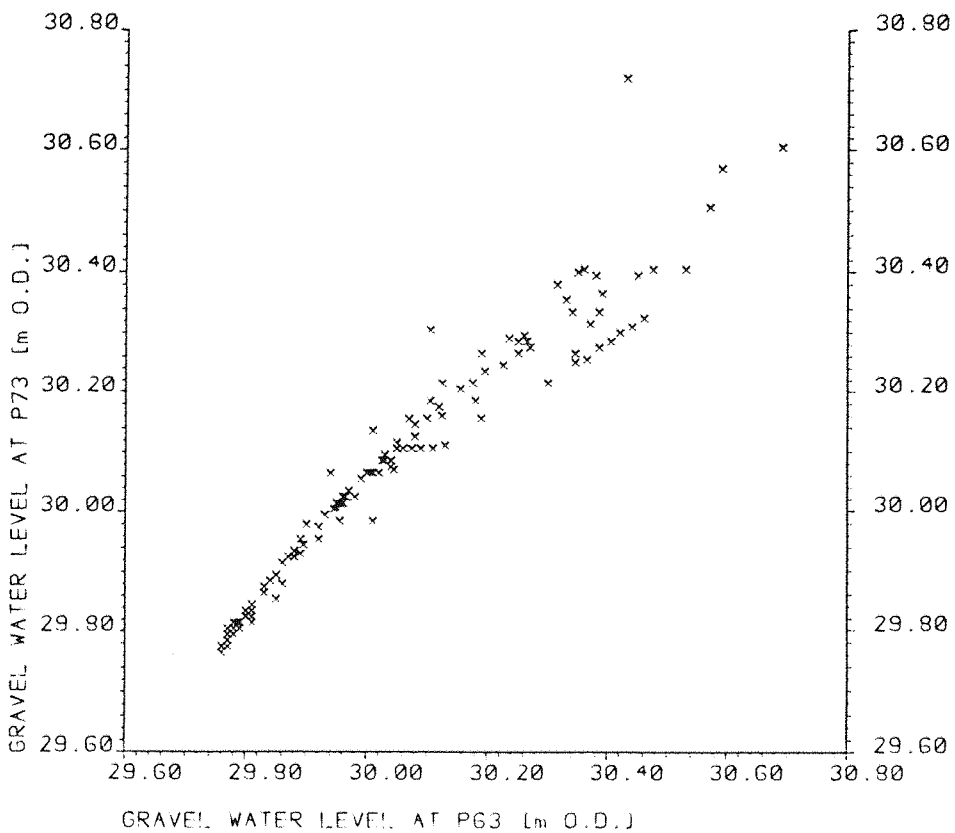

FIGURE 6.7 GRAVEL WATER LEVELS AT P61 AND P62

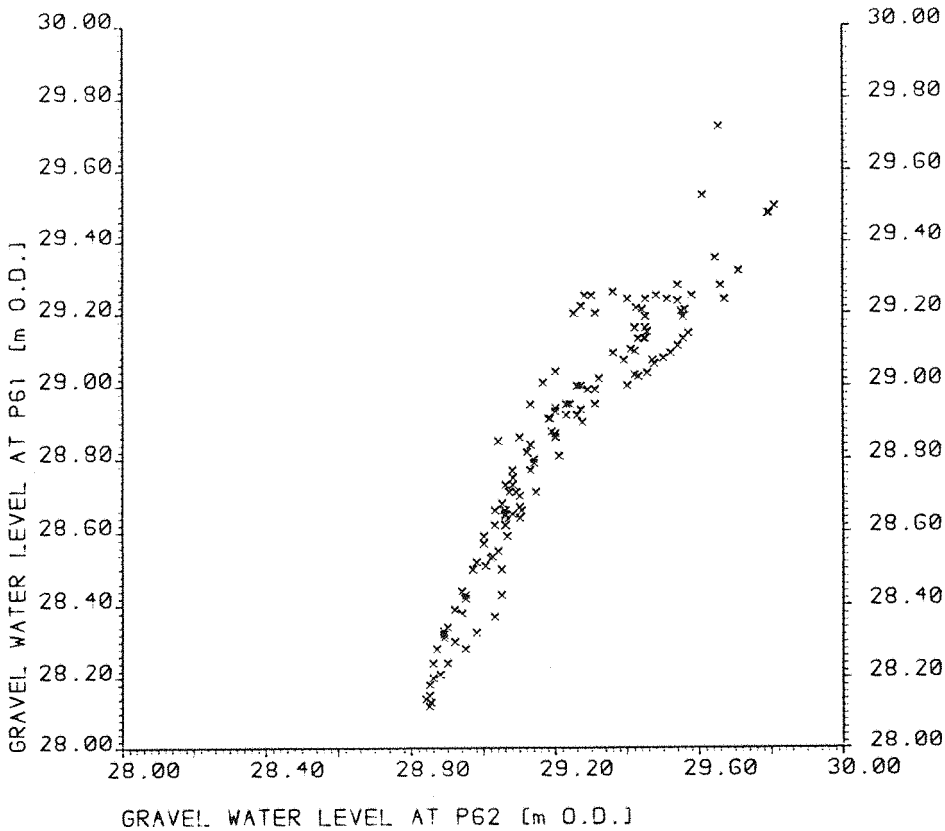

FIGURE 6.8 GRAVEL WATER LEVELS AT P60 AND P62

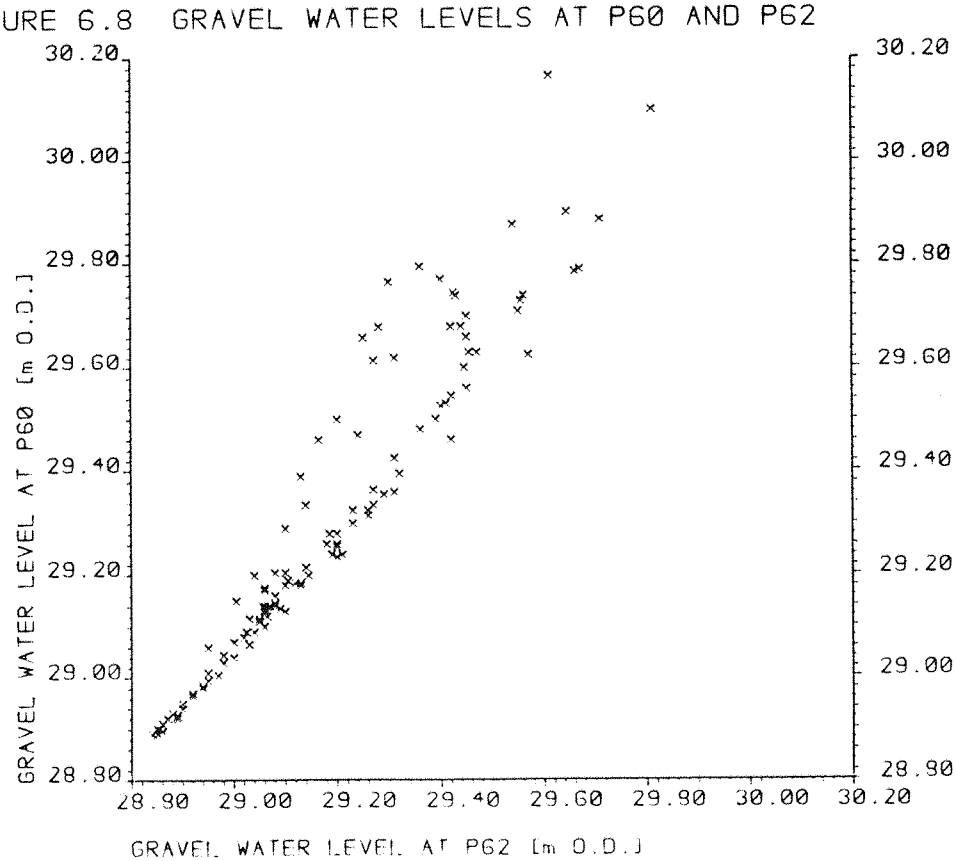

FIGURE 6.9 GRAVEL WATER LEVELS AT P62 AND P63

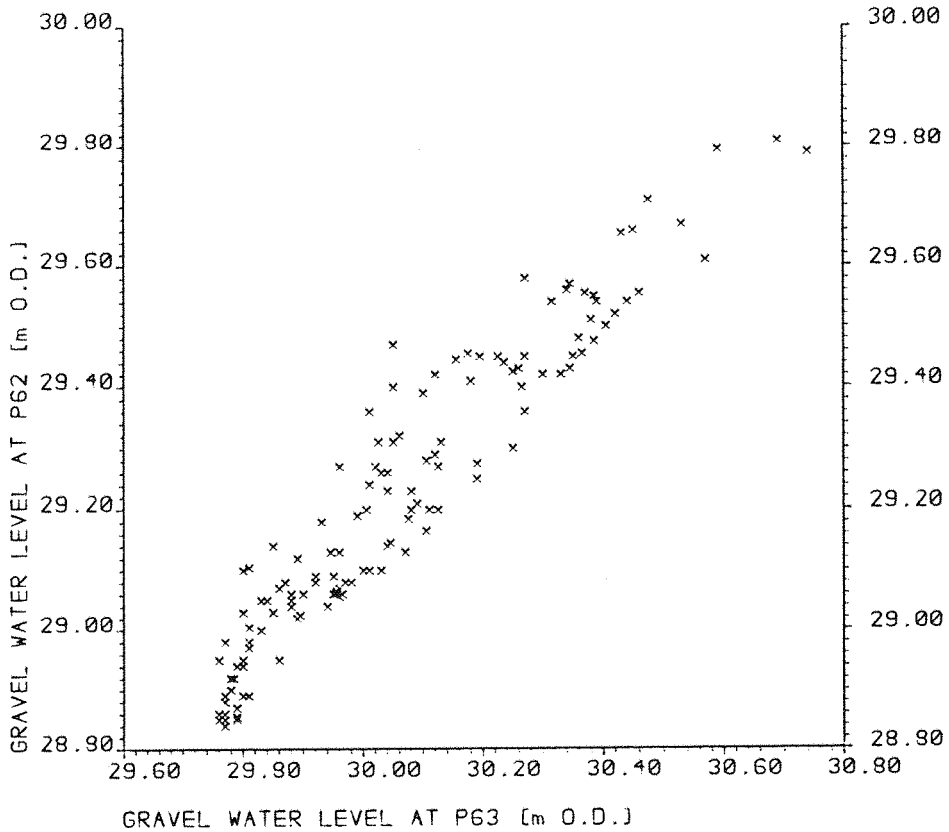

FIGURE 6.10 GRAVEL WATER LEVELS AT P63 AND P64

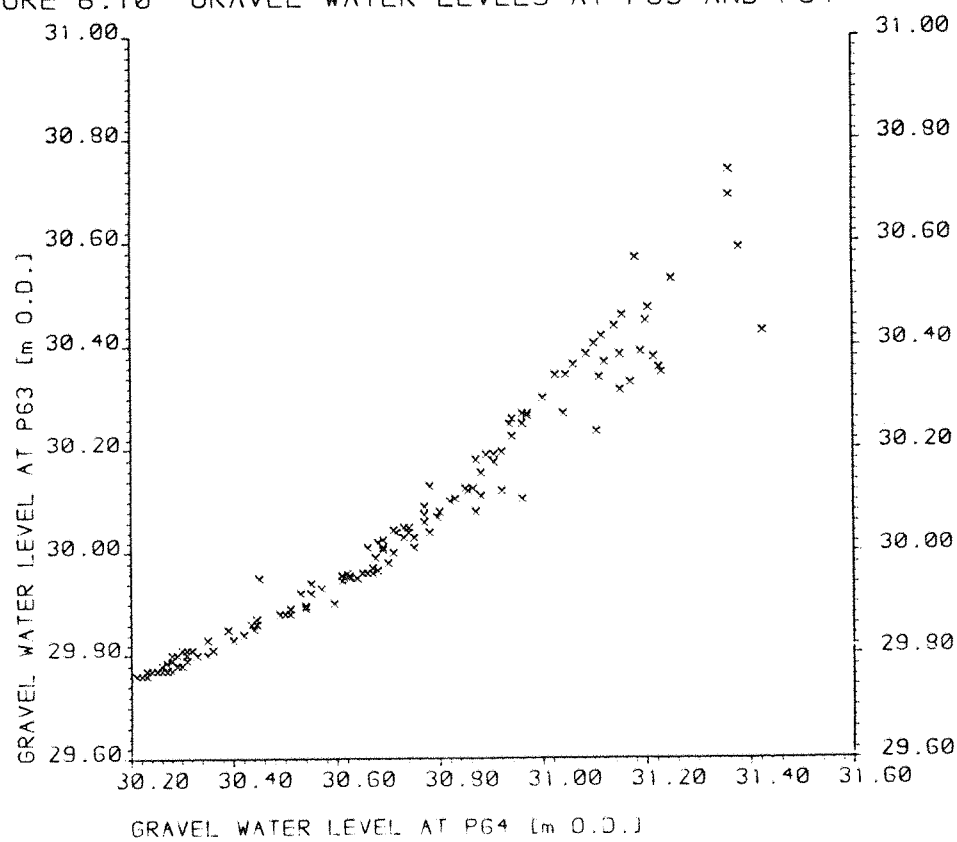

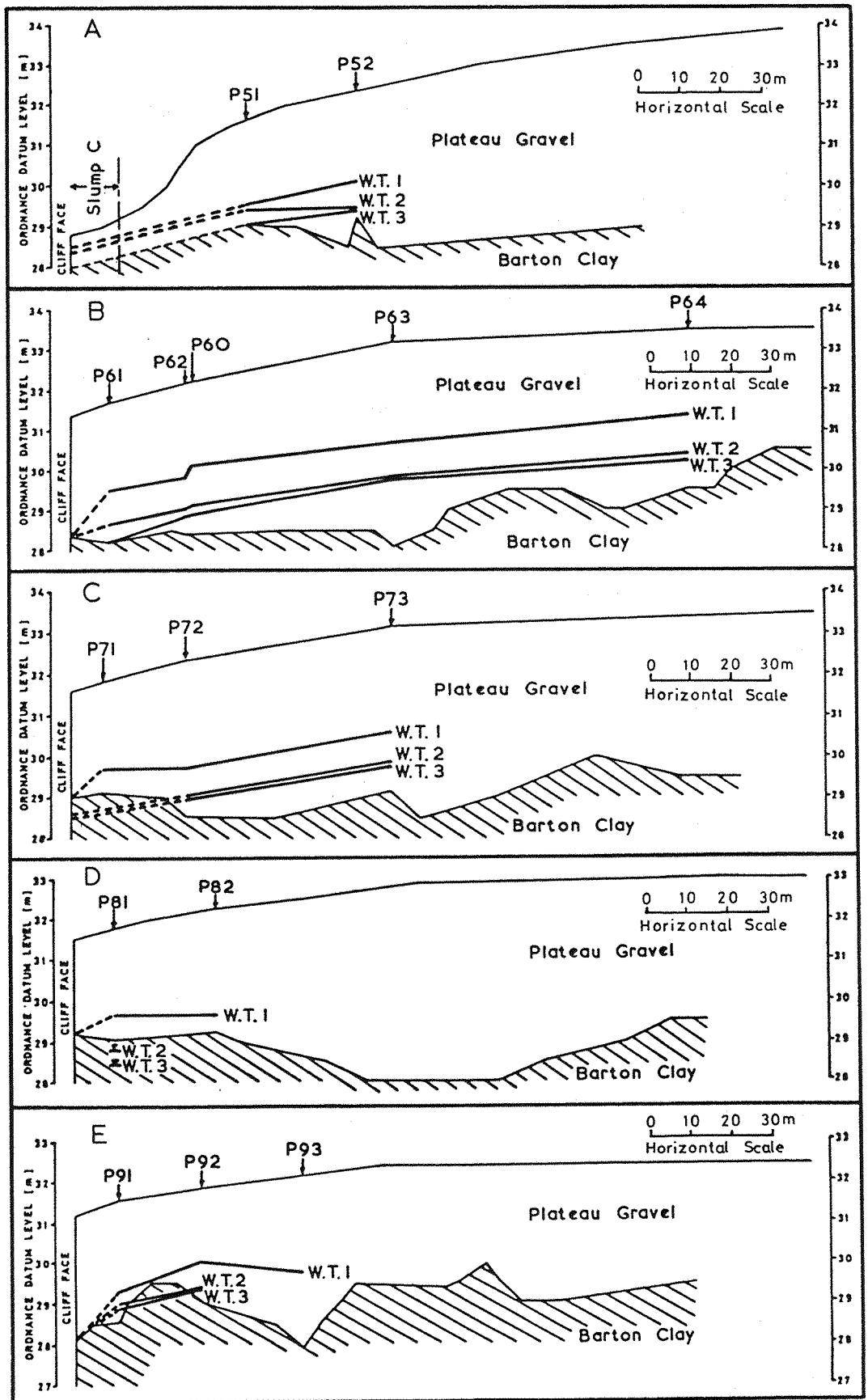

Figure 6.11 Cross sections on the cliff top perpendicular to the cliff edge showing the water table (WT) level on different dates. WT1 was on 1st February 1984; WT2 was on 11th July 1984; WT3 was on 12th September 1984.

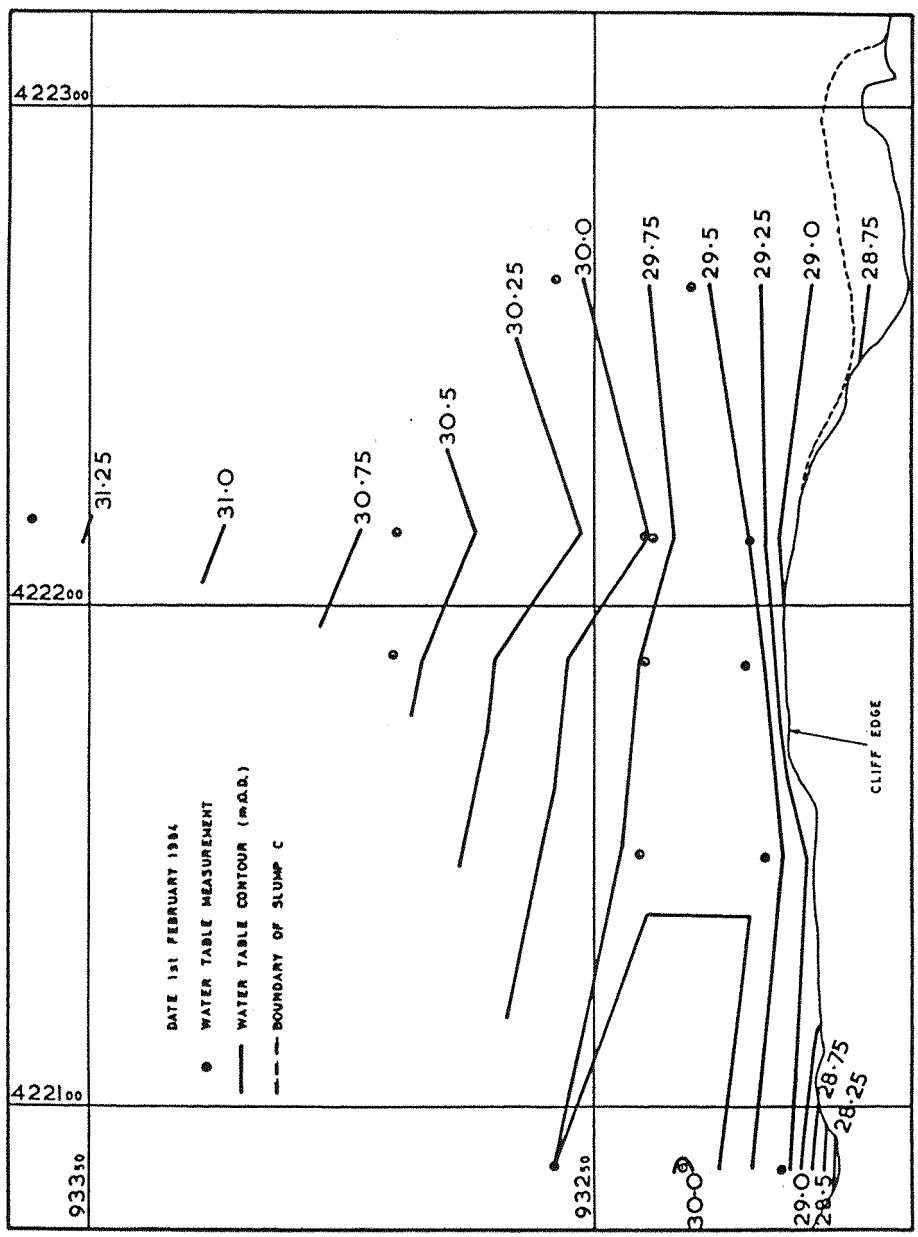

Figure 6.12 Groundwater table levels for the cliff top on 1st February 1984. Slump C refers to figure 6.3.

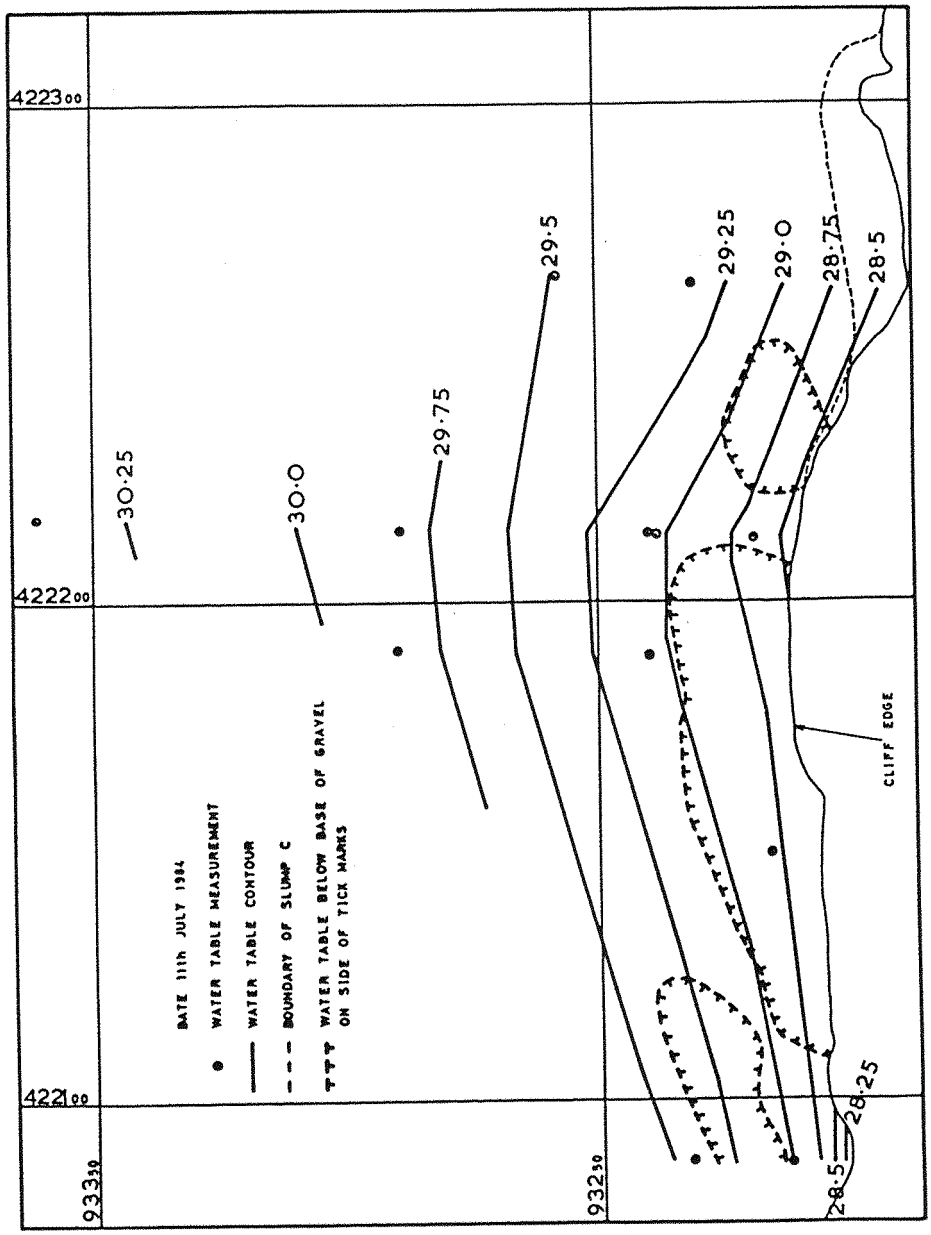

Figure 6.13 Groundwater table levels for the cliff top on 11th July 1984. Slump C refers to figure 6.3.

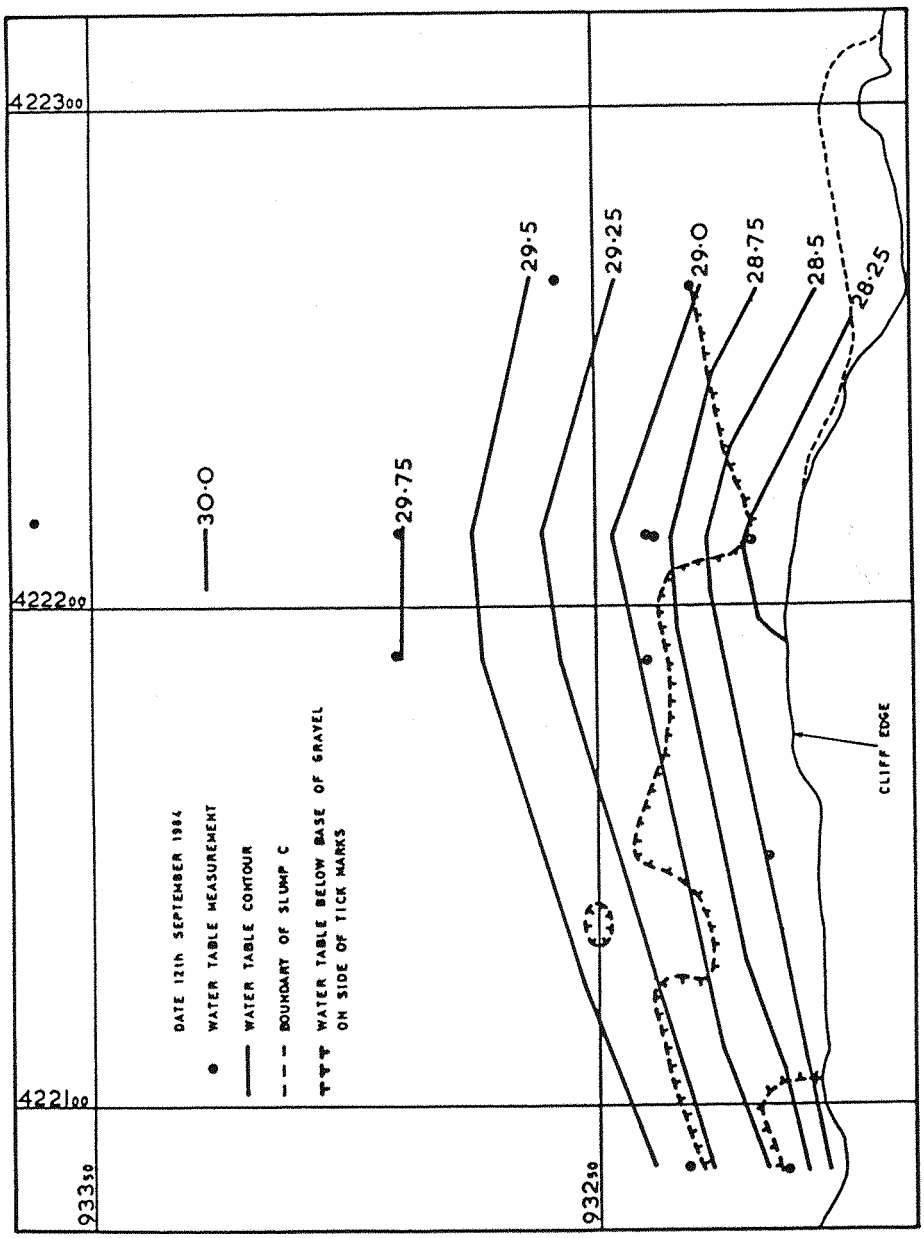

Figure 6.14 Groundwater table levels for the cliff top on 12th September 1984. Slump C refers to figure 6.3.

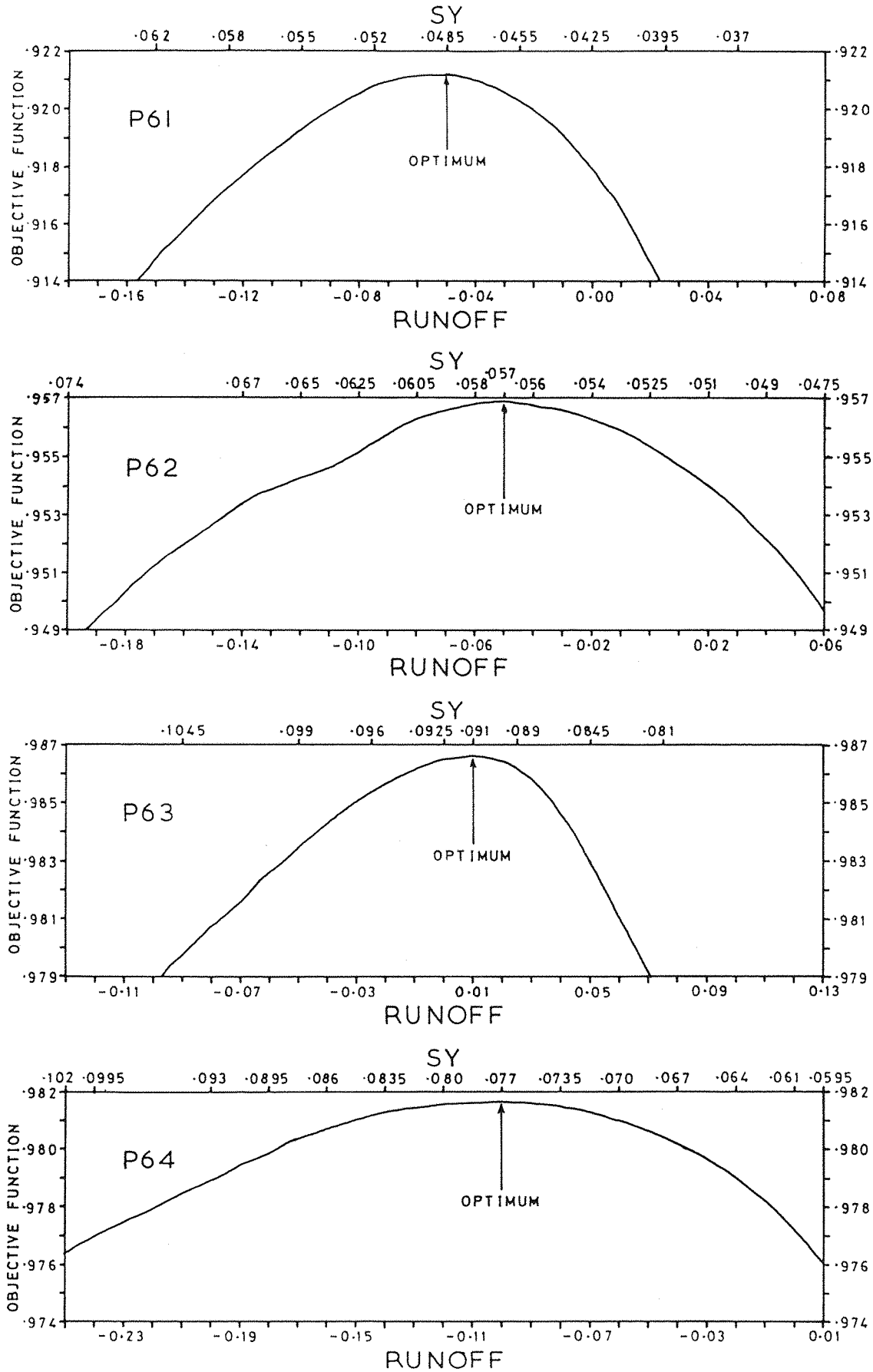

Figure 6.15 Objective function values along the ridge of interdependence between SY and RUNOFF. The other model parameters are as given in tables 6.3 and 6.4. RUNOFF is held constant whilst SY is optimised.

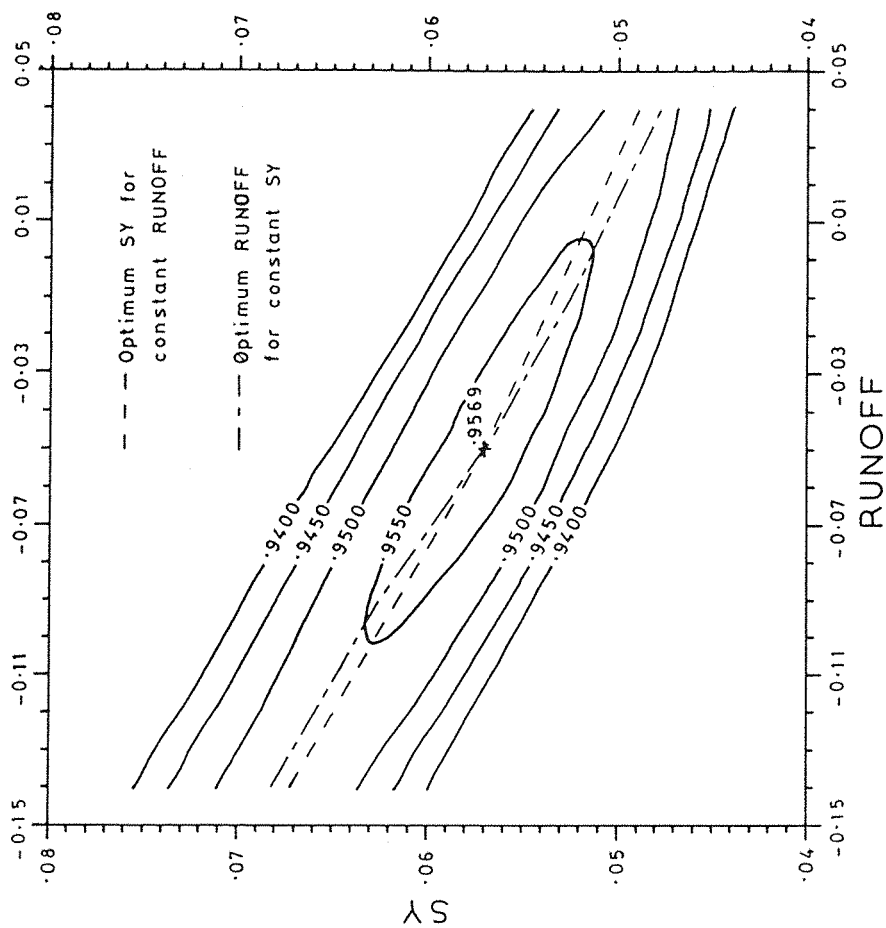

Figure 6.17 Objective function contours in SY and RUNOFF parameter space for P62. The other parameter values are as given in tables 6.3 and 6.4.

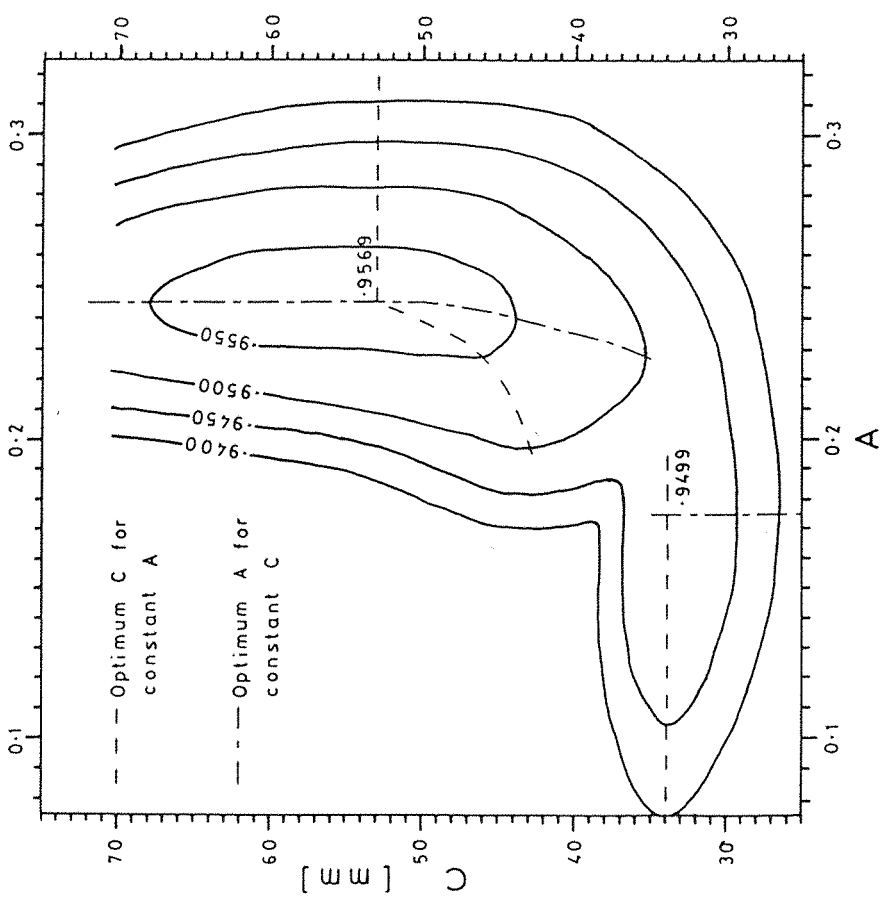

Figure 6.16 Objective function contours in A and C parameter space for P62. The other parameter values are as given in tables 6.3 and 6.4.

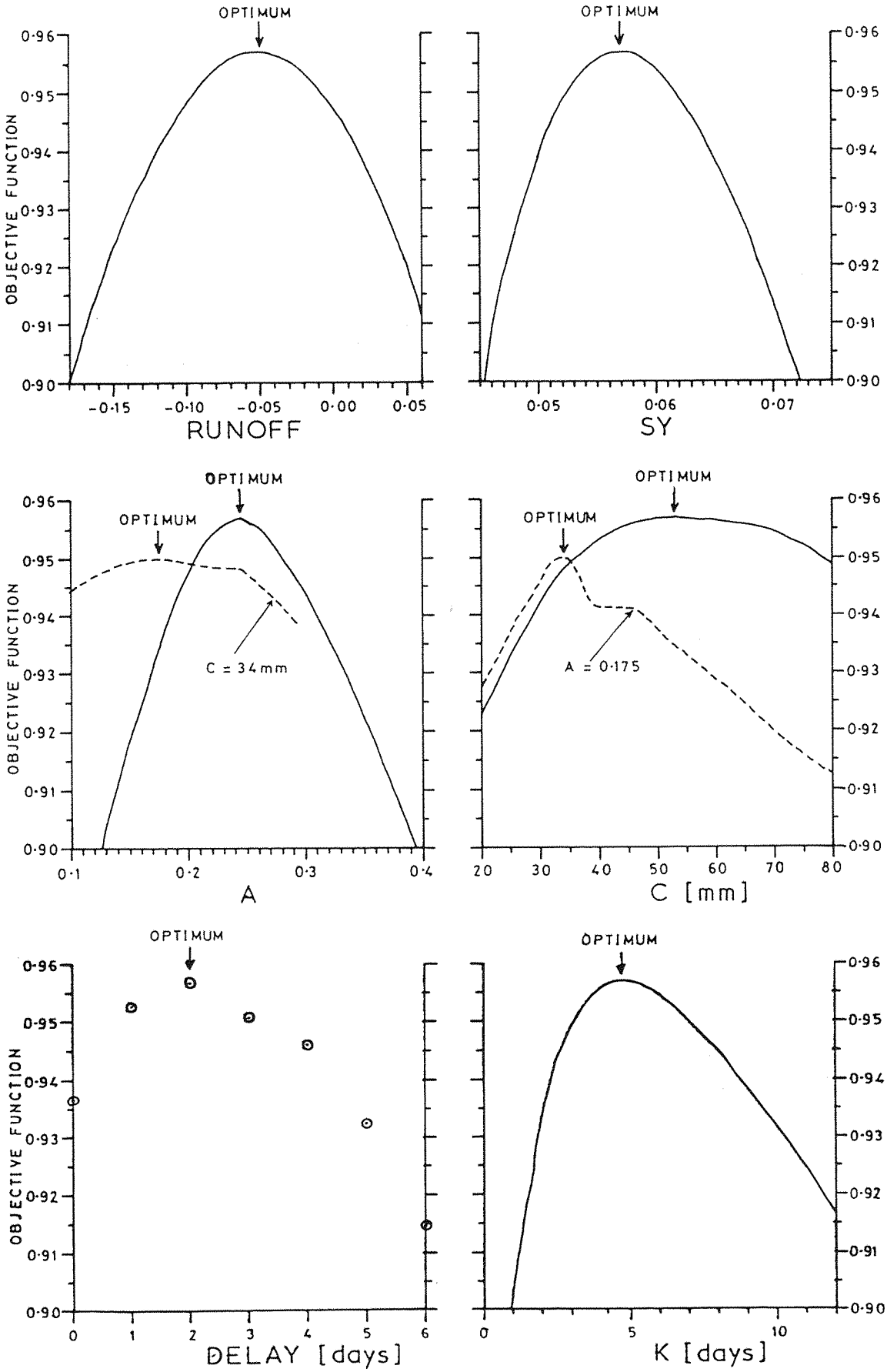

Figure 6.18 Variation of the objective function value in response to individual parameter perturbation about the optimal solution for P62. The optimal parameter values are as given in tables 6.3 and 6.4 except where indicated.

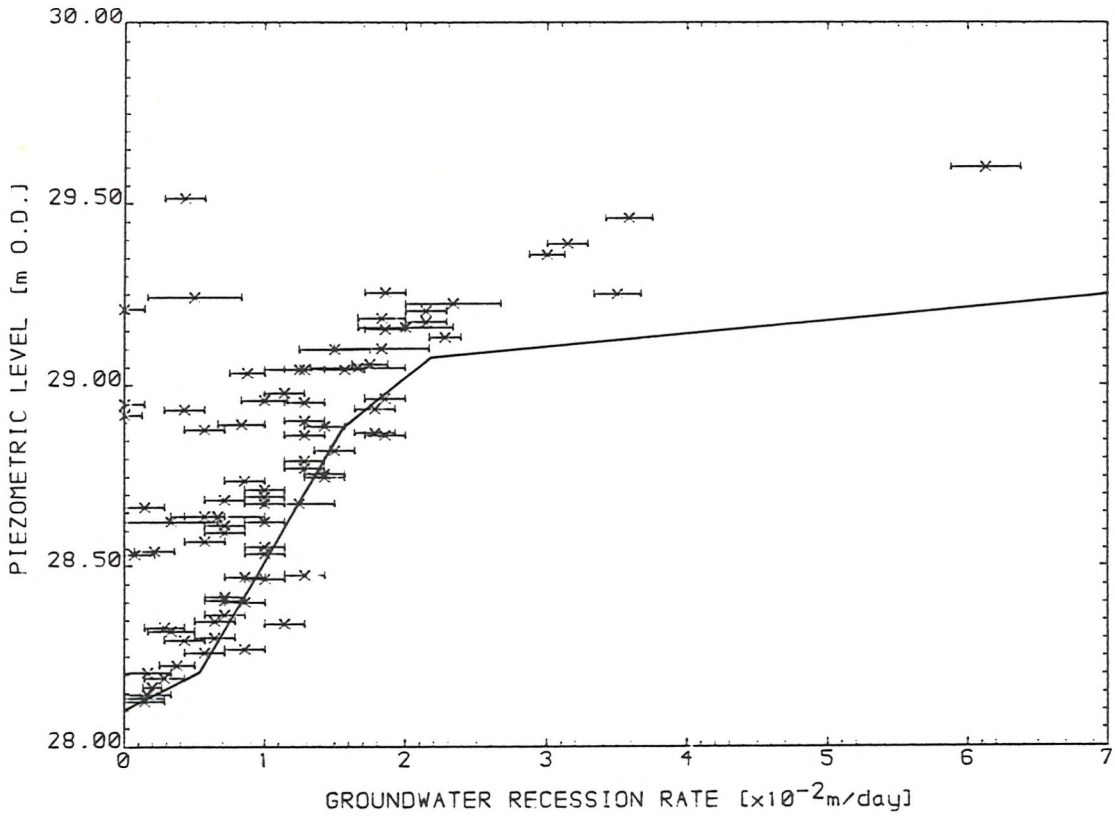

FIGURE 6.19 RELATIONSHIP BETWEEN WATER LEVEL AND GROUND WATER RECESSION DUE TO DRAINAGE AT P61

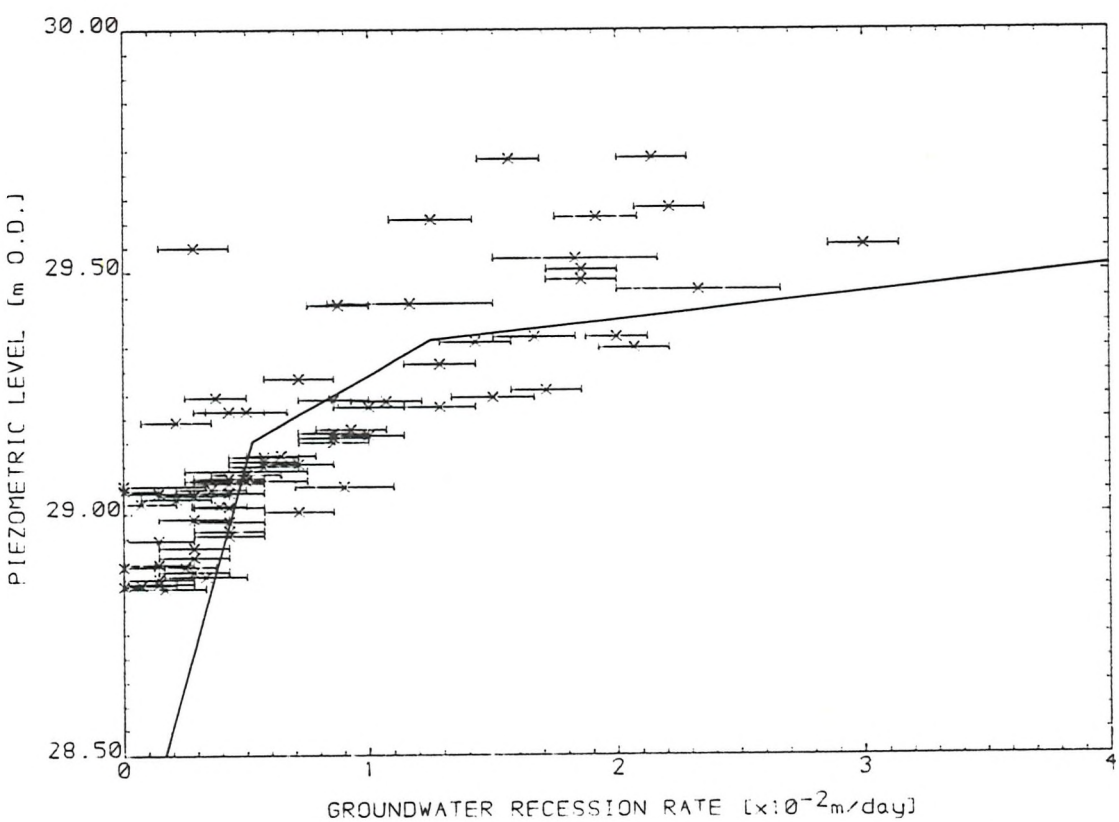

FIGURE 6.20 RELATIONSHIP BETWEEN WATER LEVEL AND GROUND WATER RECESSION DUE TO DRAINAGE AT P62

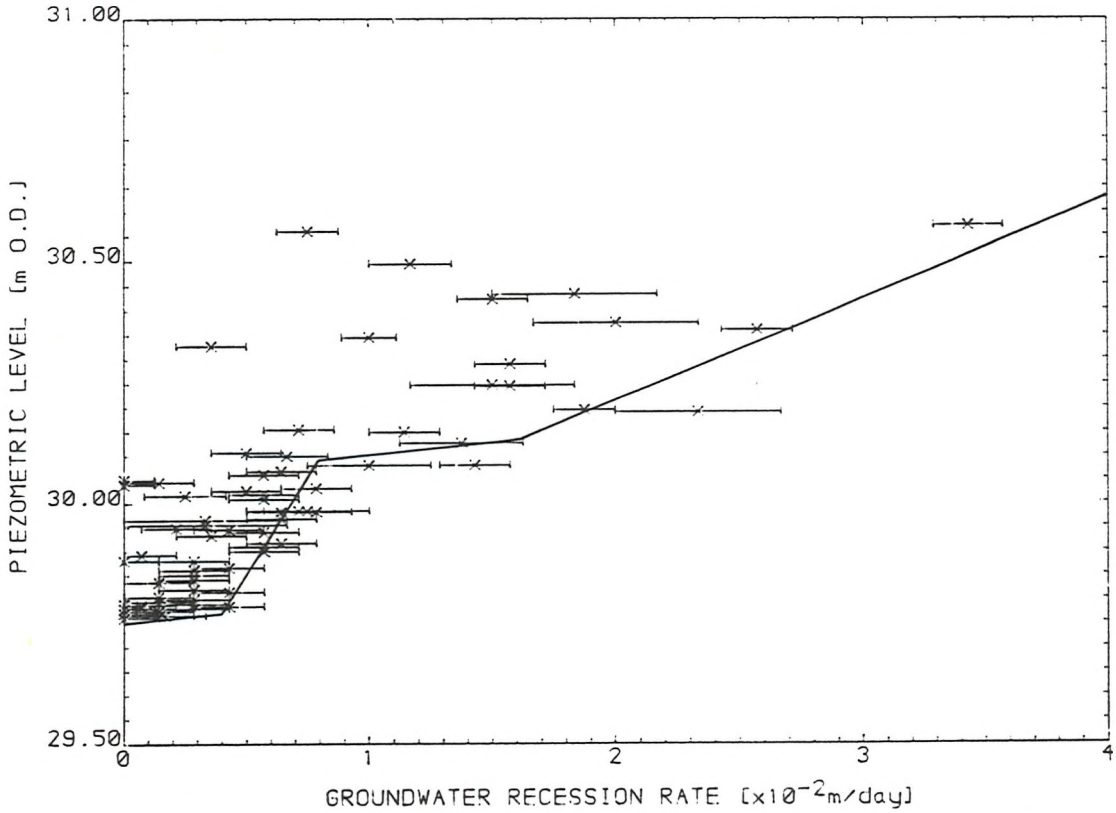

FIGURE 6.21 RELATIONSHIP BETWEEN WATER LEVEL AND GROUND WATER RECESSION DUE TO DRAINAGE AT P63

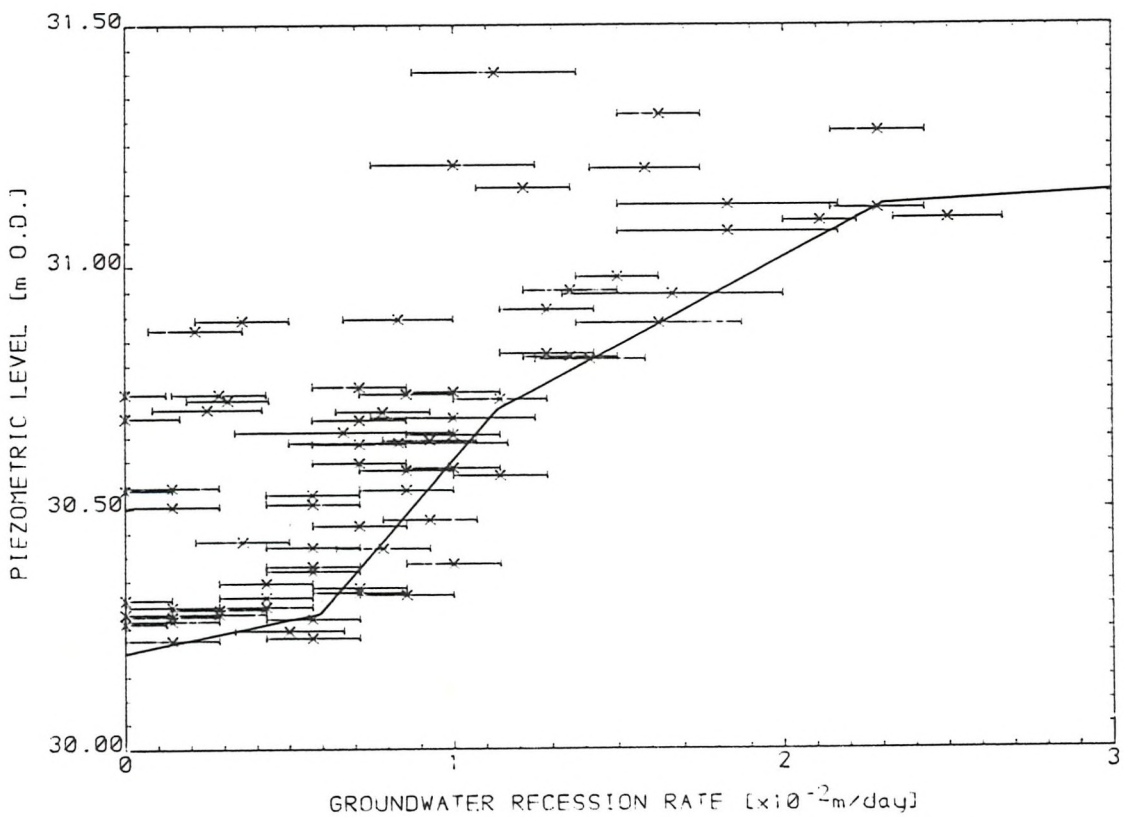

FIGURE 6.22 RELATIONSHIP BETWEEN WATER LEVEL AND GROUND WATER RECESSION DUE TO DRAINAGE AT P64

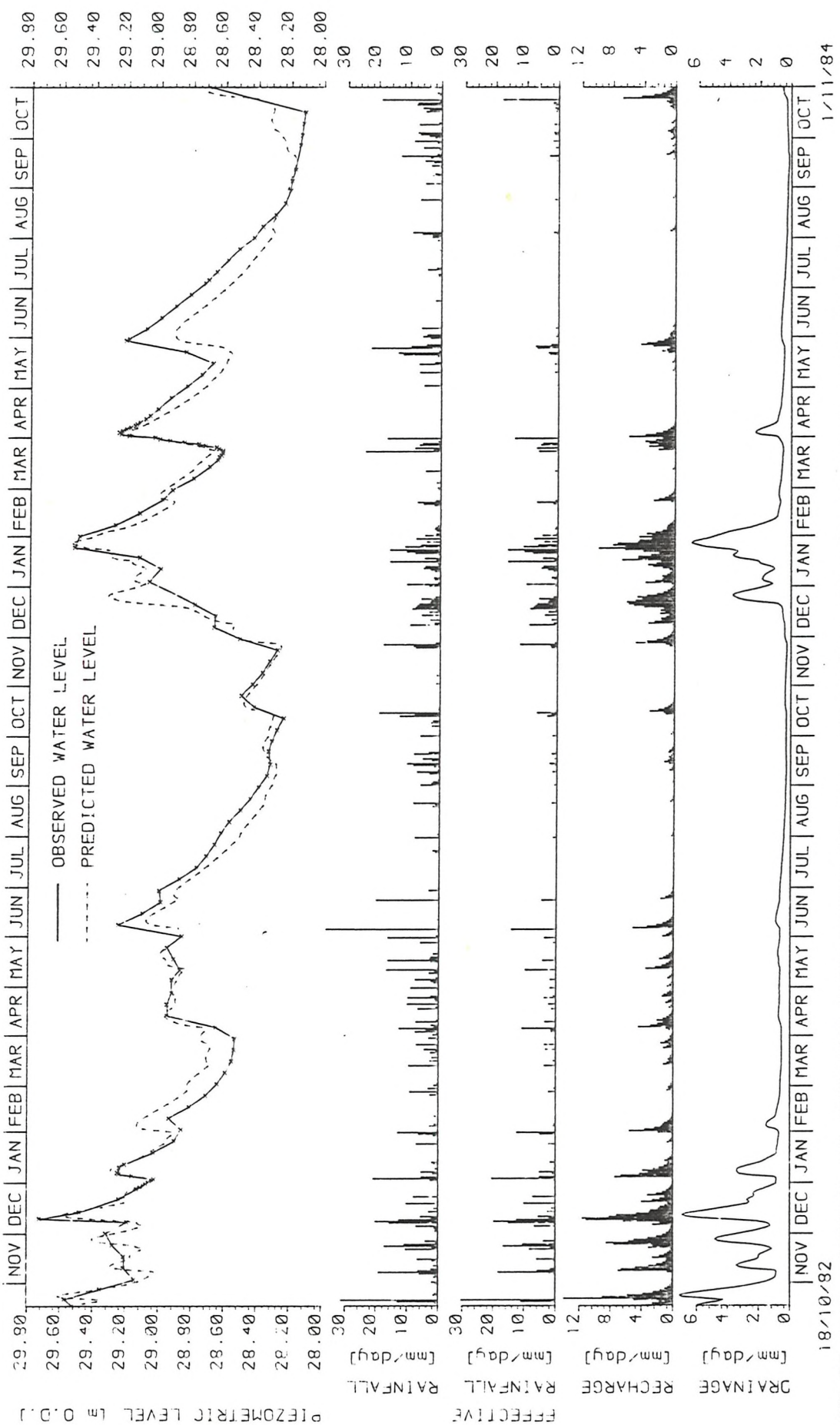

FIGURE 6.22 OBSERVED AND PREDICTED WATER LEVELS FOR P61. ALSO SHOWN ARE THE DISTRIBUTIONS OF RAINFALL, EFFECTIVE RAINFALL, RECHARGE AND DRAINAGE. PARAMETER VALUES ARE AS GIVEN IN TABLES 6.3 AND 6.6.

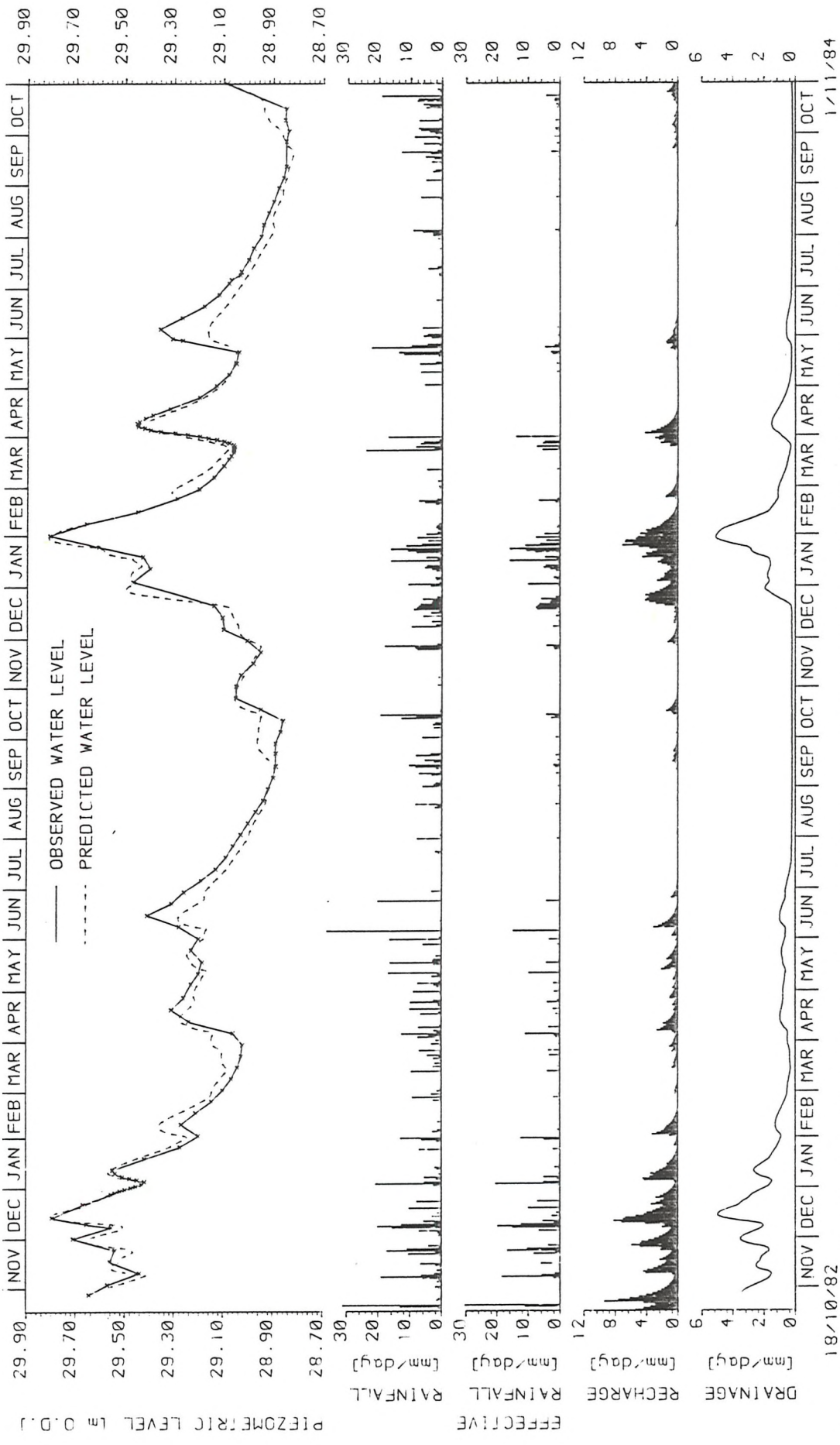

FIGURE 6.24 OBSERVED AND PREDICTED WATER LEVELS FOR P62. ALSO SHOWN ARE THE DISTRIBUTIONS OF RAINFALL, EFFECTIVE RAINFALL, RECHARGE AND DRAINAGE. PARAMETER VALUES ARE AS GIVEN IN TABLES 6.3 AND 6.6.

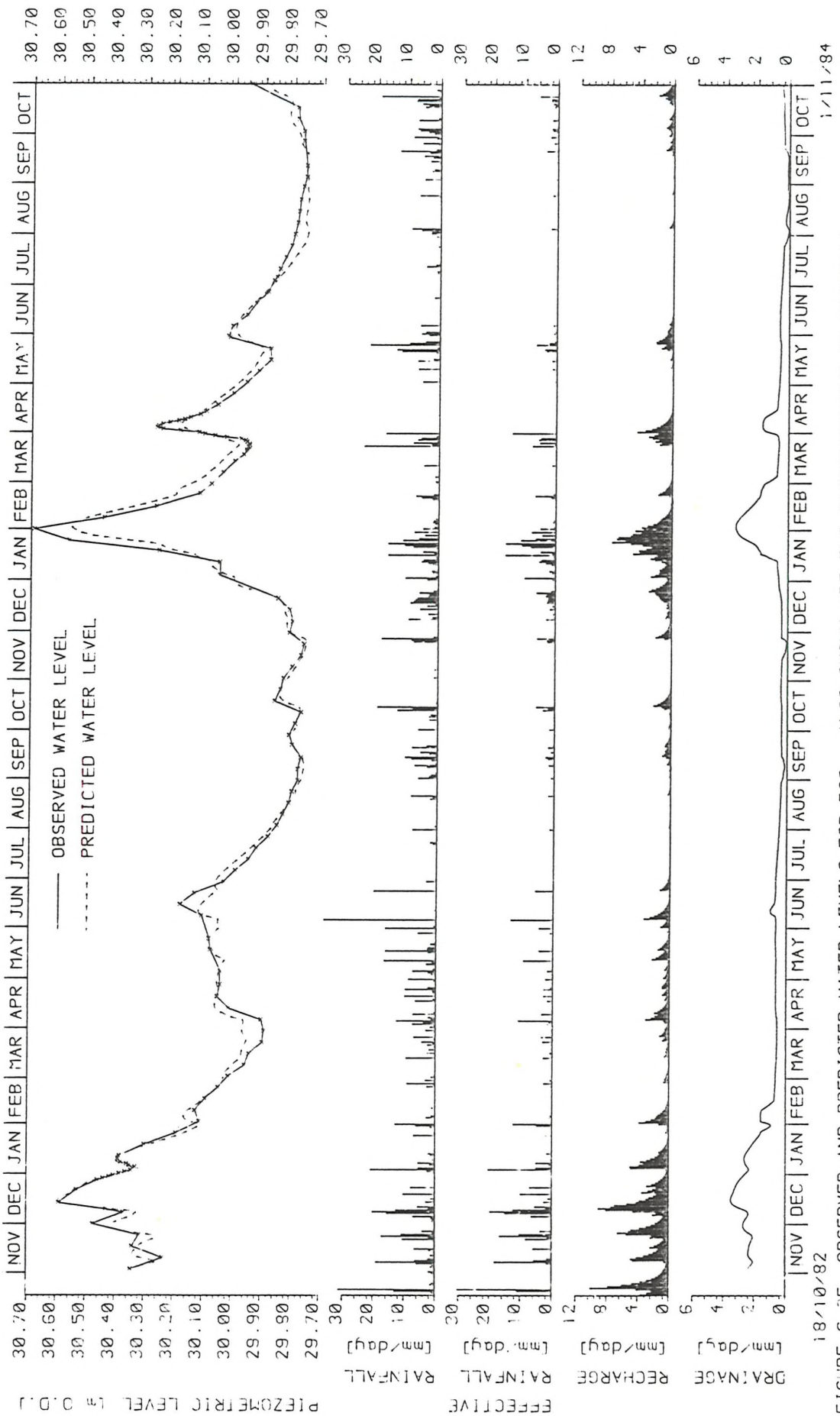

FIGURE 6.25 OBSERVED AND PREDICTED WATER LEVELS FOR P63. ALSO SHOWN ARE THE DISTRIBUTIONS OF RAINFALL, EFFECTIVE RAINFALL, RECHARGE AND DRAINAGE. PARAMETER VALUES ARE AS GIVEN IN TABLES 6.3 AND 6.6.

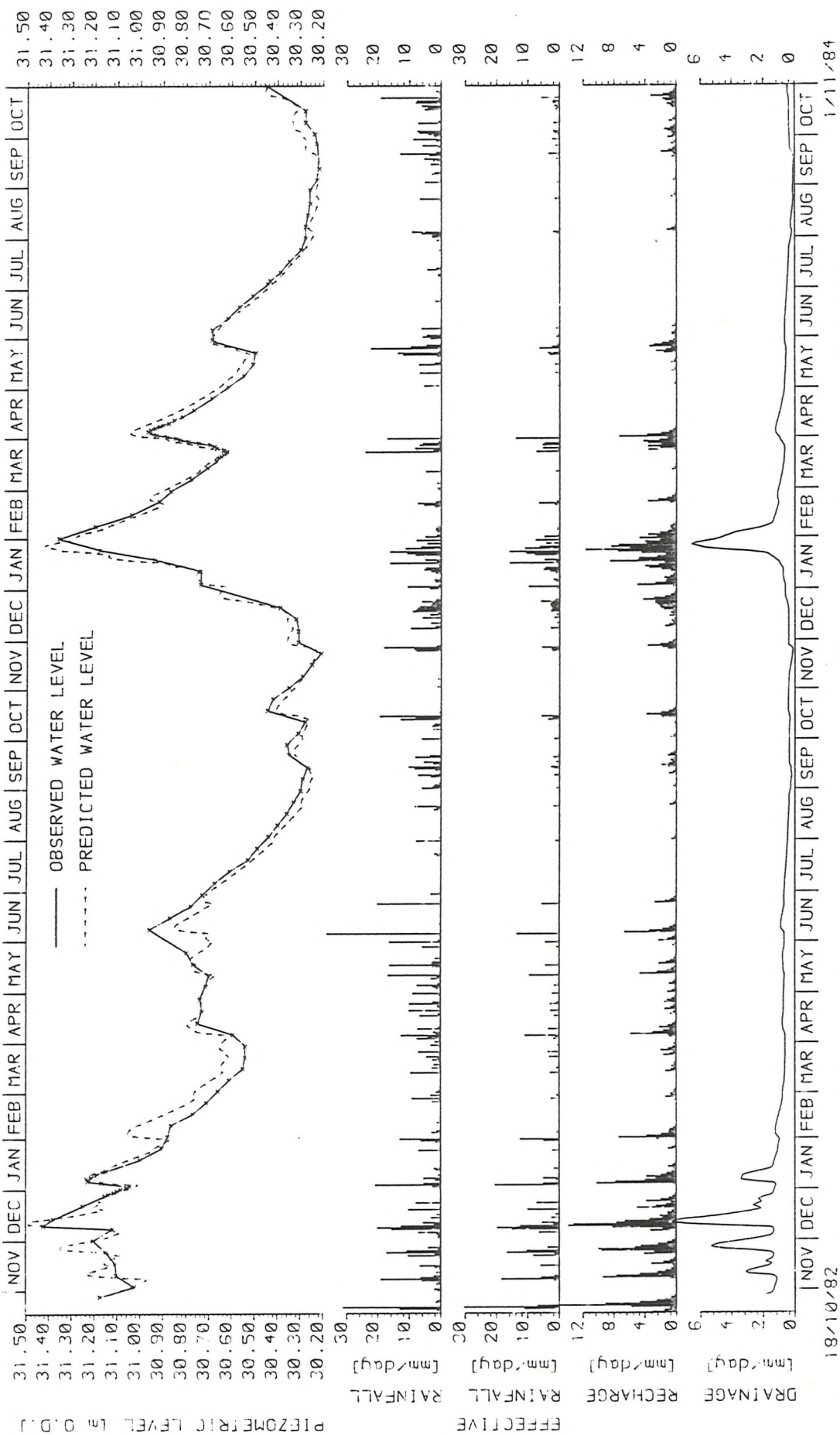

FIGURE 6.26 OBSERVED AND PREDICTED WATER LEVELS FOR P64. ALSO SHOWN ARE THE DISTRIBUTIONS OF RAINFALL, EFFECTIVE RAINFALL, RECHARGE AND DRAINAGE. PARAMETER VALUES ARE AS GIVEN IN TABLES 6.3 AND 6.6.

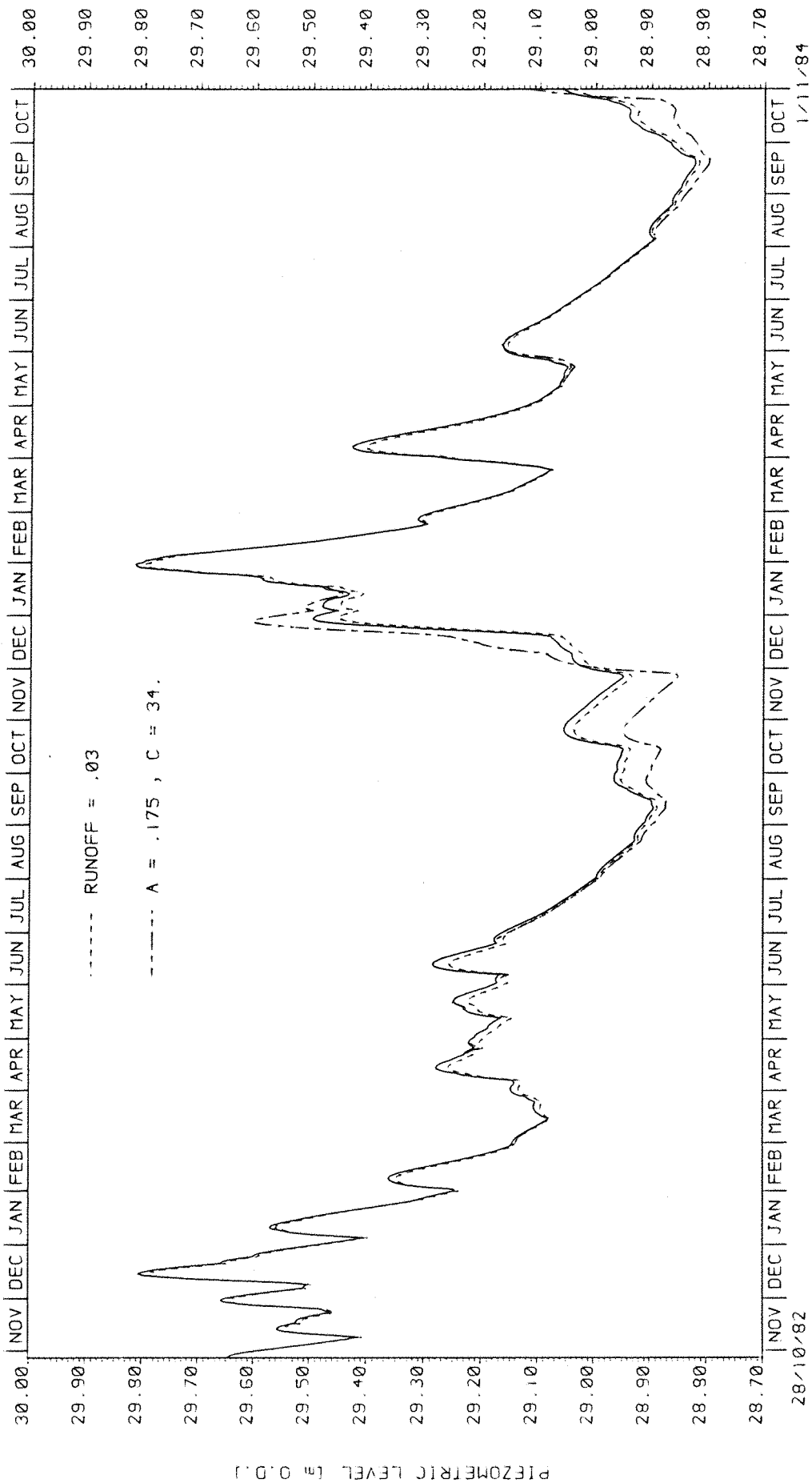

FIGURE 6.27 COMPARISON OF WATER LEVEL PREDICTION AT P62 USING DIFFERENT PARAMETER VALUES. PARAMETER VALUES ARE AS GIVEN IN TABLES 6.3 AND 6.6 EXCEPT AS INDICATED.

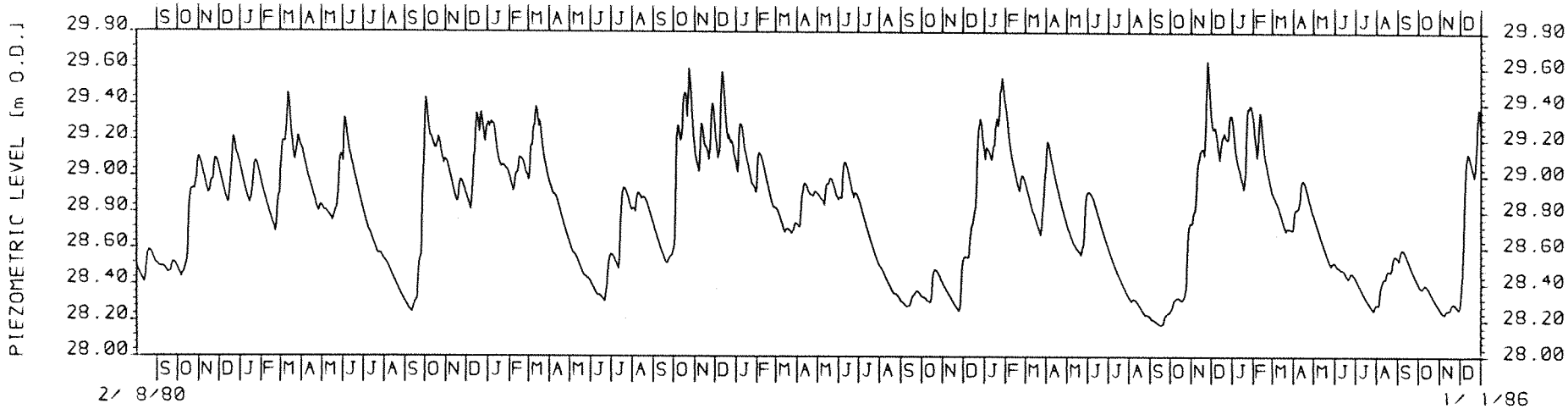

FIGURE 6.28 PREDICTED WATER LEVELS AT P61. PARAMETER VALUES ARE AS GIVEN IN TABLES 6.3 AND 6.6.

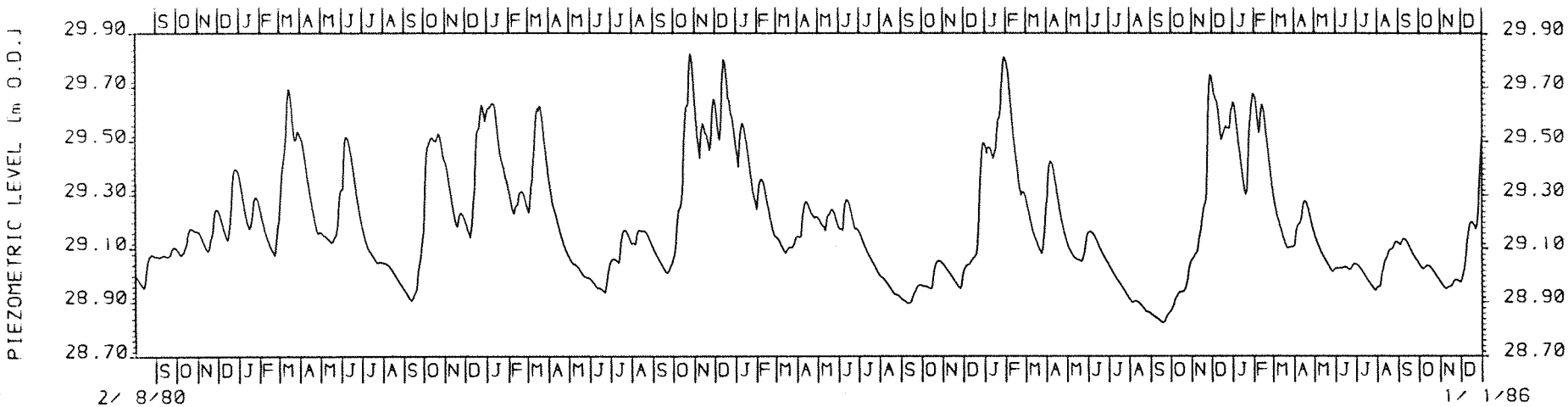

FIGURE 6.29 PREDICTED WATER LEVELS AT P62. PARAMETER VALUES ARE AS GIVEN IN TABLES 6.3 AND 6.6.

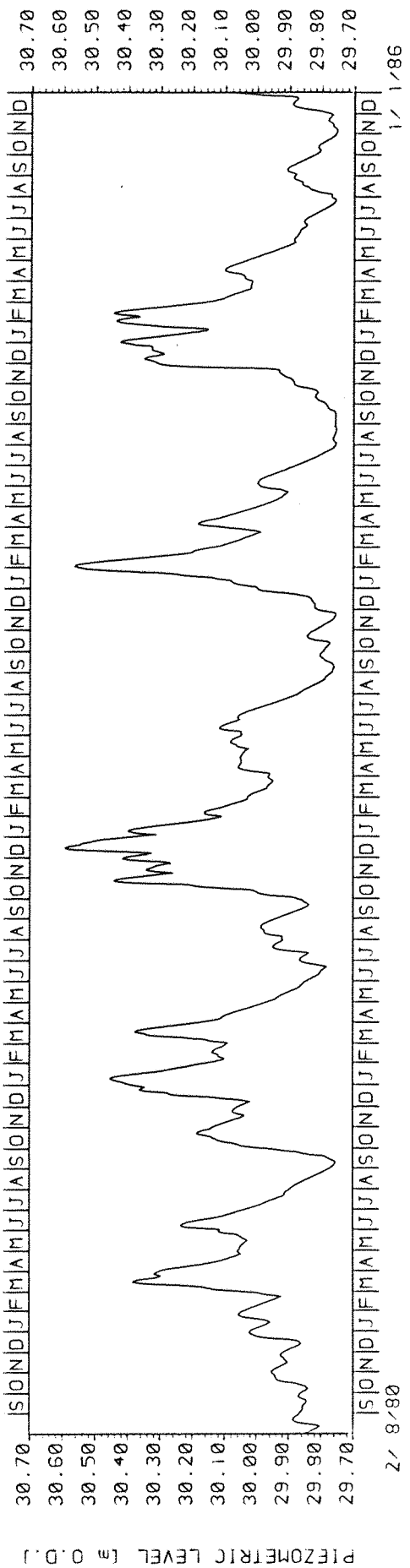

FIGURE 6.30 PREDICTED WATER LEVELS AT P63. PARAMETER VALUES ARE AS GIVEN IN TABLES 6.3 AND 6.6.

FIGURE 6.31 PREDICTED WATER LEVELS AT P64. PARAMETER VALUES ARE AS GIVEN IN TABLES 6.3 AND 6.6.

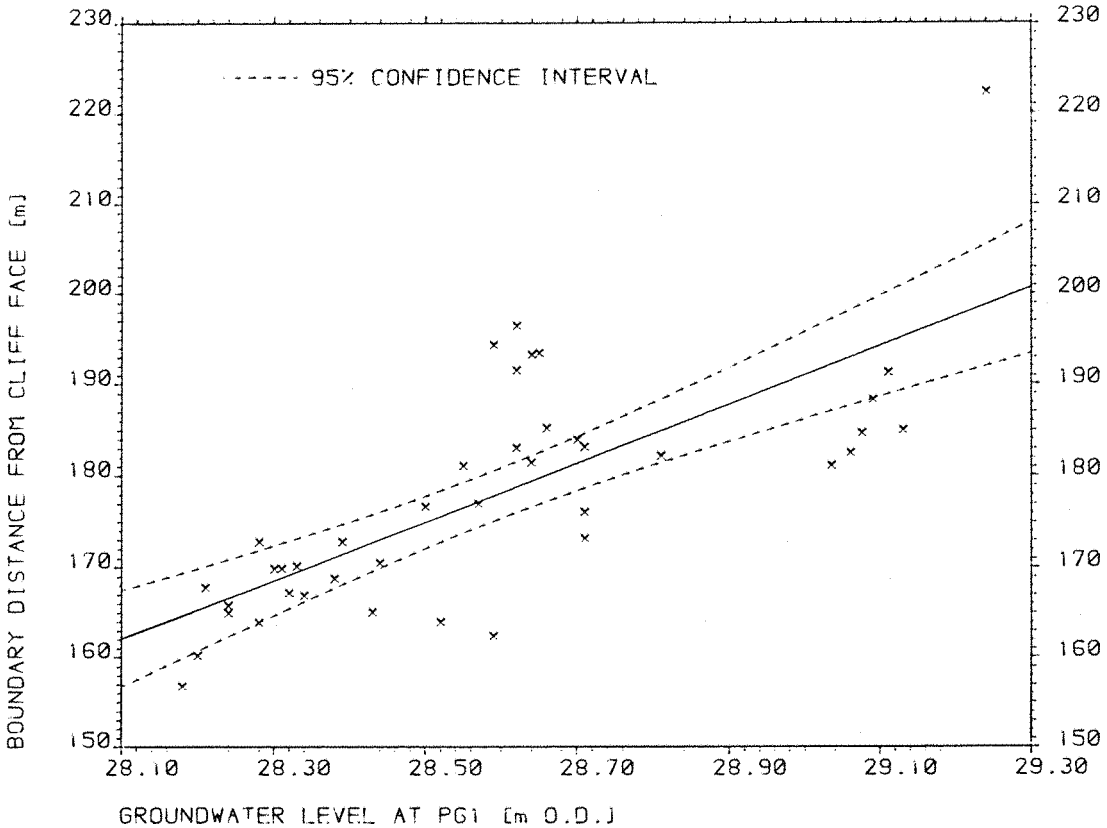

FIGURE 6.32 DISTANCE OF GROUNDWATER DIVIDE FROM CLIFF FACE AS A FUNCTION OF WATER LEVEL AT PG1

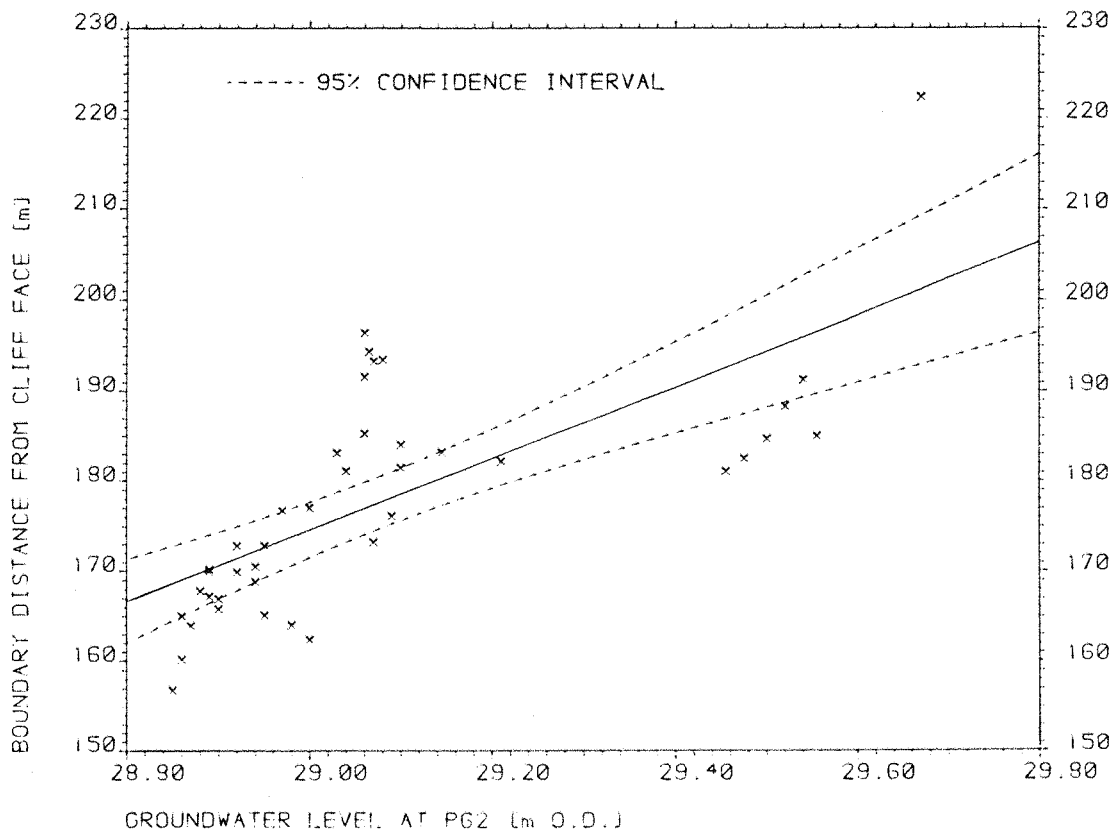

FIGURE 6.33 DISTANCE OF GROUNDWATER DIVIDE FROM CLIFF FACE AS A FUNCTION OF WATER LEVEL AT PG2

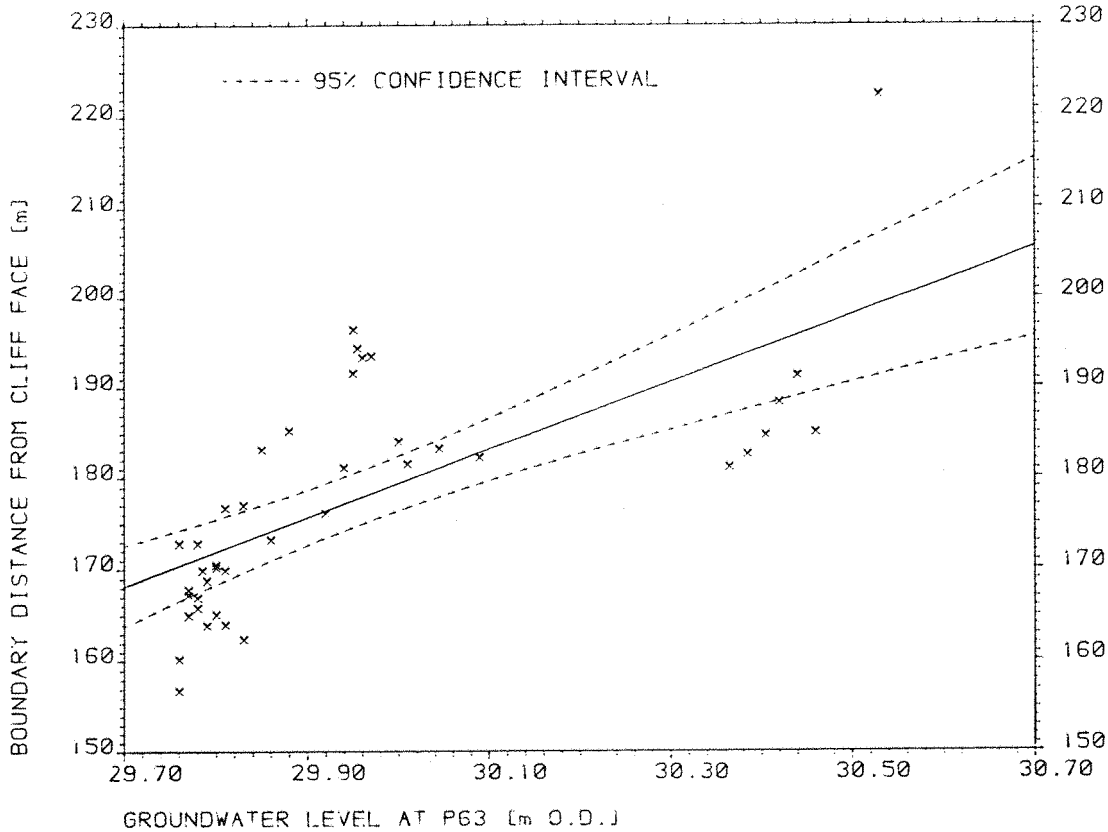

FIGURE 6.34 DISTANCE OF GROUNDWATER DIVIDE FROM CLIFF FACE AS A FUNCTION OF WATER LEVEL AT P63

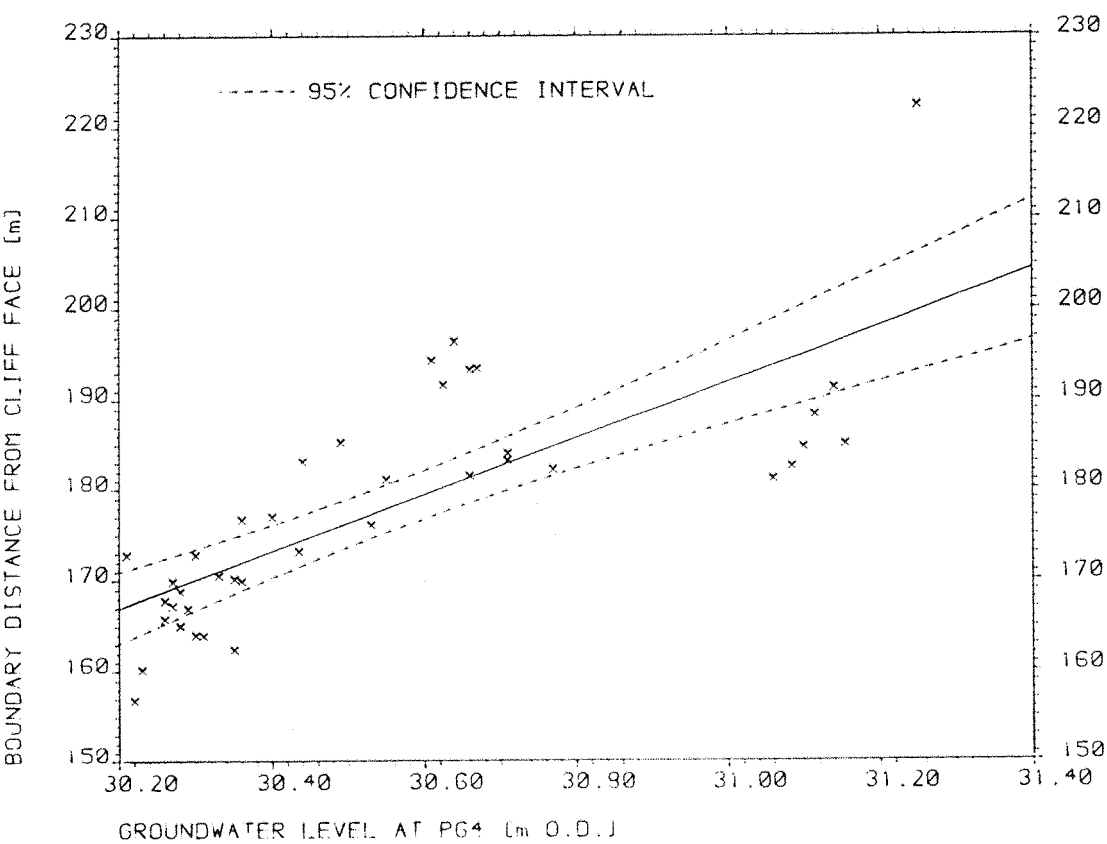

FIGURE 6.35 DISTANCE OF GROUNDWATER DIVIDE FROM CLIFF FACE AS A FUNCTION OF WATER LEVEL AT P64

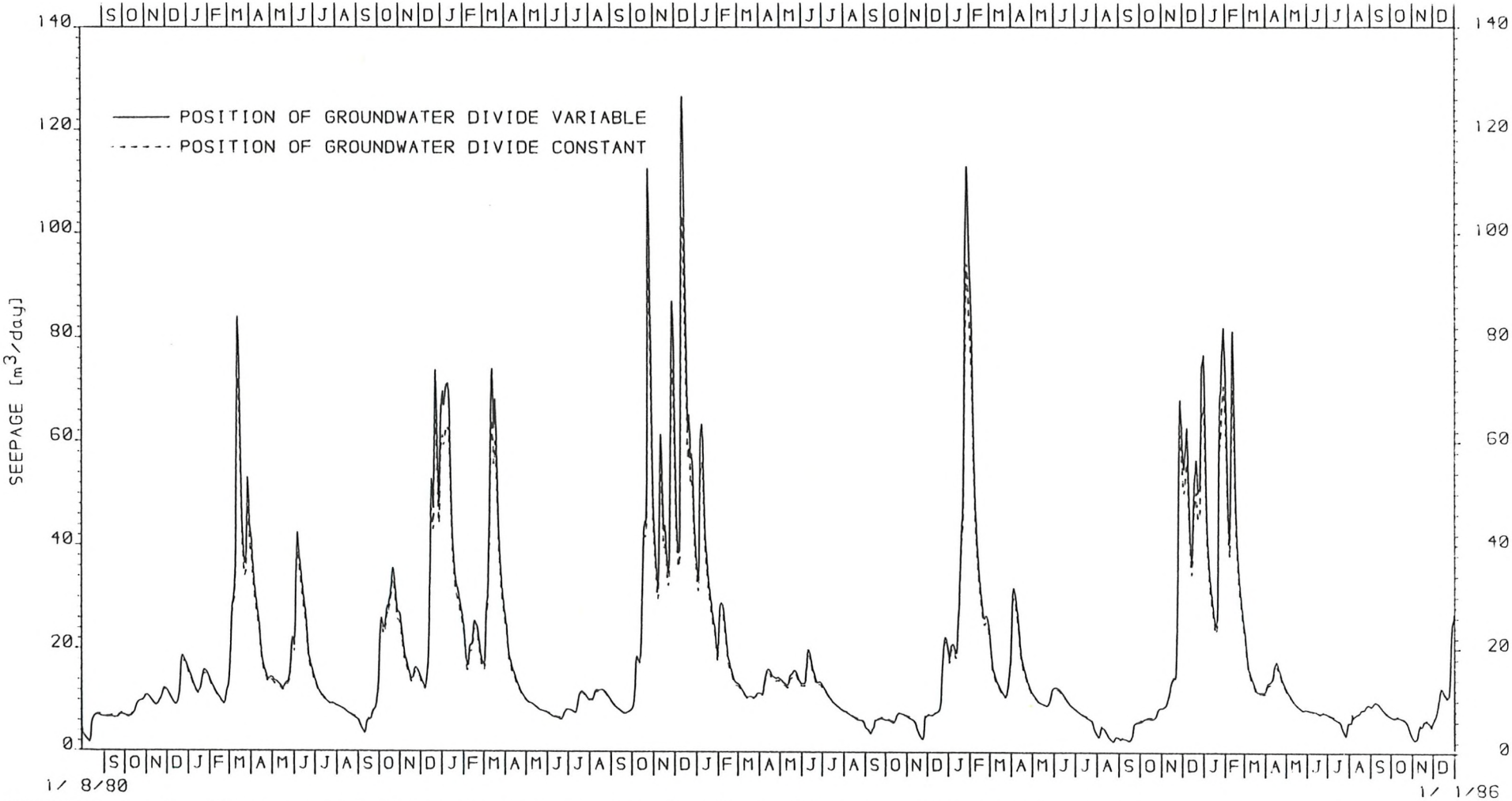

FIGURE 6.36 GROUNDWATER SEEPAGE OUT OF THE PLATEAU GRAVEL. THE GRAPH ALSO SHOWS THE ERROR WHEN THE POSITION OF THE GROUNDWATER DIVIDE IS ASSUMED CONSTANT. SEE FIGURE 6.1 FOR THE POSITIONS OF THE CONSTANT GROUNDWATER DIVIDE AND OTHER CATCHMENT BOUNDARIES.

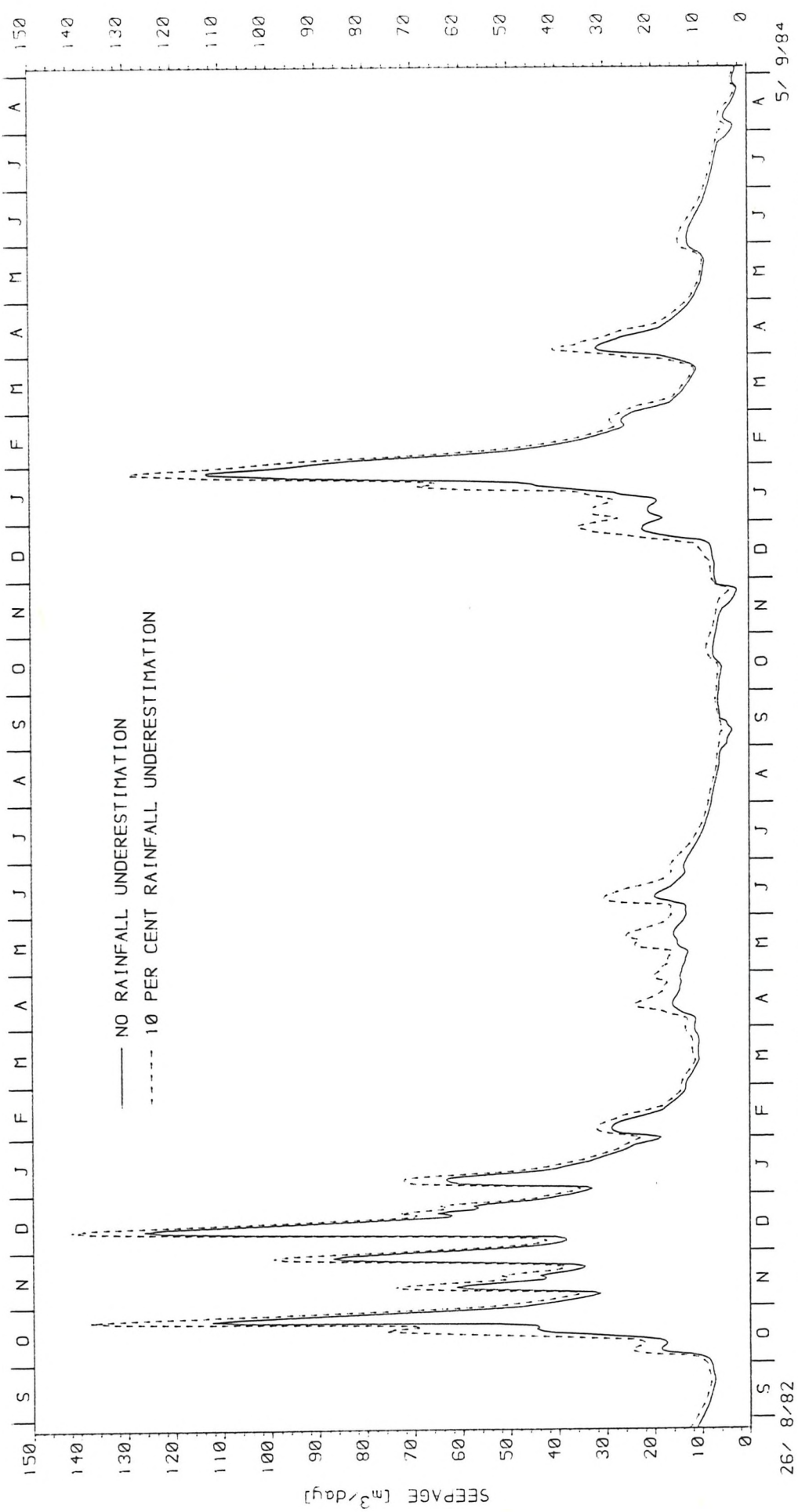

FIGURE 6.37 GROUNDWATER SEEPAGE OUT OF THE PLATEAU GRAVEL. THE GRAPH SHOWS THE ERROR DUE TO A CONSTANT UNDERESTIMATION OF RAINFALL. THE POSITION OF THE GROUNDWATER DIVIDE IS VARIABLE. SEE FIGURE 6.1 FOR THE OTHER CATCHMENT BOUNDARIES.

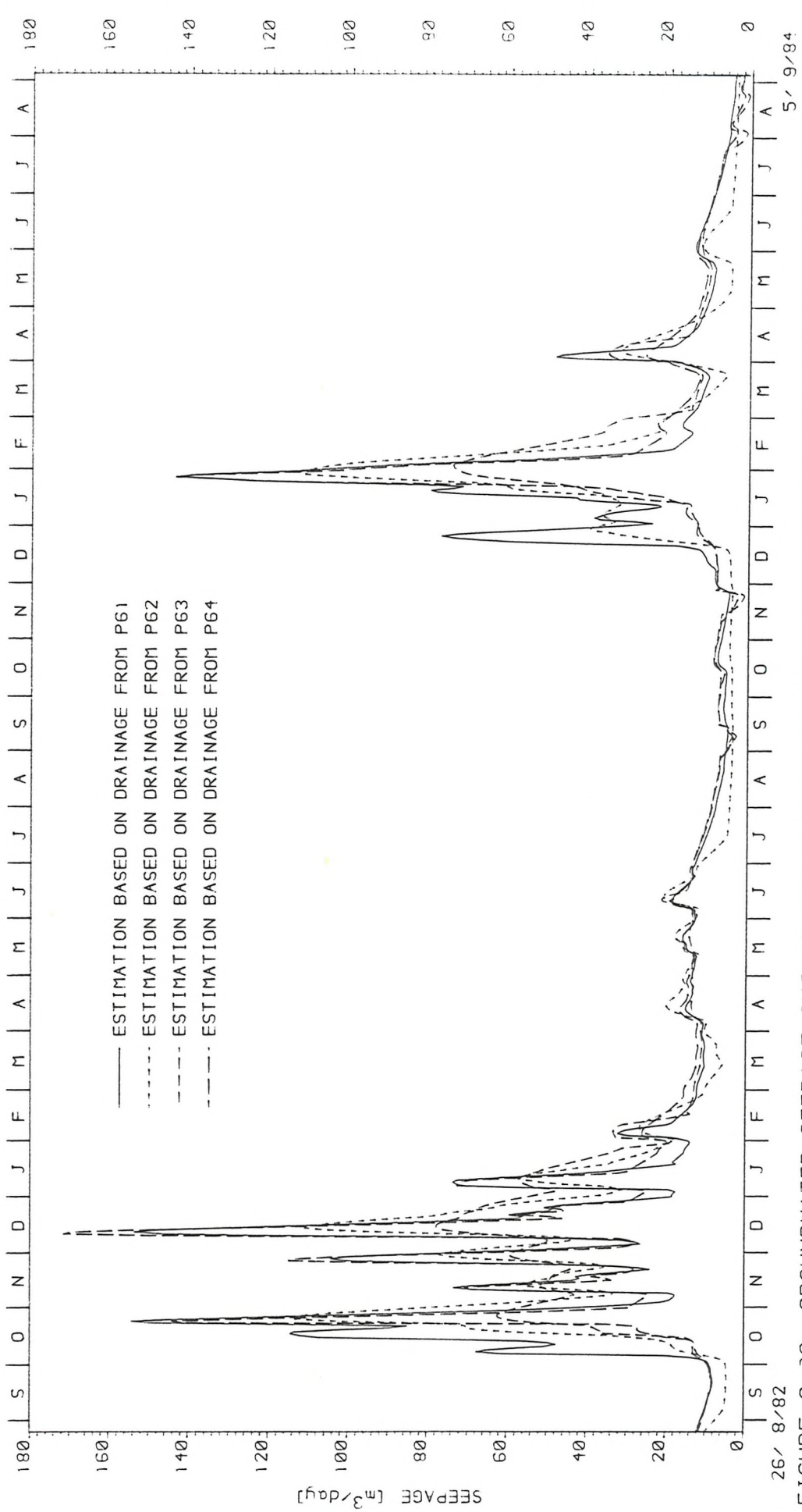

FIGURE 6.38 GROUNDWATER SEEPAGE OUT OF THE PLATEAU GRAVEL. THE GRAPH SHOWS THE VARIATION WHEN THE ESTIMATE IS BASED ON ONLY ONE PIEZOMETER. THE POSITION OF THE GROUNDWATER DIVIDE IS VARIABLE. SEE FIGURE 6.1 FOR THE OTHER CATCHMENT BOUNDARIES.

CHAPTER 7

BARTON CLAY DOMAIN

7.1 Introduction

A discussion of the hydrological role of the Barton Clay (BC) domain in the undercliff water balance was given in chapter 4. Basically, water flows in from the Plateau Gravel (PG) domain and out to the undercliff and underlying Bracklesham Beds. The significance and path of this seepage flow is considered in this chapter. Also of interest, is the hydrological role of the BC in the stability of the cliff top. The stability of the cliff top is dependent upon a number of factors, one of which is the pore pressure of any potential failure (shear) surface in the BC. This chapter also studies the influences on the pore pressures in the BC and their relative importance in stability.

7.2. Groundwater Level Observations

The study of the BC domain has centred on a number of groundwater level measurements, the locations of which are given in figure 7.1. Standpipe piezometers were used. The tips were installed in a 1 m length of filter sand which was sealed by bentonite tablets and grout. Borehole measurements, piezometer response tests, and groundwater level observations are all given in detail in Thomson (1986b).

The piezometers were all installed along the same section line. Comparison of figures 6.1 and 7.1 shows that this was the same as the section line through P61, P62, P60, P63 and P64. Due to the financial constraint it was not possible to install more than one section line of piezometers in the BC. Some areal variation of groundwater levels parallel to the cliff edge (i.e. perpendicular to the section line) is anticipated due to the slight dip of the Barton Beds.

Figure 7.2. is a geological cross section showing the depth locations of the piezometers. The zones and their thicknesses are given by Barton (1973) and shown in figure 1.3. They are based

on a borehole about 800m west of the section line (at N.G.R. 42139 09326). Barton (1973) gives the true dip of the beds as approximately ¾° ENE. This has been used together with the position of the F1/F2 boundary given in figure 4 of Barton and Coles (1984)to locate the zone boundaries in figure 7.2.

Table 7.1 is a summary of the groundwater level records of the piezometers in the Barton Clay. Readings were taken on the same dates as for the piezometers in the PG (see section 6.2).

7.3 Temporal Variation of Groundwater Levels

Variation in groundwater level observations is caused by the temporal variation of the various factors that influence groundwater levels. The factors influencing BC groundwater levels are: piezometer time lag; meteorological variations; and landslide activity.

Piezometer time lag was briefly discussed in section 6.3, paragraph 5, and is given in more detail in Thomson (1986b). Falling head tests were undertaken. The results enabled permeability estimates to be made (assuming horizontal and vertical permeabilities are equal). These are given in table 7.1. The analysis used was that of Hvorslev (1951). A few of the tests were also analysed using Gibson (1963). The results were similar to the Hvorslev (1951) method of analysis. The permeability estimates are based on assumptions made about the conditions of the piezometer tip and its location. The true conditions may be different. Therefore, the values of permeability should be considered with caution.

Piezometric observations should ideally be adjusted to allow for the time lag with the true groundwater level. This is done by using the basic time lag values given in table 7.1. The method of adjustment is described and used in Thomson (1986b) and comes from Hvorslev (1951). The amount of adjustment, in general, is dependent upon the amount of observed variation as well as the

value of the basic time lag. For the piezometers with the longest basic time lags, the readings were either fairly constant (P101), took the whole data period to equilibrate (P104), or gave a fairly constant rate of fall of water level (P102). This resulted in necessary adjustments of less than 2 or 3 cm (Thomson, 1986b). This is not much greater than the reading error ($\pm$ 1 cm), so that readings have not been adjusted for the purposes of this study.

Meteorological variations affect the amount and distribution of recharge reaching the groundwater table. This affects the position of the groundwater table which is predominantly in the PG domain (see chapter 6). In some places (see figures 6.11 to 6.14), the groundwater table may fall below the PG/BC unconformity and into the BC domain. At the two locations (P71 and P81) where this was observed to any great extent (see values of P_1 in table 6.1), the groundwater table moved up and down as rapidly in the BC as it did in the PG. Thus, for these locations the groundwater level in the top of the BC is affected by meteorological variations.

An increase in the groundwater table level increases the hydraulic gradient from the PG to the BC. This is reduced by increased leakage from the PG raising the groundwater levels in the BC. A fall in the groundwater table level will have the opposite effect. The effect is attenuated with depth such that it is less noticeable from the groundwater level measurements. The attenuation will depend upon the hydraulic connection with the groundwater table.

The results of the piezometers installed in the F zone of the BC show a definite similarity to those for the PG. This is exampled by figure 7.3 for P66. The groundwater level fluctuation (i.e. storm rainfall response) is attenuated but not delayed. The smaller response is also shown by a comparison of tables 6.1 and 7.1. The average range for the F zone piezometers is 0.66 m whereas for the PG piezometers (along the same section line) it is 1.20 m.

The results of piezometers in the E zone are more variable. P102 and P103 (figure 7.4) show no response to storm rainfall but do appear to show either a possible seasonal variation, or a gradual decline in groundwater levels. However, the data period is too small to be conclusive. The results for P105 (figure 7.5) show a more definite seasonal response. However, it also shows a small response to storm rainfall, as shown by the short rises in response to rainfall at the end of March and May.

The results of piezometers in the D zone have been complicated by the effect of landslide activity. The first half of the data record for P68 (fig 7.6) appears to show a slight 2 to 3 month delayed response to rainfall. For example, the rise in groundwater level at the end of December 1982 corresponds to the rapid rise in PG groundwater level (see figures 6.28 to 6.31) in September and October 1982. The second half of the data appears to have been affected by landslide activity. There is a downward trend in the groundwater levels after January 1984. There is also a downward trend in the groundwater levels for P69 (figure 7.7), but it is for the whole data period. P69 also shows a clear response to storm rainfall. Compared to the F zone results, there is no delay but the fluctuations are about half the size. Due to the slow response of P104, it was not possible to observe any temporal variation of groundwater level.

The slight variation in groundwater level in the A3 zone at P101 appears to be seasonal, being a maximum in the summer and a minimum in the winter. The data period is too short to say whether this is due to meteorological or landslide influences.

In section 1.9.4 it was stated that a characteristic of the equilibration of pore pressures, depressed due to unloading, is that they gradually rise with time as the soil swells. The rate at which pore pressures equilibrate may be extremely slow and, for example, has been measured by Hutchinson et al (1980) to be

0.15 m/yr in slipped Gault Clay at Folkestone Warren, Kent. Also, Dixon and Bromhead (1986) observed that the rate of equilibration in London Clay was slow. The data period may be too small to detect similar equilibration rates in the BC at Naish Farm. However, no such rising trends have been measured, and in fact, some measurements (P68, P69, and possibly P102 and P103) show a falling trend in groundwater levels. It is postulated here, that falling groundwater levels are due to changing boundary conditions, i.e. retreating cliff line, causing new equilibrium groundwater conditions at the piezometer tip, and not due to any changing volume of the soil skeleton.

On the whole, the results show that the effect of meteorological influences decreases with depth. The groundwater levels may also be complicated by landslide activity. However, for most of the piezometers the data period is too short to be sure whether landslide activity has affected the groundwater level record. Consequently, the effect has only been observed for piezometers in the D zone (P68 and P69).

7.4 Spatial Variation of Permeability

The permeability of fine sediments such as BC is low when the groundwater flow is mainly through the soil pores. The permeability is also anisotropic, being greatest parallel to the bedding. This is especially so for field permeability in sediments such as BC where there are fairly frequent changes in lithology (Barton, 1973). Fissures are present both parallel and perpendicular to the bedding. Groundwater flow through fissures increases field permeability, although the amount may be highly variable depending on the size (width) and density of fissures. Fissuring varies with lithology and stress relief (the presence of the cliff reduces lateral earth pressure and, hence, increases stress relief).

The permeability of the F2 zone was measured in the laboratory and found by West (1985) to be 1.22×10^{-10} m/s. However, the samples measured only 23-35 mm long by 38 mm diameter, and therefore did not represent the influence of fissuring. Therefore, field measurements, using falling head tests on piezometers (section 7.3, paragraph 2), have been used to estimate the permeability. It is assumed that the volume sampled is large enough to fully represent the influence of fissures on groundwater flow. In other words, for a number of piezometers of the same geometry, crossing the same bedding, and under the same stress conditions, the estimated permeability should be the same.

Estimates of the BC permeability at all the piezometers are given in table 7.1. With one of two exceptions they are greater than the laboratory estimate. Thus, fissure flow is considered to have a considerable influence on the BC permeability. The piezometer response tests were analysed assuming that the horizontal and vertical permeabilities were equal (i.e. isotropic). This is true where permeability values are mainly influenced by fissures which are as frequent in the horizontal direction as they are in the vertical direction. However, it is unlikely to be true where the permeability is mainly influenced by pore water flow (low permeability values).

The results for the F zone show that permeability decreases with increasing distance from the undercliff. The permeability varies by a factor of 50. If it is assumed that the filter length of each piezometer crosses the same bedding (figure 7.2 shows this to be approximately true), then the increase in permeability toward the undercliff can be attributed to the effect of the increase in stress relief opening up the fissures.

The results for the E zone show that permeability varies by a factor of 22, and increases with increasing distance from the undercliff. This is contrary to what is expected if just stress

relief is influencing the variation in the value of permeability. Figure 7.2 shows that the piezometers cross approximately the same bedding planes. However, there is a slight variation, such that the permeability values could be accounted for by a rapid change in the permeability of the beds with depth. Barton (1973) describes the E zone as being "locally rich in fossils". The fossil lenses are highly permeable. Thus, an alternative possibility is that piezometers P102, P103 and P105 cross fossil lenses of differing extents.

Barton (1973) describes the A3 zone as "regularly interbedded sand and grey clay". Table 4.2 gives measured particle size distributions of the A3 sand bed. Using Hazen's formula, Halcrow (1971) estimated the permeability to be 10^{-6} m/s. It is somewhat surprising, therefore, that such a low value of permeability was obtained for P101. Booth (1974) describes the sand beds as making up about 30 per cent of the total thickness of the A3 zone. If the proportion of the bedding the piezometer crossed was 30 per cent sand beds, the field permeability value in table 7.1 would suggest a permeability of the sand of 1.3×10^{-9} m/s. (This is estimated using the equation of the equivalent horizontal permeability for a layered soil given in Freeze and Cherry, 1979, p 34. The maximum sand permeability is for zero clay permeability.) This is considerably less than that estimated by Halcrow (op cit). However, this estimation does not take into account bulk density. The BC is over-consolidated and so would be expected to have a high bulk density. High bulk density (and therefore low permeability) in sand deposits is mainly due to cementation and only secondarily due to compaction (Pettijohn et al, 1972, p 392). Booth (1974) describes the A3 sand as of variable density from loose to compact and in places cemented by calcium carbonate. This is based on evidence from exposures where stress relief and leaching will make the sands appear less dense, and less cemented, than at positions such as P101. Thus, it is considered that the sand beds at P101 probably have a high bulk density due to a combination of previous consolidation pressures and cementation.

However, the A3 zone is fissured and probably increases in permeability where it is under the undercliff and subject to greater stress relief.

Apart from the estimates for the E zone, the permeability decreases with depth. However, the results are few, and due to the highly variable lithology, it is more probable that, whilst on average it may decrease, the permeability value will also greatly fluctuate with depth.

The spatial variation of permeability has only been considered with depth and perpendicular to the line of the cliff face. There will also be a variation parallel to the cliff face. The permeability for the same bedding (except where local variations, such as fossil lenses, affect permeability) will decrease from west to east due to the dip of the beds. (The increased overburden, or stress, closes up fissures. It also affects the volume of the soil matrix and,therefore, the permeability due to pore water flow.)

The permeability of the BC is spatially very variable. From the above discussion this variation may be due to: variation in stress relief; vertical variation in fissuring and lithology; and the presence of local factors such as highly permeable shelly lenses.

7.5 Spatial Variation of Groundwater Levels

Figure 7.8 shows the estimated equipotential lines for the geological cross section in figure 7.2. They are based on the piezometric readings for two particular dates (1st February 1984 and 12th September 1984). These represent the two extremes of groundwater level readings. Some of the piezometers were not read on one or both of the dates, but have been estimated from the rest of their respective groundwater level records. The groundwater level for P104 was assumed to be temporally static and equal to the single groundwater level determination of 5th

December 1984. The groundwater levels at P101, P105 and P106 were extrapolated back in time to determine the 1st February groundwater levels. For P101 it was assumed to equal the minimum recorded groundwater level (see section 7.3, paragraph 9). For P105 (figure 7.5) it was assumed to equal the maximum recorded groundwater level (the other two E zone piezometers (P102 and P103 (figure 7.4))show only a slight drop in groundwater level between the 1st February and mid March (start of readings for P105)). For P106 the groundwater level recession was extrapolated back 14 days. Any error in these estimations is not expected to make a significant difference to figure 7.8.

Groundwater level readings for both the PG and BC have been used. The PG readings give the groundwater level for the top of the BC. The equipotential lines have been estimated by linear interpolation between piezometer readings. The true groundwater level between piezometers is unlikely to vary linearly. This can be seen in figure 7.8 by the highly variable hydraulic gradient between different pairs of piezometers. It is likely that the hydraulic gradient (and therefore groundwater level) will also be highly variable in between the piezometers. The variation in hydraulic gradient is likely to be linked by a variation in permeability. (If the groundwater flow is constant in any direction, a decrease in permeability will cause an increase in hydraulic gradient as a consequence of Darcy's Law.) Thus, it is likely that the permeability of the soil in between the piezometers is highly variable.

Figure 7.8 shows that the difference in groundwater levels between the two dates decreases with depth. This is indicative of the decrease with depth of the fluctuation in groundwater levels (as discussed in section 7.3). On both dates the groundwater levels decrease toward the cliff face and with depth. This indicates that groundwater flow is both downward and toward the cliff face. For isotropic and homogeneous soil the equipotential and flow lines cross at right angles. Unfortunately, due to the highly variable value of permeability (both directionally and

spatially) it is not possible to draw flow lines on figure 7.8. The permeability estimates in table 7.1 assume isotropy (i.e. permeability is directionally constant). Errors in this assumption cause relatively small differences in the estimation of (horizontal) permeability (Thomson,1986b), whereas they could make a large difference to the angle between the flow and equipotential lines.

The equipotential lines have been estimated by assuming that the piezometer readings represent the groundwater level of the beds they cross. From the results, this appears to be in doubt for one or two piezometers. However, it would be unwise to reject results just because they do not fit the understanding of the groundwater flow. This is especially so in view of the heterogeneous nature of the BC.

P68 (figure 7.6) and P69 (figure 7.7) give very different temporal responses. Although they do cross slightly different beds, it would still be reasonable to expect similar responses. P69's greater and faster response to meteorological variations seems to indicate that it has a better hydraulic connection with the groundwater table. This may be related to the level of the PG/BC unconformity which takes a sharp drop between P103 and P69 (see section 2.5.2, paragraph 3) and is 2 m lower at P69 than at P68 (Thomson, 1986b). This could indicate a frost wedge cast (Barton, 1984a, presents evidence of such features at Naish Farm) extending down to an unknown depth. The cast, filled with PG, narrows rapidly with depth and becomes a fissure. Because its dimensions are small, the flow through the cast and fissure would be relatively small, and therefore it would have only a limited areal effect on groundwater levels. This suggests why it only affects P69 and not other piezometers slightly further away (P67 and P103). P68 and P69 have also been affected by landslide activity (see section 7.3, paragraph 8) but to a different extent. This would seem to indicate that they have different hydraulic connections with the undercliff.

The groundwater level at P104 appears to be slightly low in comparison to the other D zone piezometers (P68 and P69). This could be due to a zone of low permeability (as indicated by the permeability value for P104 in table 7.1) causing a strong hydraulic gradient (and therefore a large change in groundwater level with depth) at P104. Slight errors in the measurement of the depth of the filter length might account for the apparently low groundwater level at P104. (Borehole measurements were made to $\pm$ 0.1 m.)

The groundwater level at P105 appears to be somewhat high in comparison to the other E zone piezometers (P102 and P103). The temporal response is also different (compare figures 7.4 and 7.5), and resembles more the F zone piezometers (e.g. figure 7.3). This would indicate a better hydraulic connection with the groundwater table than P102 and P103. Figure 7.8 indicates a strong hydraulic gradient above piezometers P102 and P103 and below piezometer P105. If this hydraulic gradient was confined to a relatively small thickness of the BC, then slight differences in the levels of the E zone piezometers would account for the difference in groundwater levels. Figure 7.2 shows the filter lengths of each of the three piezometers crossing slightly different beds. This could be accentuated by slight undulations in the beds.

Halcrow (1971) measured groundwater levels in the A3 zone at Highcliffe at different locations. They show that parallel to the cliff line, the groundwater level is falling due to the dip of the beds. Extrapolation of this fall to the location of P101 (in the A3 zone), gives a groundwater level in agreement with that measured. This gives supporting evidence of the correctness of the values used in figure 7.8.

The spatial variation of groundwater levels may be influenced by stress relief induced pore pressure effects. Bromhead and Dixon (1984) and Dixon and Bromhead (1986) showed that the existing pore

pressures in a London Clay cliff on the Isle of Sheppey, North Kent, were lower than that predicted using a numerical model of steady state seepage. This is due to the long time required for pore pressures to equilibrate in London Clay as a result of stress relief following cliff failures. The permeability of the BC is greater than that of London Clay (Bromhead and Dixon, 1984, using piezometer response tests found the permeability of London Clay to vary from 3.5×10^{-10} m/s in the weathered upper surface of the clay to 4×10^{-11} m/s at a depth of 36 m: compare with table 7.1) such that the time taken for pore pressures to equilibrate is certainly less for BC. Also, the results discussed in section 7.3 do not show the characteristic rising groundwater levels associated with the stress relief induced pore pressure effects. Therefore, it is believed that pore pressures have equilibrated.

The spatial variation of groundwater level is greatly complicated by the variation in lithology, and hence permeability, and by landslide activity. However, in summary, groundwater level decreases with depth and increases with distance from the undercliff; and the temporal variation of groundwater level decreases with depth.

7.6 Leakage into the Barton Clay Domain

The groundwater level data (see figure 7.8 and section 7.5) indicates that there is a downward flow of water from the PG to the BC. This flow is termed the leakage into the BC. The areal extent of the leakage considered here is the same as that for the calculation of PG drainage (see section 6.6.2 and figure 6.1). Groundwater flow into the BC from the undercliff colluvium is considered in chapter 9.

7.6.1 Method of Estimating Leakage

The method used to estimate leakage is based on using Darcy's

Law to calculate the vertical flux at five locations (A, B, C, D and E) which are along the line of piezometers. The positions of these locations are given in table 7.2, and are determined by the piezometer readings in both the PG and the BC. The vertical flux at each location is weighted and summed to find the total areal leakage.

It is assumed that the groundwater flow between the PG/BC unconformity and the boundary between the F1 and F2 zones is vertical. It is also assumed that throughout the depth of the F1 zone the vertical hydraulic gradient is uniform, and permeability is constant and isotropic. The calculation of hydraulic gradient requires two groundwater level measurements in the F1 zone and the distance between them. These are provided by the PG and F zone piezometers. The water level in the PG piezometers represents the groundwater level in the BC at the PG/BC unconformity. The water level in the F zone piezometers is taken to represent the groundwater level at the middle of the filter length. Response tests on the F zone piezometers are also used to provide permeability estimates (see table 7.1) for the F1 zone.

The details of locations A, B, C, D and E are given in table 7.2. The necessary measurements (permeability and the groundwater levels at two different, known depths) needed to calculate the vertical flux have not been made at all these locations. The missing measurements have had to be estimated. Locations A, B, C and D use the permeability estimates and groundwater levels in the F zone at P65, P66, P67 and P106 respectively. Locations B, C, D and E use the groundwater levels in the PG at P61, P62, P63 and P64 respectively. The groundwater level at the top of the BC at location A is estimated by using the groundwater levels at P61 and P62 and assuming a constant hydraulic gradient between locations A and C. The level of the unconformity at location A was estimated by linear interpolation of the levels at P61 and the cliff face. The groundwater level near the bottom of the F1 zone at location E, was estimated by using the groundwater levels at

P67 and P106, and assuming a constant hydraulic gradient between locations C and E. The vertical position of the F zone groundwater level at location E was estimated by the average of the corresponding positions at locations C and D. The permeability of the F zone decreases with increasing distance from the cliff face. In section 7.4 this was attributed to the effect of stress relief. It is considered that stress relief has negligible effect further from the cliff face than P106. Therefore, the permeability at location E is assumed to be the same as that at location D. The F zone permeability and O.D. levels of the groundwater level measurements used for all five locations are given in table 7.2.

The estimates of leakage are made on a daily basis. This is done by using the groundwater level prediction model described in chapter 5, together with the parameter values in tables 6.3 and 6.6, to simulate groundwater levels at P61, P62, P63 and P64. The groundwater level prediction model has not been calibrated for the F zone piezometers. Instead, the F zone groundwater levels are estimated using a correlation relationship with the PG groundwater levels. As this gives a unique relationship between the two groundwater levels, there must also be a unique relationship with the hydraulic gradient. This is of more direct use in the calculation of leakage. Therefore, the hydraulic gradient has been estimated by correlating it with the PG groundwater level. The vertical flux at each location is found by multiplying the hydraulic gradient by the permeability (Darcy's Law). The groundwater level prediction model calculates the groundwater level at the end of each time step (day). In section 5.2.3 it was assumed that the groundwater level varies linearly through the time step. If the correlation between the hydraulic gradient and PG groundwater level is assumed to be linear, then the vertical flux also varies linearly through the time step. Therefore, to calculate the total leakage for each day at each location, the vertical fluxes at the start and end of the day are averaged and multiplied by 1 day.

The areal extent of the leakage considered here is the same as that for the calculation of PG drainage. It is assumed that the area represented by each location is proportional to its representative length along the cross section of figure 7.2 (same as line through P61 and P64). Thus, the calculation of areal leakage is similar to that of PG drainage (see section 6.6.3). The leakage at each location is multiplied by its representative length (as given in table 7.2) and summed to give the total leakage from the cross section of figure 7.2 (LINELEAKAGE). The total areal leakage (CATCHMENTLEAKAGE) is then calculated by using equation 6.4, with LINELEAKAGE substituted for LINEDRAINAGE, and CATCHMENTLEAKAGE substituted for CATCHMENTDRAINAGE.

7.6.2 Discussion of Results

The piezometric observations in the F zone at location D are limited. Figure 7.9 shows the linear correlation relationship used to extend the data for P106 using the data of P67 (F zone, location C). Figures 7.10 to 7.14 show the linear correlation relationships used to estimate the hydraulic gradient at each location from the PG groundwater level. They show that hydraulic gradient increases with groundwater level. This is due to the decreasing response to meteorological fluctuations in the BC with depth (see section 7.3).Figures 7.9 to 7.14 also show the 95 per cent confidence limits for the regression lines.

Figure 7.15 shows the calculated leakage from the BC. It shows both the total leakage, and the separate contributions from the areas represented by each of the five locations. The temporal fluctuation is due to the variation of hydraulic gradient with PG groundwater level (figures 7.10 to 7.14). The figure shows a decreasing contribution to leakage with increasing distance from the cliff face. This is despite the area represented by each of the locations increasing with the location's distance

from the cliff face (as signified by the representative lengths (of the cross section in figure 7.2) given in table 7.2). The decrease in leakage is due mainly to the variation in permeability, although the increase in hydraulic gradient toward the cliff face also contributes.

The assumption of a constant hydraulic gradient in the F zone between locations C and E is likely to overestimate the F zone groundwater level at location E. This would cause the vertical hydraulic gradient to be underestimated. As a consequence, the correlation between vertical hydraulic gradient and PG groundwater level (figure 7.14) gives a small upward (negative) hydraulic gradient at low groundwater levels. Upward flow is not expected and therefore the minimum allowable hydraulic gradient (as shown in figure 7.14) is zero. The underestimation of hydraulic gradient is likely to be offset by the probable overestimation of permeability (assumed equal to that at location D). The true flux at E is unlikely to be any greater than at D. Figure 7.15 shows this to be small (the areas represented by locations D and E are about the same). Therefore, any assumptions about the permeability and groundwater level at location E are unlikely to cause significant errors.

Most of the total leakage comes from the area represented by location A. Therefore, this is potentially the most significant source of error. The groundwater table level was estimated by assuming a constant hydraulic gradient between locations A and C. This is unlikely to cause serious error, as both the distance between locations A and B, and the variation in the groundwater table slope, are small.

The estimation of permeability is likely to be a more significant error. The calculation of leakage uses the vertical permeability value. The estimation of horizontal permeability, using piezometer response tests, is relatively insensitive to the degree of anisotropy (Thomson, 1986b). This makes vertical permeability very sensitive to the degree of anisotropy. Thus,

the calculation of leakage is also very sensitive to the degree of anisotropy. As an example, if the ratio of vertical to horizontal permeability is 10, then the leakage is 5.8 times greater than that shown in figure 7.15 (which assumes the ratio to be 1). The error in assuming isotropy affects all the locations but is most significant at location A.

Another source of error is the representativeness of location A. It is assumed that the leakage at location A is equal to the average leakage from 0 to 6.7 m from the cliff face (see table 7.2 for representative lengths). Both permeability and vertical hydraulic gradient increase toward the cliff face. In particular, the slope of the relationship between permeability and distance from the cliff face gets flatter with increasing distance from the cliff face (this can readily be seen from the values in table 7.2). This means that the position of the location representing the area from 0 to 6.7 m from the cliff face should be less than 3.35 m from the cliff face. Location A is 4 m from the cliff face and therefore underestimates leakage from the area it represents.

It is assumed that groundwater flow in the F1 zone is vertical. Figure 7.8 shows that this is not quite true, and that there is a component of lateral flow toward the undercliff. This will result in a slight underestimation of leakage. Assuming isotropy and constant permeability with depth, it can be calculated from figure 7.8 that this underestimation is up to 6 per cent. The assumptions of constant permeability and uniform vertical hydraulic gradient with depth are unlikely to be true. It is more likely that permeability decreases with depth. (Stress increases with depth and causes fissures to close, and hence permeability to decrease.) To maintain the same vertical flow, the vertical hydraulic gradient would need to increase with depth. Thus, the vertical flow past the F1/F2 boundary would be greater than the leakage calculated in figure 7.15 (due to the greater hydraulic gradient). The increase in hydraulic gradient with depth would cause the equipotentials to be more vertical in the

upper part of the F1 zone. Coupled with the greater permeability, this would result in an increase in lateral flow in the F1 zone. Thus, the leakage from the PG into the BC would be even greater. The errors in these assumptions are not known, but it is clear that they may lead to some underestimation of the leakage into the BC.

In section 6.6.4 errors in both the estimation of rainfall and the position of the groundwater divide, were shown to have a significant effect on the estimation of PG drainage. For the calculation of leakage, the position of the groundwater divide only affects the area represented by location E. The small vertical flux at location E means that large errors in the area represented by it would have negligible effect on the total leakage. The calculation of leakage uses the groundwater level prediction model calibrated for the PG groundwater levels. This relies upon rainfall input. However, calibration of the model accounts for any constant error in rainfall estimation by adjusting the value of SY (see section 6.5). Therefore,a constant error in the estimation of rainfall does not cause any significant error in the calculation of leakage.

From the above discussion,it is clear that leakage may be significantly underestimated, especially near the cliff face. A clearer indication of the possible underestimation may be gained by comparing figures 7.15 and 6.36 (PG drainage). Drainage from the PG is comprised of leakage to the BC and seepage to the cliff face. Figure 6.13 shows that there was some cliff face seepage on 11th July 1984 (for the catchment area shown in figure 6.1), whereas figure 6.14 shows that there was none on 12th September 1984. This means that leakage was about 2 m^3/day on 12th September, and less than 7 m^3/day on 11th July (values taken from figure 6.36). This compares reasonably well with figure 7.15 where the leakage values are 1.75 and 2 m^3/day respectively for the two dates. However, it was stated in section 6.6.4, paragraph 7, that the PG drainage may be underestimated at very low groundwater levels (due to the form of the drainage

relationship). This suggests that the true minimum PG drainage may be as much as 6 m^3/day. This infers that leakage is up to 3.5 times that shown in figure 7.15. Of course, it could alternatively be that figure 6.36 slightly overestimates PG drainage at low groundwater levels. However, comparison of figures 6.36 and 7.15 does support the contention that figure 7.15 gives the right order of magnitude to the leakage component. This infers that any lateral flow in the F1 zone (as discussed in paragraph 7 of this section) does not cause a significant underestimation of leakage.

7.7 The Effect of Installing a Cut Off Drain on the Cliff Top

To protect the cliffs from further degradation, it would be necessary to undertake certain stabilization works. One of these might be to install a cut off drain on the cliff top. This would intercept groundwater flow in the PG and prevent it from getting to the undercliff. To examine the effect of such a scheme, it is necessary to establish the amount of water it would intercept. If the scheme intercepted all the groundwater flow in the PG, then the amount would be the PG drainage in figure 6.36 less the leakage in figure 7.15, i.e. the cliff face seepage.

The annual leakage in figure 7.15 is about 10 per cent of the annual PG drainage in figure 6.36. Figure 7.15 shows that leakage (and therefore PG drainage) occurs throughout the year. It also shows that the amplitude of the fluctuations is very small in comparison to PG drainage. Therefore, leakage could be approximated as an average value when estimating the cliff face seepage. Thus, cliff face seepage is as variable as PG drainage, and a cut off drain would, at times, intercept considerable quantities of water.

A cut off drain "may take the form of either (i) a trench drain or (ii) a cut off diaphragm with drainage outlets" (Barton and Thomson, 1986c). The latter was used for the cliff protection

scheme at Highcliffe (Halcrow, 1971, and Mockridge, 1983). A diaphragm wall ensures that all the water is intercepted even if the drainage outlets are overwhelmed. The water is allowed to dam up behind the wall, and is subsequently lead away over a period of time. The total capacity of the drainage outlets will affect the amount of water damming up against the diaphragm wall. If the capacity is reduced, the cost of the scheme is reduced, but the risk of overtopping the wall is increased. For the scheme at Highcliffe, Halcrow (1971) suggests that the groundwater levels would be raised by up to 0.5 m. This is equivalent to a storage of 593 m^3 in the catchment area of figure 6.1 if the value of SY is taken to be .062 (average of the values in table 6.6).

The diaphragm wall at Highcliffe was generally located at least 20 m from the cliff edge except at the western end where, owing to restricted access, the distance was reduced, in part, to about 12 m. For the area seaward of the cut off, improved surface drainage was used to minimise percolation toward the cliff face. If a cut off at Naish Farm was located 20 m from the cliff edge, the catchment area would be reduced by 12½ per cent and, therefore, so would the PG drainage. Whether the other 12½ per cent reaches the undercliff would depend on whether or not the scheme provided surface drainage.

The raising of PG groundwater levels increases leakage. This is due to an increase in hydraulic gradient in the BC (see figures 7.10 to 7.14). Most of the leakage would occur seaward of any possible diaphragm wall (see figure 7.15 and the representative lengths in table 7.2). Therefore, the increase in leakage is only slight, and not significant to the estimation of the amount of water intercepted. However, the increase in PG groundwater levels will cause an increase in the BC groundwater levels. This may affect the stability of the cliff. However, stability is also dependent on other factors (see section 7.9), such that the increase in groundwater levels in the BC may not be critical. Also, because

the cut off is sited at some distance from the cliff face, the BC groundwater levels relevant to stability may not be affected.

7.8 Groundwater Flow to and from the Barton Clay Domain

Groundwater flow to and from the BC domain includes the flow at the boundaries with the PG, undercliff colluvium, sea, and the Bracklesham Beds. However, this discussion is limited to the flow across arbitrary boundaries within the BC. The areal position of these boundaries is the same as that for the PG. This is for the calculation of flow across the upper boundary, the PG/BC unconformity. There are arbitrary vertical boundaries at the cliff face and the PG groundwater divide. The lower boundary is the A3 zone. This is the level of the deepest piezometer. Although the groundwater flow between the undercliff colluvium and the BC is outside these boundaries, it is considered in chapter 9.

Figure 7.8 shows that groundwater flow is downward and toward the undercliff. Groundwater flow into the BC crosses the PG/BC unconformity, and the boundary under the PG groundwater divide. Due to the lack of piezometric measurements, it is not possible to estimate the latter. However, some indication of its importance may be gained by making certain assumptions. These are that Darcy's Law is applicable; the direction of flow in a horizontal plane is parallel to the cross section in figure 7.8; the horizontal permeability and hydraulic gradient are constant with depth between midway positions of piezometers; permeability is isotropic and its variation with depth is the same as that at location D (see table 7.2); the hydraulic gradient is the same as the average between locations C and D. This gives an estimated lateral flow between the PG/BC unconformity and the bottom of the A3 zone for the catchment area shown in figure 6.1 of .016 m^3/day. This is insignificant in comparison to the leakage (see figure 7.15). However, the piezometers are insufficient to give a good representation of the variation in permeability. In particular, P105 is thought to cross fossil lenses (see section 7.4,

paragraph 5).As these are isolated,the piezometer merely acts as though it has a larger tip, so that the relevant permeability of the ground is overestimated. Conversely, the permeability at P104 appears to be exceptionally low (see table 7.1). An upper estimate of the lateral flow could be made by assuming that the permeability of the entire depth of BC is the same as that at P105. The largest recorded horizontal hydraulic gradient is that between P103 and P105. Assuming this to occur throughout the depth of the BC, the lateral flow is estimated to be .07 m^3/day. This is still insignificant. Therefore, lateral flow across the boundary under the PG groundwater divide is ignored.

In section 7.6 leakage flow from the PG to the BC was calculated so as to estimate the cliff face seepage from a partitioning of PG drainage. This is needed in chapter 9 as an input to the undercliff water balance. The leakage flow may still reach the undercliff via permeable lower horizons. Large joints and fossil lenses are very permeable, but will only be effective as a drainage outlet where they connect with the undercliff colluvium. It is most likely that this will be the case for leakage within a short distance of the cliff face. It is noticeable from figure 7.15 that most of the leakage occurs within a few metres of the cliff face. It is therefore anticipated that this will be intercepted by large joints and fossil lenses and seep to the undercliff. It is probable, therefore, that most of the leakage calculated in section 7.6 will still reach the undercliff.

Leakage which does not reach the undercliff will eventually seep down to the Bracklesham Beds. It is difficult to estimate this quantity from the groundwater level records. It could be assumed that the vertical groundwater flow between the D and A3 horizons (see figures 7.2 and 7.8)does not reach the undercliff. However, this ignores lateral flow within the A3 sand beds to the lower part of the undercliff. Also, the BC is highly variable between the D and A3 zone piezometers which makes it difficult to

estimate the vertical flow between them. It is considered that P68 (D zone) and P101 (A3 zone) are in relatively permeable horizons, such that the assumption of a uniform hydraulic gradient between them will overestimate the seepage flow. However, if it is assumed that the hydraulic gradient is uniform, and the permeability homogeneous and isotropic and equal to that at P101, then the groundwater flow between the D and A3 zones over the whole catchment area is 0.84 m^3/day. This is approximately equivalent to assuming that none of the leakage into the BC from the areas represented by locations B,C, D and E reaches the undercliff. This quantity is very small in comparison to the total PG drainage at any time. Therefore, any error in its estimation will not cause a significant error in the input to the undercliff water balance. In chapter 9 the input to the undercliff water balance from the PG and BC domains will use all the PG drainage less 0.84 m^3/day. This assumes that the daily fluctuation of the groundwater flow out of the BC to the undercliff is the same as that of leakage. Any error in this assumption will be small, because the fluctuation of leakage is small.

7.9 Relationship between Groundwater Levels and Landslide Activity

Landslide activity at Naish Farm involves a number of mass degradational processes (Barton and Coles, 1984). The processes act on both in situ and colluvial material. When a slope fails (i.e. becomes unstable) sliding occurs along a surface where the soil strength is less than the net force tending to cause the movement. The geohydrological influences on stability are the pore pressure (as a head of water, it is the groundwater level minus the gravitational head) and the hydraulic gradient. The latter affects the seepage force and the former, as well as being a destabilizing force, controls the effective stress upon which the soil strength depends. Both the groundwater level and hydraulic gradient at any location depend on the groundwater flow

regime, and therefore, the surrounding groundwater levels. Thus, other groundwater levels in the groundwater flow regime may give an indication of the likelihood of landslide activity. The occurrence of landslide activity changes the groundwater flow regime, and therefore, affects groundwater levels. Thus, groundwater levels both influence and are influenced by landslide activity.

7.9.1 Influence of Landslide Activity on Groundwater Levels

In chapter 6 the effect of landslide activity was only discussed in reference to cliff top slumps. This is because the PG groundwater regime is only significantly affected by changes in the position of the cliff face, its main drainage outlet. However, the BC groundwater regime can be affected by movement of both the in situ material (slumping) and the undercliff colluvium. The effect of landsliding may be twofold.

The first effect is where the groundwater flow regime is changed due to the alteration of the boundaries. The loss of soil material causes the groundwater boundary at the undercliff to move inland. Figure 7.8 shows that there is a fall in groundwater levels toward the undercliff. Therefore, as the boundary moves inland, the distance between it, and any location within the BC, will reduce. This causes a decrease in groundwater levels within the BC. The precise effect on the groundwater level at any location will depend upon the hydraulic connection between the boundary and that location. The change in groundwater level will not be complete as soon as landslide activity ceases, but will occur gradually over a much longer period of time.

The second effect is due to a reduction in total stress causing swelling of the BC. At any point within a soil, the total stress (caused by the overburden) is made up of the stress taken by the water in the soil voids (pore water pressure), and the stress

taken by the soil skeleton (effective stress). The removal of material from the cliff slope by landslide activity causes a reduction in the total stress within the BC. This is immediately accommodated by a reduction in pore pressure. There is then an increased flow into the BC (due to an increase in hydraulic gradient) which causes the soil skeleton to swell, and the pore pressure to rise until it reaches equilibrium. The time that this takes depends upon the compressibility and permeability of the BC. In permeable and incompressible soils, such as sand or gravel, it is effectively immediate, whereas for compressible clays of low permeability it may take many years. In order to determine whether pore pressures are depressed due to stress relief, it is necessary to either, (a) have a long period of data (e.g. as used by Hutchinson et al, 1980), or (b) to use a numerical model of the groundwater flow regime assuming a rigid soil skeleton (e.g. as used by Bromhead and Dixon, 1984). Although the groundwater measurements are limited, and a numerical model has not been used to describe groundwater levels in the BC, it is considered, from the discussion in section 7.5, that pore pressures are no longer influenced by stress changes in the soil caused by previous cliff failures.

Landslide activity is intermittent. Therefore, groundwater levels will not necessarily be affected by landslide activity at all times. Only a few of the groundwater level records are long enough to determine whether they have been influenced by landslide activity. These are in the F and D zones, and only the latter are affected (see section 7.3).

The F zone piezometers could be affected by cliff top slumps (figure 7.8 shows that the groundwater level is dependent on the distance from the cliff face - a cliff top slump would reduce this distance), but it is unsure whether they could be significantly affected by slumping of lower scarps, or by sliding of the undercliff colluvium. The effect of a cliff top slump should diminish with increasing distance from the cliff face

(this can be seen in figure 7.8 by the decrease in hydraulic gradient in the F zone with distance from the cliff face). Figure 6.3 shows the location of cliff top slumps affecting the study area. Slumps B and G cross the piezometer line (see figure 7.1). Slump B occurred near the start of the study period but does not appear to have affected groundwater levels. The much larger slump G must have affected groundwater levels but it occurred after the end of the study period. The F zone groundwater levels may have been affected by other slumps which do not cross the piezometer line. Of these, only slump C occurred during the study period but appears to have had no effect.

The D zone piezometers could probably be affected by cliff top or F scarp slumps, or movement of the undercliff colluvium. It is unsure whether they would be significantly affected by failure of lower scarps. The long period D zone piezometers (P68 and P69) have both been affected by landslide activity (see figures 7.6 and 7.7). The start of the effect on P68 coincides with the initial failure of slump C. This is in contrast with P51 (see section 6.3, paragraph 7), which was only affected 6 months later, when the slump had moved down sufficiently to expose the PG. The drainage of the D zone at P68, however, was obviously immediately affected. The large slump C utilized the shear surface in the D zone, the bedding plane of which occurs 2.6 m below the level of P68. Although the slump and undercliff colluvium did not initially move far, the new failure surface would have provided a rapid drainage path, and so would have affected groundwater levels in the Barton Clay. It is somewhat puzzling why slump C affected P68, and not P69 or the F zone piezometers. It could be due to their being in different horizons. P69 is 3.8 m above the bedding plane in the D zone which is used as a shear plane in slumping. This is greater than the 2.6 m for P68 and may be significant. The nature of landslide activity causing the groundwater levels at P69 to have a downward trend throughout the study period is uncertain. It is surprising that P68 was not similarly affected.

Although there appear to be different causes for the landslide influences on P68 and P69, they do both show a downward trend in groundwater levels. This suggests that the dominant effect of landslide activity is the change in the groundwater flow regime.

7.9.2 Influence of Groundwater Levels on Landslide Activity

The stability of a slope is influenced by the pore pressures (as a head of water, it is the groundwater level minus the gravitational head) and the hydraulic gradient. The pore pressure is a force per unit area tending to decrease stability. An increase in pore pressure also adversely affects the soil strength parameters. The hydraulic gradient determines the direction and magnitude of the seepage force. If this is downward stability is increased (compared to no groundwater flow) and if it is upward stability is decreased.

In the absence of pore pressure measurements, slope stability analyses are based on hypothetical conditions of pore pressure, such that the groundwater flow is assumed to be parallel to the slope, or even that the conditions are hydrostatic. When in situ measurements are made, they tend to show that the real situation deviates significantly from these hypothetical approximations due to the geologic conditions. Hodge and Freeze (1977) and Lafleur and Lefebvre (1980) studied the influence of various geometric and stratigraphic factors on the groundwater regime, and on the stability of slopes, using numerical models. It was found that such factors could make a large difference to the factor of safety of a slope. The results of such models, and the assumptions of geologic conditions, should be verified by in situ measurements. Although no stability analysis has been undertaken here, a study of the geohydrology of the slope should elucidate some factors affecting instability in the cliffs.

Failure of in situ BC involves slumping, either at the cliff top, or any one of the scarps in the undercliff (F, D or A3). Slumping has been described by Barton and Coles (1984) to use a preferred bedding plane shear plane as its basal surface. The reasons for using these particular bedding planes is unknown (although suggestions have been made in the past (see section 1.8.6)). However, the choice of bedding is probably due to a combination of a comparatively low shear strength and adverse permeability characteristics. The latter will affect the pore pressure and hydraulic gradient.

Hutchinson et al (1981) and Sterrett and Edil (1982) present examples of high hydraulic gradients causing seepage erosion in fine sand layers, and eventually leading to failure of the slope. The A3 zone contains fine sand layers which may similarly be subject to seepage erosion. This could be the cause of slumping of the D scarp.

Figure 7.16 shows the vertical variation of pore pressure at location B (as defined in table 7.2) on 1st February 1984. At this location, cliff top slumps mainly utilize the preferred bedding plane shear plane in the F zone, but also occasionally use the one in the D zone (the last time being during the winter of 1977/8). They do not use the one at the bottom of the A3 zone. Because of the paucity of groundwater level readings, and the vertical variation of lithology, it is difficult to determine the actual pore pressure at the preferred bedding plane shear plane in the D zone. The pore pressure given by figure 7.16 could be erroneous if the assumption of linear interpolation is invalid. Figure 7.8 shows that the average hydraulic gradient is small above the D zone piezometer, and large below it. There is unlikely to be a sudden change at the location of the piezometer. Therefore, if the true hydraulic gradient continues to be small for a few metres below the D zone piezometer, then it may be that the pore pressure is higher, and the hydraulic gradient is lower, at the preferred bedding plane shear plane in the D zone. This possible pore pressure variation

is shown as a dashed line in figure 7.16. This shows that the pore pressure could be at a maximum at the level of the preferred bedding plane shear plane in the D zone. This may be the reason why this level is sometimes used for cliff top failures. The pore pressure variation about the level of the preferred bedding plane in the F zone is such that it is probable that some other factor (such as soil strength) causes its utilization as a shear surface. A more detailed investigation of this aspect could be the source of further work.

There is a temporal variation in groundwater level as a result of meteorological variations (see section 7.3). This will affect both pore pressure and hydraulic gradient and therefore the stability of the cliff. Figure 7.8 shows that the downward hydraulic gradient increases with groundwater level (the groundwater level fluctuation increases with decreasing depth (see section 7.3)). Thus, at the same time as stability decreases due to rising groundwater levels, it increases due to increasing hydraulic gradient. Therefore, for the purpose of this discussion, the effect on stability of a temporal variation in hydraulic gradient is assumed to be small in comparison to that of the variation in pore pressure.

Ideally, the discussion should be of the groundwater levels at the failure plane at the time the slump occurred. This would only be possible for cliff top slumps and if the piezometer were very close to the cliff edge. It is also unlikely that measurements would have been taken at the exact location of a slump. However, the F zone piezometers have been installed at the same horizon as the F shear plane. The behaviour of the groundwater level at these piezometers is likely to be similar to that causing failure due to slumps based on the F shear plane. The timing of the rise and fall in groundwater levels (i.e. the response to meteorological variations) at the F zone piezometers is also similar to that at the PG piezometers. This means that there is a good correlation between the groundwater levels in

the different horizons. This is useful as the groundwater level prediction model of chapter 5 has not been calibrated for the F zone piezometers. For groundwater levels outside the study period, comparison can be made between the simulated PG groundwater levels and the occurrence of landslide activity.

The location and dates of cliff top slumps affecting the study area between July 1982 and October 1985 are given in figure 6.3. Figures 6.28 to 6.31 show simulated PG groundwater levels at various locations within the PG (see figure 6.1 for their location). Figure 7.3 gives an example of the observed groundwater level at a location (P66) in the F zone during the study period. All the small slumps (not C and H) used the shear surface in the F zone. Slumps A and B occurred after a period of about 6 weeks of very high groundwater levels (see figures 7.3 and 6.28). The time of the occurrence of slumps D and E is uncertain. Figures 6.28 to 6.31 show that the groundwater levels were very high at the time. However, they also show that the slumps occurred at least a week after the highest groundwater level. From the above evidence it is clear that slumps utilizing the shear surface in the F zone occur when groundwater levels are very high. Therefore, it is likely that slumps F and G occurred in February 1985 when groundwater levels were high.

It is also apparent from the above evidence that slumps do not necessarily occur immediately groundwater levels reach a high level. This indicates that other factors also contribute to the failure of cliff top slumps utilizing the shear surface in the F zone. This will likely be the lateral support provided by the undercliff colluvium. As will be discussed in chapter 9, the rate of movement of undercliff colluvium is highly variable depending on the groundwater levels in the colluvium. The colluvium moves down the undercliff and away from the cliff face. This reduces the lateral support given to the in situ material and therefore decreases cliff top stability. Thus, the failure

of slumps using the shear surface in the F zone is due to a combination of a reduction in lateral support and high pore pressures.

High pore pressures will be present all along the cliff line. The location of a slump will depend upon the amount of lateral support provided by both the undercliff colluvium and the line of the cliff edge. (There will be more support where the cliff edge curves inland than where it curves seaward.) Thus, the prediction of slumps utilizing the shear surface in the F zone needs to be based on the variation of both the lateral support and pore pressure. If the prediction is for a slump to occur anywhere along the cliff, this may be possible by using a combination of the groundwater level, and the length of time that the groundwater level has been maintained (perhaps, as indicated by the amount of recent undercliff movement). This sort of analysis is beyond the scope of this study.

Cliff top slumps in the study area generally utilize the shear surface in the F zone. However, slumps C and H utilized the shear surface in the D zone instead. No piezometric measurements have been made on the cliff top at this horizon. Therefore, it is not possible to say whether groundwater levels would be affected by meteorological variations. Added to this, piezometers at a slightly higher horizon (P68 and P69, figures 7.6 and 7.7 respectively) show conflicting evidence. However, if it is initially assumed that the temporal groundwater level variation at the shear surface in the D zone is similar to that in the PG, some observations can be made. (See figures 6.3 and 6.28 to 6.31.) Slump C occurred at high groundwater levels just before they rose to a maximum. However, slump H occurred at very low groundwater levels.

One possible explanation for the timing of the failure of slump H is the second effect (described in section 7.9.1) of landslide activity on groundwater levels, i.e. the equilibration of pore

pressure after unloading (from previous failure). The gradual rise in pore pressure eventually reaches a value that is critical to stability. However, the evidence from the groundwater level records suggests that this is probably not taking place. Also, due to the fact that the BC is fissured with a number of fossil lenses, the drainage paths are small, and therefore the time needed for the equilibration of pore pressures is also thought to be small. Thus, this is not considered to be the explanation.

The low PG groundwater levels when slump H occurred, would indicate that the pore pressure had very little influence on the failure. It might also indicate that meteorological variations do not influence groundwater levels at the preferred bedding plane shear plane (i.e. groundwater levels are static). Another possible explanation for the timing of the failure of slump H could be a reduction in lateral support. Barton and Coles (1984) determined a 7 to 8 per cent loss of colluvial volume during 1981/82. It took place "during a time of increasing overall slope angle and decreasing slope stability". Chapters 8 and 9 also present evidence for a loss of colluvium during the study period (1982/84).

Barton and Coles (1984) also describe another large slump based on the shear surface in the D zone. This occurred between approximately NGR 42213 09320 and 42225 09319 during 1977/78. Prior to this "accelerated degradation in 1976 (Hurn Airport recorded 550 mm of rain between September and December 1976: using the Normal distribution parameters in table 3.4, the probability of non-exceedance for each month's rainfall from September to December 1976 was .81, .93, .79 and .77 respectively) caused slumping along the D surface (i.e. of the F scarp) to extend back to the cliff top".

This is similar to the situation for slump H. For some years prior to the failure of slump H there were very few cliff top slumps along that part of the cliff top. Therefore, repeated

failure of the F scarp and movement of the undercliff colluvium, caused a steepening slope angle and loss of lateral support. This eventually resulted in the failure of slump H. The slump would have been triggered off by the undercliff movement just prior to failure. However, as groundwater levels were low, the rate of undercliff movement would have been slow. It is therefore likely that the cliff top was on the point of failure for several months. Thus, the prediction of slumps utilizing the shear surface in the D zone needs to be based on the variation in lateral support and not pore pressure.

It is clear from the above discussions that failure of the cliff top involves a combination of a number of factors. The role of lateral support and undercliff movement is crucial. This is especially true for large slumps based on the shear surface in the D zone, where there is very little temporal fluctuation in groundwater level to influence the time of failure. The temporal fluctuation of groundwater level is a more significant factor in the timing of the failure of the smaller slumps based on the shear surface in the F zone. The discussion has centred on the slumping of the cliff top scarp. Slumping of the F and D scarps in the undercliff would probably also be due to a combination of variations in the lateral support and pore pressure. The relative importance of pore pressure and lateral support in determining the time of failure would depend upon their respective variations.

7.10 Summary

An investigation of the BC domain has been carried out using a number of standpipe piezometers installed at various depths and distances from the cliff face. Five piezometers were observed for 2 years, and six for up to one year. The effect of meteorological variations on the temporal variation of groundwater

level decreased with depth. The readings can also be influenced by landslide activity, but this was only observed for two long period piezometers in the D zone.

Piezometer response tests were used to estimate the permeability of the BC at the piezometer tip. Permeability is important with respect to the path and quantity of seepage flow. Permeability varied spatially due to: variation in stress relief; vertical variation in fissuring and lithology; and the presence of local factors such as highly permeable shelly lenses. The spatial variation of groundwater level showed a large spatial variation of hydraulic gradient, which is also an indication of the spatially variable permeability.

Groundwater flow is downward and toward the undercliff. Groundwater flow down to the Bracklesham Beds, although difficult to estimate, is small and not very significant. The groundwater flow from that part of the BC inland of the PG groundwater divide was determined to be negligible. The BC domain is recharged via leakage from the PG domain. It was variable, being greatest when groundwater levels were high. The variation was considerably less than the PG drainage, such that the annual total for leakage amounted to only 10 per cent of that for PG drainage. Leakage decreased with increasing distance from the cliff face. A large proportion of the leakage occurred within a few metres of the cliff face. Most of this probably reaches the undercliff due to the presence of fossil lenses and stress relief joints causing high permeabilities near the undercliff. Apart from this, the role of the BC domain, as a source of seepage to the undercliff, is not very significant.

The relationship between groundwater levels and landslide activity was investigated. Landslide activity causes a downward trend in groundwater level due to the change in groundwater flow regime (i.e. the moving boundary at the undercliff). However, the effect is not always present due to the intermittent nature of landslide activity. The importance of groundwater level in the timing of landslide activity depends upon its temporal variation at the

failure plane. Thus, groundwater level is considered to be a contributing factor to the timing of small slumps based on the shear plane in the F zone, but not to large slumps based on the shear plane in the D zone. Another important factor contributing to the timing of slumps is considered to be the variation in lateral support.

Table 7.1 Summary of the Barton Clay Groundwater Level Records

Location	Observation Period		Maximum	Minimum	Range	Basic Time[C]	Permeability[D]
	From	To	(m O.D.)	(m O.D.)	(m)	Lag	(m/s)
P65	18.10.82	29.01.85	27.18	26.58	0.60	0.64 hrs	5.0×10^{-8}
P66	28.10.82	29.01.85	28.01	27.24	0.86	2.3 hrs	1.4×10^{-8}
P67	28.10.82	29.01.85	28.91	28.34	0.57	6.5 hrs	5.0×10^{-9}
P68	28.10.82	29.01.85	22.55	21.74	0.81	12 hrs	2.7×10^{-9}
P69 [A]	03.01.83	29.01.85	24.04	23.00	1.04	25 hrs	1.3×10^{-9}
P101	06.03.84	29.01.85	9.14	9.04	0.10	120 hrs	4.0×10^{-10}
P102	19.01.84	29.01.85	23.32	22.90	0.42	16 days	1.2×10^{-10}
P103 [B]	01.02.84	05.12.84	24.00	23.68	0.32	54 hrs	8.8×10^{-10}
P104	05.12.84	05.12.84	22.46	22.46	-	58 days	3.4×10^{-11}
P105	23.03.84	29.01.85	28.42	27.96	0.46	18 hrs	2.6×10^{-9}
P106	15.02.84	29.01.85	29.74	29.11	0.63	48 hrs	9.9×10^{-10}

Notes: The observation period is taken from when the piezometer water level has equilibrated with the groundwater level.

A. Prior to the 3rd January 1983 there was difficulty in making consistent piezometer readings. Therefore, the results were unreliable.

B. The 29th January 1985 reading is dubious.

C. As defined by Hvorslev (1951). It is the time taken for 63 per cent recovery of the piezometric head during a falling head test.

D. Assuming the vertical and horizontal permeabilities are equal.

Table 7.2 Details of the Locations used for the Estimation of the Vertical Flux from the Plateau Gravel to the Barton Clay

Location	Position (1) (m)	Representative Length (m)			F1 zone		
		From(1)	To (1)	Length	Top (2) (m O.D.)	Bottom (3) (m O.D.)	K (4) (m/s)
A	4	0	6.7	6.7	28.25	24.18	5.0×10^{-8}
B	9.4	6.7	19.45	12.75	28.17	24.36	1.4×10^{-8}
C	29.5	19.45	54.05	34.6	28.37	24.17	5.0×10^{-9}
D	78.6	54.05	114.9	60.85	28.09	24.15	9.9×10^{-10}
E	151.2	114.9	165-205(5)	50.1-90.1	29.49	24.16	9.9×10^{-10}

Notes:
1. These measurements are the distances from the cliff face along the section line XX on figure 7.1
2. This is the level of the PG/BC unconformity.
3. This is the middle of the F zone piezometer filter length.
4. This is the permeability estimated from piezometer response tests.
5. This is determined by the position of the groundwater divide in the PG which varies with PG groundwater level.

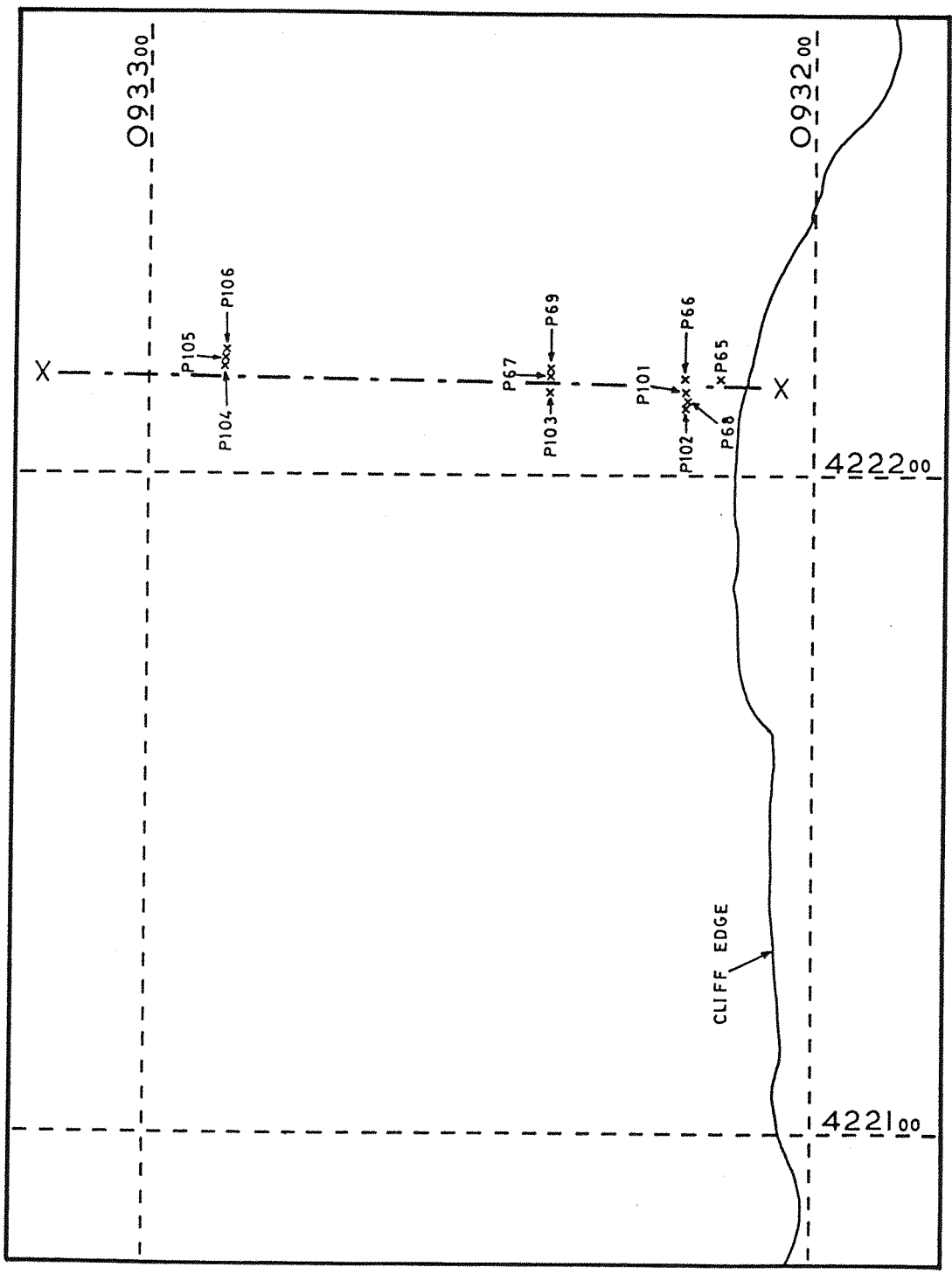

Figure 7.1 Location map for piezometers in the Barton Clay.
XX is the line of the cross section used in figure 7.2.

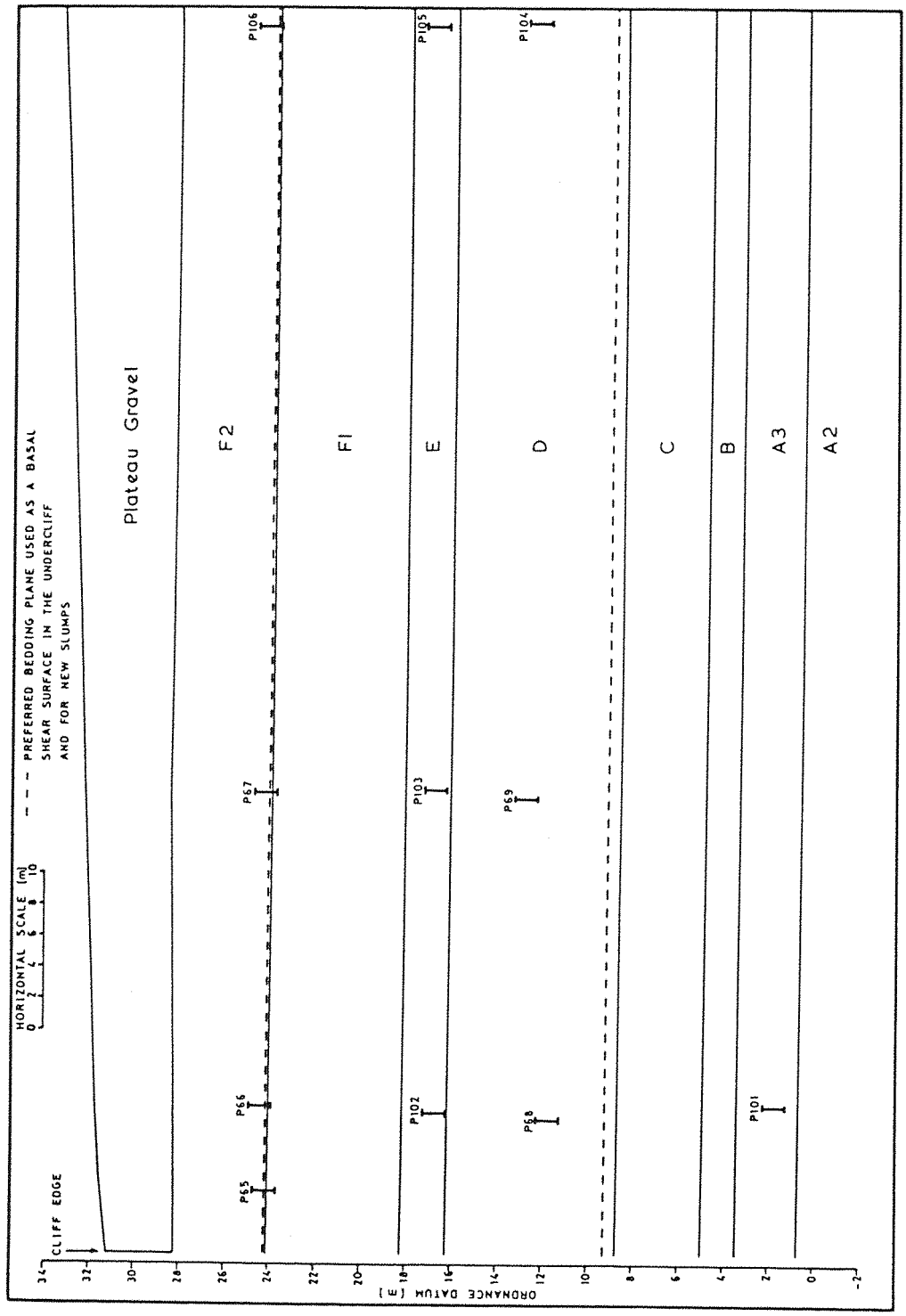

Figure 7.2 Geological cross section showing the depth location of piezometers in the Barton Clay. The line of the cross section is XX on figure 7.1.

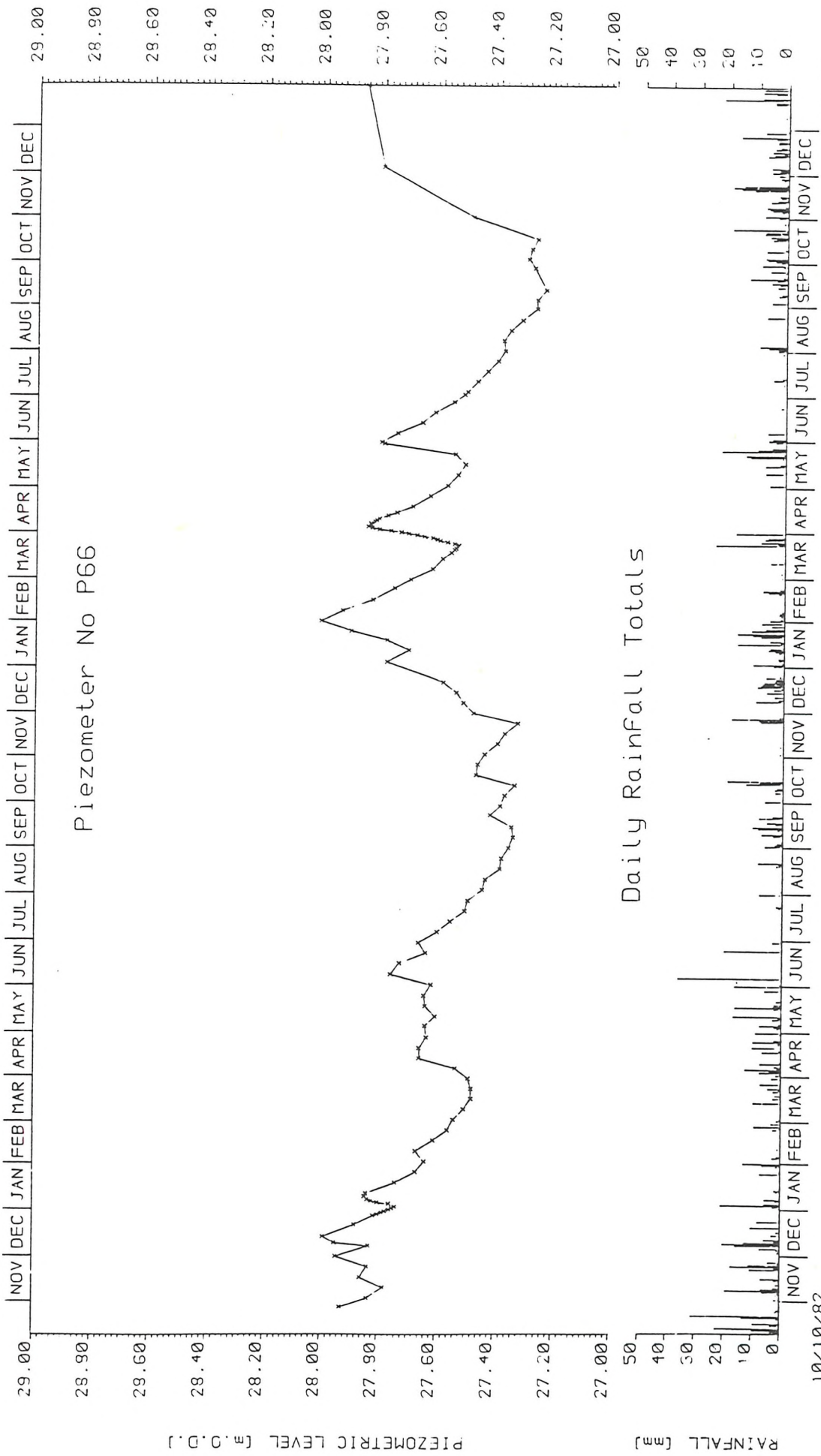

Figure 7.3 Groundwater level record in the Barton Clay at P66. See figures 7.1 and 7.2 for location.

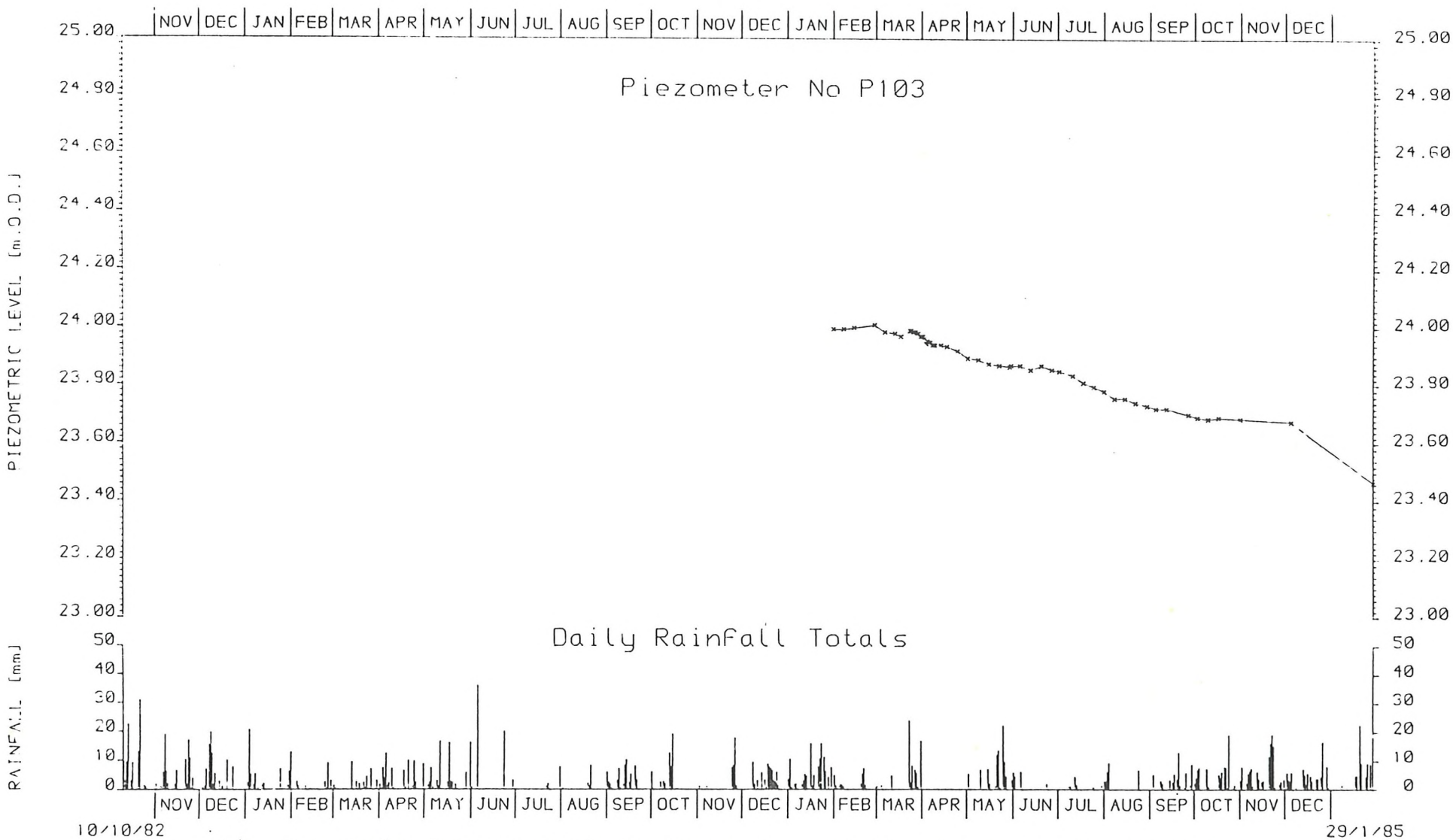

Figure 7.4 Groundwater level record in the Barton Clay at P103. See figures 7.1 and 7.2 for location.

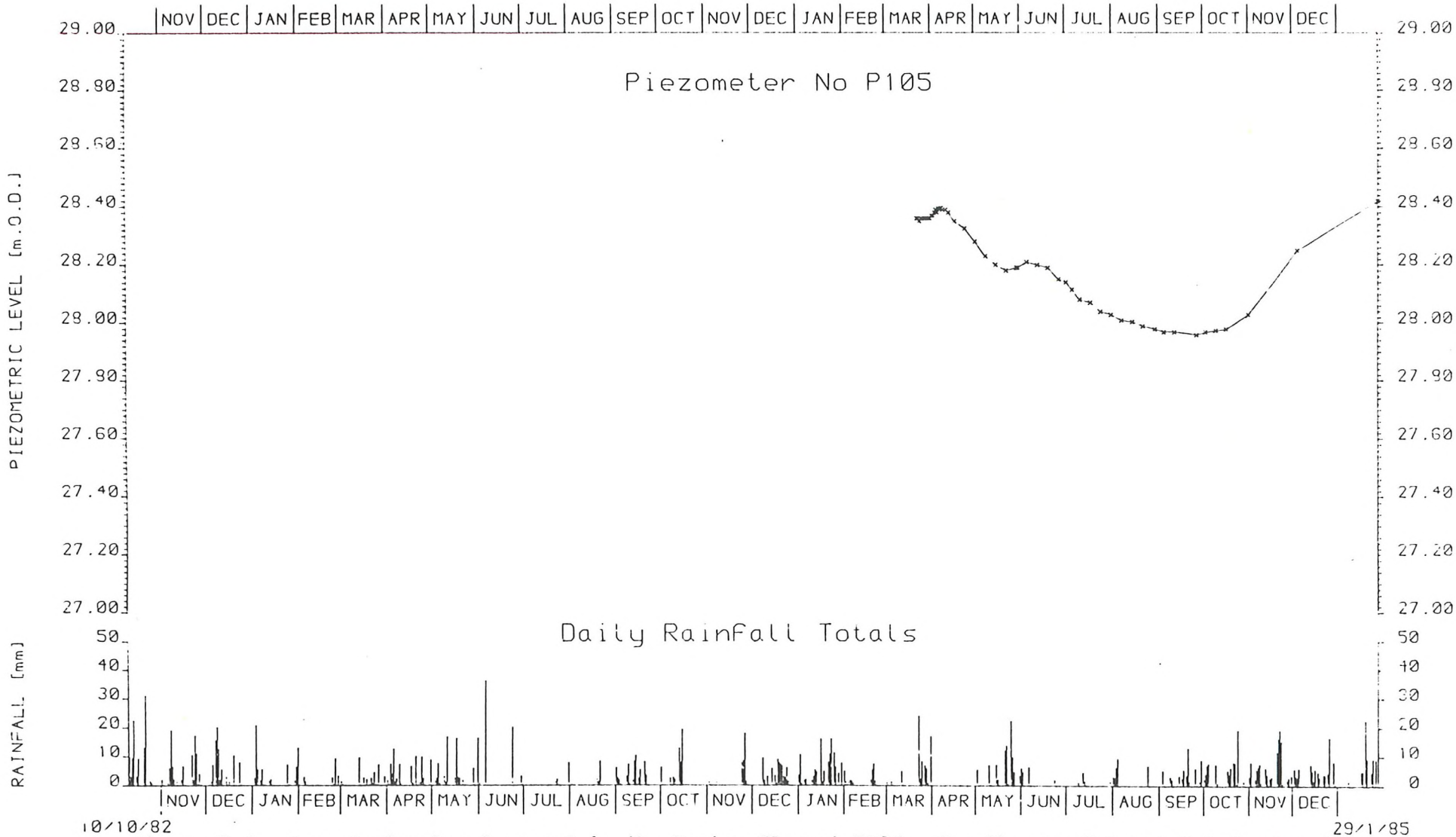

Figure 7.5 Groundwater level record in the Barton Clay at P105. See figures 7.1 and 7.2 for location.

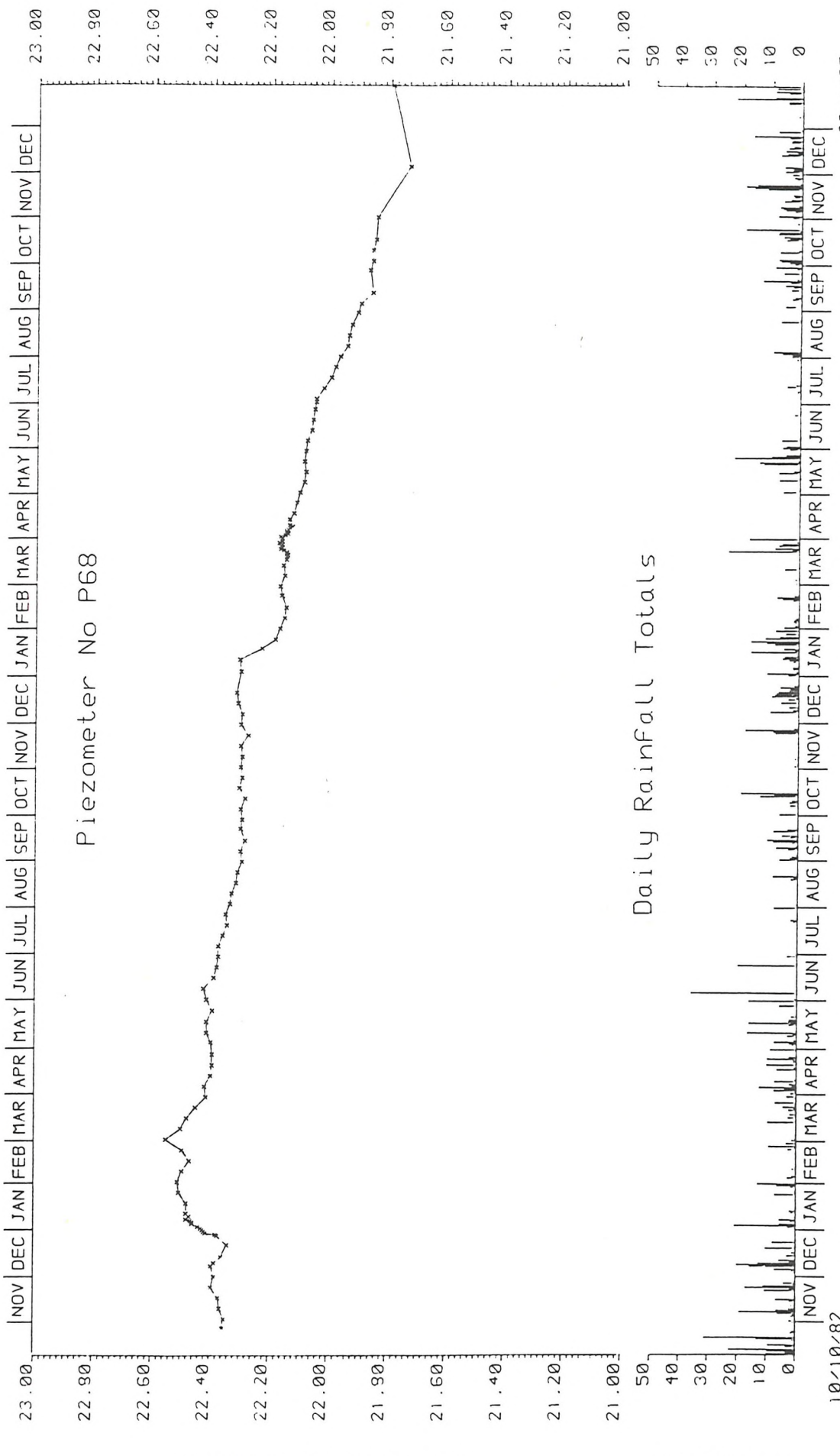

Figure 7.6 Groundwater level record in the Barton Clay at P68. See figures 7.1 and 7.2 for location.

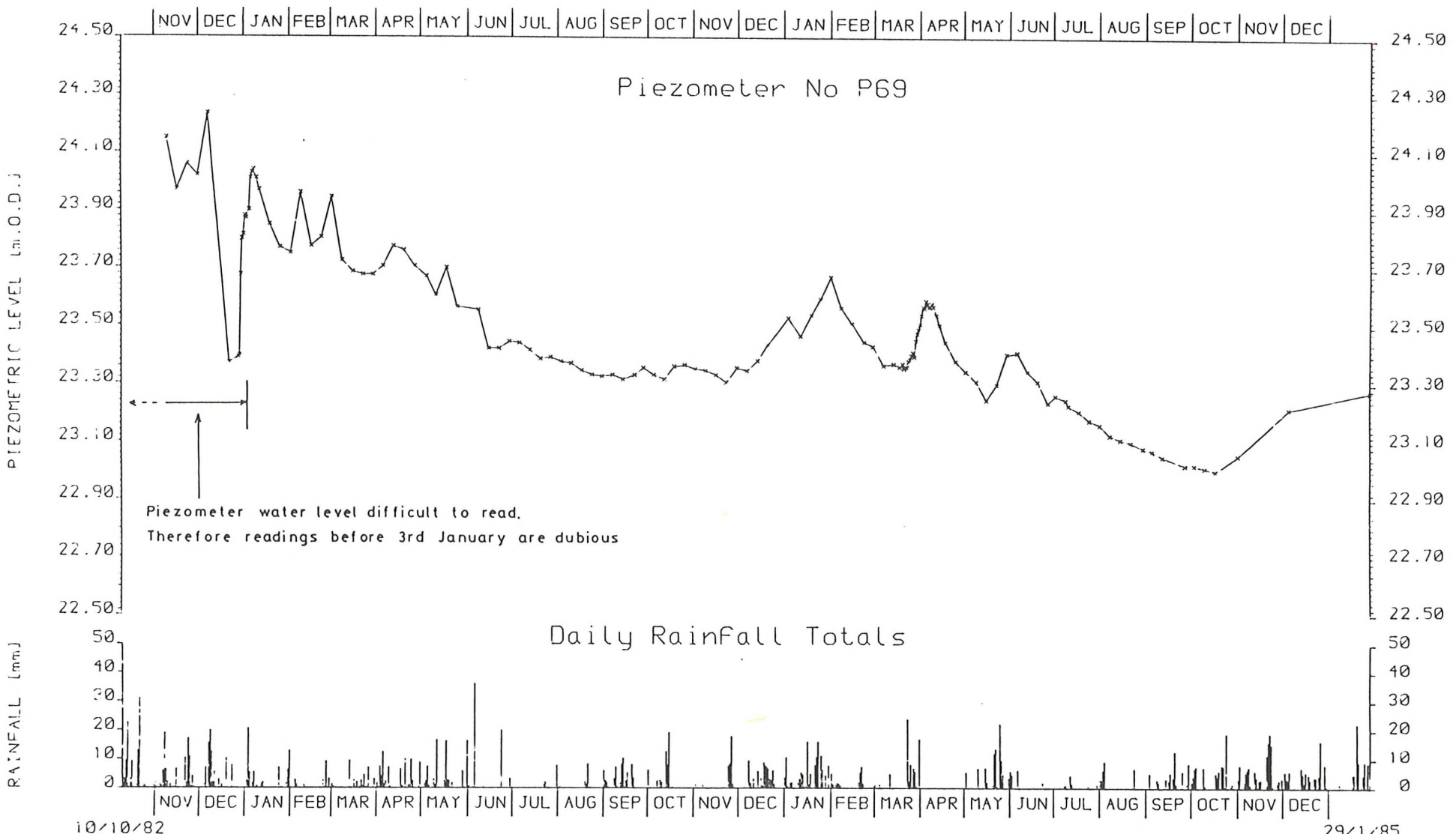

Figure 7.7 Groundwater level record in the Barton Clay at P69. See figures 7.1 and 7.2 for location.

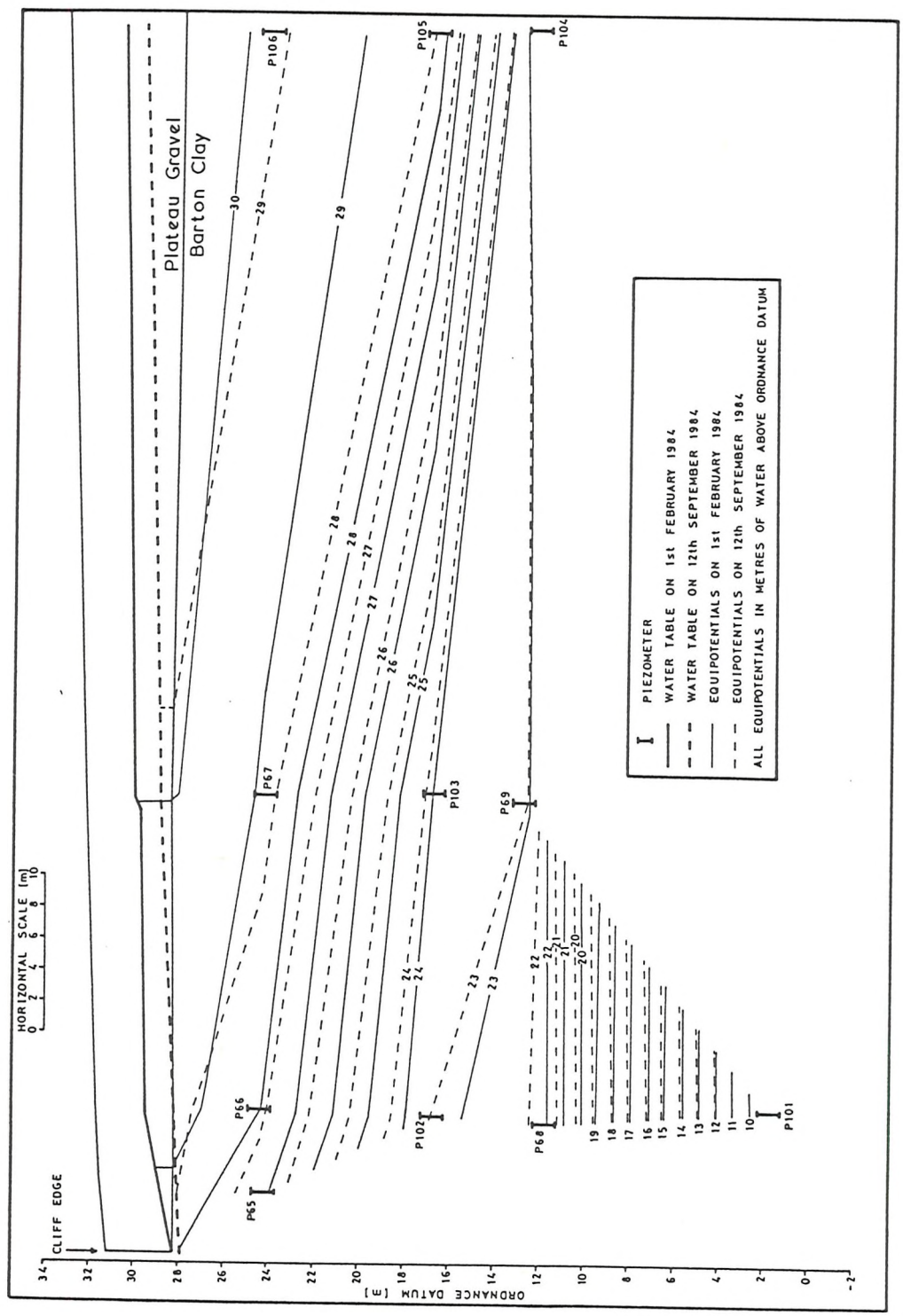

Figure 7.8 Cross section showing estimated equipotentials in the Barton Clay.

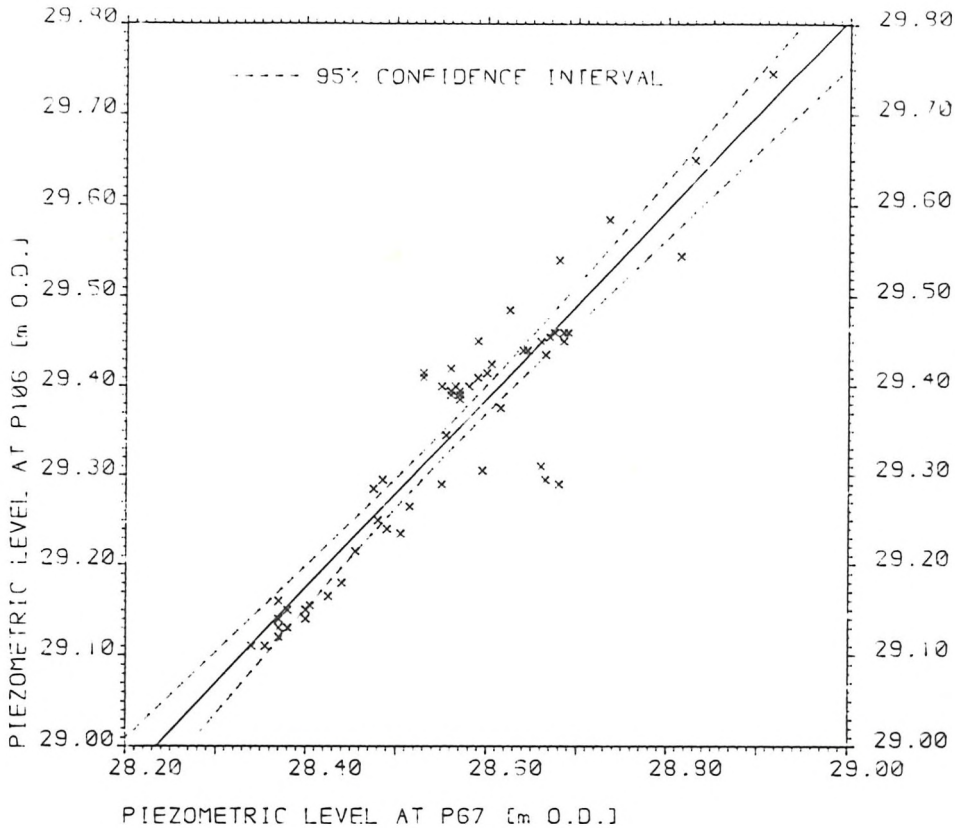

FIGURE 7.9 F ZONE PIEZOMETRIC LEVELS AT P106 AND P67

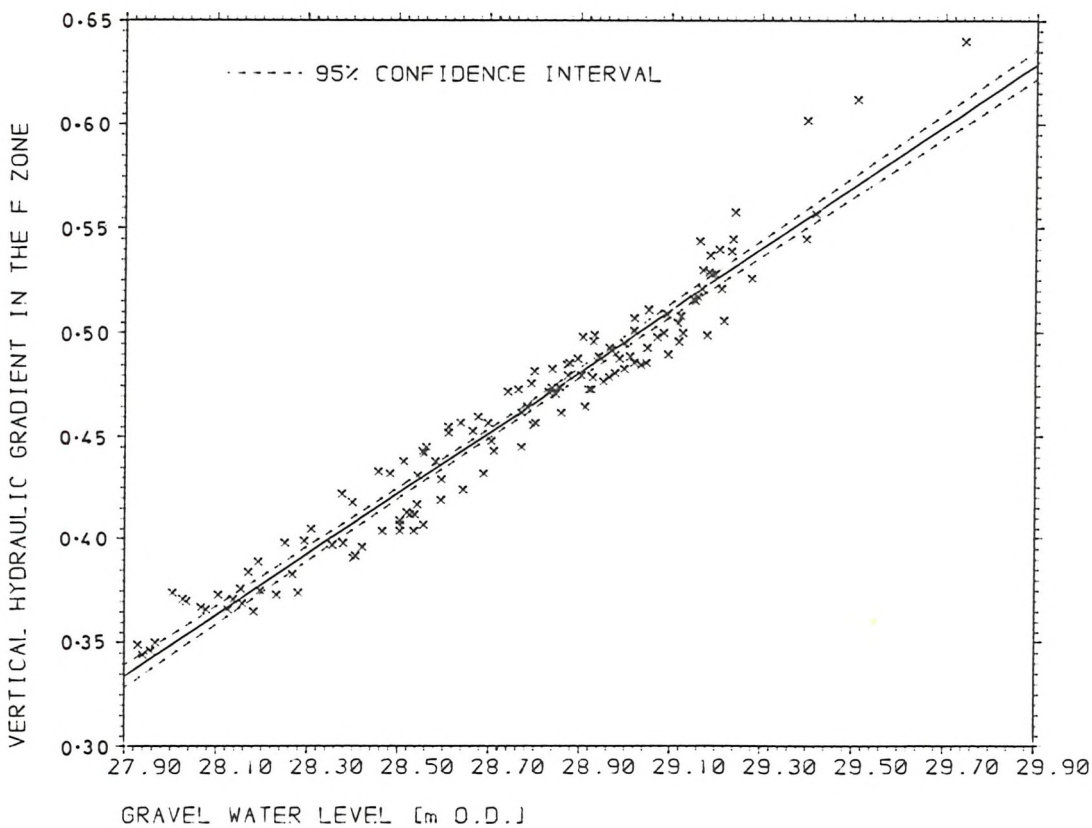

FIGURE 7.10 VERTICAL HYDRAULIC GRADIENT IN THE F ZONE AND GRAVEL WATER LEVEL AT LOCATION A

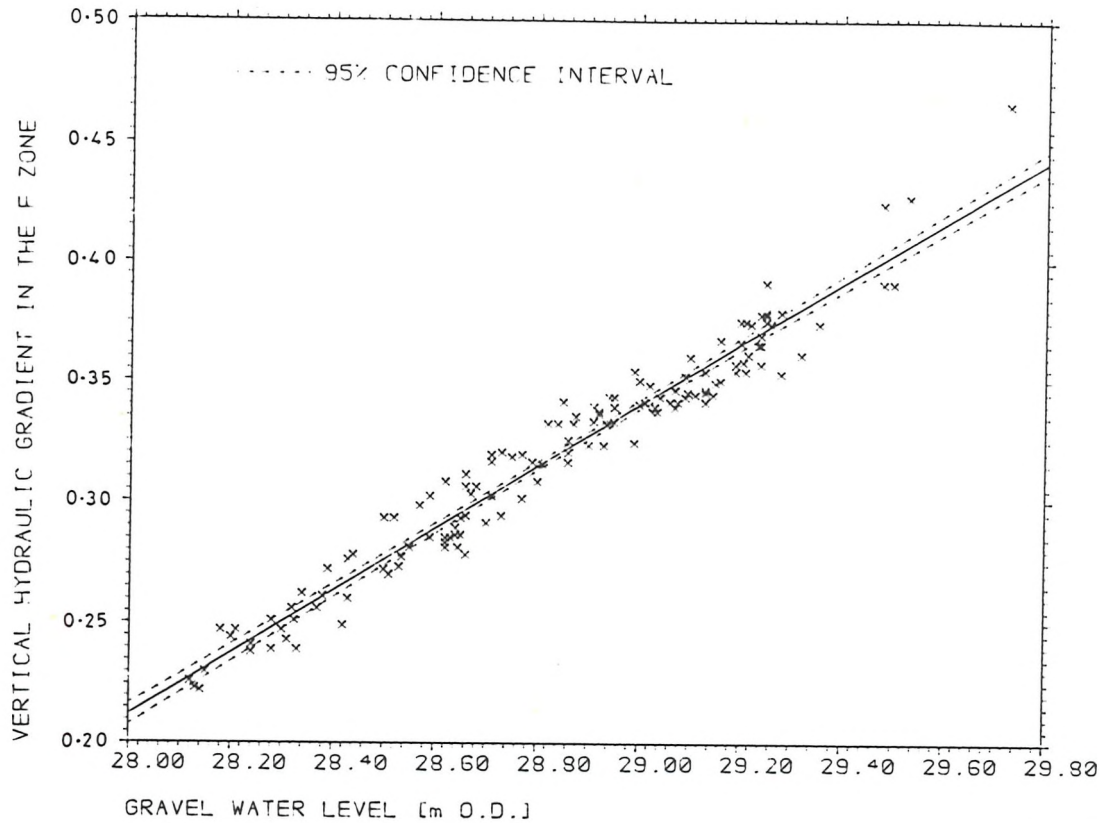

FIGURE 7.11 VERTICAL HYDRAULIC GRADIENT IN THE F ZONE AND GRAVEL WATER LEVEL AT LOCATION B

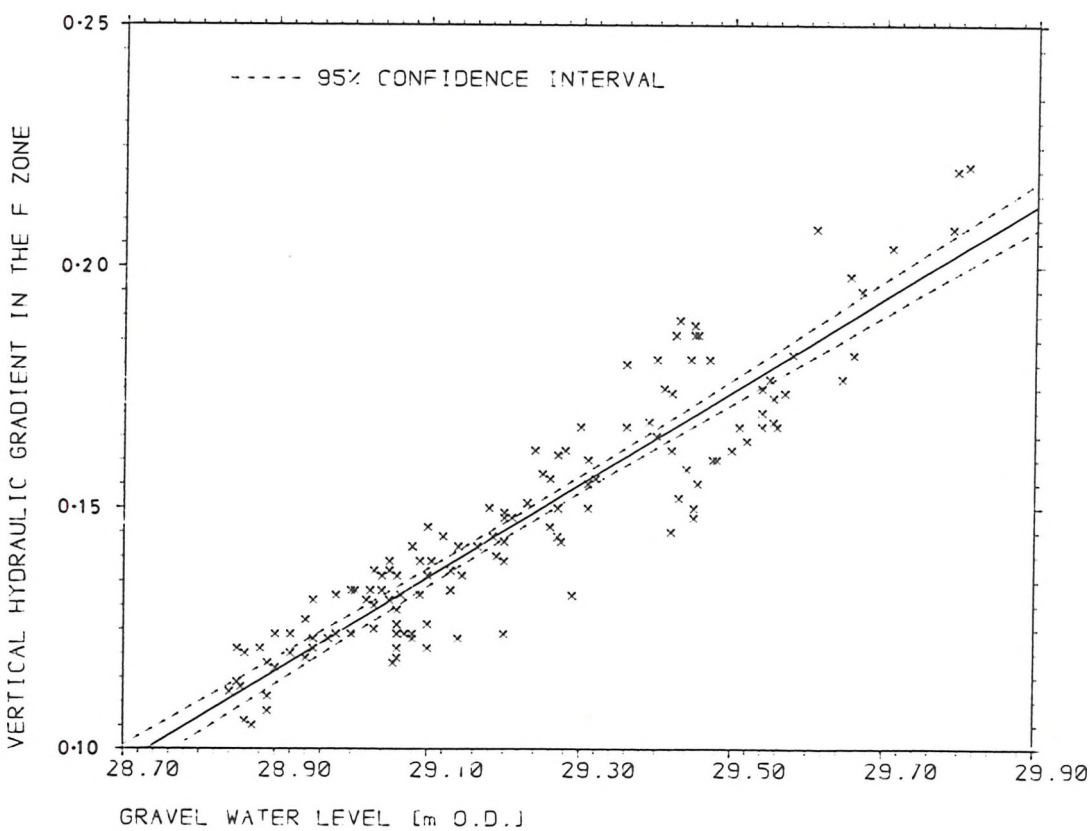

FIGURE 7.12 VERTICAL HYDRAULIC GRADIENT IN THE F ZONE AND GRAVEL WATER LEVEL AT LOCATION C

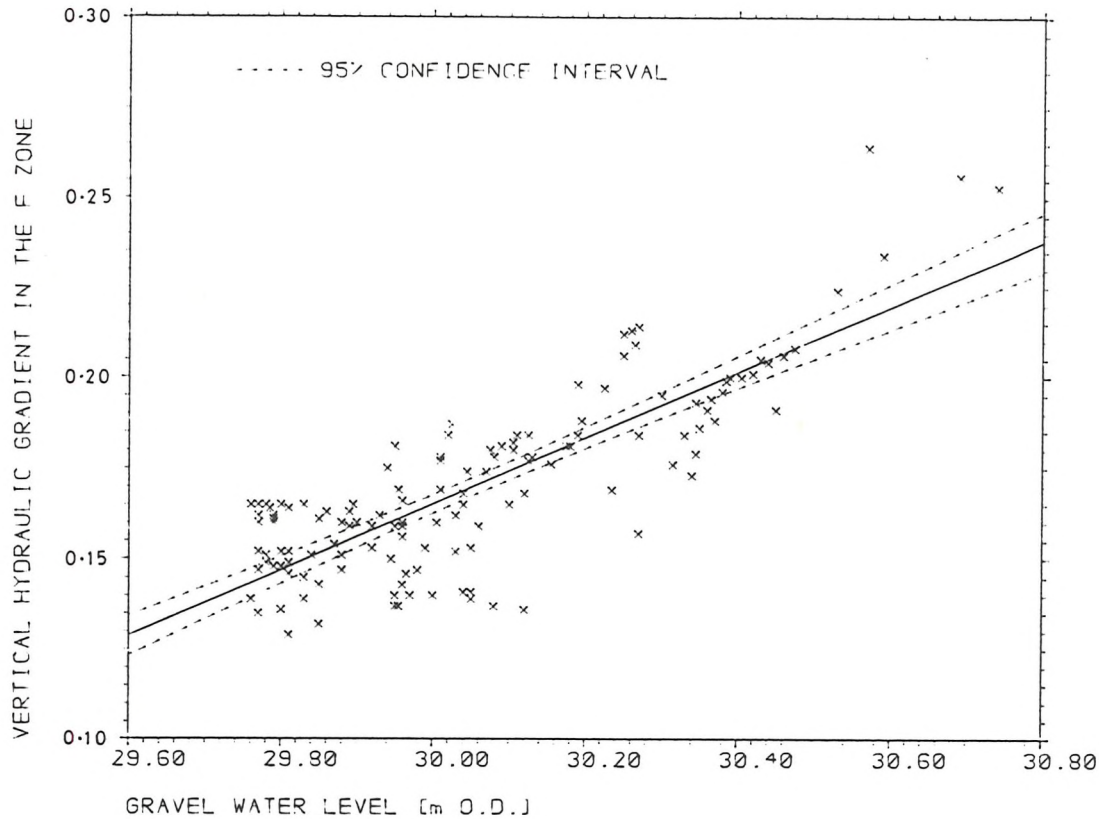

FIGURE 7.13 VERTICAL HYDRAULIC GRADIENT IN THE F ZONE AND GRAVEL WATER LEVEL AT LOCATION D

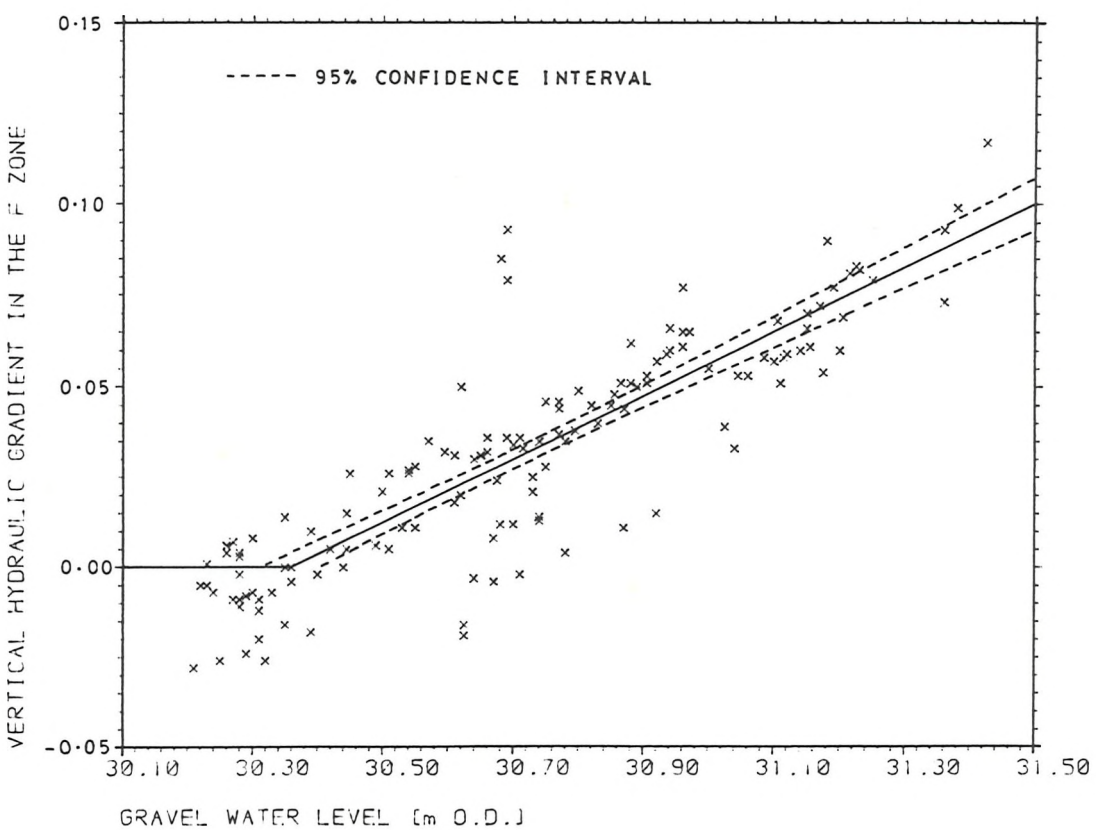

FIGURE 7.14 VERTICAL HYDRAULIC GRADIENT IN THE F ZONE AND GRAVEL WATER LEVEL AT LOCATION E

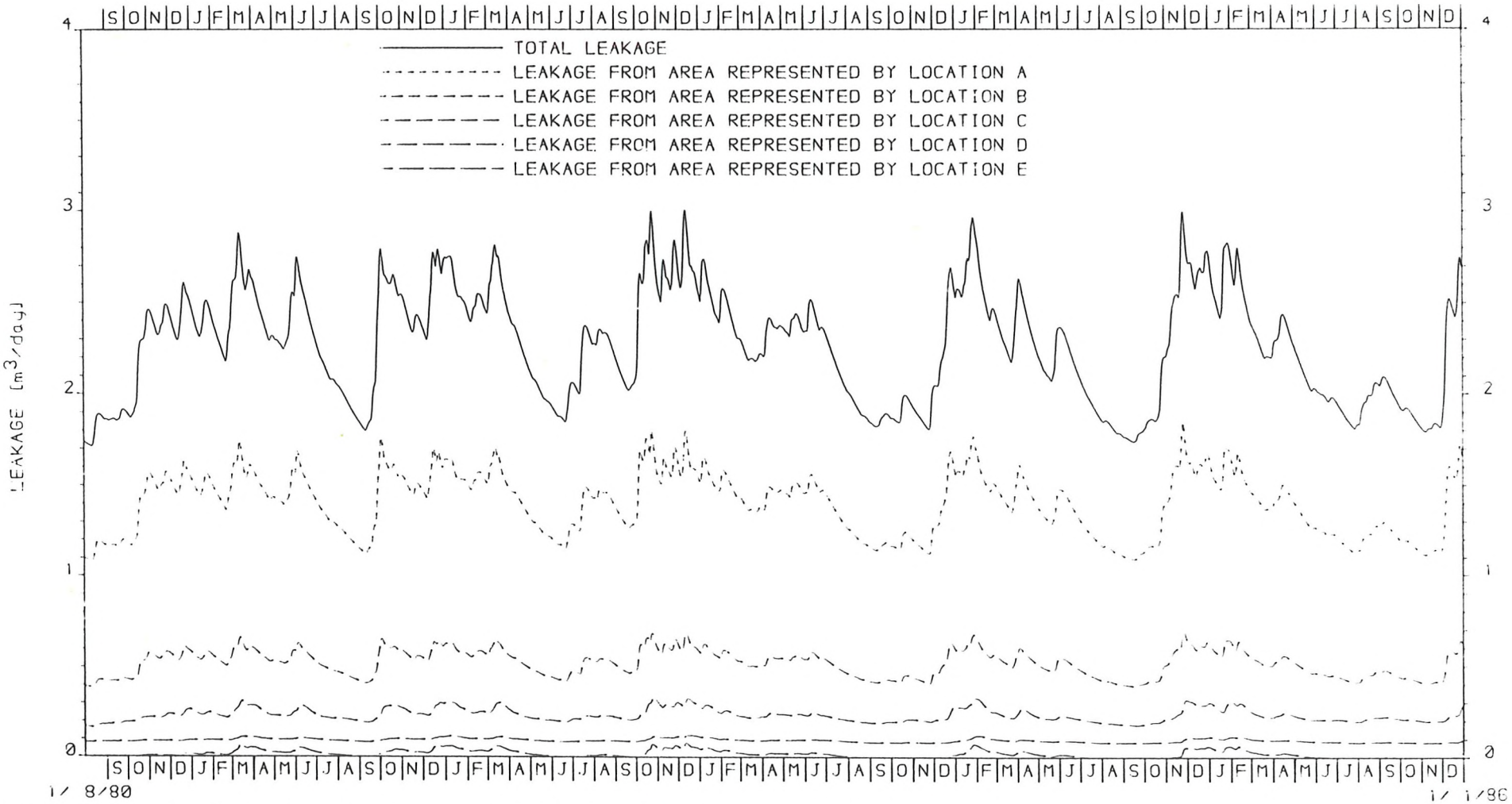

FIGURE 7.15 GROUNDWATER LEAKAGE FROM PLATEAU GRAVEL TO BARTON CLAY.
THE GRAPH SHOWS THE TOTAL AREAL LEAKAGE AND FROM THE AREAS REPRESENTED BY EACH OF THE LOCATIONS AT WHICH VERTICAL FLUX IS CALCULATED.
SEE TABLE 7.2 FOR THEIR LOCATION.

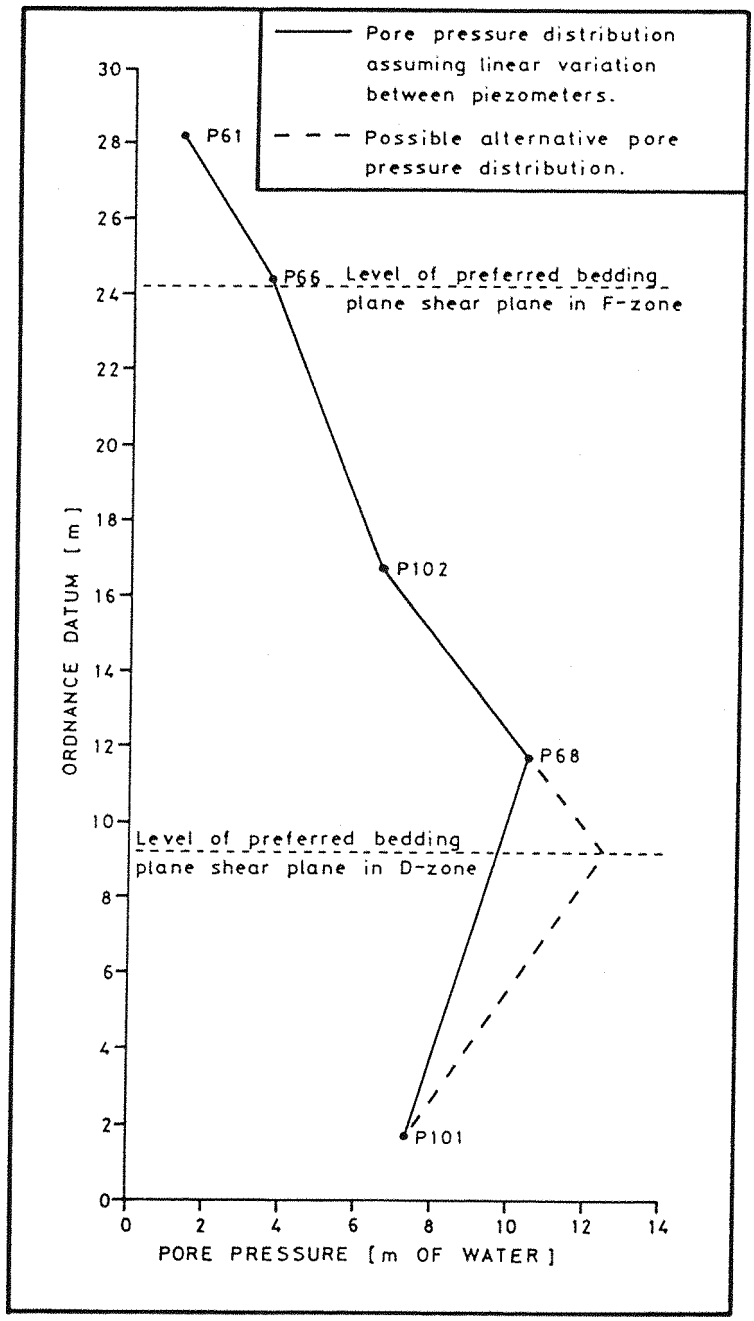

Figure 7.16 Variation of pore pressure with depth at location B on 1st February 1984. See table 7.2 for the position of B.

CHAPTER 8

THE MEASUREMENT OF SOIL MOISTURE IN THE UNDERCLIFF COLLUVIUM

8.1 Introduction

In any hydrological study an investigation of the subsurface water also requires a knowledge of the unsaturated zone of soil between the surface and the groundwater table. The unsaturated zone is subject to both seasonal and weekly variations in moisture content. To carry out a water balance, the changes in moisture content need to be evaluated. To do this, periodic measurements of the vertical distribution of moisture content need to be taken down to a depth where the moisture content does not vary, either seasonally, or weekly (ideally to below the lowest water table position).

The method used in this study to acquire this information is that of neutron scattering. It is the most widely used method in practice. This is because it is simple, quick, non-destructive, repeatable in the same soil matrix, and can be applied to the entire moisture range.

This chapter briefly describes some aspects of the basic technique, and then in more detail, its application and the use of the results to estimate changes in soil moisture storage in the undercliff. A more detailed description of the basic technique can be found elsewhere (e.g. Bell, 1976). All the results are given in Thomson (1986c). Only the areal average results for the undercliff are presented here.

8.2 Basic Principles of the Neutron Scattering Technique

A probe containing a source emitting high energy (fast) neutrons and a detector of low energy (slow) neutrons, is lowered down an access tube into the soil. The fast neutrons collide with the atoms of the soil. With each collision they lose some energy and their direction of movement is changed. Some slow neutrons return to the probe and are counted by the detector. The soil

element with the greatest ability to reflect neutrons is hydrogen. The amount of hydrogen in the soil, in the form of water, varies. Therefore, the count rate of slow neutrons is related to the soil moisture content. The precise relationship is also dependent upon the other elements in the soil, and this depends upon the soil chemistry and bulk density. This requires calibration using the direct gravimetric method of moisture determination. This measures the moisture lost by a soil sample of known volume which has been in an oven at 105°C for 24 hours.

When a reading is being taken, the further the emitted neutrons travel from the probe, the less likely they are to be reflected back to the detector. Thus, the reading is influenced largely by soil close to the probe, with a diminishing influence by soil further away from the probe. Because the direction of emission is random, the volume of measurement is a sphere and has been called the sphere of influence (Bell, 1976).

The calibration of count rate with moisture content is normally for a homogeneous soil of uniform moisture content. Where there is an abrupt change in the moisture profile, which the sphere of influence intersects, the normal calibration curve will not give an accurate estimation of the true moisture content. The soil surface is an abrupt change. Therefore, a special calibration is needed for readings near the soil surface.

Drifts in the electronic components cause drifts in the readings (for the same soil horizon at a constant moisture content) from one reading date to the next. To avoid this problem, all readings of count rate in soil are divided by a standard reference count. This is carried out in an access tube set in a large tub of water.

The emission of fast neutrons and the detection of slow ones is a random process. There is thus a random error associated with

the reading of count rate. The resulting standard error* in moisture content determination is given by (Bell, 1976):

$$E_m = \frac{1}{G} \cdot \frac{R}{R_W} \cdot \left(\frac{1}{R.t} + \frac{1}{R_W.t_W} \right)^{\frac{1}{2}} \quad (8.1)$$

where R is the count rate in soil,

R_W is the standard count rate in water,

t is the integration time for the count rate in soil,

t_W is the integration time for the count rate in water,

G is the change in R/R_W per unit change in moisture content (by volume).

8.3 Access Tube Installation at Naish Farm

The construction and installation of the aluminium alloy access tubes was as described in Bell (1976). The access tube needs to have a good tight fit so as not to leave any unnatural voids between the soil and the tube which may lead to non-representative readings. An exception to this is when the access tube goes through a tension crack which is a natural void in the soil. As the soil had been remoulded and in an easily compressed state, it was found to be difficult to avoid enlargening of the hole near the ground surface. This could also be true at depth as well, as it was noted during installation that tightness of fit varied considerably (this was dependent on the soil material, as the clay varied from very soft and loose to very stiff). However, after installation, the ground heaves, and within a few days closes up to give a satisfactory contact with the tube.

Access tubes were installed to a depth of 2m. The problem with deeper tubes is that they have to be well sited and fortunate

*The standard error is defined such that there is a 68 per cent probability that the deviation of the true value from the estimated value is less than the standard error.

not to fail* after only a short time in use.(The greater the depth of tube, the greater the chance of failure due to differential rates of movement of the debris material.) This increases the difficulties of obtaining a representative network of tubes. However, 2 m has been found satisfactory for obtaining changes in soil moisture storage.

The method of access tube installation was not suited to gravelly soils. The debris material of the undercliff is made up of mainly clayey soil. However, there are substantial areas of gravel at the surface (for example, see plate 1.4) and in layers at depth. It is difficult, and often not possible, to install a tube in these conditions with this method. Other researchers have tried other methods in gravelly soil.

Cline and Jeffers (1975) hammered a steel rod into the ground which was then withdrawn and an access tube pushed into the soil. The method relies upon the soil being cohesive enough for the hole not to collapse after the rod is withdrawn and before the tube is put in. The soil is displaced, causing local compaction (higher bulk density) next to the tube. This makes the method advisable only as a last resort. The method is not suitable at Highcliffe as the loose gravel debris is highly collapsable.

Carpenter (1972) used a method for gravel soils liable to collapse. He hammered a hollow rod into the ground. Inside the rod was an access tube. The rod was withdrawn leaving the access tube behind. The method requires heavy expensive equipment which would not be accessible to the undercliff.

Another way of installing access tubes in the gravelly soils in the undercliff, might be to dig a big pit and put a tube in and backfill. This would be difficult and require considerable work for just one tube. As a compromise, shallow surface (less than 30 cm) gravel has been dug out before installing the tube in clay and the surface gravel backfilled to the original ground

*An access tube is said to have failed when the probe can no longer be lowered to the bottom. The probe has only a slight clearance inside the tube and only a slight curvature of the tube is necessary for the tube to have failed.

level. To dig out and backfill material around a tube in normal ground is not advisable as the natural state would be disturbed. However, the undercliff soils are already in a highly disturbed state, such that backfilling around a tube will still be representative of the surrounding soil. With the equipment available, some success has been achieved in installing tubes through gravelly clay or sandy layers. The major criterion in being able to do so, seems to be that the layer should not contain any large gravel, or cause the hole to collapse.

8.4 Access Tube Network Design at Naish Farm

To make an areal estimate of the changes in soil moisture storage, a number of access tubes need to be installed in representative locations of the undercliff. The number of access tubes is limited by the time taken for each reading and the number of readings for each access tube. The depths at which readings were taken were:

10cm, 20cm, 30 cm, 40cm, 60cm, 80cm, 100cm, 120cm, 140cm, 160cm.

The readings were more frequent near the surface where the moisture gradients were likely to be strongest and where the moisture fluctuations were greatest. The less frequent deeper readings were subject to smaller moisture fluctuations and, therefore,to less error in the evaluation of the changes in total profile moisture content. There was no point in using less than a 10 cm reading depth interval near the surface as "no greater resolution can be gained by decreasing this figure" (Bell, 1976).

The probe used had preset integration times for count rate of 16 sec, 64 sec, 16 min, and 64 min. From equation 8.1 it can be seen that the longer the integration time, the smaller the random error. As the standard reference count was taken only once for each reading date, a 16 min integration time was used. A

64 sec integration time was used for the more numerous readings in the undercliff soil. This meant that there was sufficient time in the day for approximately 12 access tubes. A shorter integration time (i.e. 16 sec) would have allowed more access tubes to have been read. This would mean that the results of individual access tubes would be less accurate, but that the network would be more representative of the study area. However, due to the moving environment, the life expectancy of an access tube is limited. From time to time new access tubes need to be installed in order to maintain the size of the network. The access tubes also need to be regularly checked and cleared of stones, sticks, mud, and water. The more access tubes there are in the network, the more time consuming this all becomes. In the end, there is a limitation as to the size of the network that can be maintained. For this reason, a network of 12 access tubes and an integration time of 64 sec. was used.

The installation of access tubes was done in dry periods when the undercliff was reasonably trafficable. In wet periods, access to many parts of the undercliff is either dangerous or impossible (for example, see plate 1.8). The continual state of movement in the undercliff causes access tubes to fail from time to time due to the differential movement. Sometimes, the failure was such that readings could still be taken down to the failure point. Often, however, a new tube had to be installed. To improve the life expectancy of access tubes in the undercliff, care had to be taken with their location. Areas of shallow differential movement, or where material was prone to fall and bury the tube, tended to be avoided. Another problem of siting was vandalism, although it can be reduced by careful siting.

In choosing the sites for the access tube network, the major factor decided upon was the position on the slope (from cliff toe to cliff top). However, limitations were set by installation difficulties (i.e. gravel), wet areas, differential movement, and vandalism considerations. It was difficult to find sites in the upper part of the undercliff due to many areas having

gravel either on the surface or at depth. In winter, the lower part of the undercliff was not only mostly inaccessible, but was also subject to large movements, such that the life expectancy was unacceptably low (a few weeks). Thus, in the end, the network design came down to using sites as varied and widely spaced as possible, whilst avoiding the above problems as much as possible so as to achieve as constant (long life) a network as possible. Figure 8.1 shows the location of the access tubes.

8.5 Soil Calibration

8.5.1 The Use of Special Calibration Equations or those given by the Neutron Probe Instruction Manual

The Instruction Manual (IOH, 1979) for the probe used, gives a number of typical calibration curves for different soil types, and suggests that for intermediate soils an intermediate curve should be used. The manual suggests that a special calibration should only be performed if a high degree of accuracy is required. The equations given are:

$$MVF = 0.790 \cdot \frac{R}{R_W} - 0.024 \qquad (8.2)$$

$$MVF = 0.867 \cdot \frac{R}{R_W} - 0.016 \qquad (8.3)$$

$$MVF = 0.958 \cdot \frac{R}{R_W} - 0.012 \qquad (8.4)$$

where MVF is the moisture volume fraction of the soil. Equation 8.2 is for "sandy, silty or gravelly soils (i.e. predominantly silica)". Equation 8.3 is for "loams". Equation 8.4 is for "clay soils (also peat)".

For values of R and R_W equal to 500 and 1000 counts per second respectively, the error in using an "average" equation (instead of equation 8.2 or 8.4) for the determination of the absolute moisture content is $\pm$ 11.5 per cent, and for the change in moisture content it is $\pm$ 9.7 per cent. The soil chemistry can vary between soils of the same texture, and Lal (1974) showed that this can make a significant difference to the estimation of both the absolute moisture content, and the change in moisture content.

The manual curves make no allowance for variation in dry bulk density. Vachaud et al (1977), using the theoretical model of Couchat (1974), showed that for a typical soil, at a typical count rate of 500 counts per second, a 14 per cent variation in dry bulk density will produce only a 1.7 per cent variation in slope (change in moisture content) of the calibration equation, but a 6 per cent variation in absolute moisture content. This is an example based on a theoretical model. Other researchers using field calibrations have also found that dry bulk density affects the calibration (e.g. Luebs et al (1968) found that dry bulk density mainly affected the intercept, with little change to the slope of the calibration equation).

From the above discussion, it would seem to be advisable to perform a special calibration (as most researchers do), whether absolute moisture contents, or changes in moisture content are required. This special calibration should take into account the dry bulk density of the soil if absolute moisture contents are required. However, if only changes in moisture content are important (as is the case in this study), then a single calibration representing all dry bulk densities should be sufficient.

8.5.2 The Derivation of Special Calibration Equations

There are three basic methods of calibration: theoretical; laboratory; and field. Bell (1976) points out that the results

from theoretical calibrations can sometimes be poor; and laboratory calibrations rely upon good experimental technique, and are unsuitable for clay soils. Because of these drawbacks, field calibrations are usually performed.

For a field calibration, access tubes are installed at sites representative of the study area. For each tube, precise count rates are taken at a known depth, and six known volume soil cores are then obtained from that depth. The moisture content is determined by oven drying. A large number of points are needed along the whole range of moisture contents, as there is a large scatter due to soil heterogeneity and various sampling errors. Soil compression is a source of error which can be very large in some soils (notably clays). The debris material of the undercliff, being a remoulded mix of mostly clay, is very compressible, such that it is very difficult to take known volume soil cores for calibration by the usual field method. An alternative method was used to determine the volume of soil. It is based on the sand replacement method (large pouring cylinder method) of measuring the in situ soil density (BS 1377, 1975, Test 15B). Two calibrations are necessary: one for readings affected by the presence of the ground surface (i.e. 10 cm depth); and one for deeper readings not so affected (i.e. 20 cm depth and below).

8.5.2.1 The Method of Calibration used at Naish Farm for Readings affected by the Soil Surface (i.e. at 10 cm depth).

Due to the effect of the sphere of influence (see section 8.2), the count rate decreases as the probe nears the ground surface. Long and French (1967) used the ground surface to investigate the size of the sphere of influence, which they defined as the depth at which the reading reached 99 per cent of the value corresponding to the true moisture content. They showed that wet soil has a smaller sphere of influence than does dry soil. At 20 cm and below, the underestimate was less than 5 per cent.

As the depth decreased below 20 cm, the underestimate sharply increased. Therefore, it was decided that a special calibration was needed for the 10 cm depth reading. The error at 20 cm depth was not considered significant enough for a separate calibration.

A short access tube was installed in level ground to a depth of 20-30 cm. A neutron probe count rate (using a 16 min integration time) was taken at 10 cm depth. With the access tube at its centre, a 20 cm diameter hole was dug down to just below the bottom of the access tube (about 25 cm depth). The soil was bagged and sealed. The volume of the hole was determined by using the in situ density apparatus (BS 1377, 1975, Test 15B). From this was subtracted the volume of the access tube below ground surface. This gave the volume of the soil. The soil was weighed, oven dried, and re-weighed to give the moisture content and bulkdensity of the soil.

In using this method, it was found that the presence of tension cracks in the soil was a source of possible error. If there is a tension crack in the side of the hole dug, it will fill with the sand used for estimating the volume of the hole. This will cause an overestimate of the volume of the hole. Before the hole was filled with sand, it was carefully checked for tension cracks, and any present were sealed with a plug of wet clay.

8.5.2.2 The Method of Calibration used at Naish Farm for Readings not affected by the Soil Surface

The calibration work was carried out near access tube no 15. The pond nearby (see figure 8.1) was not considered to have had any significant effect on the readings.

An access tube was installed in a clay profile to a depth of 2 m. The ground was levelled, and neutron probe readings (using a 64

second integration time) taken at 10 cm intervals from the ground surface to a depth of 60 cm. Then a 10 cm layer of soil was removed to a distance of at least 30 cm from the tube. 30 cm is the maximum radius of influence that might be expected, and only when the soil is very dry (Long and French, 1967). Thus, 30 cm was thought to be sufficient to ensure that the sides of the removed layer do not affect readings. Neutron Probe readings were repeated at 10 cm intervals to a depth of 60 cm. The procedure of taking readings and removing a 10 cm layer of soil, was repeated several times. The results are presented in table 8.1.

For each soil horizon, a series of readings are obtained with the horizon at different depths below a "moving ground surface". The moisture content of the soil horizon does not change. To obtain its moisture content, the count rate when it is at 10 cm depth is used with the calibration equation for 10 cm depth (obtained by the method described in section 8.5.2.1). The count rate for the same soil horizon when it is not affected by the ground surface, is used to obtain a calibration point for the required calibration.

Although the exercise was carried out in the summer when it was dry, the readings obtained were not as low as have been obtained in some profiles. To ensure readings at the dry end, a second pit was dug and an access tube installed in its centre. The pit was filled with 10 cm layers of gravelly sand (taken from the undercliff) up to the original ground level. As before, neutron probe readings were taken down the profile after each layer was placed. As can be seen by a comparison of equations 8.2 and 8.4, gravelly sand does not give the same calibration as clay. However, the difference is only slight at the dry end. Also, low readings in the undercliff are commonly due to gravelly sand layers, or gravel and sand mixed with clay (except where numerous tension cracks in the clay reduce the readings). The results are presented in table 8.2.

8.5.2.3 The Results of Calibration at Naish Farm

Table 8.3 summarises the results of calibration work for the 10 cm depth readings. Figure 8.2 is a plot of the results and shows the regression line. Moisture content (as MVF) is taken as the independent variable, and count ratio is the dependent variable, i.e. scatter is due to errors in the count ratio. These are due to:

i) Random counting errors (see section 8.2). This error was minimised by using a 16 min integration time.

ii) Depth location errors. Because the influence (on the reading) of the presence of the ground surface varies with depth, an error in the depth location of as little as 1 cm can cause a significant error. Great care was taken to ensure that the ground surface was even, and that the height of the top of the access tube above the ground level was a whole number of centimetres.

iii) Moisture gradients. It is assumed that the moisture content is uniform. If a moisture gradient is present, the reading of count rate will be affected. The moisture gradient, and therefore its effect, will be different for each calibration point.

iv) Soil chemistry and dry bulk density. It was previously explained (section 8.5.1) that these properties affect the count rate. As they differ for each calibration point, they will contribute to the scatter.

Although moisture content is taken not to be in error, some error can occur. The only significant error is due to the influence of tension cracks. It is always possible that a tension crack may not be noticed, or that the clay plug is breached by the sand. The lower the count reading, the more tension cracks there probably are, with a greater likelihood of error. This makes

calibration at the dry end of the relationship very difficult. The regression equation is:

$$\frac{R_{10}}{R_w} = 1.041 \times MVF + 0.0133 \qquad (8.5)$$

where R_{10} is the count rate at 10 cm depth. The standard error for the slope is 0.13. This means that there is a 68 per cent chance that the changes in soil moisture storage calculated from equation 8.5 are up to 13 per cent different from the true values. This is a bias error, i.e. the percentage error in the change in soil moisture storage is constant for all results.

The results for the calibration of readings at depths of 30 cm and greater, are summarized in table 8.4, and plotted in figure 8.3. The regression equation is:

$$\frac{R_D}{R_w} = 1.085 \times MVF + 0.0475 \qquad (8.6)$$

where R_D is the count rate for depths 30 cm and greater. The values of MVF for the calibration points are derived from the use of equation 8.5. Therefore, the error in using equation 8.6, is due not only to the scatter of the calibration points in figure 8.3, but also to the error in using equation 8.5. As the scatter of the calibration points in figure 8.3 is small, the error in using equation 8.6 is approximately the same as that for equation 8.5 (i.e. the standard error of the slope is 0.13). This is taken into account by the 95 per cent confidence limit for equation 8.6 that is drawn on figure 8.3. The intermediate equation (equation 8.3) given by the Instruction Manual (IOH, 1979) lies within these limits, although it is not used in this analysis.

At the wet end, the count rate at 20 cm depth is not significantly different from that at 30 cm depth and below. Although the difference is significant at the dry end, it is not great, and as

most of the readings for 20 cm depth are at the wet end, it was decided to adopt equation 8.6 for the 20 cm depth calibration.

Rearranging equation 8.5 gives:

$$MVF = 0.961 \times \frac{R_{10}}{R_W} - 0.013 \qquad (8.7)$$

Rearranging equation 8.6 gives:

$$MVF = 0.922 \times \frac{R_D}{R_W} - 0.044 \qquad (8.8)$$

8.6 Calculation of the Total Profile Moisture Content

Equations 8.7 and 8.8 were used to convert count rate readings into values of MVF, each of which was assumed to be the average for a layer of soil as defined in table 8.5. The layer moisture contents were summed to give the total profile moisture content. The change in profile moisture storage between any two dates was calculated as a rate in mm depth of water per day.

8.7 Calculation of the Changes in Undercliff Water Storage

The average rate of change of soil moisture storage between reading dates was found for each profile. Each tube is given a weighting to reflect the area of the undercliff it represents. The daily change in soil moisture storage for each tube is multiplied by its weighting factor, and the result is summed for all the tubes to give a value of the daily rate of change in undercliff soil moisture storage.

The fact that the same set of tubes were not used every time

readings were taken (due to failures or new installations), makes it difficult to assign individual weightings. It is also very subjective to say for what area of undercliff a tube is representative. It was therefore decided to use an equal weighting factor for all the tubes, i.e. to assume that each tube is representative of an equal area of the undercliff.

It is assumed that the network of access tubes also represents the changes in pond storage (for example, the pond in plate 1.7). Ideally, the changes in pond storage should be measured separately. However, this would require considerable and frequent field work, as movement continually causes the ponds to change in level (with changes in the general level of the colluvium) and shape.

8.8 Results and Discussion

The results for individual access tubes have been presented and discussed in Thomson (1986c). They show that for any profile and depth, the MVF of the soil varies due to the undercliff movement, as well as in response to changes in meteorological conditions. Undercliff movement can cause changes in the local topography around a tube (topography influences soil moisture conditions); tension cracks to open and close (affecting drainage conditions around the tube); variations in dry bulk density (affecting the count rate (see section 8.5.1) which, as the calibration does not allow for dry bulk density, gives an apparent change in MVF). These effects of undercliff movement are assumed to be averaged out over the network of access tubes, such that the calculated change in undercliff water storage is not influenced by them. The depth to which meteorological conditions noticeably affect the MVF of the soil varies from tube to tube, but is never more than 1.5 m.

Figure 8.4 shows the calculated moisture storage in the undercliff

throughout the study period. The initial moisture storage is arbitrarily given a value of 100 cm of water. This is approximately equal to the areal average of moisture storage in the top 2.4 m of colluvium at the start of the study period. The figure shows the water storage to be influenced by meteorological conditions. However, there is also a downward trend in water storage throughout the study period. It is difficult to accurately determine the trend from such limited data. However, assuming the two winter periods to be in a comparable state of wetness, the trend is about minus 2 cm per year. The reason for this trend is uncertain, but it is postulated here that there could be three possible causes.

The first possibility is that the effects described above, of undercliff movement on individual profiles, may not be averaged out over the access tube network, i.e. some bias may exist.

The other two possibilities are as a result of the net loss of debris material from the undercliff. The colluvial budget for the undercliff has been given in Barton and Coles (1984) for the year previous to the study period (i.e. July 1981 to July 1982). They calculated a 7 per cent loss of undercliff colluvium. The area of undercliff covered by their study was slightly larger, but included all the area covered by this study. Only one small slump occurred during their study period. Figure 6.3. shows that only two small slumps occurred in the study area, and one large one just to the east of it, during the study period. Therefore,it is expected that the rate of loss of undercliff colluvium in the study period is similar to that of Barton and Coles (1984). Further evidence of this, is the drop in ground level at the access tubes that has occurred throughout the study period (Thomson, 1986c). The colluvial budget is characterised by intermittent large sudden inputs (large slumps, such as the one depicted in plates 1.10 and 1.11), followed by an initial short period of high output (to the sea), and then a long period of reduced output until the next large slump. Although there

is always a small amount of input (in the form of spalling and small slumps, such as the one depicted in plate 1.12), it is never as large as even the reduced output. It is postulated here that this temporal change in the colluvial budget could cause the trend in figure 8.4 in two possible ways. The first is through changes in groundwater flow, and the second is through changes in the average dry bulk density of the undercliff.

The large slump causes a sudden large increase in weight at the back of the undercliff. The increased load is initially taken by an increase in pore water pressure. This causes an increased flow of groundwater down the undercliff. This causes groundwater levels in the rest of the undercliff to rise and the surface soils to increase in moisture content. Subsequently, as colluvium is lost to the sea, the load on the upper part of the undercliff decreases, which decreases pore water pressures, and therefore groundwater flow. Thus, groundwater levels in the undercliff fall, reducing the moisture content of the surface soils. The amount of undercliff colluvium lost varies seasonally (Barton and Coles, 1984). This has also been noted from movement records of the access tubes (Thomson, 1986a) during the study period. This would imply a variation of the trend in a loss of moisture storage in the undercliff (as characterised by figure 8.4), although the variation may be attenuated. However, for simplicity the trend is assumed constant.

When a large slump occurs, a large amount of material tries to fit into an already occupied space (undercliff). It is in part accommodated by movement of material along the undercliff and into the sea; and by a rise in ground level of the colluvium. It is probable that an increase in average dry bulk density (for the whole undercliff) also occurs. When there is a net loss of material from the undercliff, this is partly accommodated by a drop in ground level, and partly by a decrease in average dry bulk density of the undercliff. It was stated in the first paragraph of this discussion that undercliff movement causes

variations in dry bulk density, but that these were assumed to average out over the network of access tubes. It was assumed that the average dry bulk density remained constant. However, if the access tube network is representative of the undercliff for which there is a variation (gradual reduction) in the average dry bulk density, then this could explain the trend in figure 8.4. Unfortunately, it has not been possible to measure the temporal variation of dry bulk density in the undercliff.

The purpose of this analysis is to determine the changes in undercliff moisture storage as part of a water balance for the undercliff. Which of the above postulates is assumed will affect this analysis. If the trend in figure 8.4 is due to an unrepresentative network, or to a decrease in average undercliff dry bulk density, then it should be removed before applying the results to an undercliff water balance. However, if the trend is due to long term changes in groundwater flow due to the loss of colluvium, then the trend represents a real loss of water and should be included in the undercliff water balance. Of course, the reality may well be a mixture of all three causes.

Figure 8.5 shows the rate of change of undercliff moisture storage during the study period. It has been calculated as explained in section 8.7, and is equal to the gradient of figure 8.4 (without the trend being removed). If the trend were removed (assuming a constant trend throughout the study period), then the rates would need to be increased by 0.054 mm/day. The random standard error (see section 8.2) in figure 8.5 varies from week to week, but is, on average (for a seven day period), about $\pm$ 0.07 mm/day (Thomson, 1986c). In the short term, the effect of the trend of figure 8.4 is negligible and is less than the random error. In the long term, the trend is more important as the "error" is cumulative. The uncertainty in the slope of the calibration (see section 8.5.2.3) leads to a bias standard error of $\pm$ 13 per cent in the rates of figure 8.5. This is by far the most significant source of possible error.

Figure 8.5 also shows the effect of reducing the rate of change in soil moisture storage by 13 per cent. This of course would also reduce the trend of figure 8.4 by 13 per cent (i.e. from 2 cm per year to 1.74 cm per year). This last error is used in an error analysis of the undercliff water balance in chapter 9.

8.9 Summary

The changes in undercliff soil moisture storage during the study period have been evaluated using the neutron scattering technique. A network of access tubes was set up, and the vertical distribution of moisture content measured weekly. The measurements were taken down to depths where the moisture content did not significantly vary, either weekly, or seasonally. Because of the compressible nature of the soil, an original (to the knowledge of the author) method of calibration was devised. The estimation of the slope of the calibration is the most significant error in estimating the rates of changes in soil moisture storage (standard error 13 per cent).

A downward trend in the undercliff soil moisture storage was observed for the study period. The trend is not significant for the short periods (a few days) for which the analysis of the water balance is of most interest. However, for longer periods it is significant, and amounts to an estimated 40 mm for the 2 year study period. It is assumed that this loss is due to the gradual net loss of undercliff colluvium affecting the groundwater flow, although in reality, other effects, such as a gradual reduction in the average dry bulk density of the colluvium, and bias in the access tube network, may also be significant.

Table 8.1 Results of an Examination into the Ground Surface Interface Effect. I Clay Profile

Soil Removed (cm)											
0		10		20		30		40		50	
Z	R	Z	R	Z	R	Z	R	Z	R	Z	R
0	59										
10	278	0	64								
20	413	10	353	0	78						
30	455	20	448	10	403	0	86				
40	479	30	473	20	475	10	429	0	94		
50	493	40	487	30	491	20	490	10	436	0	103
60	511	50	511	40	518	30	514	20	512	10	462
		60	519	50	514	40	521	30	516	20	514
				60	522	50	522	40	519	30	522
						60	497	50	504	40	499
								60	503	50	505
										60	503

Notes: Date: 5th July 1984

Location: Near access tube AT15

Count rate in water, R_W = 963.8 counts/sec

Integration time in water, t_W = 16 min

Integration time in soil, t = 64 sec

Z Depth below ground surface in cm

R Reading in counts/sec

Table 8.2 Results of an Examination into the Ground Surface Interface Effect. II Sand Profile

Depth below original ground level (cm)											
0		10		20		30		40		50	
Z	R	Z	R	Z	R	Z	R	Z	R	Z	R
0	18										
10	68	0	19								
20	84	10	53	0	18						
30	76	20	65	10	41	0	23				
40	93	30	92	20	78	10	59	0	33		
50	261	40	267	30	253	20	236	10	210	0	108
60	485	50	492	40	496	30	488	20	479	10	457
		60	511	50	508	40	507	30	511	20	509
				60	446	50	448	40	451	30	462
						60	391	50	392	40	392
								60	494	50	489
										60	520

Notes: Date: 5th July 1984

Location: Near access tube AT15

Count rate in water, R_W = 963.8 counts/sec

Integration time in water, t_W = 16 min

Integration time in soil, t = 64 sec

Z Depth below ground surface in cm

R Reading in counts/sec

Table 8.3 Calibration Results for 10 cm Depth

Location	Particle Size %			DBD (gm/cc)	MVF	R_{10}/R_w
	Clay	Silt	Sand			
AT 1	35	39	26	1.57	.382	.399
AT 13	37	37	26	1.66	.304	.344
AT 15	55	42	3	1.27	.307	.295
AT 8	51	34	15	1.39	.152	.161
AT 17	58	38	4	1.41	.364	.394
AT 3	-	-	-	1.36	.290	.340
AT 6	-	-	-	1.32	.286	.333
AT 15	30	66	4	1.32	.253	.275

Notes: The location is described by the nearest access tube (see figure 8.1).
For the particle size classification see BS 1377 (1975).
- denotes debris material derived from the Barton Clay.
DBD is dry bulk density
MVF is moisture volume fraction
R_w and R_{10} are the count rates in water and at 10 cm depth in soil respectively.

Table 8.4 Calibration Results for Depths 30 cm and Below

R_{10}	R_{10}/R_w	MVF	R_D	R_D/R_w
41	.043	.028	76	.079
59	.061	.046	93	.096
403	.418	.389	455	.472
429	.445	.415	476	.494
436	.452	.422	490	.508
462	.479	.448	513	.532

Notes: R_w and R_{10} are the count rates in water, and at 10 cm depth in soil respectively.

R_D is the average count rate in soil at 30 cm depth and below.

MVF is the moisture volume fraction calculated using equation 8.5.

Table 8.5 Definition of the Soil Layering used in the Calculation of the Profile Moisture Storage

Reading Depth (cm)	Layer Depth (cm)
10	0 - 15
20	15 - 25
30	25 - 35
40	35 - 50
60	50 - 70
80	70 - 90
100	90 - 110
120	110 - 130
140	130 - 150

Note: The value of MVF calculated for the reading depth is taken to be the average for the given layer.

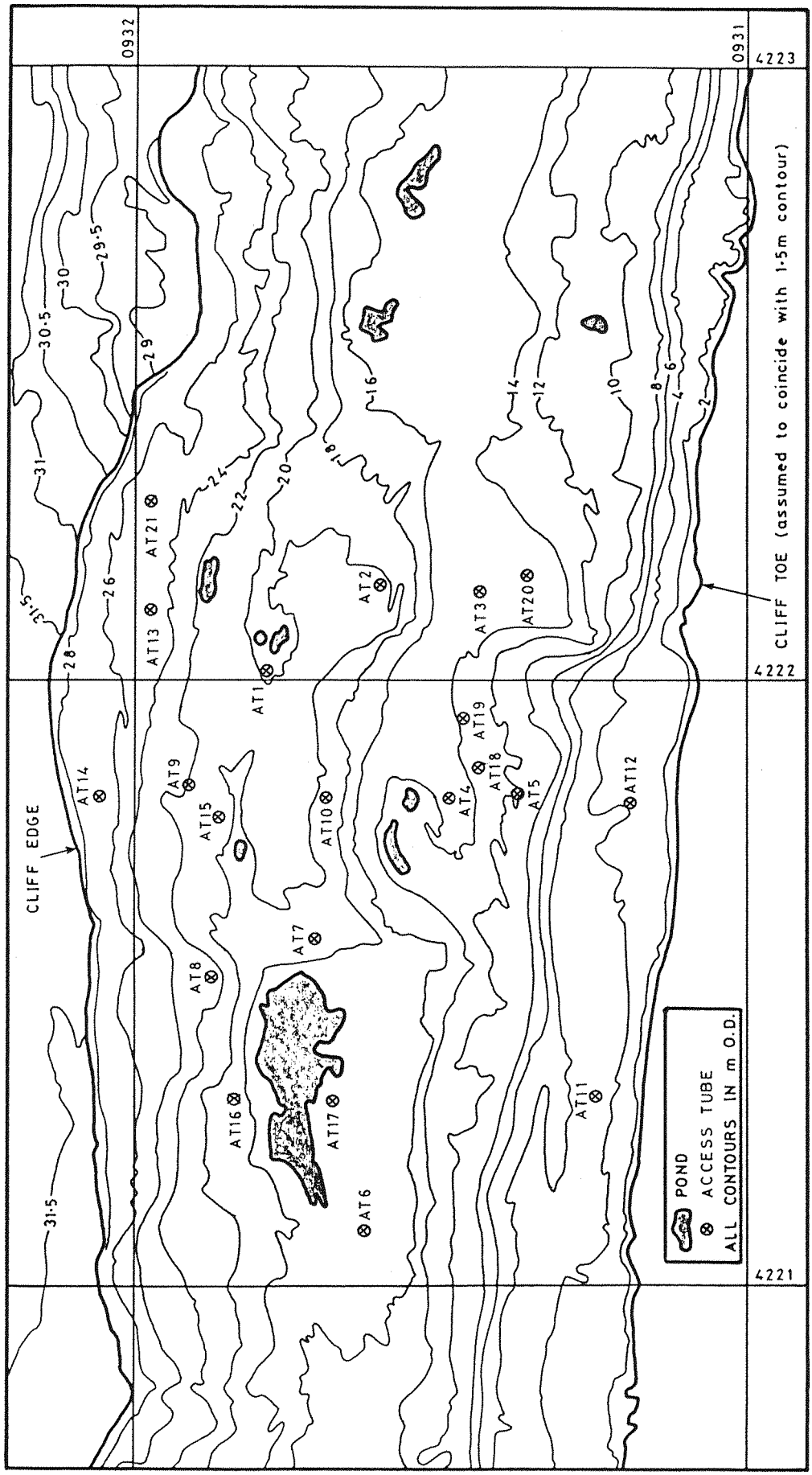

Figure 8.1 Access tube location map. The positions shown are as on the first survey date for each access tube.

Figure 8.2 NEUTRON PROBE CALIBRATION FOR READINGS AT 10cm DEPTH

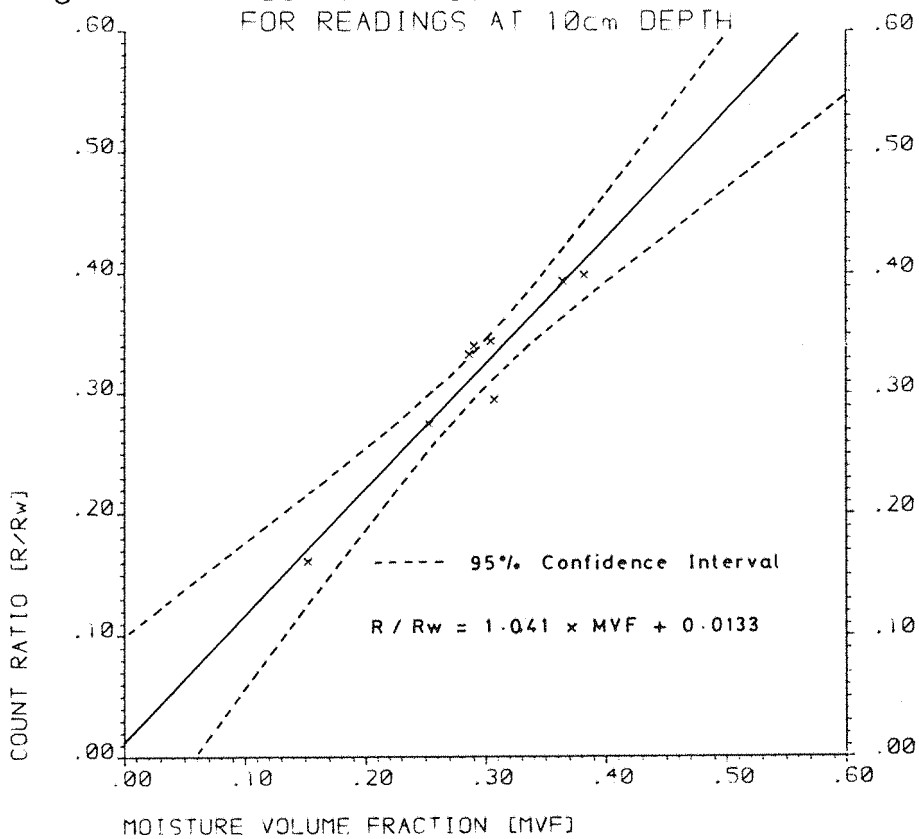

Figure 8.3

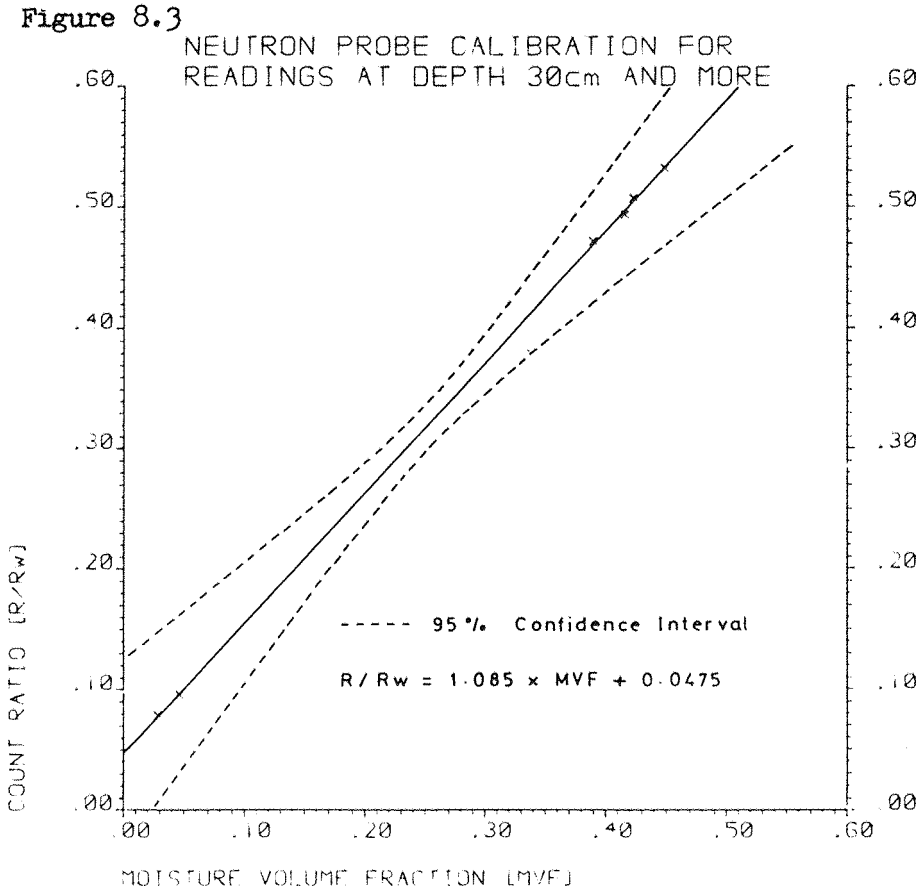

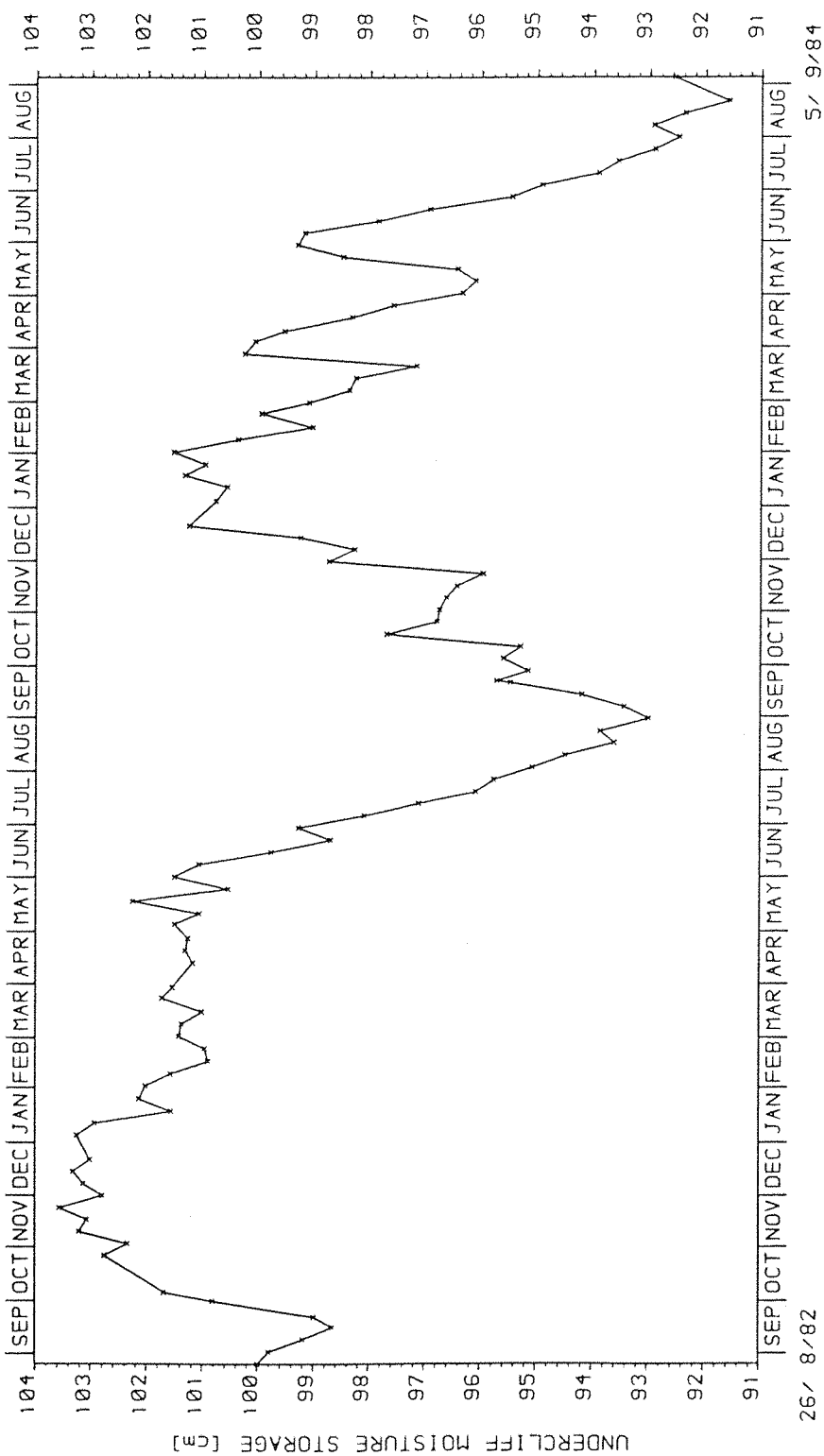
MOISTURE STORAGE IN THE UNDERCLIFF
UNDERCLIFF MOISTURE STORAGE [cm]
104
103
102
101
100
99
98
97
96
95
94
93
92
91
SEP OCT NOV DEC JAN FEB MAR APR MAY JUN JUL AUG SEP OCT NOV DEC JAN FEB MAR APR MAY JUN JUL AUG
26/ 8/82
5/ 9/84

Figure 8.4

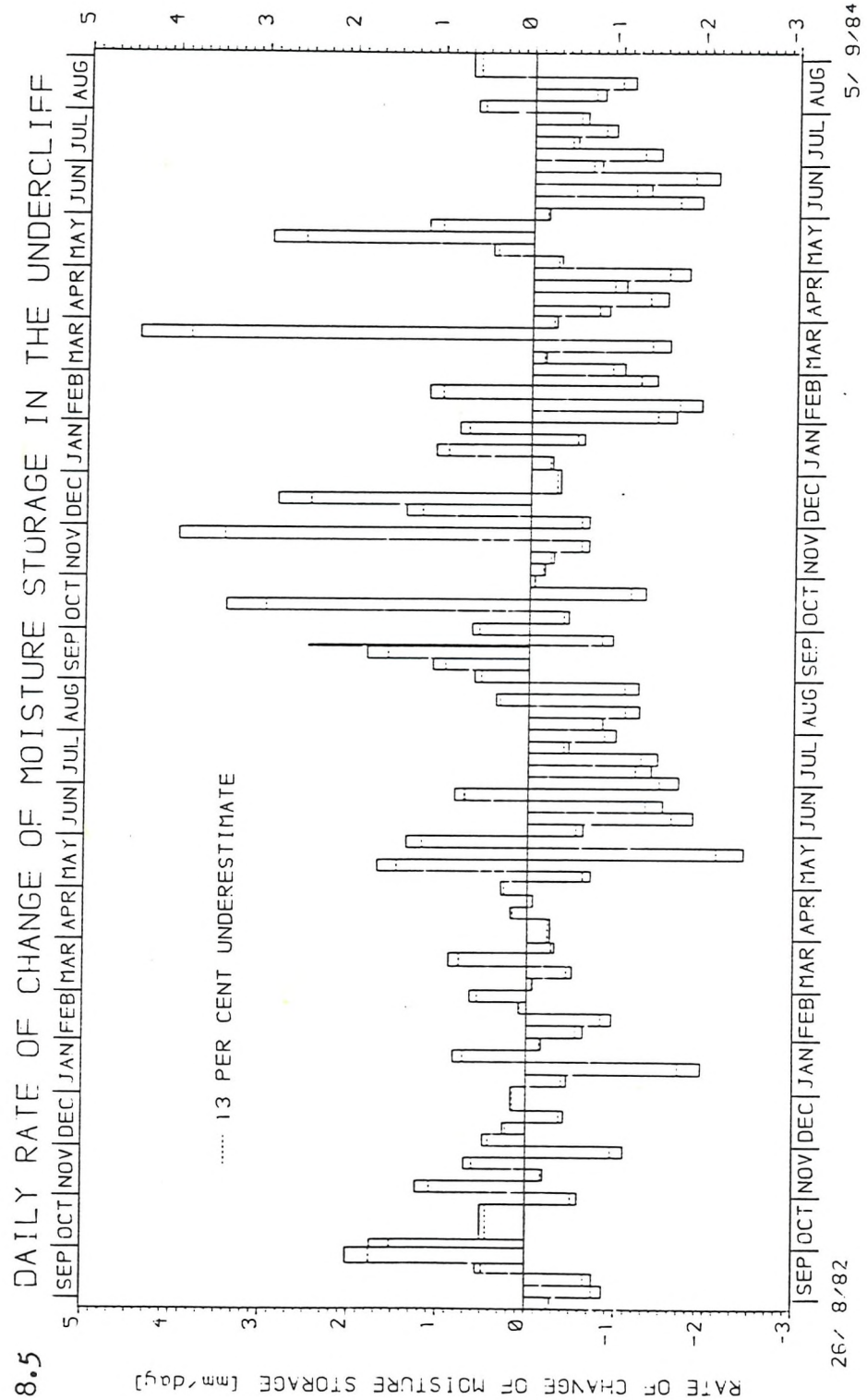
DAILY RATE OF CHANGE OF MOISTURE STURAGE IN THE UNDERCLIFF
SEP OCT NOV DEC JAN FEB MAR APR MAY JUN JUL AUG SEP OCT NOV DEC JAN FEB MAR APR MAY JUN JUL AUG
5 4 3 2 1 0 -1 -2 -3
13 PER CENT UNDERESTIMATE
RATE OF CHANGE OF MOISTURE STORAGE [mm/day]
26/ 8/82
5/ 9/84

Figure 8.5

CHAPTER 9

UNDERCLIFF COLLUVIAL DOMAIN

9.1 Introduction

A discussion of the hydrological role of the undercliff colluvial domain was given in chapter 4. The measurement of soil moisture in the colluvium was described in chapter 8. A number of piezometric measurements have been made in the colluvium. This chapter uses these measurements to discuss the seepage flow in the colluvium. The undercliff water balance is solved to estimate the groundwater flow out of the colluvium. The relationship between the hydrology and stability of the cliff is discussed. The effect of possible stabilization works on the water balance and stability of the cliff is considered.

9.2 Groundwater Level Observations

A number of piezometric observations have been made in the colluvium. Their locations are given in figure 9.1. Installation, borehole measurements, response tests, and water level observations are all given in detail in Thomson (1986b).

A variety of methods were used to install the piezometers. P94, P95 and P96 were drive-in piezometers. P202 and P203 were installed using a powered auger. The rest were installed by hand augering. At first, piezometers (those numbered up to P25) were installed in a small diameter auger hole. This provided a tight fit for the piezometer tubing such that no backfilling was necessary. Subsequent piezometers were installed in a large diameter auger hole. The piezometer tip was installed in a sand filter, and then backfilled with bentonite tablets and grout. This method was used to: (a) improve the piezometer response time; (b) gain a better knowledge of the colluvium into which the piezometer was installed; (c) install piezometers to greater depths.

The siting and depth of piezometers were severely restricted by the presence of gravel, either on the surface, or at depth. Soft clay (causing auger holes to close)was sometimes overcome using casing. There was a physical (human) limit to the depth which

could be achieved, especially when stiff clay was encountered. The maximum depth achieved by hand augering was 6.5 m. Drive-in piezometers were found to be unsuitable for the undercliff colluvium. The depth was limited by the stiffness of the clay. Also, the clay around the tip was probably compacted and smeared, which gave rise to unacceptably long response times (25 to 150 days). The maximum depth achieved using a powered auger was 8.5 m. However, the auger used a diamond drill bit which was highly susceptible to damage by gravel. Therefore, its possible use was extremely limited. Siting and life expectancy of piezometers was also limited by vandalism and undercliff movement. Piezometers in areas of rapid movement, or at the top or foot of scarps, were short lived. Differential movement (i.e. an upper mass of colluvium (e.g. a debris slide) moving more rapidly than the lower mass of colluvium) caused numerous failures, and, where it was recognised, limited the siting and depth of piezometers.

The most important, or informative, pore pressures in any slope stability study are those at the shear surfaces. Therefore, the aim of many of the piezometer installations was to try to obtain readings at, or as close as possible to, the basal shear surfaces. However, due to the difficulties described above, this was only possible in a few instances. These tended to be short lived due to rapid or differential movement. The presence of a shear surface is characterised by seepage (indicating increased permeability) followed by an increase in clay stiffness.

Piezometer response times are highly variable, both spatially and temporally. This is due to movement opening and closing tension cracks near the piezometer tip. Piezometers were installed at various times from December 1981 to September 1984. Their life varied from 1 day up to 32 months. Readings were taken weekly at the same time as the cliff top piezometers.

9.3 Temporal Variation of Groundwater Level

Figures 9.2 to 9.9 show the considerable variation of groundwater

level fluctuation that exists in the undercliff colluvium. The temporal variation of groundwater observations may be affected by piezometer time lag, meteorological variations, and landslide activity. The figures show pore pressure, movement, and rainfall data for each of the piezometers. P97 (figure 9.6), P202 (figure 9.8) and P203 (figure 9.9) were only surveyed once such that no movement data is possible. The survey data is from Thomson (1986a) The results for all the other piezometers are in Thomson (1986b).

Piezometer time lag was briefly discussed in section 6.3, paragraph 5, and is given in more detail in Thomson (1986b). The response of a piezometer is characterised by its basic time lag (Hvorslev, 1951). This is equivalent to the time taken for a 63 per cent recovery of piezometer water level during a slug, or bail, test. The time lag depends upon the soil permeability and the geometry of the piezometer intake area. These factors vary spatially. Therefore, the time lag varies between piezometers. The time lag may also vary temporally. This is due to: variation in soil permeability as a result of the opening and closing of cracks; disruption of the sand filter around the piezometer tip; and sedimentation and clogging of the piezometer. The first two are a result of undercliff movement. Ideally, the measured water levels should be adjusted for piezometer time lag (Thomson, 1986b). However, the necessary adjustment is small for the data presented here, and is therefore ignored (although values of basic time lag are included on the figures).

Figures 9.2 to 9.9 show that the observations of groundwater level in the undercliff are affected by both meteorological variations and landslide activity. To some extent, the influence of landslide activity has been reduced by plotting in terms of pore pressure at the tip. This is because pore pressure relates groundwater level to the moving piezometer tip and not to the static O.D. as the reference level.

P46 (figure 9.5) shows a large response to meteorological variations and is unaffected by landslide activity. It is situated on the F

bench (see figure 9.1) with the piezometer tip at the basal shear plane. The data shows no movement of the F bench at this location between April 1983 and September 1984. (P41 moved 1.9 m during the same period showing that other parts of the F bench were moving.) Other piezometers show that during this period the D bench moved during January 1984 (P31 and P32 moved 0.6 m; P33 and P45 moved 1 m). The lack of movement of the F bench shows the stability at this location of the cliff top against slumps based on the preferred bedding plane shear plane in the F zone. The movement on the D bench shows a reduction in lateral support and, therefore, also stability of the cliff top against slumps based on the preferred bedding plane shear plane in the D zone. P46 is at the location of the big slump H which occurred in October 1985 (see figure 6.3 and plates 1.10 and 1.11). It is believed that this slump failed due to a reduction in lateral support (see section 7.9.2, paragraphs 11 to 15).

P9 (figure 9.2) has been affected by considerable colluvial movement. The piezometer was initially at the top of a scarp within the colluvium (see figure 9.1). As the colluvium subsequently moved forward, scarp slump failures occurred. These caused the piezometer to move down the scarp. The entire piezometer must have been in a single slump block of colluvium moving down the scarp, as it was not sheared by differential movement. The block was part of a scarp slump failure which occurred in October 1982. The pore pressure subsequent to this date was relatively higher and more erratic. The change in the response to meteorological variations probably reflects a decrease in the basic time lag of the piezometer. This would have been due to movement causing tension cracks to open up around the tip. Unfortunately, this cannot be positively verified, as a response test was not carried out before October 1982. The figure shows a continuing upward trend of pore pressures throughout the period subsequent to October 1982. This reflects the piezometer's changing position relative to the scarp.Pore pressures at the foot of a scarp will be higher than at the top.

P35 and P44 (figures 9.3 and 9.4) show the pore pressure response at the same location but at different depths. The response to meteorological variations is much greater at the shallow depths. P35 was installed at a shear plane in the colluvium. Spatially, at any given time, there is a fall in groundwater level from the back of the bench to the front (see section 9.5). The pore pressures at both piezometers show a downward trend. This reflects the change in position of the piezometers relative to the D bench as a whole. The results of figures 9.2 to 9.4 show that the effect of movement on the observed pore pressure is complicated by both changes in local topography and the relative position in the undercliff.

P97 and P98 (figures 9.6 and 9.7) are examples of pore pressure readings in the A3 bench. The piezometer tips are both situated at the basal shear plane. The readings show the effect of movement along the A3 bench. The topography is not as variable as that of the D bench. Thus, the drop in pore pressure is due to the change in relative position along the A3 bench. This can also be seen by comparison of the two sets of readings and their positions. Figure 9.1 shows their initial positions. Although the readings are taken at different times, the initial pore pressure at P97 is slightly higher than at P98 due to it being 1.25 m further back in the A3 bench. The readings between October and December 1983 are higher at P97 as it is 4.25 m further back on the A3 bench.

P202 and P203 (figures 9.8 and 9.9) show gradually rising groundwater levels probably in response to meteorological variations. No movement data is available as the piezometers were surveyed only once. However, P203 was installed in the in situ Barton Clay (BC). Therefore, as soon as there was any undercliff movement, it failed (15th to 22nd November 1984). P202 was installed at the basal shear plane of the D bench. The reason why the piezometer tip of P203 is at a higher level than P202 is because it is situated on the F scarp (i.e. the back of the D bench).

Landslide activity affects both the local topography of a piezometer and its relative position in the undercliff. The results show that the interpretation of the temporal variation of piezometric readings can be considerably complicated by landslide activity. However, the results also show that the groundwater level can be significantly affected by meteorological variations. This suggests that, if the effect of landslide activity was removed, groundwater level could be modelled using the groundwater level prediction model described in chapter 5. This could prove useful in relating groundwater level to movement in the colluvium. This should be done for groundwater level records in relatively stable areas (e.g. P46), where the effect of landslide activity is minor in comparison to meteorological variations. This could be a topic of further research.

9.4 Spatial and Temporal Variation of Permeability

The permeability of the undercliff colluvium is highly variable. The presence of much Plateau Gravel (PG) derived material, together with numerous deep tension cracks, promotes areas of relatively high permeability.

The permeability varies temporally due to the effect of clay swelling and landslide activity. Active slope movements open new tension cracks and widen old ones. As movement slows down, the tension cracks close (due to the weight of the overburden) and fill with loose material. When the clay is dry it shrinks and cracks occur. This is most prevalent at the ground surface where it considerably affects rainfall infiltration. As the clay absorbs water, it swells, and the shrinkage cracks close. These effects are not in phase. Therefore, the temporal variation of permeability is complicated. The permeability near the ground surface is probably greatest in summer when clay shrinkage is most prevalent. The permeability at depth is probably greatest during active slope movement.

Measurements of permeability in the colluvium have been made using piezometer response tests. However, the piezometers are not a very representative sample. Most of the piezometers are in clay due to the difficulty of augering through gravel. The depth of augering was often limited by the clay stiffness. There are less tension cracks (and therefore lower permeability) where the clay is stiff. Also, the piezometer may not sample a large enough volume of soil to be representative of the effect of tension cracks (this would tend to underestimate the permeability of the colluvium). Permeability estimates were made using the analysis of Hvorslev (1951). (A few of the tests were also analysed using Gibson, 1963. The results were similar to the Hvorslev, 1951, method of analysis.) The assumption of a homogeneous, isotropic and incompressible soil will not be true. In some cases the compressibility of the soil may have lead to: smearing of the borehole by the auger; soft clay causing installation difficulties and clogging of the piezometer tip. This would have reduced the estimate of permeability. Thus, the estimates are, at best, a rough guide as to the spatial variation in permeability. These can be found in Thomson (1986b) to vary from 1×10^{-6} to 8.4×10^{-11} m/s. The higher value is for a piezometer installed in the top of a gravel seam. The lower value is for a drive-in piezometer, where it is believed compaction and smearing of the clay around the tip has occurred.

The temporal variation of permeability has not been measured. Hardly any of the piezometers had more than one response test. Also, piezometers tend to fail when significant tension cracks form around them.

9.5 Spatial Variation of Groundwater Levels

The spatial variation of groundwater level in the colluvium will be influenced by the position of its boundaries. The geology of the in situ BC affects the position of the basal shear surface

of the undercliff colluvium. Surface topography is influenced by the position of the basal shear surface and the history of landslide activity. Both of these vary parallel to the cliff edge. Therefore, the spatial variation of groundwater level is complicated, and will be different for different cross sections perpendicular to the cliff edge. It has not been possible to investigate this due to the paucity of groundwater level measurements. However, the cross section used for figures 9.10 and 9.11 is fairly representative of the study area.

The cross section includes part of the in situ material, as this influences, and helps determine, groundwater levels in the colluvium. There is relatively little local variation in topography perpendicular to the cross section (see figure 9.1). The surface topography is derived from a photogrammetric plot* produced from aerial photography taken in July 1982. The positions of the F and D shear surfaces are given by piezometers P46 and P202 respectively. The position of the A3 shear surface is calculated from its position at P97 and P98, and assuming the shear surface to dip $\frac{3}{4}^{o}$ ENE. The position of a back scarp of a shear surface is generally not known, except at P203. It has otherwise been estimated.

The piezometers on the F and D benches lie along the cross section. However, those on the cliff top and the A3 bench are at some distance from the cross section. There is relatively little variation in topography from their true position to the line of the cross section. Therefore, the error in using them is not considered to be significant. The position of those on the A3 bench has been determined by their distance from the exposure of the A3 shear surface. The position of those on the cliff top has been determined by their distance from the cliff edge. The piezometer positions are from surveys on 27th October 1983 for P97 and P98; 9th February 1984 for P31, P32,

*Produced by Cartographical Services (Southampton) Limited , Landford Manor, Salisbury, Wilts.

P33 and P46; and 5th October 1984 for P202 and P203. There will be some difference in the surface topography between these dates and July 1982. This can be seen by the discrepancies in the position of the ground levels at P33 and P203. Also, the pond level dropped from 17.1 m O.D. in July 1982, when it was relatively dry, to 16.8 m O.D. on 1st February 1984 when it was very wet. This is due to a fall in the elevation of the ground surface of the D bench.

Figures 9.10 and 9.11 show the estimated equipotentials for the 1st February 1984 and 12th September 1984 respectively. Because it was not possible to take readings at all the locations on these dates, some estimation has been made. The estimation of high and low groundwater levels at P97 and P98 is somewhat difficult. The readings are both complicated and limited by movement of the A3 bench. Between late October and late November 1983, they are both fairly static, with no indication of whether they are high or low. Elsewhere, at the same time, groundwater levels were either fairly low (e.g. figures 6.23 to 6.26 and 9.4), intermediate (e.g. figures 9.2 and 9.3), or fairly high (e.g. figure 9.5). Without further information, it was decided to use the readings for the 27th October 1983 for both figures 9.10 and 9.11. It is probable that the groundwater levels on the 1st February 1984 were higher than that indicated. This would steepen the equipotentials, and hence reduce stability, both due to adverse pore pressure and hydraulic gradient. P33 was dry on 12th September 1984. The data is insufficient to accurately extrapolate the recession curve. The data was, however, sufficient to extrapolate the recession curves for P46 (by 7 weeks) and P32 (by 7 days), so as to estimate the 12th September 1984 groundwater levels. The observed groundwater level at P31 varied only slightly between May 1983 and January 1984. Therefore, the average recorded groundwater level was used to estimate both groundwater levels. The groundwater levels at P202 and P203 are the maximum and minimum of the groundwater level records (see figures 9.8 and 9.9). The groundwater level at P101 on 1st

February 1984 is as assumed in figure 7.8 (see section 7.5, paragraph 1).

Figures 9.10 and 9.11 show that groundwater level falls both with depth and towards the cliff toe. Linear interpolation of groundwater levels between piezometers has been used. This may lead to some error in the estimation of groundwater levels other than at piezometer locations. This is because of the paucity of groundwater level measurements and the highly variable hydraulic gradients. However, it does provide a rough indication of the spatial variation of groundwater levels.

The groundwater table was estimated using a number of assumptions. These are:

i) it is given by the water levels in piezometers P61, P46 and P32 on both dates; by P33 on 1st February 1984; and by P97 and P98 on 12th September 1984;

ii) it is coincident with the pond level on both dates;

iii) it is coincident with ground level on the D scarp on both dates; and the unconformity at the cliff face, the F scarp, and the A3 bench on 1st February 1984;

iv) it can be estimated by straight lines between points estimated by i to iii above;

v) it is coincident with ground level where iv would cause it to be above ground level.

Figures 9.10 and 9.11 show the large temporal variation in the groundwater table level, and the influence of the surface topography. The surface topography limits the height of the groundwater table, which affects the distribution of groundwater levels.

Groundwater flow in the colluvium is mainly along shear surfaces,

tension cracks, and gravel seams. Groundwater flow in the clay matrix itself will be negligible. This will affect the fluctuation and, therefore, distribution of groundwater levels within the colluvium. When the groundwater table level is high, the groundwater levels in the tension cracks will be higher than in the clay matrix. This will cause a small flow of water into the clay matrix. Conversely, when the groundwater table level is low, the groundwater levels in the tension cracks will be lower than in the clay matrix. This will cause a small flow of water out of the clay matrix. Thus, the variation in groundwater level in the clay matrix is much smaller than that in the tension cracks. The size of the variation depends upon the distance from nearby tension cracks. This will lead to a spatial distribution of groundwater levels which is much more complicated than that shown in figures 9.10 and 9.11.

The effect of a variation in response between tension cracks and the clay matrix, is in contrast to the reduction in pore pressures due to unloading of the clay. If this were the case, the slow equilibration of pore pressures would mean that the groundwater level in the clay matrix, would be lower than that in the surrounding tension cracks, at all groundwater table levels.

Bromhead and Dixon (1984) found a sharp reduction in pore pressure across the shear surface of a deep rotational landslide at the Isle of Sheppey. This was due to the slow equilibration of pore pressures, in the in situ London Clay, following a reduction of loading. The higher pore pressures in the colluvium were thought to be cliff top pressures "carried down" by the landslides. Unfortunately, there is little evidence with which to investigate any similar phenomenon occurring at Naish Farm. However, the evidence of P203 appears to suggest that it does not occur, and that pore pressures in the in situ BC under the colluvium have equilibrated.

There is insufficient information to give a true indication of the complicated spatial variation of groundwater levels in the colluvium. However, when considering the groundwater flow and stability of

the colluvium, the groundwater levels of interest are those in the tension cracks and at the shear surface. Ideally, figures 9.10 and 9.11 should at least reflect the spatial variation in these groundwater levels. This may be doubtful due to the assumption of a linear variation of groundwater level between only a few measurements. Also, some measurements may not be in tension cracks, gravel seams, or at shear surface. P31 has a basic time lag of 7 days and hardly any temporal variation in groundwater level. This suggests that it is not near a tension crack. If this is the case, then the use of P31 causes the groundwater levels in the surrounding tension cracks to be underestimated at high groundwater table levels, and overestimated at low groundwater table levels. Thus, the equipotentials near the front of the D bench would be steeper and flatter than those shown in figures 9.10 and 9.11 respectively. This would cause the slope of the equipotentials in both figures to be more or less the same. This suggests that (during the observation period) the groundwater level at P31 is in equilibrium with the fluctuation in groundwater levels in the surrounding tension cracks, and not in the process of equilibrating due to the unloading of the clay.

Apart from P31, the groundwater level measurements are believed to be in tension cracks, gravel seams, or at a shear surface. The use of P31, and the assumption of a linear variation in groundwater levels, limits the accuracy, but figures 9.10 and 9.11 are still considered to be a useful guide as to the spatial variation of groundwater levels.

9.6 Groundwater Flow in the Colluvium

Groundwater flow is influenced by permeability (section 9.4) and hydraulic gradient (spatial rate of change of groundwater level (section 9.5)). Groundwater flow occurs predominantly where the permeability is greatest. In the colluvium, this is along tension cracks, shear surfaces, and gravel seams. Figures 9.10

and 9.11 show that it is both toward the sea and the basal shear surface. Groundwater flow at the basal shear surface is either lateral toward its exposure or into the in situ BC. The flow into the BC either percolates down to the Bracklesham Beds or toward the back of a lower colluvial bench. The permeability of the in situ BC is likely to increase toward the front of the bench due to stress relief. This will cause an increase in groundwater flow into the BC. This is similar to what was found to occur at the PG/BC unconformity. Likewise, it is probable that the percolation rapidly finds its way to the lower bench via permeable layers (e.g. fossil lenses) and joints which have widened due to stress relief.

9.7 Water Balance for the Colluvium

The area of the undercliff to which the water balance has been applied is shown in figure 9.1. The cliff face boundary is the same as the one used in section 6.6 to calculate PG drainage. The cliff toe boundary is taken to be the 1.5 m contour which coincides with the A3 scarp. The two other boundaries are continuations of two of the boundaries used to calculate PG drainage (see figure 6.1). These boundaries have been defined such that they are parallel to the line through the cliff top piezometers P61 and P64, and that they pass through the positions of access tubes AT6 and AT21 (see figure 8.1).

The components of the water balance were described in chapter 4. A number of assumptions have been made to solve the water balance. These are:

i) There is no flow across the boundaries parallel to the line through P61 and P64 in either of the undercliff, PG, or BC domains.

ii) Rainfall is spatially constant, both on the undercliff and on the cliff top, and is equal to that measured at the Naish Farm weather station (see figure 3.2 and section 3.4.1.2).

iii) The PE in the undercliff from vegetation, bare ground, and ponds is equal to that on the cliff top from short grass, bare ground, and open water respectively (see section 3.4.1.1).

iv) The actual evaporation can be estimated by the same method as used in section 5.2.1. This uses a relevant value of PE, a direct effective rainfall component, and the SMD model given in figure 5.1.

v) The access tube network (see chapter 8) is representative of the colluvium, such that figure 8.5 gives the change in moisture storage in the undercliff catchment area of figure 9.1.

vi) The change in moisture storage due to the net gain or loss of colluvium is negligible.

vii) Sea spray and waves can be neglected.

viii) When the groundwater table is below the PG/BC unconformity and in the BC, it can be treated, for storage calculations, as though it were in the PG.

ix) The change in storage in the BC domain is negligible.

x) The groundwater seepage out of the PG domain is as described in section 6.6 and given by figure 6.37.

xi) The groundwater flow across the inland boundary of the BC domain is negligible (see section 7.8, paragraph 2).

xii) The amount of PG drainage contributing to percolation to the Bracklesham Beds is constant, and equal to 0.84 m^3/day (see section 7.8, paragraph 4).

Using the above assumptions the water balance equation is given by:

$$Q = R + P - AE - \Delta S \qquad (9.1)$$

where R is the rainfall falling on the undercliff; P is the combined groundwater seepage to the undercliff from the PG and BC; AE is the actual evaporation from the undercliff; ΔS is the change (positive for an increase) in the water stored in the undercliff colluvium; Q is the combined surface and groundwater outflow from the undercliff colluvium.

R is calculated using assumption ii. P is calculated using assumptions i and viii to xii. The calculation of PG drainage (assumption x) uses assumption viii and can be split into two components: cliff face seepage, which is an immediate input to the undercliff; and leakage to the BC. From assumption ix, the leakage entering the BC must immediately displace an equal volume of water out of it. The amount displaced to the Bracklesham Beds is given by assumption xii. From assumption xi, the rest of the leakage is displaced to the undercliff. Thus, all the PG drainage, less 0.84 m^3/day, immediately reaches the undercliff. From assumption i, it must reach the catchment area used for the undercliff water balance.

The actual evaporation is calculated using assumptions iii and iv. The evaporation is calculated separately for vegetation, bare ground and ponds, and then summed to give the total evaporation from the undercliff catchment area. The areas of vegetation, bare ground, and ponds, as a proportion of the catchment area, are given in table 9.1. Also given are the values of the initial SMD and the parameters A, C and D. The cliff face seepage is assumed to bypass the surface soil moisture store, such that the rainfall is the only input affecting the calculation of SMD. Runoff is taken to be zero.

The change in moisture storage in the colluvium is calculated

using assumptions v and vi. The downward trend in figure 8.4 is considered to be due to the net loss of colluvium from the undercliff. However, the effect is complicated (see section 8.11), such that the loss of moisture due to the loss of colluvium may not be entirely passed on to figure 8.4. From assumption vi, the resulting error will not be great. The trend (and hence, loss of colluvium) does not significantly affect the soil moisture change over short periods (see section 8.8).

The outflow from the undercliff may be either: surface flow from the A3 bench to the beach; groundwater seepage out of the A3 scarp and onto the beach; or groundwater flow to the BC which does not return to the colluvium. The latter either percolates to the sea, or down to the Bracklesham Beds.

Equation 9.1 has been solved for the period from 26th August 1982 to 5th September 1984 over irregular intervals of approximately 7 days. These factors were determined by the length of the moisture storage data, and the intervals at which it was collected. Also, a time step of 7 days (instead of 1 day) reduces errors in the distributions of PE (see section 3.4.2.2, paragraph 11) and PG drainage (see section 6.6.4, paragraph 10). Actual evaporation was calculated daily, using weekly values of PE. Daily values of rainfall, actual evaporation, and PG drainage were summed and averaged over the length of the water balance time step.

The results are given in figure 9.12. The peak outflows for each winter are in December 1982 (165 m^3/day) and in January 1984 (140.5 m^3/day). These are average values for 7 day periods. The peak outflow over shorter periods, say 1 day, will be greater. Negative values of outflow are not possible. Therefore, the three slight negative values of outflow are due to errors in the other water balance components. Both bias and random errors could exist in all the estimated values of outflow. They can either be determined by direct measurement, or by consideration of the possible errors in the other water balance components.

It has not been possible to measure the outflow independently. A structure to measure the surface and groundwater flows from the A3 bench would be fraught with difficulties (see plate 1.8):

i) Outflow crosses the entire length of the cliff toe. It would be necessary to intercept and measure all of this outflow.

ii) Movement of the colluvium causes the calibration of the structure to continually shift (i.e. there would be calibration difficulties) and its life to be short.

iii) For much of the winter, most of the A3 bench is not trafficable. This would limit the ability to read, calibrate and maintain the structure.

iv) During the summer, when the structure might survive the conditions of the undercliff, it would be vandalised.

Errors in the estimation of the change in water storage were discussed in section 8.8. The random counting error was insignificant. The uncertainty in the slope of the neutron probe calibration (see section 8.5.2.3) leads to a bias standard error of $\pm$ 13 per cent in the rate of change of water storage in the undercliff. The water storage change in figure 9.12 varies from -25 to +44 m^3/day, for which the bias error varies from + 3.2 to -5.7 m^3/day (for a -13 per cent error in the slope). This is not very significant to the calculation of outflow. There may be some error in assuming that the access tube network is representative of the undercliff. Some estimation could be made by examining the spatial variation of the measured water storage changes. A large variation and a small number of access tubes, would give a large possible error in the estimation of the true water storage change in the undercliff catchment area. This assumes that the network is random. Unfortunately, due to the difficulty of installing access tubes in some areas, and the short life expectancy in others, it was not possible to install a truely random network. Thus, there are unknown

errors in estimating the true water storage change in the catchment area due to the size and randomness of the access tube network. In figure 9.13 it is arbitrarily assumed that the true change in water storage is 50 per cent of that used in figure 9.12. This leads to a slight redistribution of computed outflow. The effect on peak outflows is negligible. The peaks are increased by 0.5 m^3/day in December 1982 and 4.5 m^3/day in January 1984.

The error in the estimation of PG drainage was discussed in section 6.6.4. Errors in the distribution of drainage are likely to be present, due to the method of estimation, and to the representativeness of the four modelled piezometers. These errors are reduced by using PG drainage values totalled over longer periods (i.e. 7 days). Significant errors can occur due to the method of estimating the rainfall and the catchment area. It is likely that these errors will cancel. However, as an extreme case, figure 9.14 examines the effect of assuming the estimation of the cliff top catchment area to be correct, and the true rainfall to be 10 per cent more than that measured (see section 3.4). The error in rainfall measurement also affects the estimation of rainfall on the undercliff. The increased rainfall and PG drainage reaching the undercliff significantly increases most values of outflow. The peak outflows in December 1982 and January 1984 were both increased by 20 m^3/day.

Error in the estimation of actual evaporation may be due to: the estimation of PE; the model used and its parameter values; and the estimated proportional areas of ponds, vegetation and bare ground. The estimation of PE may be in error (see section 3.4) due to the method of its computation, and the assumption that it is the same on the undercliff as on the cliff top. A 10 per cent reduction in the value of PE made no significant difference to the computed values of outflow. This is especially so for the peak values which occur in winter when the value of PE is least. The calculation of actual evaporation from PE involves the use of a number of parameters. Each of these parameters was changed in

turn (initial SMD halved; A doubled; C reduced by 40 per cent; D reduced by 20 per cent; the value of the ratio AE/PE when SMD is greater than C was halved), but was found to only slightly affect summer values of outflow. The peak winter values were unaffected. Changing the structure of the model used to calculate actual evaporation, would similarly only affect summer values of outflow. Changing the areal proportion of ponds, vegetation, and bare ground will have an effect similar to a mixture of the above changes. Therefore, the effect of an error in these areal proportions is not significant.

There will be a small error in the estimation of the catchment area using a planimeter (repeated measurements suggest the estimate to be within 3 per cent of the true value). The estimation was based on aerial photographs taken in July 1982. The area will vary during the period of the water balance due to cliff top and A3 scarp failures. The areas involved are not large (for the cliff top, it is the area of slumps A and B and a small part of slump C in figure 6.3) and they will cancel each other out. Under-estimation of the area will underestimate the rainfall, actual evaporation, and water storage change. The error in rainfall will be offset by the errors in actual evaporation and water storage change when applying the water balance. Therefore, the error in the computed outflow is unlikely to be significant. Figure 9.15 applies the water balance to only the F and D benches (defined as all the undercliff above 9.5 m O.D.). This is an extreme example, and represents a reduction in undercliff catchment area of 20.5 per cent. Most of the outflows have been slightly reduced. The peak outflows in December 1982 and January 1984 have been reduced by 15 and 8 m^3/day respectively.

Errors in the estimation of outflow are considered to be mainly due to the methods of estimating rainfall and PG drainage reaching the undercliff. Errors in the distribution of PG drainage have been reduced by using a 7 day time step. Errors in the totals of PG drainage are due to errors in the estimations of rainfall and the cliff top catchment area. Errors in the estimation of the under-

cliff catchment area, water storage change, and actual evaporation are not considered to cause a significant error in the computed outflow.

9.8 Relationship between the Hydrology and Stability of the Undercliff

The stability of the undercliff colluvium is influenced, to varying extents, by a number of factors. These factors, and, therefore, also stability, vary temporally. They are:

i) Meteorological variations causing changes in groundwater levels and the weight of the colluvium.

ii) Variation of the distribution of loading due to failure of the in situ material and the movement of colluvium along the undercliff to the sea.

iii) Soil strength and pore pressure variations due to clay swelling, or consolidating, as a result of past unloading, or loading.

iv) Removal of colluvial material by the sea.

Rainfall runs off the clay surfaces of the undercliff and either collects in ponds, or infiltrates via gravel, tension cracks, or shrinkage cracks at the ground surface. This causes the weight acting on the basal shear surface to increase. However, this only has a minor effect on stability (Carson, 1976).

Groundwater flow in the colluvium is mainly through the numerous permeable tension cracks, shear surfaces, and gravel seams. Some of this reaches the basal shear surface and therefore affects groundwater levels (i.e. pore pressures). As groundwater levels rise, stability decreases due to both increased pore pressures and

hydraulic gradient along the basal shear surface (compare figures 9.10 and 9.11). The stability decreases until eventually the colluvium starts sliding along the basal shear surface. If groundwater levels rise still further, the out of balance force causing movement increases. This accelerates the movement (Newton's 2nd Law of Motion). As groundwater levels fall again, the out of balance force decreases to zero, and the rate of movement becomes constant (Newton's 1st Law of Motion). At even lower groundwater levels, the out of balance force resists movement, such that the rate decelerates until it reaches zero.

This is very much a simplistic view, and the true dynamics of the colluvial movement will be more complex. Firstly, the soil strength may be a function of the rate of movement. Secondly, the movement of colluvium redistributes the loading on the basal shear surface such that stability (of the colluvium) is increased. Thirdly, movement opens new tension cracks and widens old ones. This increases permeability, and therefore drainage of the colluvium, which lowers the groundwater level. This effect will vary with the rate of movement. Fourthly, failure of the in situ material at scarp faces adversely affects the distribution of loading and decreases stability of the colluvium.

Movement of the colluvium along a bench increases its stability by decreasing the load at the back of the bench. However, this also decreases the lateral support for the in situ material behind the back scarp of the bench. This decreases the stability of the in situ material until eventually a failure occurs. Failure of an in situ scarp increases the loading at the back of the bench, and thereby decreases the stability of the colluvium. Scarp failure also decreases the lateral support, and therefore also the stability, of the colluvium on the higher bench.

In situ failure, and movement of the colluvium, occurs in order to improve the overall stability of the cliff. The overall slope angle is reduced, i.e. there is a redistribution of loading, by removal of material at the top of the slope and accumulation

lower down. The cliff slope would eventually stabilize itself, and movement stop, if it were not for the removal of colluvial material by the sea.

Brunsden and Jones (1976) describe two dominant mechanisms occurring in the Fairy Dell cliffs of Dorset. These are rotational landsliding (i.e. slumping) and block disruption, which are also in evidence at Naish Farm. Block disruption is the breakup of originally large landslide units as they move downslope and over time. The loss of structure is accompanied by a decrease in bulk density and an increase in moisture content. This leads to a reduction in shear strength and resistance to movement of the colluvium. By the time it reaches the cliff toe the colluvium is far more readily removed by the sea than is the in situ material.

Movement of the colluvium causes a temporal variation of loading. A change in load is immediately taken up by the pore water. There is thus a sudden change in pore water pressure. Subsequently, the clay matrix gradually takes the load by either swelling, or consolidating, depending on whether the load has decreased, or increased. This causes the soil strength and pore water pressure to gradually change. The time taken for the swelling, or consolidation, to stop, i.e. for pore pressures to equilibrate, depends on the coefficient of swelling, or consolidation, and the boundary conditions. Because of the high permeability (giving a high value of the coefficient of swelling or consolidation) of the tension cracks and shear surfaces, the equilibration of pore pressures at the basal shear surface is considered to be immediate. This may not be the case for the rest of the colluvium (i.e. the clay matrix). However, it is probable that the boundary conditions (i.e. drainage distance to a nearby tension crack) are such that the time taken for the equilibration of pore pressures in the clay matrix is not long.

An example of a temporal change in loading is a failure of the in situ material. This causes an increase in loading at the back of the bench in front. Apart from adversely affecting the

distribution of loading, this also affects pore pressures. The increased load is immediately taken up by an increase in pore pressure. The increased hydraulic gradient and high permeability of the tension cracks causes water to rapidly flow from the area of increased loading. This allows the tension cracks to narrow, such that the colluvial soil takes up the load and the pore pressure falls. The excess water flowing from the area of increased loading is accommodated by a rise in the groundwater table level. The equilibrium pore pressure value is rapidly reached, although the higher groundwater table level indicates that it may well be higher than the value before loading. Thus, a failure of the in situ material reduces the stability of the colluvium by adversely affecting the pore pressure and distribution of loading. This explains why, after such failures, a large increase in colluvial movement is observed. This increased rate decreases (probably exponentially) with time as redistribution of the load increases stability.

A similar effect to the above, occurs when colluvium moves from an upper bench to a lower bench. This has also been described by Bromhead (1979) as a contributing cause to the occurrence of mud slides. Adverse conditions of loading and groundwater conditions will be localised and extreme for mud slides, whereas they will be more uniform (along the cliff line) for bench sliding.

Previous research has sought to correlate rainfall with landslide activity. Examples are Bertini et al (1984a, b) and Canuti et al (1984,1985) in Italy; Lumb (1975) and Brand et al (1984) in Hong Kong; Guidicini and Iwasa (1977) in Brazil; Campbell (1974) in California; and Sidle and Swanston (1982) in Alaska. Various measures of rainfall were used. These included the rainfall totals of both several hours and several days before failure. Campbell (1974) comments that shallow failures occur during, and only during, heavy rainfall, whereas deep failures depend on deep percolation of groundwater and may not respond to the effects of heavy rainfall until some time after a storm. It is therefore

probable that shallow failures depend almost on the rainfall intensity, whereas deeper failures are dependent on the effects of rainfall over several days or even weeks. For shallow failures in Hong Kong, Premchitt et al (1986) note that groundwater response to rainfall is far too rapid for rainfall infiltration to be transmitted via pore water. They therefore suggested that natural voids (soil pipes) in the soil were being used as preferred drainage paths (cf the tension cracks and shear surfaces at Naish Farm). Bertini et al (1984a,b), Canuti et al (1984) and Sidle and Swanston (1982) also correlated groundwater levels with the onset of movement.

Correlations of rainfall and pore pressure with landslide activity have not been attempted here, due to the complicating effect of the other factors discussed in this section. These other factors would have to be included in any relationship (or model) describing the rate of movement of undercliff colluvium. The development of such a model would need to make use of data in Thomson (1986b) and Coles (1983). This could be a topic of further research.

9.9 The Effect of Possible Stabilization Works on the Hydrology and Stability of the Undercliff

The first step in the stabilization of a coastal cliff is the halting of marine erosion. This generally constitutes the construction of a barrier across the toe of a slope. Without further protection the cliff slope would continue to fail until it reached a stable overall slope angle. This could cause damage to the toe protection and involve a considerable loss of land on the cliff top. Therefore, it is often desirable to also undertake slope stabilization works. This usually involves modification of the slope profile and drainage. A detailed description of these, and other methods of slope stabilization, is given in Hutchinson (1977, 1983).

Modification of the slope profile by excavation and filling causes a redistribution of the load. Hutchinson (1977, 1983) suggests

using the influence line concept (from structural engineering) to analyse the optimum positioning of cuts and fills. Excavation upslope or filling downslope of the influence line will increase stability. However, care should be taken to determine the influence lines for all possible types of failure. Increasing the stability against one type of failure may decrease the stability against another. For example, the stability of the colluvium on the D bench could be increased by excavation at the back or filling at the front of the bench. However, this would decrease the stability against in situ failure of the F or D scarps respectively. Similarly, shallow failures within the colluvium may be promoted by ill considered positioning of cuts and fills. Thus, it is important to recognise the different modes of failure and their occurrence in the cliff slope.

The purpose of drainage is to reduce pore pressures at the potential or existing failure surfaces, whether they be within the in situ material, at the basal shear surface, or a shear surface within the colluvium. This may be done either by leading water away from the shear surface, or by intercepting it before it reaches the shear surface. The former is more effective in controlling pore pressures at the shear surface. However, it will be increasingly more expensive for deeper shear surfaces. For deep failure surfaces, it may be more effective and economic to modify the slope profile. This is in evidence from the controlling factors for in situ failure (see section 7.9.2). It is believed that the loss of lateral support is the major influence, especially for deep failures based on the preferred bedding plane shear surface in the D zone. Thus, it would probably be more effective, and economic, to use cut and fill to improve the stability against this type of failure.

To maintain stability against in situ failure, the colluvium must be stabilized. Movement along the basal shear surface is seasonal (Barton and Coles, 1983), and is mainly in the winter when ground-water levels are high. (Figures 9.5 to 9.8 show that the pore pressures at the basal shear surfaces of the F and D benches respond to meteorological variations, whereas for the A3 bench they are too

complicated by landslide activity to determine any similar response.) However, it has also been observed to be affected by a change in the spatial distribution of loading (section 9.8). Therefore, stability should be improved by a combination of cut and fill and drainage measures. Shallower shear surfaces are even more responsive to meteorological variations and drainage would greatly improve their stability. Even though shallow failures do not constitute the major portion of the total colluvial movement (Barton and Coles, 1984, give it as 10 per cent), it is important to stabilize them, otherwise the redistribution of loading could lead to instability of the basal shear surface or the in situ material.

Drainage of shallow shear surfaces would lower the groundwater table, which in turn would lower pore pressures at the basal shear surface (compare figures 9.10 and 9.11). This is an example of intercepting water before it reaches the (basal) shear surface. Other methods of interception are:

i) To lead away surface water in ponds and tension cracks.

ii) To increase evaporation by the establishment of vegetation.

iii) To intercept surface and groundwater on the cliff top before it reaches the undercliff (Barton and Thomson, 1986c).

Vegetation also helps to control surface erosion by breaking the fall of raindrops, increasing infiltration, and reducing the speed of overland flow (by increasing surface roughness).

The study area is part of an unprotected 1.4 km length of cliff line in the BC. The landsliding within this unprotected length changes due to the dip of the bedding. This will affect the design of a protection scheme. This is in evidence by comparison of the two schemes on either side of the unprotected length.

To the west (Highcliffe), a 5 to 6 m thick deposit of PG rests unconformably on the BC. To the east, the PG rests on Barton Sand. The Barton Sand outcrops about 170 m east of the study area. The dip of the beds causes the bottom of the Barton Sand to be about 15 m below ground level at the eastern edge of the unprotected length of cliff line. The depth is even greater further to the east where the Barton-on-Sea protection works are situated. Both the Barton Sand and PG provide permeable horizons which allow large flows of water to reach the undercliff. The scheme at Highcliffe prevented groundwater flow in the PG from reaching the undercliff by using a diaphragm wall and counterfort drains (Halcrow, 1971, and Mockridge, 1983). The wall was constructed on the cliff top and caused the groundwater to dam up behind it. The water was channelled straight down the cliff slope to the sea via counterfort drains. At Barton-on-Sea the Barton Sand is too deep for a similar scheme to be economic. Because of its depth, the groundwater table in in the Barton Sand is in intimate contact with the groundwater table in the colluvium. Therefore, the cut off was installed in the undercliff colluvium, where the depth to the groundwater table was considerably less than on the cliff top. This consisted of a deep drainage trench (not used at Highcliffe) with a diaphragm installed down into the in situ BC. Counterfort drains led the water to the sea. This reduced the groundwater table level throughout the colluvium.

A drainage scheme for the unprotected length of cliff line would similarly need to intercept groundwater flow from inland. The scheme would probably be a combination of the methods used at Highcliffe and Barton-on-Sea, the former being used in the east, and the latter in the west part of the unprotected cliff. The study area is in the east, and therefore, the design of the cut off would probably be similar to that at Highcliffe. Figure 9.16 shows the effect on the water balance for the study area, of a cliff top cut off drain whose installation is similar to the one at Highcliffe. It is assumed that the amount of leakage reaching the undercliff is the same as that without the cut off drain. (Due to the damming effect of a diaphragm wall, the leakage would in fact increase

slightly, although it is unlikely to do so by a significant amount (see section 7.7).) The effect on the undercliff water balance is considerable. The size and timing of the peak outflows have been affected. The peak outflow in the first winter is two months earlier and 78.5 m^3/day less than without a cut off drain. The peak outflow in the second winter is a week earlier and 68 m^3/day less than without a cut off drain. The groundwater flow to the undercliff to the east of the study area will be much larger due to the increase in catchment area (see figure 4.2). Thus, a cut off drain along the entire length of unprotected cliffs would intercept a large amount of water and have a considerable effect on the water balance of the undercliff.

Figure 9.16 shows that even with a cut off drain there is still a considerable amount of outflow from the undercliff. This is derived from direct rainfall onto the undercliff which needs to be collected and channelled to the sea via drainage within the undercliff colluvium. In both the Highcliffe and Barton-on-Sea schemes, this includes drains to collect both the surface and groundwater flows. The latter includes both the deep counterfort drains and shallower drains. The Highcliffe scheme was also designed to intercept water seeping out of the sand beds in the in situ A3 zone. In section 7.8 it was considered that, inland, the seepage in this zone is small, due to the unexpectedly low permeability (for sand). However, nearer to the undercliff, stress relief is likely to greatly increase permeability, such that the flow may be considerable. Stress relief also increases the permeability of other zones of the BC near the D scarp. Therefore, the major source of the groundwater flow out of the A3 zone is considered to be from the D bench, and not from inland. In the Highcliffe scheme, it was found to be difficult to locate and follow the A3 zone sand beds. It would probably be easier, and just as effective, to intercept the groundwater flow in the D bench colluvium before it could seep down to the A3 zone.

The rapid interception and channelling away of the surface and groundwater flows will reduce pore pressures at the shear surfaces.

This, together with modification of the slope profile, should suitably increase the stability of the cliff slope against all types of failure. However, this will be useless unless the toe of the cliff is adequately protected against erosion by the sea.

9.10 Summary

A number of piezometers were installed in the colluvium. Various methods were tried in order to achieve greater depth, and to decrease the piezometer time lag. These met with variable success, and problems were encountered with soft clay and gravel. The observation period of a piezometer was limited by differential movement and vandalism.

The temporal variation of the groundwater observations was spatially variable, and was affected by the piezometer time lag, meteorological variations, and landslide activity. The piezometer time lag was influenced by the method of installation, and the presence of tension cracks, shear surfaces, or gravel seams near the piezometer tip. This is affected by movement. Therefore, the time lag varies temporally. The time lag was used to estimate permeability. It was found to be highly variable spatially, and is also considered to vary temporally. The response to meteorological variations increases near tension cracks, shear surfaces, and gravel seams and decreases with depth. Piezometer observations are affected by landslide activity due to changes in both the local topography of the piezometer and its relative position in the undercliff.

From the groundwater observations the direction of groundwater flow is both vertical and horizontal toward the sea. At the basal shear surface, groundwater flows out of the colluvium and into the in situ BC. The amount is considered to increase rapidly toward the front of a bench due to stress relief, and to seep to the lower bench via permeable layers (e.g. fossil lenses) and joints widened by the stress relief.

The water balance for the undercliff was solved in order to estimate the combined surface and groundwater outflow from the colluvium. The change in soil moisture storage was calculated over intervals of approximately 7 days. The variation between successive 7 day intervals was large. Therefore, the daily variation is likely to be even larger. Thus, the water balance was solved over the same intervals as the change in soil moisture storage. The 7 day interval also reduces distribution errors in PE and PG drainage. The largest source of possible error in the water balance was considered to be due to the estimation of rainfall. This probably leads to an underestimation of the outflow. To stabilize the cliffs, it would be necessary to intercept and convey this outflow off the undercliff before it adversely affected groundwater levels. It would be necessary to both intercept the large amount of groundwater flow from the inland catchment area, and to drain the colluvium itself. The effect of intercepting the groundwater flow from the inland catchment area has been estimated using the water balance (see figure 9.16). The effect was found to be considerable, and shows the necessity of a suitable cut off drain (in any possible future design of stabilization works) in order to effectively drain the undercliff.

The stability of the undercliff colluvium is influenced by meteorological variations causing changes in pore pressures at the shear surfaces, and by variation of the distribution of loading due to failure of the in situ material and movement of the colluvium. The effect of the sea is to remove lateral support at the cliff toe. This decreases the stability of the colluvium. The first step in the stabilization of a coastal cliff is to halt marine erosion. The cliff slope is then stabilized by a combination of drainage and modification of the slope profile. The former reduces pore pressures at shear surfaces, and the latter optimises the distribution of loading. The relative importance of each depends upon the type of failure. Care should be taken in modifying the slope profile, as improving stability against one type of failure may decrease the stability against another.

Table 9.1 Parameter Values used in the Undercliff Water Balance

Parameter	Bare Ground	Pond	Vegetation
Area[1](%)	73	7	20
Area[2](%)	66	9	25
A	0.3	0.3	0.3
C(mm)	25	∞	65
D(mm)	40	∞	100
Initial SMD (mm)	25	0	65

Notes:

1. Total undercliff area above 1.5 m O.D. was 11200 m^2
2. Total undercliff area above 9.5 m O.D. was 8900 m^2
   It is assumed that all the colluvium between 1.5 and 9.5 m O.D. is bare ground.

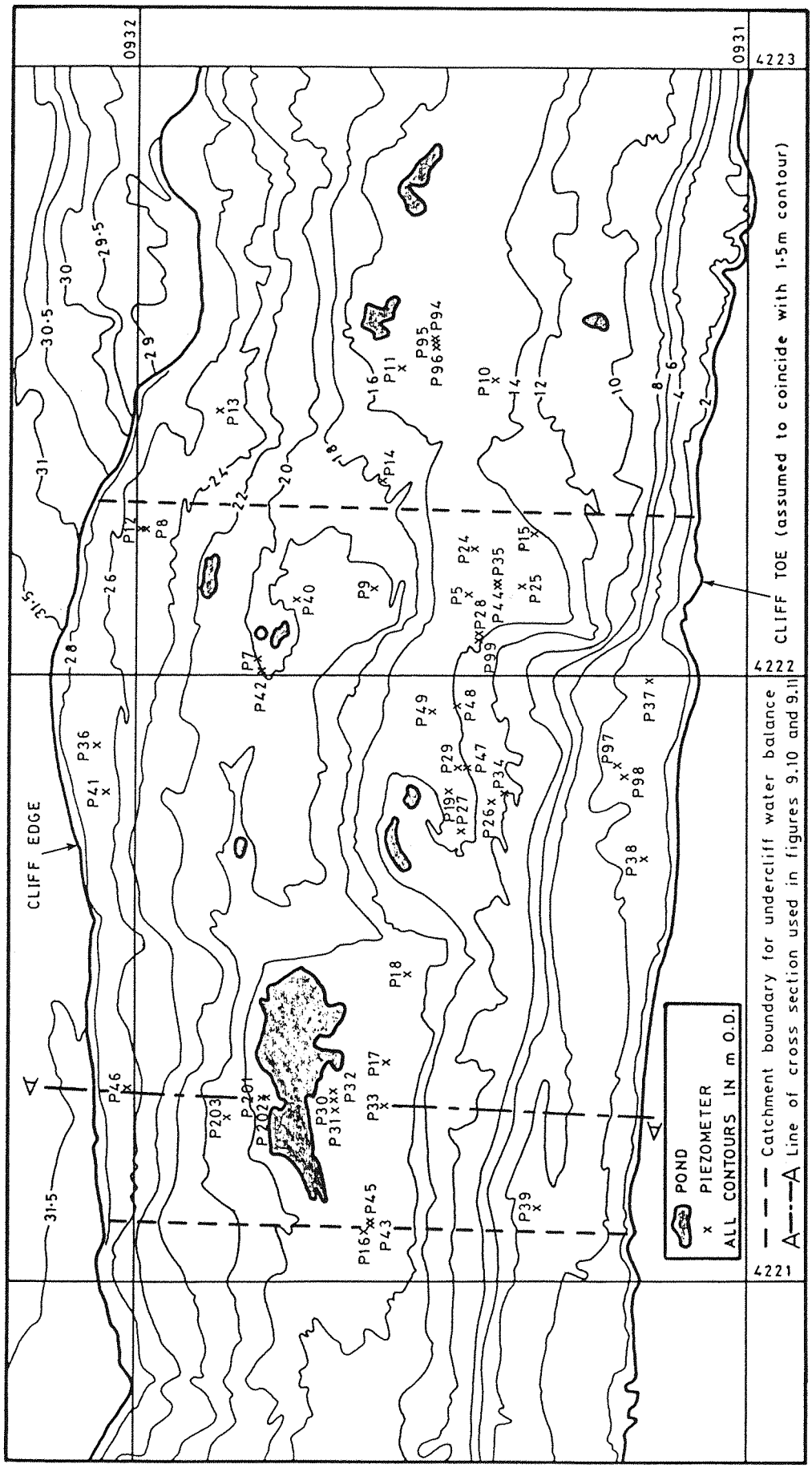

Figure 9.1 Location map for piezometers in the undercliff. The positions shown are as on the first survey date for each piezometer.

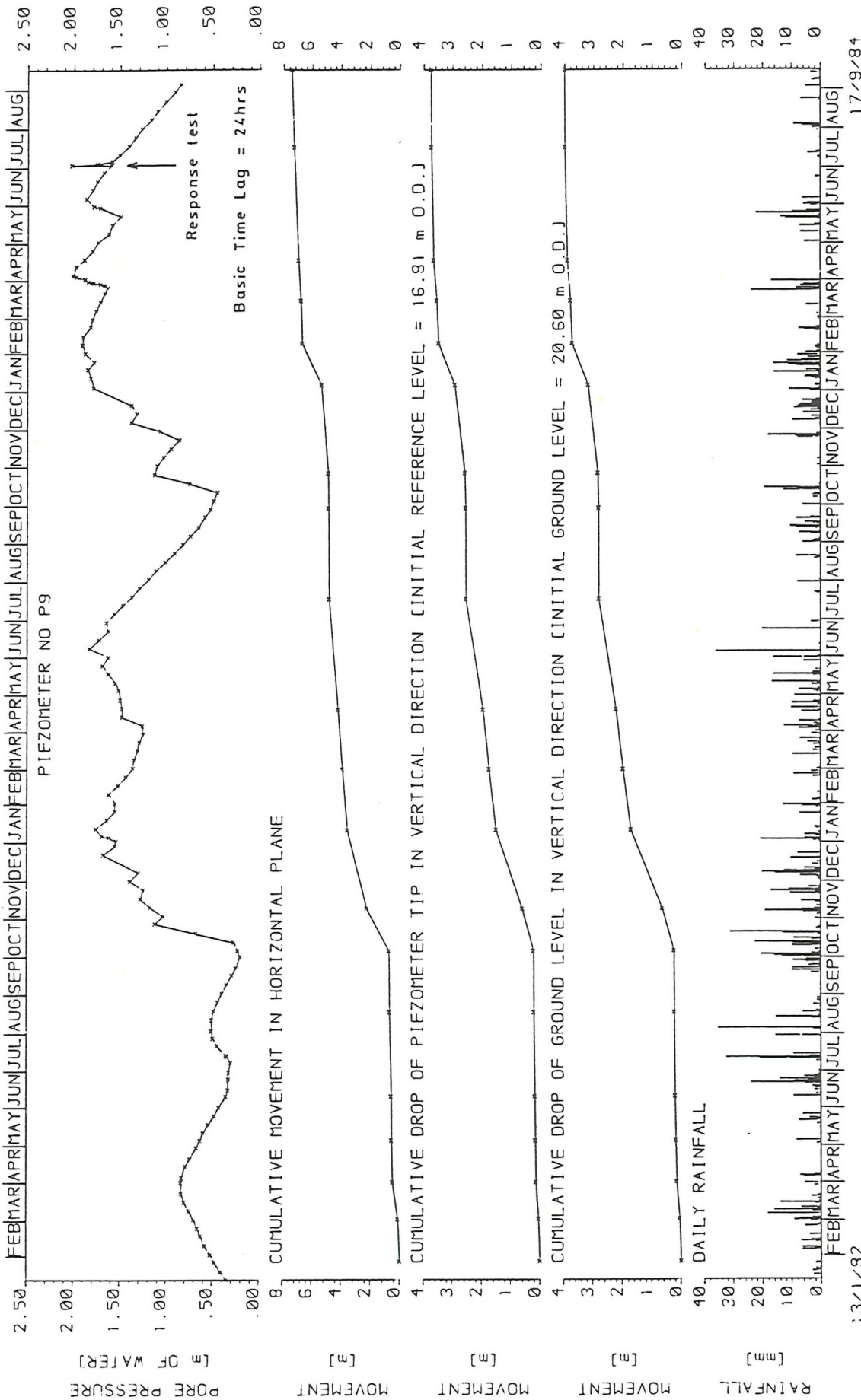

Figure 9.2 Groundwater level record at P9. See figure 9.1 for location.

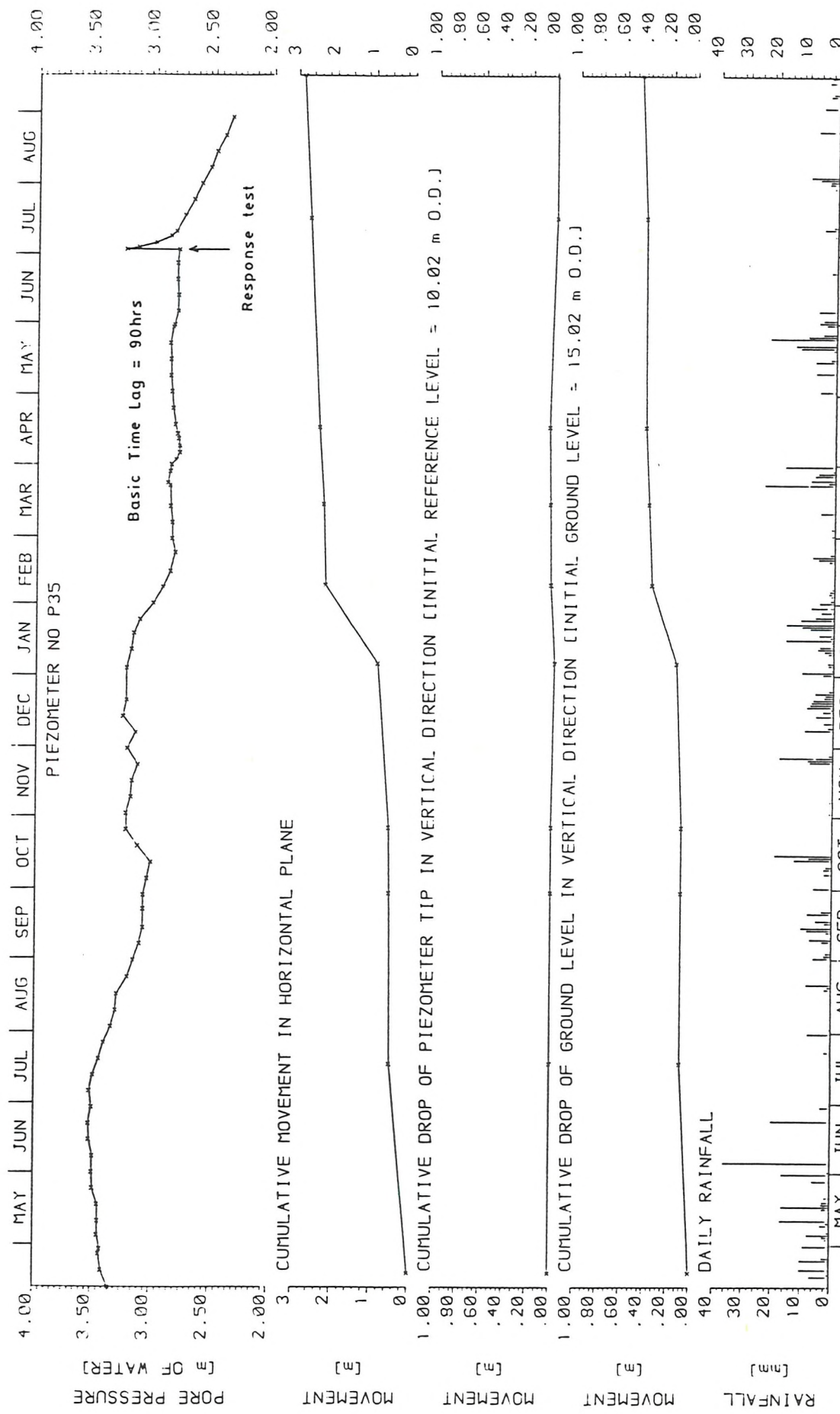

Figure 9.3 Groundwater level record at P35. See figure 9.1 for location.

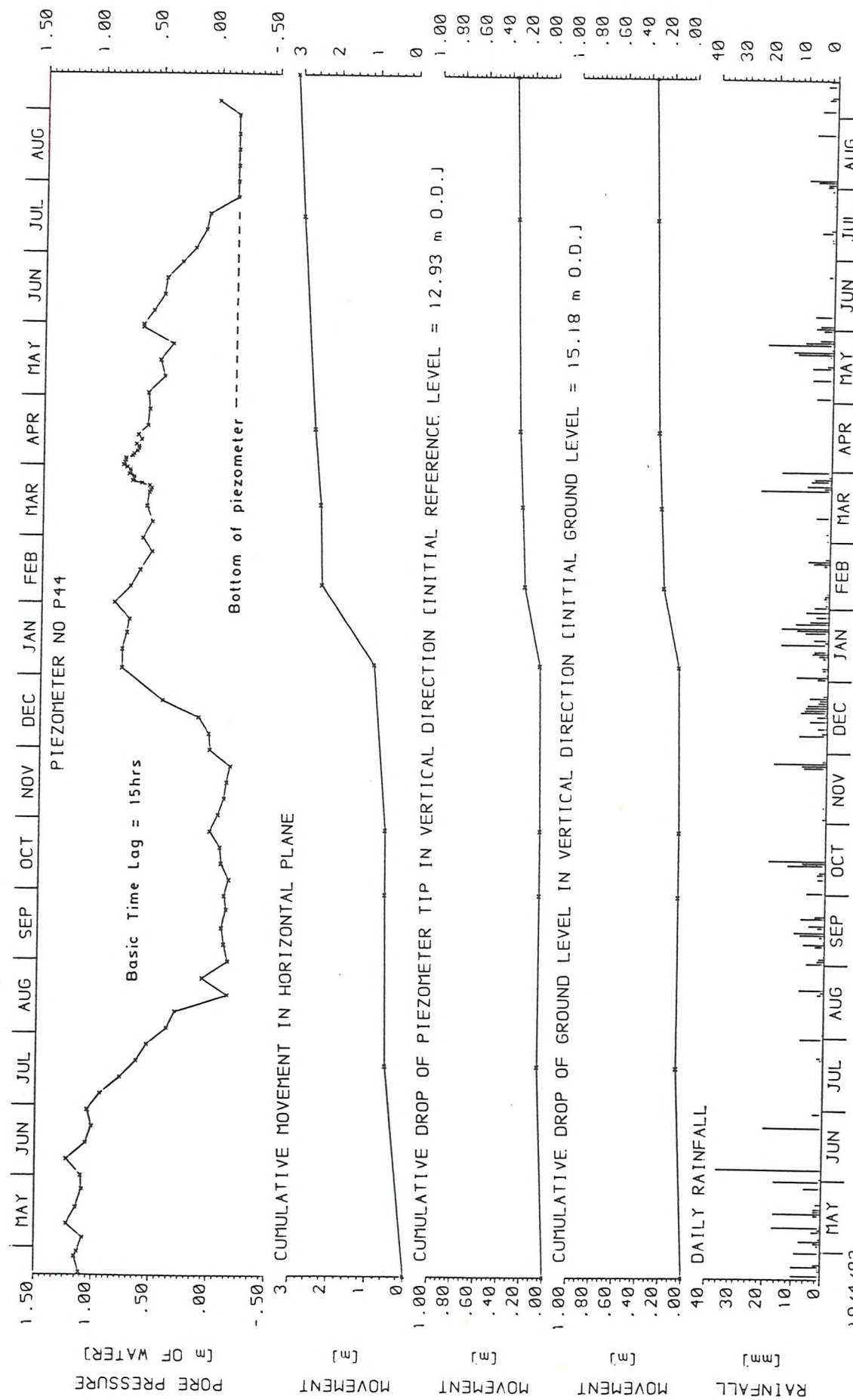

Figure 9.4 Groundwater level record at P44. See figure 9.1 for location.

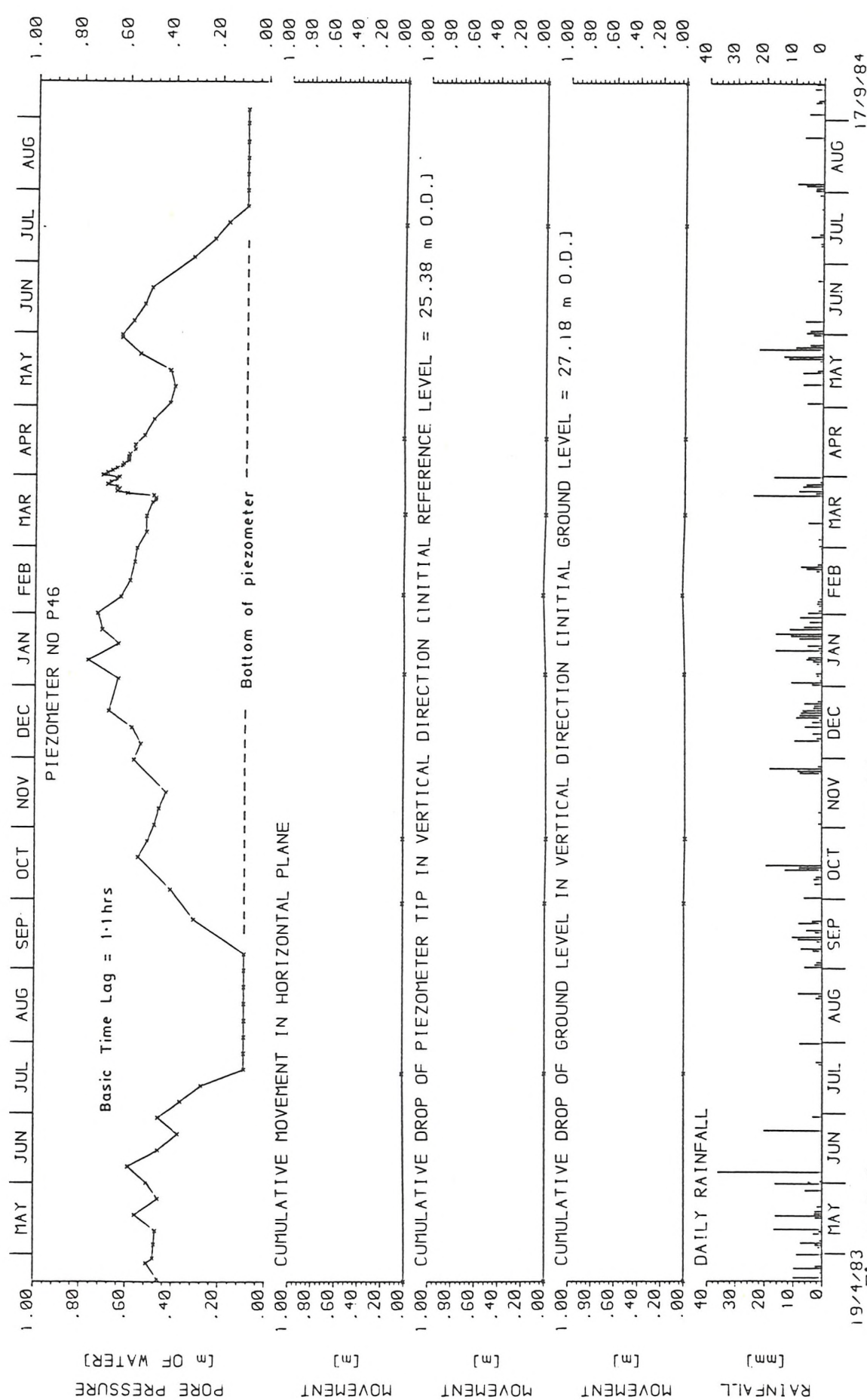

Figure 9.5 Groundwater level record at P46. See figure 9.1 for location.

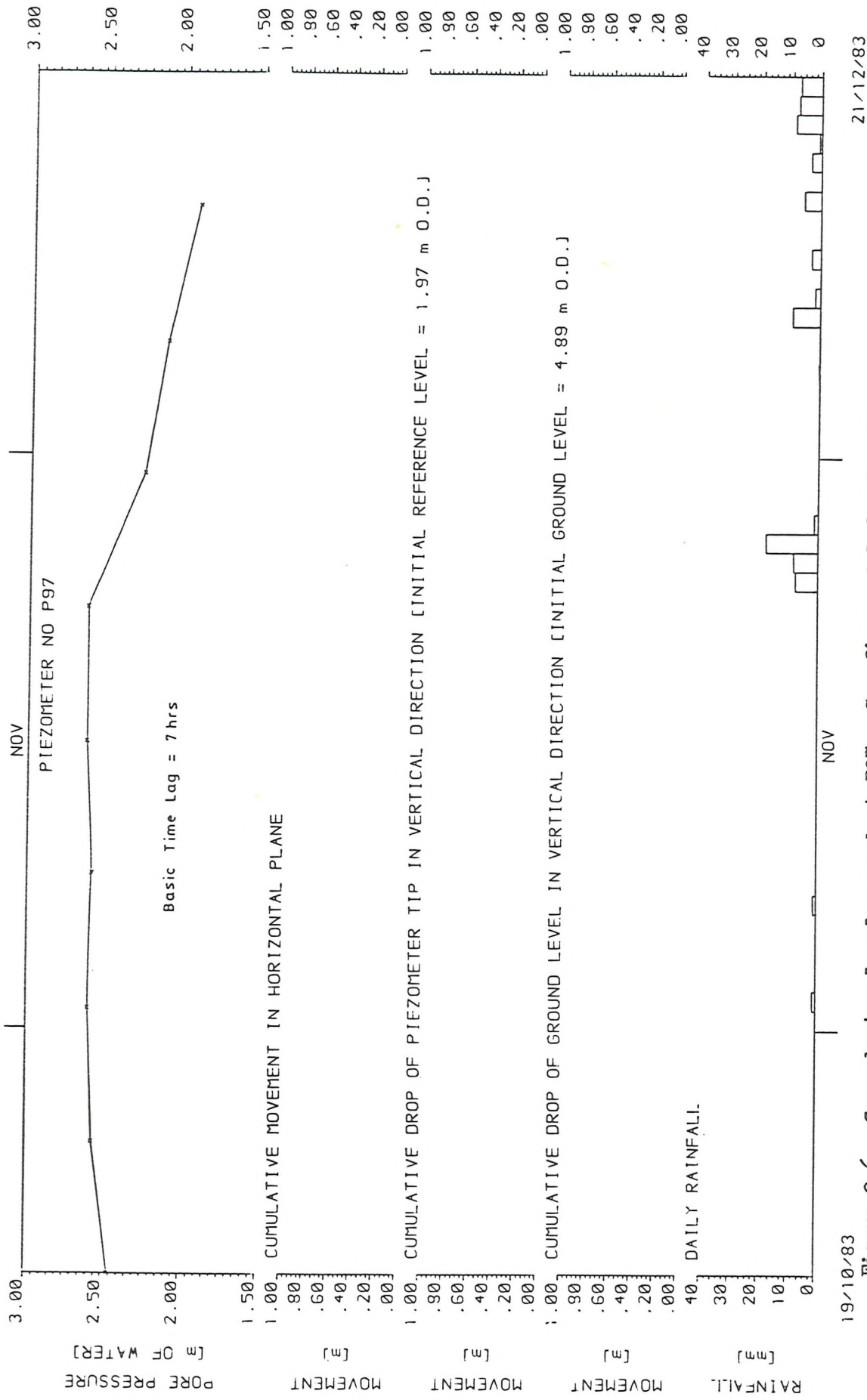

Figure 9.6 Groundwater level record at P97. See figure 9.1 for location.

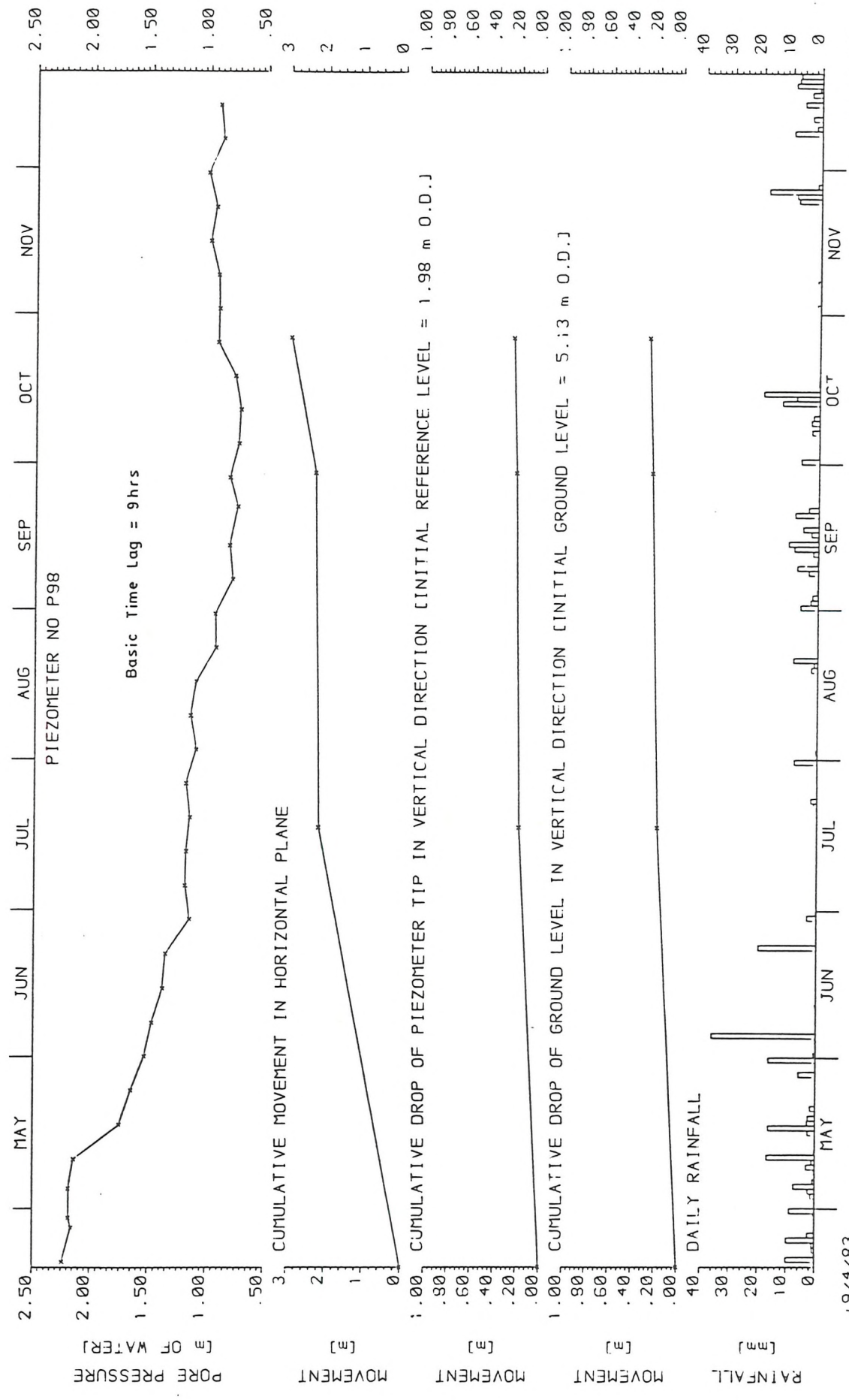

Figure 9.7 Groundwater level record at P98. See figure 9.1 for location.

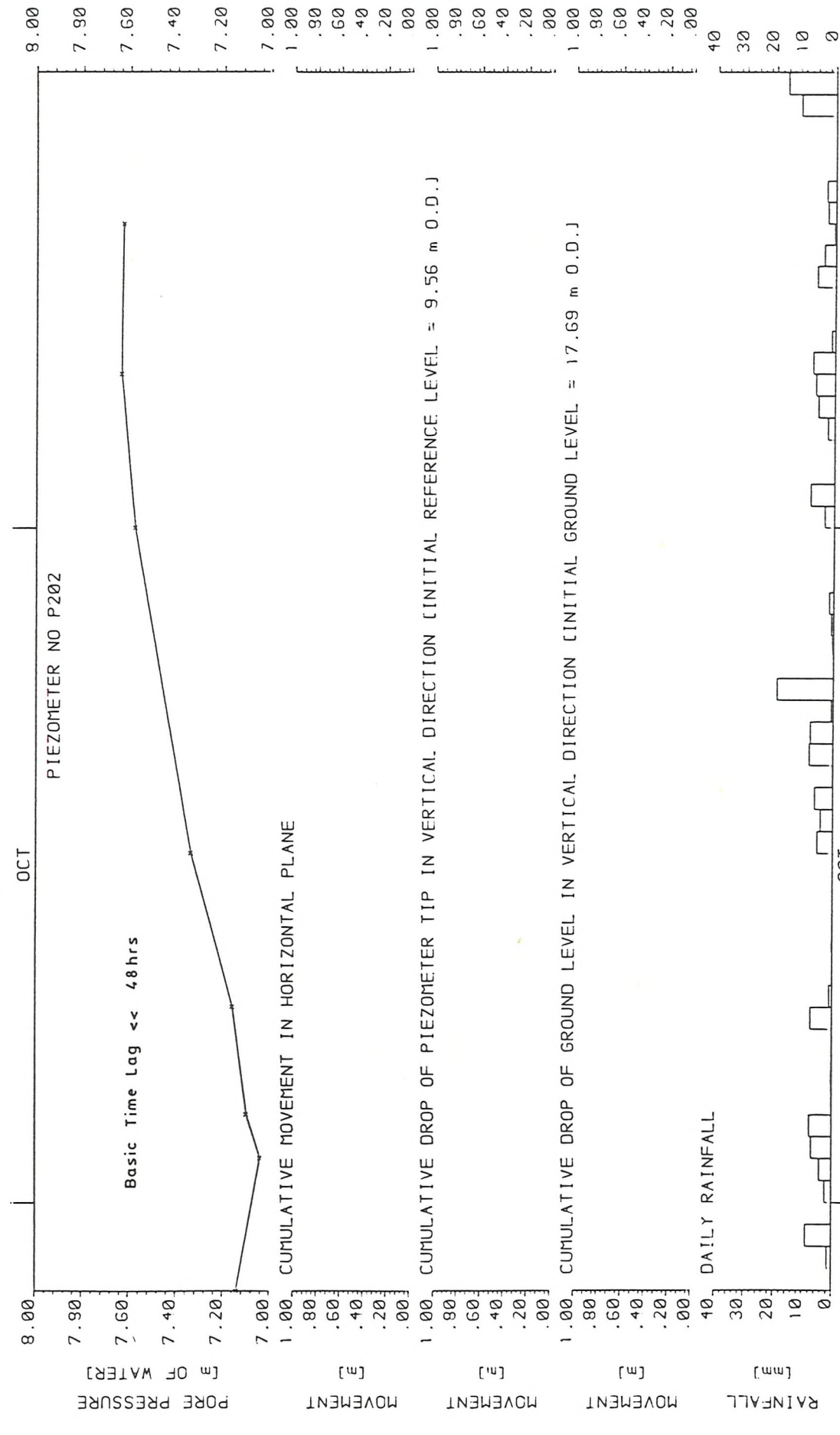

Figure 9.8 Groundwater level record at P202. See figure 9.1 for location.

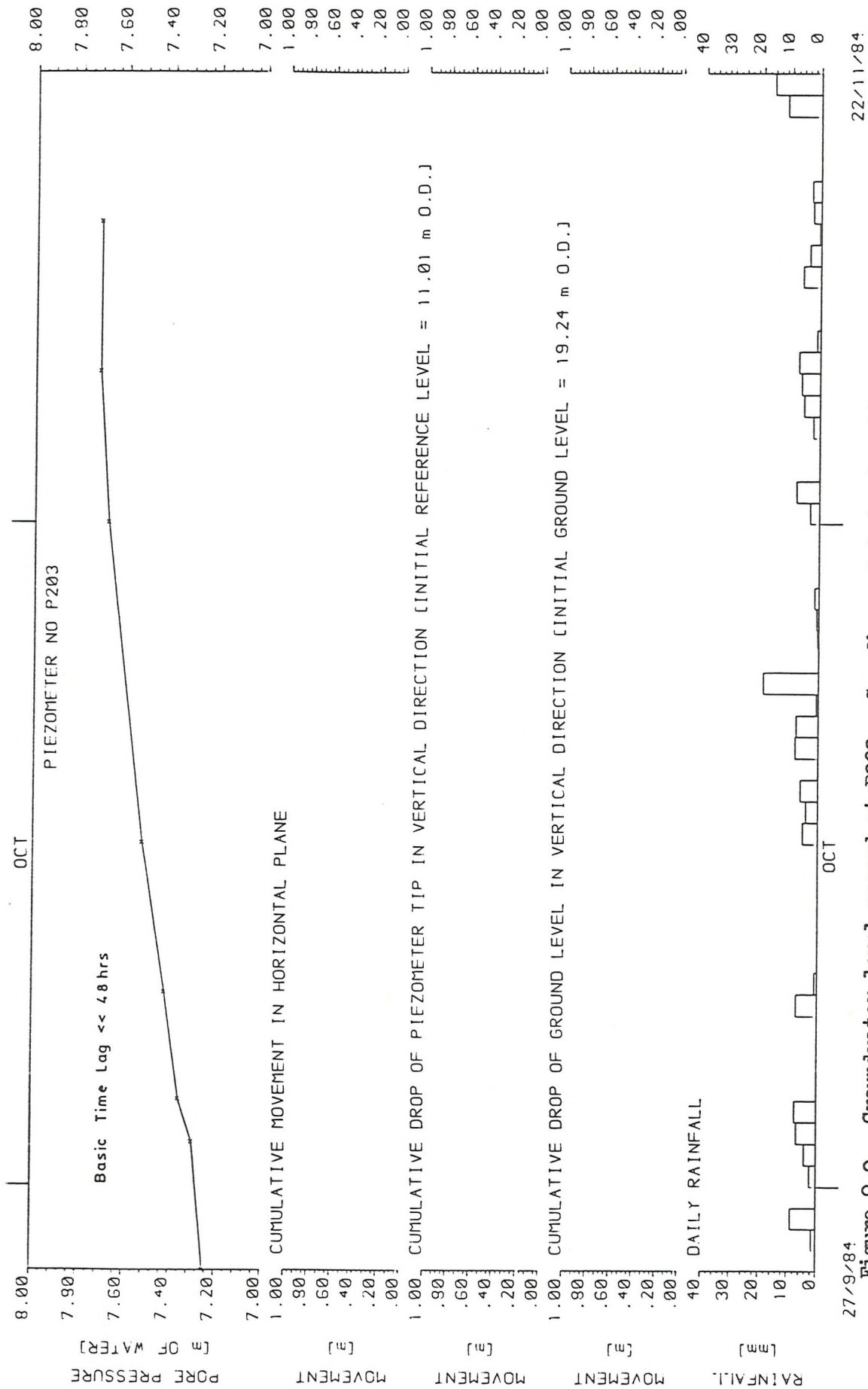

Figure 9.9 Groundwater level record at P203. See figure 9.1 for location.

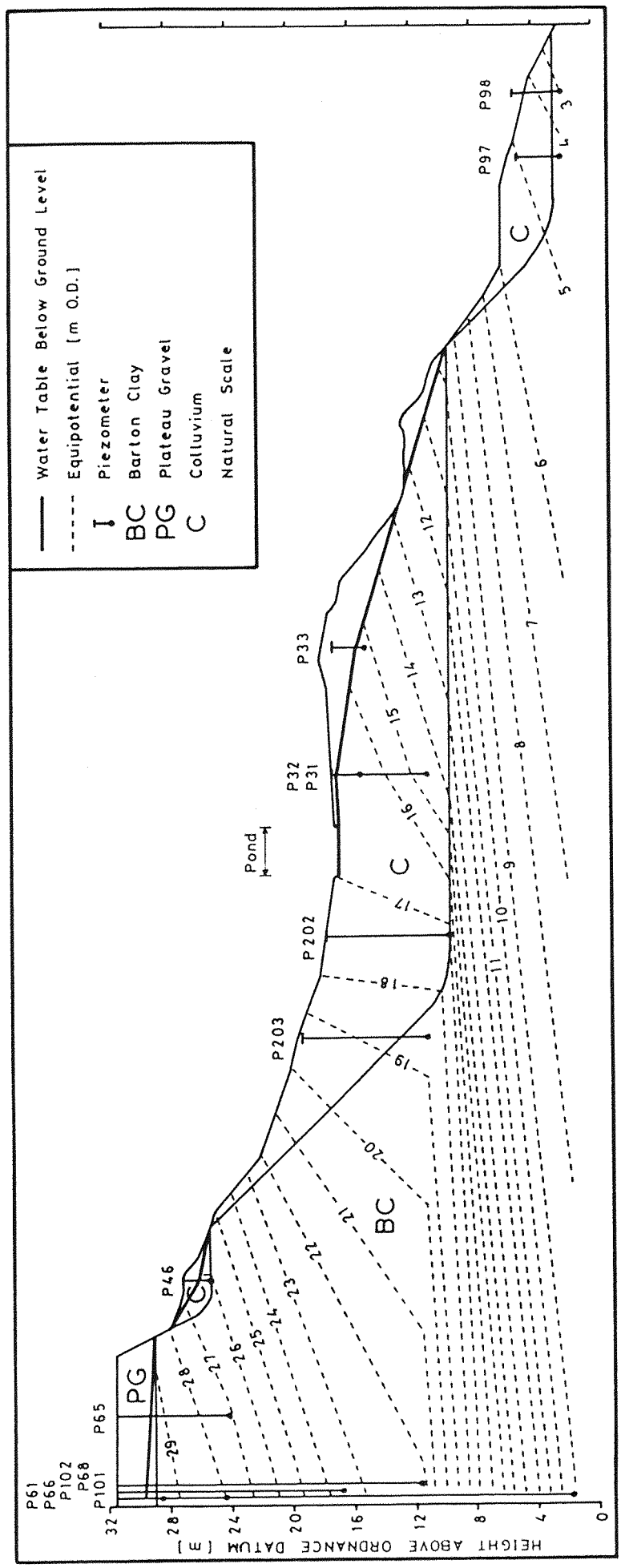

Figure 9.10 Cross section of the undercliffs showing estimated equipotentials for the 1st February 1984. The line of the section is along A-A as shown on figure 9.1.

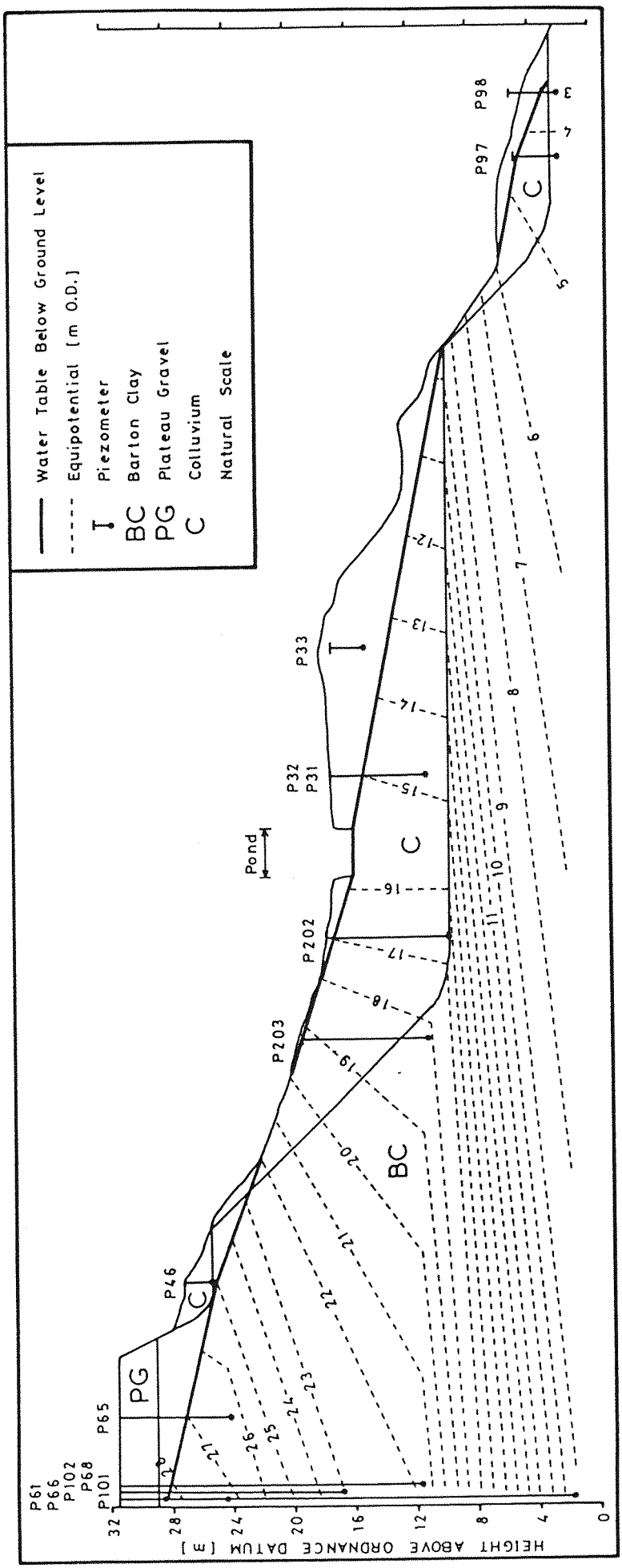

Figure 9.11 Cross section of the undercliffs showing estimated equipotentials for the 12th September 1984. The line of the section is along A-A as shown on figure 9.1.

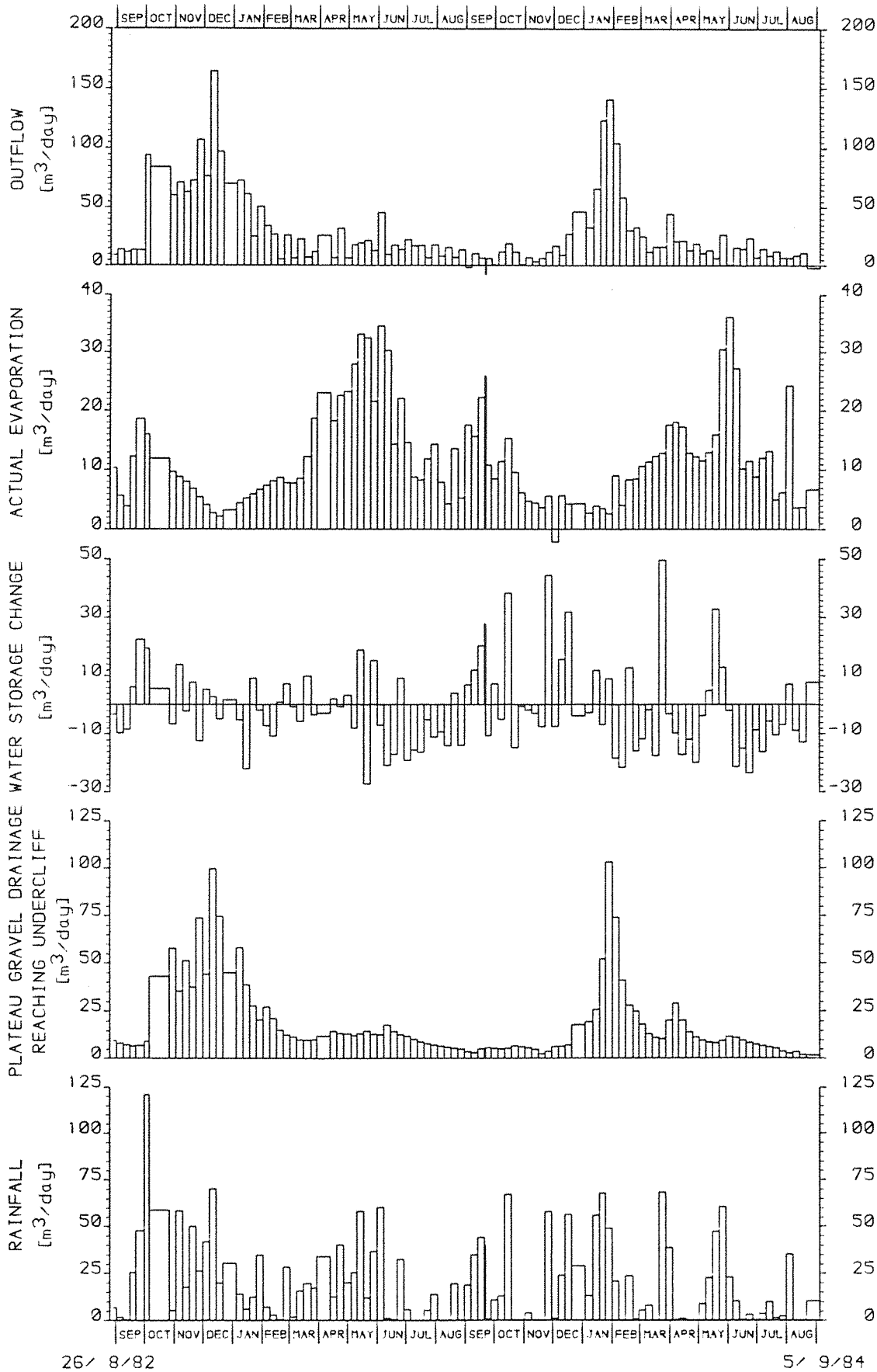

FIGURE 9.12 UNDERCLIFF WATER BALANCE.

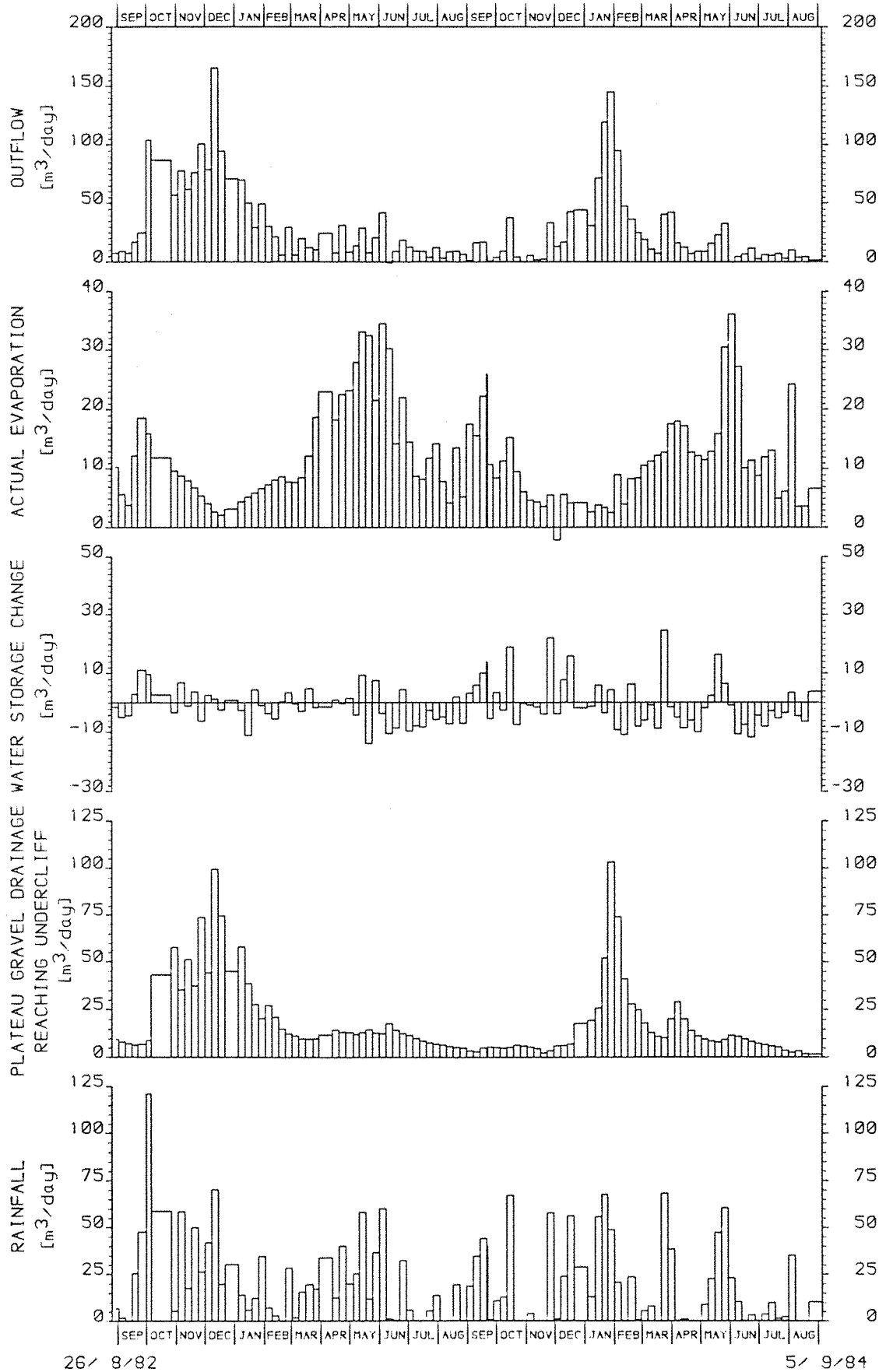

FIGURE 9.13 UNDERCLIFF WATER BALANCE. THE ANALYSIS OF THIS FIGURE ASSUMES THAT THE TRUE VALUE OF WATER STORAGE CHANGE IS 50% OF THE MEASURED VALUE.

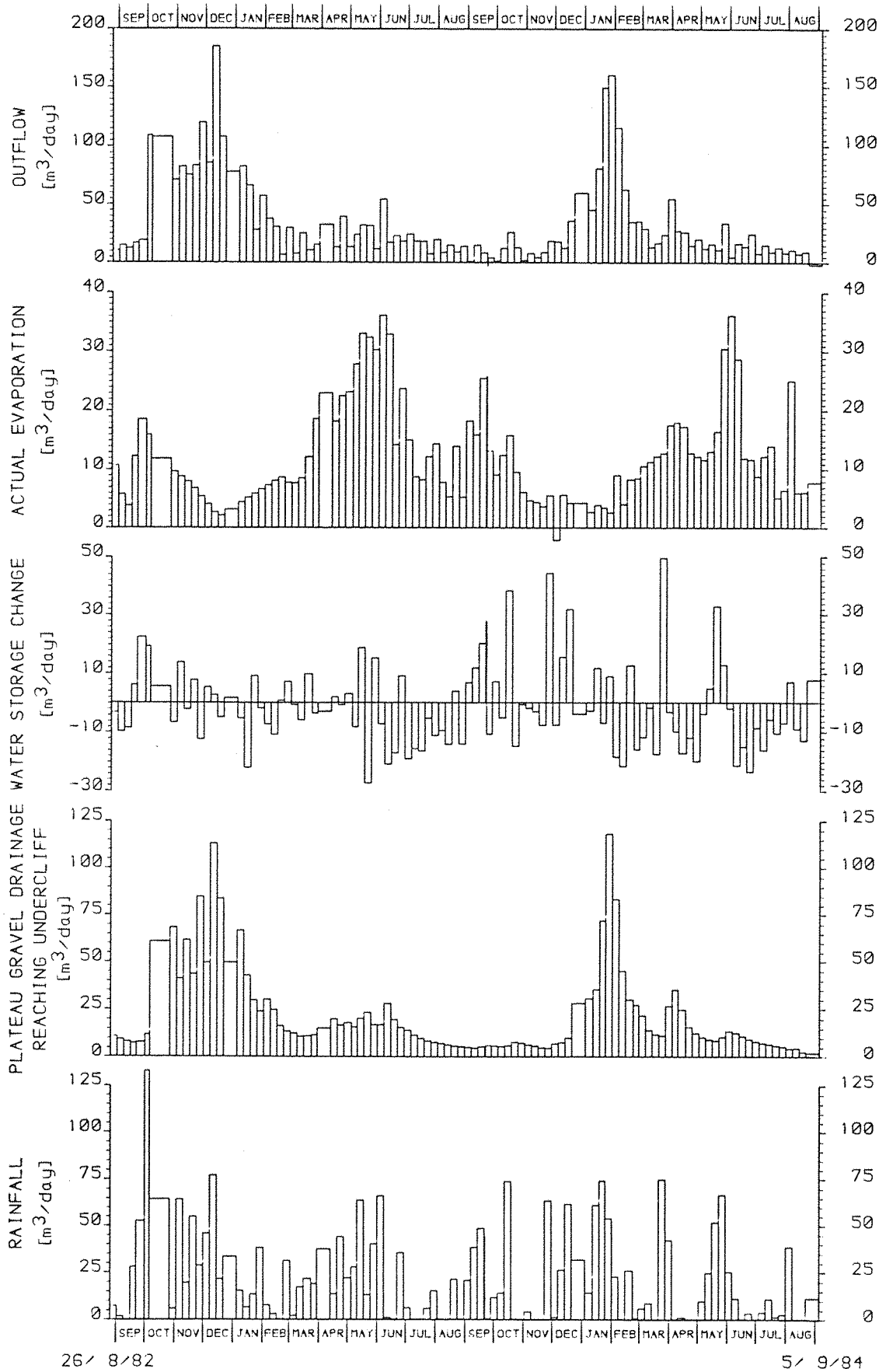

FIGURE 9.14 UNDERCLIFF WATER BALANCE. THE ANALYSIS OF THIS FIGURE ASSUMES THAT THE TRUE VALUE OF RAINFALL IS 10% MORE THAN THE MEASURED VALUE.

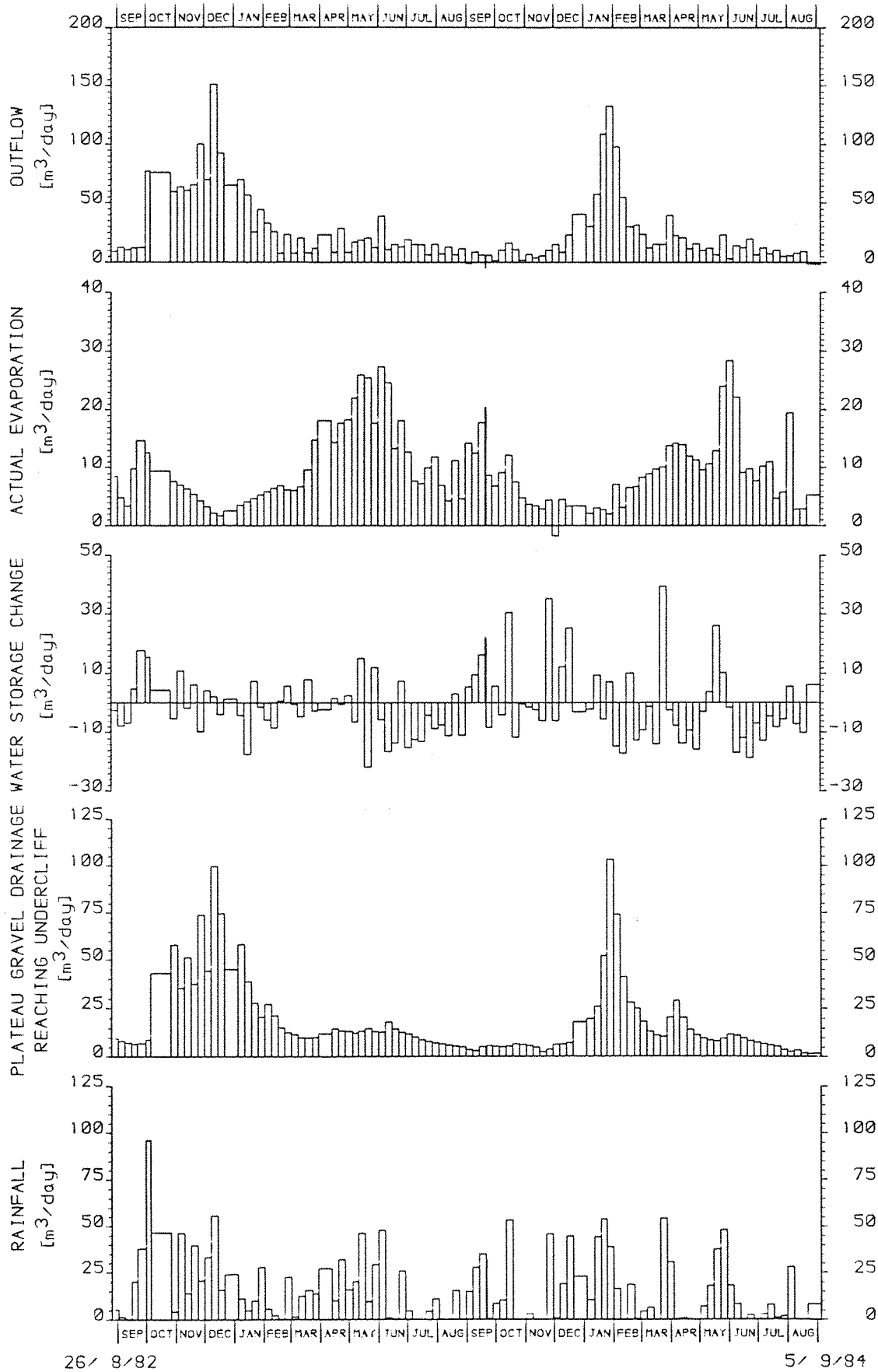

FIGURE 9.15 UNDERCLIFF WATER BALANCE.
THE ANALYSIS OF THIS FIGURE EXCLUDES THE A3 BENCH.
I.E. IT IS THE WATER BALANCE OF THE F AND D BENCHES.

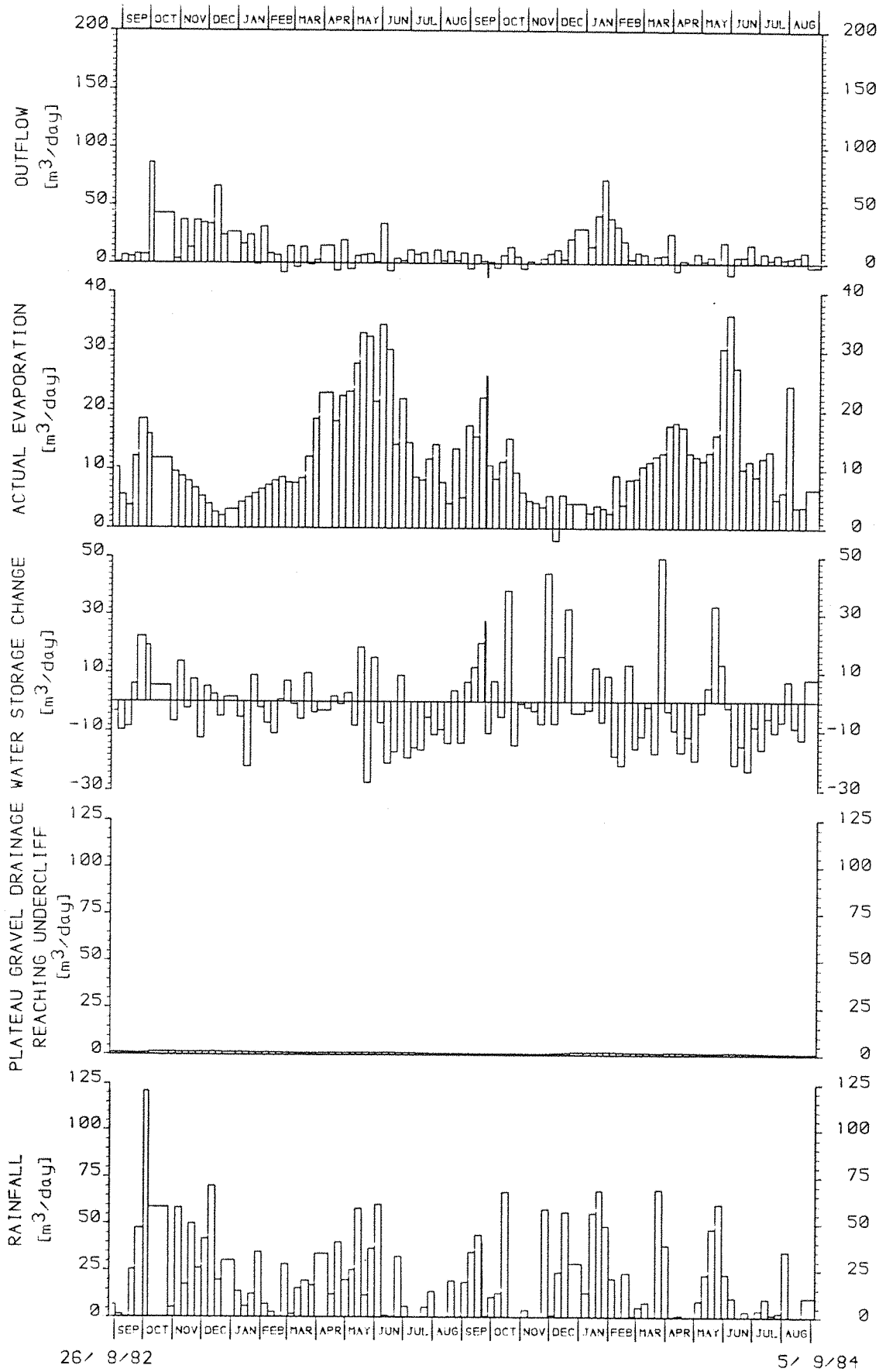

FIGURE 9.16 UNDERCLIFF WATER BALANCE. THE ANALYSIS OF THIS FIGURE EXAMINES THE EFFECTIVENESS OF A POSSIBLE CUT OFF DRAIN INSTALLED ON THE CLIFF TOP.

CHAPTER 10

SUMMARY AND CONCLUSIONS

The study has set out to investigate the hydrology of a degrading soil cliff. The purpose of the study was to increase understanding of the inter-relationship between hydrology and mass movements in such areas. It has long been recognised that the hydrology, through its influence on pore pressures, can affect the stability of a slope. However, studies of such areas have been neglected in the past, possibly due to the complicating nature of specific problems which do not arise elsewhere. In the past, studies have been confined to pore pressure measurements and some stability analysis. The latter is a major field of investigation in itself. As such, it has not been tackled here, although it would provide a natural extension to this work, and enable it to be related to other work, which has been conducted at the same site, into the volumes and rates of the various processes of degradation (Barton and Coles, 1984).

The study was of a stretch of the undefended Barton Clay (BC) cliffs of Christchurch Bay. Although this is site specific, it is believed that many of the difficulties, techniques used, and ideas evolved are of relevance to other similar areas. The cliffs are composed of Plateau Gravel (PG) overlying the BC. Meteorological and groundwater measurements have been made, and seepage to the undercliff estimated. Groundwater measurements and a water balance have also been made for the undercliff colluvium. The study has investigated the inter-relationship between these measurements and mass movement.

10.1 Difficulties Encountered

Conducting such an investigation in an area of active slope movement has been fraught with difficulties. Piezometers and access tubes installed in the undercliff have had limited life expectancies due to their either being engulfed by debris, or sheared by differential movement. Even when this did not occur, the often highly variable (both temporally and areally) rates of movement made interpretation of the results very difficult.

The materials of the undercliff often made the installation of instrumentation impossible. This was particularly true when

encountering gravel, nodules, soft clay and stiff clay. This also limited the depth which could be achieved by hand augering. The use of powered augers was limited by cost and portability. Although a portable powered auger was used for the installation of two piezometers, its use was limited to areas completely devoid of gravel, of which there were very few.

Considerable areas of the undercliff are either difficult, or impossible, to traverse in winter. Conversely, in summer, when the cliffs are more easily traversed, the instrumentation is subject to vandalism.

All the above difficulties severely limited the siting, and therefore representativeness, of the instrumentation. This was particularly true of the neutron probe access tube network. Also, the soils of the undercliff were highly compressible, such that the normal field calibration of the neutron probe was not suitable. An alternative, original method was devised instead.

There is believed to be some climatic variation between the undercliff and cliff top. Ideally, to measure the variation in climate between the undercliff and the cliff top, a long period of data should be collected from enough locations to be representative of both the undercliff and cliff top variability. However, investigation of the undercliff micro climate proved to be difficult due to vandalism, and the errors due to the method of measurement (variability of the aerodynamic effect) and non-representativeness of readings.

10.2 Geological Investigations

Geological investigations in this study have centred on the nature of the PG/BC unconformity. This marks a sharp division between the PG and BC with no mixing of the two. In the study area, the top of the BC is an irregular erosion surface cut in zone F. In places it has been periglacially disturbed, showing frost wedge casts, involutions and cryoturbation structures.

All this is in evidence at the cliff face. However, in order to investigate the continuity of the gravel deposit and the level of the unconformity back from the cliff face, a geophysical resistivity survey was undertaken. This confirmed the continuity of the PG deposit and detected the presence of channels and ridges in the top of the clay. These were generally aligned in a NE-SW direction. They are considered to be palaeo-current indicators for the deposition of the gravels. The presence of channels and ridges (linear trends) in the top of the BC at Highcliffe were noted to have a N-S orientation. This change in current direction during deposition is attributed to the locality being near to the confluence of the ancient rivers Avon (south flowing) and Solent (east flowing).

The continuity of the gravel is of significance in estimating the extent of the area contributing groundwater flow to the undercliff. The presence of channels is of relevance to the design and construction of a possible cut off drain as part of cliff stabilization works. They may also significantly affect the pattern of groundwater flow.

10.3 Meteorological Investigations

Rainfall and Potential Evaporation (PE) were measured at Naish Farm over a two year period. The statistical properties of the data were examined and the possibility of extending and modelling the data considered. The data record was extended to cover the period August 1980 to December 1985 in order to have adequate data for use in other analysis work.

The meteorological measurements were assumed to be spatially constant over the study area. However, it was recognised that there may be some error in this assumption, due to the presence of the sea and the variation in topography (the cliffs). The method of measurement was also subject to error. It was estimated that rainfall was underestimated by up to 10 per cent.

In order to put the data into historical perspective, the data for

Hurn Airport was examined in detail. No significant trend or periodicity was found. The significance (of the difference from the mean) of individual months of the study period was examined and found to be highly variable. Over the two year period, rainfall was found to be about average, although it was high in the first year and low in the second. PE was found to be high in both years.

The hydrologic significance of individual months of the year was examined. It was found that October to January was the most significant period. This means that it is during this period that rain induced slope movements are most likely to occur.

The regional variation of average annual and monthly rainfall and PE was investigated. There was little variation in PE. There was a much greater variation of rainfall. It increases northwards due to the influence of the coast. There was a significant variation in wetness (difference from the mean) of individual months between Naish Farm and Hurn Airport. This limits the accuracy to which data at Naish Farm can be extended using just Hurn Airport data. Ideally, data from several, suitably placed, weather stations should be used to extend the Naish Farm data.

10.4 Groundwater Level Prediction Model

A deterministic model was developed for the simulation of groundwater levels in response to meteorological changes. The model was based on a soil water balance approach and used existing groundwater level records for the estimation of the parameter values. The model was applied to groundwater level records for the PG. The model fit deteriorated toward the cliff face. This was ascribed to model assumptions being increasingly violated toward the cliff face. In particular, this was considered to be the case with the assumption that the drainage relationship was a unique function of groundwater level. However, the results still showed a good model fit to the observed data. The range, peaks, and recessions in groundwater levels were generally well predicted. Groundwater levels were

simulated for the period August 1980 to December 1985 using the extended meteorological data record (section 10.3).

The optimisation was complicated by the presence of more than one optimal solution; interdependence of parameters; persistence; and the dependence of the solution on the initial parameter values, the order of parameters in optimisation, and the calibration period. This meant that great care had to be taken in reaching the final solution. This was exampled by a detailed examination of the objective function surface for one particular piezometer. Of particular note was the strong interdependence of the parameters SY and RUNOFF. (The parameter SY relates changes in groundwater storage to changes in groundwater level; the parameter RUNOFF is the fraction of the rainfall that becomes surface runoff.)

The value of RUNOFF is due to a combination of surface runoff and a bias in the estimation of rainfall. As surface runoff is zero, the value was due to bias in the rainfall. The values obtained indicated that rainfall was on average underestimated by 4.75 per cent. This compares well with other investigations (see section 10.3 and chapter 3). However, there was considerable spatial variation such that the areal average was not significantly different from zero.

10.5 Cliff Top Water Balance

The water balance for the cliff top was investigated with a view to estimating the amount and distribution of the groundwater flow to the undercliff colluvium. With no significant surface runoff, all the effective rainfall was considered to infiltrate the ground surface and reach the water table in the PG. Groundwater was present in the PG at all times except near the cliff face when the water table was low. The temporal fluctuation of the water table was rapid. The rises were due to rainfall recharge, and the falls were due to lateral flow in the PG and downward leakage into the BC. As the permeability of the PG is much greater than that of the BC, the lateral flow was much greater than the leakage. The direction of lateral groundwater flow was considered to be locally complicated

by the undulation in the PG/BC unconformity. However, in the area studied, groundwater flow was generally found to be approximately perpendicular to the cliff face.

The area contributing groundwater flow to the undercliff between Highcliffe and Barton-on-Sea was estimated. It varies along the coastline, and the maximum is about 4.5 times the average for the study area. The position of the groundwater divide was calculated as a function of groundwater level. (The catchment area increased with higher groundwater levels.)

The calibrated groundwater level models of four piezometers in the PG (see section 10.4) were used to estimate the total drainage from the gravel. Considerable errors were found to be possible by not accurately determining the rainfall and catchment area. (It has already been noted (sections 10.3 and 10.4) that there is evidence to suggest that rainfall is underestimated.) These errors affected the amounts of gravel drainage. The use of only four calibrated locations was considered to cause some error in the estimated distribution of gravel drainage. This error was reduced when the values were totalled over longer intervals of 7 days for use in the undercliff water balance. Despite these possible errors, the estimation of gravel drainage was still considered useful. A considerable temporal variation in gravel drainage was found to occur, showing considerable amounts in the winter when groundwater levels were high.

Groundwater levels in the BC were used to estimate the leakage from the PG to the BC and the groundwater flow from the BC to the undercliff colluvium. Permeability is important with respect to the path and quantity of seepage flow. It varied spatially due to: variation in stress relief; vertical variation in fissuring and lithology; and the presence of local factors such as highly permeable shelly lenses.

Groundwater flow is downward and toward the undercliff. Groundwater flow down to the Bracklesham Beds is small and not very significant. The groundwater flow from that part of the BC inland of the PG

groundwater divide is negligible. The BC domain is recharged via leakage from the PG domain. It was variable, being greatest when groundwater levels were high. The variation was considerably less than that of the PG drainage, such that the annual total for leakage amounted to only 10 per cent of that for PG drainage. In summer, the PG drainage was almost entirely due to leakage, whereas in winter it was only a small proportion. Leakage decreased with increasing distance from the cliff face. A large proportion of the leakage occurred within a few metres of the cliff face. Most of this reaches the undercliff due to the presence of highly permeable fossil lenses (spatially, these are present everywhere, and not just near the undercliff) and stress relief opening joints near the undercliff. Apart from this, the role of the BC domain, as a source of seepage to the undercliff, is not very significant.

10.6 Undercliff Water Balance

The water balance for the undercliff was solved in order to estimate the surface and groundwater outflow from the colluvium. The input from the PG and BC was assumed to equal the gravel drainage less a small amount to allow for deep percolation to the Bracklesham Beds. Groundwater flow within the colluvium is mainly via gravel seams, tension cracks, and shear surfaces. Groundwater levels indicate that the general direction of groundwater flow within the colluvium is both downwards and seawards. The majority of flow at the base of the colluvium will be along the permeable shear surface separating colluvium from the BC. The downward percolation into in situ BC increases rapidly toward the front of a bench due to stress relief increasing permeability. The majority of this percolation returns to the undercliff colluvium via the back of a lower bench. Thus, the appearance of seepage from exposed in situ BC does not necessarily indicate that it entered the BC at a great distance inland.

The changes in undercliff soil moisture storage during the study period were evaluated using the neutron scattering technique. Large seasonal variations of moisture storage were observed within the top

1.5 m of colluvium. The readings were taken at approximately 7 day intervals.

The water balance was solved over the same intervals as the change in soil moisture storage. The 7 day interval reduced distribution errors in PE and PG drainage. However, it also averages outflows, the peak values of which are likely to be much higher, but over shorter periods. The largest source of possible error in the water balance was considered to be due to the estimation of rainfall. This may well lead to an underestimation of the outflow.

The water balance showed that there was a considerable outflow from the undercliff during wet periods in winter. To stabilize the cliffs, it would be necessary to intercept this outflow before it adversely affected groundwater levels at existing or potential failure surfaces. This would require intercepting the large amount of groundwater flow in the PG, and to drain the colluvium itself.

10.7 The Relationship between the Hydrology and Stability of the Cliffs

The geohydrological factors affecting the stability of a slope are the pore pressure and hydraulic gradient at a potential or existing shear surface. These factors depend upon the surrounding groundwater flow regime, which has been found to be affected by both meteorological variations and landslide activity. The effect of landsliding may be twofold.

The first effect is where the groundwater flow regime is changed due to the alteration of the boundaries. This effect has been noted in all three domains (PG, BC, and undercliff colluvium), although not all groundwater measurements have been affected. The effect is a gradual downward trend in groundwater level and soil moisture measurements. In the undercliff colluvium, this is highly variable and one or two measurements even show an upward trend.

The second effect is due to a reduction in total stress causing

swelling of the clay. The reduction in total stress causes pore pressures to be depressed. The subsequent swelling of the clay leads to a gradual rise in pore pressure. There is no evidence to suggest that any of the measured pore pressures are still equilibrating (i.e. rising). Therefore, the equilibration of pore pressures is not considered to be important in the timing of cliff failures at this locality. (I.e. although it is recognised that pore pressures will be depressed following a cliff failure, it is contended here that at Naish Farm they have equilibrated long before any subsequent failure.)

Meteorological variations have been found to cause fluctuations in groundwater levels, the magnitude of which decreases with depth. Fluctuations were still large at the F zone preferred bedding plane shear plane. Small cliff top slumps based on this bedding plane were observed to occur when groundwater levels were high. The existence of groundwater level fluctuations at the D zone preferred bedding plane shear plane is uncertain. However, large cliff top slumps based on this bedding plane were found to occur even when groundwater levels in the PG were low. Therefore, groundwater level fluctuation due to meteorological variations is reasoned to be minimal. The timing of these large slumps could be due to either, the slow equilibration of pore pressures as a result of previous slumping, or a gradual loss of lateral support due to the seaward movement of the colluvium on the undercliff. As mentioned in the previous paragraph, the equilibration of pore pressures, depressed following previous slumps, is considered to be complete long before the next failure takes place. Therefore, it is believed that failure is due to a loss of lateral support for the in situ material. This is probably also a contributing factor to the timing (at any particular location) of small slumps.

The choice of a particular bedding plane as a basal shear surface is due to a combination of a comparatively low shear strength and adverse permeability characteristics. The latter will affect the pore pressure and hydraulic gradient. The vertical variation of pore pressure is such that it may well be near the maximum at the

preferred bedding plane shear surface in the D zone. The vertical variation in pore pressure will be due to the vertical variation in permeability. Thus, there will be a peak in the vertical variation of pore pressure at about the same stratigraphic location at other cross sections along the coastline. This may well be the major cause of this vertical location sometimes being used for cliff top failures, although the precise bedding plane will also depend upon the local variation of the soil strength parameters. The F zone preferred bedding plane shear plane does not show a similar maximal pore pressure. It is probable that some other factor (such as shear strength) causes its utilization as a shear surface.

The stability of the undercliff colluvium is influenced by meteorological variations causing changes in pore pressures at the shear surfaces, and by variations of the distribution of loading due to failure of the in situ material and movement of the colluvium. The effect of the various mass movements is to cause an overall increase in the stability of the cliff as a whole. However, this is negated by the action of the sea in removing accumulated debris and in situ material at the cliff toe.

The temporal variation in colluvial movement is highly variable. The rate of movement varies from very high during wet periods in winter, to virtually zero at the end of a dry summer. This causes groundwater measurements to be affected by landslide activity considerably more than on the cliff top. The rate of equilibration must be very high in the immediate vicinity of the basal shear surfaces owing to their high permeability. Thus, groundwater levels are affected by landslide activity as a result of the changing groundwater flow regime. This makes the interpretation of readings somewhat complicated. However, they are mostly affected by meteorological variations and are high when movement occurs.

The stability analysis of a slope is normally based on static (i.e. whilst no movement is occurring) forces just prior to failure. The application of stability analysis to improve understanding of the colluvial movement, would need to account for the inertia of the soil mass and the changing geometry of the slope (i.e. distribution of loading). At any moment in time, there would be

a critical state of groundwater levels. If the actual groundwater levels were above this critical state, movement would accelerate (or be initiated), and if they were below it, movement would decelerate. The critical state would vary in time due to the changing geometry of the slope. Once movement is initiated, the inertia will tend to keep it going, even after groundwater levels have fallen below the critical state. Barton and Coles (1984) recorded rates of colluvial movement in the summer at Naish Farm (albeit at a much reduced rate). During a one year study period, they recorded that the lower part of the undercliff (A3 bench) continued to move throughout the year (albeit at a highly variable rate), whereas the rest of the undercliff stopped moving for only a one month period in summer. Thus, correlations between colluvial movement and meteorological conditions should be made with reference to the onset or acceleration of movement.

The undercliff is composed of three benches, and stability of the colluvium can be conveniently discussed with reference to a single bench. The initiation of movement of colluvium on the bench is as a result of rising groundwater levels in response to meteorological conditions. The movement will increase stability by decreasing the slope angle. Material will move from the front of the bench onto the lower bench. Similarly, material will move onto the back of the bench from a higher bench. This will increase the slope angle and so decrease stability. However, the input of material to the whole cliff by spalling is much less than that removed by the sea. Thus, there is a net loss of colluvium (Barton and Coles, 1984) and decrease in slope angle of individual benches. This causes a decrease in the lateral support, and hence stability, for the back scarp of the bench. Eventually, the in situ back scarp fails. This increases the loading at the back of the bench and thereby decreases the stability of the colluvium. This can lead to a sudden large acceleration in colluvial movement.

The above discussion suggests that either in a direct or indirect way meteorological variations are a causative factor in the various

processes of degradation. The concept of a critical state of groundwater levels has been introduced as a measure of stability. This state will fluctuate due to colluvial movement. The actual groundwater level will fluctuate due to the influence of meteorological variations and colluvial movement (the effects of loading and changing boundary conditions of the groundwater flow regime). The combination of the two fluctuating levels will determine the onset or change in the rate of movement. Thus, the relation between meteorological conditions and colluvial movement will be complex, and any correlation between the two should take this into account.

10.8 Recommendations for Further Work

Inevitably, an investigation of this nature falls short of being a final definitive account of the hydrology of the cliffs and its relation to their degradation. It is always desirable to have taken more measurements, and done more analysis work. However, resources are limited. Also, an increased understanding of the cliffs leads to the realisation of how other measurements and analysis work could yield important information. Finally, the work can only go so far, and has to stop somewhere. Although some consideration has been given to the relation between hydrology and mass movement, a natural extension of this work would be to take this still further.

It would be useful to investigate still further the vertical variation of pore pressure in the BC. In particular, measurements at the preferred bedding plane shear plane in the D zone would explore the response to meteorological changes and help elucidate whether, as suggested in section 7.9.2 paragraph 4, the pore pressure was at a maximum. More measurements along the section line would also be useful. For instance, measurements are lacking in the in situ BC below the undercliff colluvium. This would considerably reduce the uncertainty in the estimation of the equipotentials in figures 9.10 and 9.11. It would also provide further evidence as to whether pore pressures in the BC are still equilibrating. (If

they were, there would be a sharp drop in the vertical variation of pore pressure beneath the basal shear surface.) It is not anticipated that further measurements in the BC would identify paths and quantities of significant seepage flow. However, they would more accurately define the spatial distribution of pore pressures upon which a consideration of the stability of the cliffs depends. Unfortunately, measurements beneath the colluvium would be short lived (due to colluvial movement), and could only be made when groundwater levels were low (in summer). It would also require portable powered auger equipment able to work in gravel and soft ground.

The calculation of PG drainage was subject to a number of errors. These were the estimation of rainfall, catchment area, and the temporal distribution of drainage. More groundwater level measurements in the PG, if suitably placed, would identify local variations in flow caused by undulations in the unconformity. This would enable a more accurate estimation of the catchment area. If they were long period measurements, the parameters of the groundwater level prediction model could be estimated. This would yield a more accurate estimation (and maybe significant) of the areal rainfall (through the parameter RUNOFF and the measured rainfall). It would also reduce distribution errors due to the variability of the calculated drainage of the separate calibrated models. Further measurements at existing piezometers, as well as new ones, and their long term continuation, would also give useful information as to the effect on groundwater levels of the long term recession of the cliff top.

The groundwater level prediction model has only been applied to the PG groundwater levels. It could also be applied to some of the groundwater levels in the BC (see section 5.4.3) and possibly in the undercliff colluvium (see section 9.3 paragraph 9). This would provide a useful topic of further research. It would also be useful to predict historical groundwater levels for longer than the 5 years of section 6.5.3. This would enable the probability (return period)

of specific groundwater levels to be estimated. It would also enable the PG drainage to be calculated over a much longer period.

The use of a gamma probe (for measuring bulk density) would also provide a useful area of further research. It would increase the accuracy of soil moisture measurements. It would also provide information as to the spatial and temporal variation in bulk density in the colluvium. Bulk density values are used in stability analysis and in the calculation of the volumes and rates of movement of colluvial material. Hence, greater accuracy in these analyses would also be possible.

Seepage holes in the top of the BC (section 4.2) have been noted. Laboratory tests suggest that the clay is not susceptible to seepage erosion. It was suggested that tiny burrowing animals such as molluscs might be responsible. Further investigation of this is necessary, as seepage in the BC is of relevance to the effectiveness of any future possible cliff top cut off drain.

The study area is a part of the cliffs where the PG overlies BC. To the east, where it overlies Barton Sand, the behaviour of the groundwater flow to the undercliff may be different. This is of importance in the design of any scheme to intercept the groundwater flow before it affects the cliff stability. A useful topic of further work would be to compare the hydraulic behaviour of the PG with that of the different zones of the Barton Sand. Also, the Brickearth in this area would affect the temporal distribution of recharge to the groundwater table, and should therefore be investigated as well.

A natural extension of this work would be to relate it to that of Barton and Coles (1984). This might lead to the development of a model to simulate the inter-relation between the hydrology of the cliff with that of mass movement. This would need to take account of both meteorological conditions and the removal of material by the sea.

10.9 Final Remarks

Observations have shown that soil moisture and groundwater level fluctuations are influenced by both meteorological conditions and landslide movement. The effect of these influences differs spatially. The effect of meteorological conditions decreases with depth. In the undercliff colluvium this was additionally complicated by the presence of tension cracks. The effect of landslide movement is generally that of a downward trend in some of the readings. From this it is suggested that pore pressures have generally equilibrated such that the phenomenon does not play a part in the timing of failures.

A model was developed which related meteorological conditions to groundwater levels. The model was used to help identify the relative level of groundwater levels at the time of occurrence of a number of slumps. This showed that small slumps, based on the F zone preferred bedding plane shear plane, occurred when groundwater levels were high, but that their timing was also dependent upon the slow loss of lateral support in front of them. The groundwater levels at the D zone preferred bedding plane shear plane, upon which the large slumps are based, are not thought to be affected by meteorological conditions, such that the timing of failure is due to the gradual loss of lateral support afforded by the undercliff colluvium. Failure can occur at any time, although it is most likely while there are large movements of the undercliff colluvium causing a rapid loss of lateral support. This occurs when groundwater levels in the colluvium are high.

Landslide movement is influenced by both the distribution of loading and the fluctuation of pore pressures due to meteorological conditions. The distribution of loading itself is affected by landslide movement. Also, landslide movement can affect pore pressures. Thus, the inter-relation between landslide movement and meteorological conditions is complex.

The water balance of the undercliff colluvium was studied. The PG

contributed a considerable amount of groundwater flow to the undercliff. An estimate was made of its temporal variation. The direction of groundwater flow in the BC is both downward and seaward. The permeability of the BC increases near the undercliff due to the effect of stress relief opening up fissures. The leakage from the PG to the BC is small and increases toward the cliff face due to the increase in BC permeability. Most of this leakage quickly finds its way to the undercliff colluvium.

Groundwater flow in the colluvium is both downward and seaward. It is mainly via permeable tension cracks, shear surfaces and gravel seams. These, and the rough topography, provide a considerable storage of water. However, they are quickly filled at the end of summer, and subsequently large quantities of water flow from the undercliff.

The studies have shown that any future stabilization works should be designed to beneficially affect both pore pressures and the distribution of loading. The distribution of loading may be affected by regrading. This may be the most suitable method of improving stability against large failures. However, care needs to be taken, as improving the stability against one mode of failure, may decrease the stability against another mode of failure. A cliff top cut off drain would prevent considerable quantities of water from affecting groundwater levels in the undercliff. However, it would still be necessary to drain the cliff slope in order to deal with the effect of direct rainfall on the undercliff. Ideally, to be most effective at controlling pore pressures, drainage should be installed at the shear surfaces. Vegetation should also be established to minimise surface erosion. Should any such stabilization works be undertaken, it would be invaluable to estimate their effectiveness by measuring their performance.

REFERENCES

Adamowski, K. and Hamory, T. (1983). A stochastic systems model of groundwater level fluctuations. Journal of Hydrology, vol 62, pp 129-141.

Allerup, P. and Madsen, H. (1980). Accuracy of point precipitation measurements. Nordic Hydrology, vol 11, pp 57-70.

Alley, W.M. (1984). On the treatment of evapotranspiration, soil moisture accounting, and aquifer recharge in monthly water balance models. Water Resources Research, vol 20, pp 1137-1149.

Anderson, M.G. and Howes, S. (1985). Development and application of a combined soil water-slope stability model. Quarterly Journal of Engineering Geology, vol 18, pp 225-236.

Anderson, M.G. and Pope, R.G. (1984). The incorporation of soil water physics models into geotechnical studies of landslide behaviour. 4th International Symposium on Landslides, Toronto, Canada. Vol 1, pp 349-353.

Ashmore, S.E. (1944). The rainfall of the Wrexham district. Quarterly Journal of the Royal Meteorological Society, vol 70, pp 241-269.

Atkinson, T.C. (1978). Techniques for measuring subsurface flow on hillslopes. Ch 3 in "Hillslope hydrology" (ed. M.J. Kirkby). Wiley, Chichester.

Bailey, S.F. (1983). A further study of the shear strength characteristics of the Highcliffe Plateau Gravel. B.Sc. dissertation, Department of Civil Engineering, University of Southampton.

Barton, M.E. (1973). The degradation of the Barton Clay cliffs of Hampshire. Quarterly Journal of Engineering Geology, vol 6, pp 423-440.

Barton, M.E. (1977). Landsliding along bedding planes. Bulletin of the International Association of Engineering Geology, No 16, pp 5-7.

Barton, M.E. (1984a). Periglacial features exposed in the coastal cliffs at Naish Farm, Near Highcliffe. Proceedings of the Hampshire Field Club and Archaeological Society, vol 40, pp 5-20.

Barton, M.E. (1984b). The preferred path of landslide shear surfaces in over-consolidated clays and soft rocks. 4th International Symposium on Landslides, Toronto, Canada. Vol 3, pp 75-79.

Barton, M.E. and Coles, B.J. (1982). The overall pattern and rates of movement in the undercliffs at Naish Farm, Highcliffe, Hampshire. Progress report to SERC, October 1982. Department of Civil Engineering, University of Southampton.

Barton, M.E. and Coles, B.J. (1983). Rates of movement of soil slopes in Southern England using inclinometers and surface peg surveying. Proceedings of the International Symposium on Field Measurements in Geomechanics, Zurich. Vol 1, pp 609-618. Balkema, Rotterdam.

Barton, M.E. and Coles, B.J. (1984). The characteristics and rates of the various slope degradation processes in the Barton Clay cliffs of Hampshire. Quarterly Journal of Engineering Geology, vol 17, pp 117-136.

Barton, M.E., Coles, B.J. and Tiller, G.R. (1983). A statistical study of the cliff top slumps in part of the Christchurch Bay coastal cliffs. Earth Surface Processes and Landforms, vol 8, pp 409-422.

Barton, M.E., Palmer, S.N. and Wong, Y.L. (1986). A geotechnical investigation of two Hampshire Tertiary Sand Beds: are they locked sands? Quarterly Journal of Engineering Geology, vol 19, pp 399-412.

Barton, M.E. and Thomson, R.I. (1984). Studies of the water balance in a rapidly degrading soil cliff. Proceedings of the 4th International Symposium on Landslides, Toronto, Canada. Vol 1, pp 355-361.

Barton, M.E. and Thomson, R.I. (1986a). Seepage characteristics and landsliding of the A3 horizon of the Barton Beds. Pp 107-114 in "Groundwater in Engineering Geology" (ed. by J.C. Cripps, F.G. Bell, M.G. Culshaw). Geological Society, Engineering Group Special Publication No 3.

Barton, M.E. and Thomson, R.I. (1986b). A model for predicting groundwater level response to meteorological changes. Pp 299-312 in "Groundwater in Engineering Geology" (ed. by J.C. Cripps, F.G. Bell, M.G. Culshaw). Geological Society, Engineering Group Special Publication No 3.

Barton, M.E. and Thomson, R.I. (1986c). Interceptor drains for cliff top and above the crest of slopes and cuttings. Pp. 487-496 in "Groundwater in Engineering Geology" (ed. by J.C. Cripps, F.G. Bell, M.G. Culshaw).Geological Society, Engineering Group Special Publication No 3.

Beard, L.R. (1967). Optimization techniques for hydrologic engineering. Water Resources Research, vol 3, pp 809-815.

Bell, F.C. (1969). Generalized rainfall-duration-frequency relationships. Journal of the Hydraulics Division, Proceedings of the American Society of Civil Engineers, vol 95, no HY1, pp 311-327.

Bell, J.P. (1976). Neutron Probe Practice. Natural Environment Research Council, Institute of Hydrology, Wallingford, Report No 19.

Belmans, C., Wesseling, J.G. and Feddes, R.A. (1983). Simulation model of the water balance of a cropped soil: SWATRE. Journal of Hydrology, vol 63, pp 271-286.

Bergstrom, S. and Sandberg, G. (1983). Simulation of groundwater response by conceptual models - three case studies. Nordic Hydrology, vol 14, pp 71-84.

Bertini, T., Cugusi, F., D'Elia, B. and Rossi-Doria, M. (1984a). Climatic conditions and slow movements of colluvial covers in Central Italy. Proceedings of the 4th International Symposium on Landslides, Toronto, Canada. Vol 1, pp 367-376.

Bertini, T., Cugusi, F., D'Elia, B. and Rossi-Doria, M. (1984b). Pore water pressure variations governing slow movements in a colluvial slope. Proceedings of the 4th International Symposium on Landslides, Toronto, Canada. vol 3, pp 81-83.

Bleasdale, A. and Farrar, A.B. (1965). The processing of rainfall data by computer. Meteorological Magazine, vol 94, pp 98-109.

Booth, A.I. (1974). Degradation of the cliffs of the Barton Clay outcrop in West Hampshire. Ph.D. Thesis, University of Southampton.

Brand, E.W.,Premchitt, J. and Phillipson, H.B. (1984). Relationship between rainfall and landslides in Hong Kong. Proceedings of the 4th International Symposium on Landslides, Toronto, Canada. Vol 1, pp 377-384.

British Standard 1377 (1975). Methods of test for soils for Civil Engineering purposes. British Standards Institution, London.

Bromhead, E.N. (1979). Factors affecting the transition between the various types of mass movement in coastal cliffs consisting largely of overconsolidated clay with special reference to Southern England. Quarterly Journal of Engineering Geology, vol 12, pp 291-300.

Bromhead, E.N. and Dixon, N. (1984). Pore water pressure observations in the coastal clay cliffs at the Isle of Sheppey, England. Proceedings of the 4th International Symposium on Landslides, Toronto, Canada. Vol 1, pp 385-390.

Brunsden, D. and Jones, D.K.C. (1976). The evolution of landslide slopes in Dorset. Philosophical Transactions of the Royal Society of London, Series A, vol 283, pp 605-631.

Buishand, T.A. (1978). Some remarks on the use of daily rainfall models. Journal of Hydrology, vol 36, pp 295-308.

Buishand, T.A. (1982). Some methods for testing the homogeneity of rainfall records. Journal of Hydrology, vol 58, pp 11-27.

Burton, E. St. J. (1933). Faunal horizons of the Barton Beds in Hampshire. Proceedings of the Geologists' Association, vol 44, pp 131-167.

Calder, I.R., Harding, R.J. and Rosier, P.T.W. (1983). An objective assessment of soil moisture deficit models. Journal of Hydrology, vol 60, pp 329-355.

Campbell, R.H. (1974). Debris flows originating from soil slips during rainstorms in Southern California. Quarterly Journal of Engineering Geology, vol 7, pp 339-349.

Canuti, P., Focardi, P. and Garzonio, C.A. (1985). Correlation between rainfall and landslides. Bulletin of the International Association of Engineering Geology, No 32, pp 49-54.

Canuti, P.,Focardi, P., Garzonio, C.A., Rodolfi, G. and Zanchi, C. (1984). Analysis of the dynamic of a mass movement on silty clayey Lacustrine deposits in North-Central Italy (Mugello, Tuscany). Proceedings of the 4th International Symposium on Landslides, Toronto, Canada. Vol 1, pp 391-397.

Carpenter, C.D. (1972). Note: installation of soil moisture access tubes in gravels and cobbles. Soil Science, vol 113, pp 453-455.

Carson, M.A. (1976). Mass-wasting, slope development and climate. Chapter 4 in "Geomorphology and Climate" (ed. E. Derbyshire). Wiley, Chichester.

Cedergren, H.R. (1977). Seepage, drainage, and flow nets (2nd edition). Wiley, London.

Chandler, R.J. and Skempton, A.W. (1974). The design of permanent cutting slopes in stiff fissured clays. Géotechnique, vol 24, pp 457-466.

Chatfield, C. (1983). Statistics for technology (3rd edition). Chapman and Hall, London.

Chidley, T.R.E. and Pike, J.G. (1970). A generalised computer program for the solution of the Penman Equation for evapotranspiration. Journal of Hydrology, vol 10, pp 75-89.

Clarke, R.T. (1973). A review of some mathematical models used in hydrology, with observations on their calibration and use. Journal of Hydrology, vol 19, pp 1 -20.

Cline, R.G. and Jeffers, B.L. (1975). Installation of neutron probe access tubes in stony and bouldery forest soils. Soil Science, vol 120, pp 71-72.

Coles, B.J. (1983). Periodic surveying of the undercliffs at Naish Farm, Highcliffe from June 1981 to July 1983: Survey data. Data report, December 1983. Department of Civil Engineering, University of Southampton.

Couchat, P. (1974). Mesure neutronique de l'humidité des sols. Thesis, Institut National de Polytechnique, Toulouse.

Davis, S.N., Thompson, G.M., Bentley, H.W. and Stiles, G. (1980). Ground-water tracers - a short review. Ground Water, vol 18, pp 14-23.

Dawdy, D.R. and Bergmann, J.M. (1969). Effect of rainfall variability on streamflow simulation. Water Resources Research, vol 5, pp 958-966.

Diskin, M.H. and Simon, E. (1977). A procedure for the selection of objective functions for hydrologic simulation models. Journal of Hydrology, vol 34, pp 129-149.

Dixon, N. and Bromhead, E.N. (1986). Groundwater conditions in the coastal landslides of the Isle of Sheppey. Pp 51-58 in "Groundwater in Engineering Geology" (ed. by J.C. Cripps, F.G. Bell, M.G. Culshaw). Geological Society, Engineering Group Special Publication No 3.

Dooge, J.C.I. (1960). The routing of groundwater recharge through typical elements of linear storage. International Association of Scientific Hydrology, General Assembly, Helsinki. Publication No 52, pp 286-300.

Faust, C.R. and Mercer, J.W. (1980). Ground-water modelling: numerical models. Ground Water, vol 18, pp 395-409.

Freeze, R.A. and Banner, J. (1970). The mechanism of natural ground water recharge and discharge: 2. Laboratory column experiments and field measurements. Water Resources Research, vol 6, pp 138-155.

Freeze, R.A. and Cherry, J.A. (1979). Groundwater. Prentice-Hall, Englewood Cliffs, New Jersey, U.S.A.

Gibson, R.E. (1963). An analysis of system flexibility and its effect on time lag in pore water pressure measurements. Gēotechnique, vol 13, pp 1-11.

Gillham, R.W. (1984). The capillary fringe and its effect on water-table response. Journal of Hydrology, vol 67, pp 307-324.

Griffiths, D.H. and King, R.F. (1981). Applied Geophysics for Geologists and Engineers (2nd edition). Pergamon, Oxford.

Guidicini, G. and Iwasa, O.Y. (1977). Tentative correlation between rainfall and landslides in a humid tropical environment. Bulletin of the International Association of Engineering Geology, No 16, pp 13-20.

Gupta, V.K. and Sorooshian, S. (1983). Uniqueness and observability of conceptual rainfall-runoff model parameters: the percolation process examined. Water Resources Research, vol 19, pp 269-276.

Halcrow, Sir William & Partners (1971). Highcliffe: report on the instability of the cliffs and recommended remedial works. Consulting engineer's report to the Borough of Christchurch.

Harper, T.R. (1975). The transient groundwater pressure response to rainfall and prediction of rock slope instability. International Journal of Rock Mechanics, Mining Science and Geomechanics Abstract, vol 12, pp 175-179.

Headworth, H.G. (1972). The analysis of natural ground water level fluctuations in the chalk of Hampshire. Journal of the Institution of Water Engineers, vol 26, pp 107-124.

Hendrick, R.L. and Comer, G.H. (1970). Space variations of precipitation and implications for raingage network design. Journal of Hydrology, vol 10, pp 151-163.

Henkel, D.J. (1967). Local geology and the stability of natural slopes. Journal of the Soil Mechanics and Foundations Division, Proceedings of the American Society of Civil Engineers, Vol 93, No SM4, pp 437-446.

Hodge, R.A.L. and Freeze, R.A. (1977). Groundwater flow systems and slope stability. Canadian Geotechnical Journal, vol 14, pp 466-476.

Houston, J.F.T. (1982). Rainfall and recharge to a Dolomite aquifer in a semi-arid climate at Kabure, Zambia. Journal of Hydrology, vol 59, pp 173-187.

Houston, J.F.T. (1983). Ground-water systems simulation by time series techniques. Ground Water, vol 21, pp 301-310.

Howard, K.W.F. and Lloyd, J.W. (1979). The sensitivity of parameters in the Penman evaporation equations and direct recharge balance. Journal of Hydrology, vol 41, pp 329-344.

Hurley, G.A. (1986). The prediction of groundwater levels using computer based mathematical models. Pp 321-325 in "Groundwater in Engineering Geology" (ed.by J.C. Cripps, F.G. Bell, M.G. Culshaw). Geological Society, Engineering Group Special Publication No 3.

Hutchinson, J.N. (1977). Assessment of the effectiveness of corrective measures in relation to geological conditions and types of slope movement. Bulletin of the International Association of Engineering Geology, No 16, pp 131-155, Krefeld.

Hutchinson, J.N. (1983). The geotechnics of coastal cliff stabilisation. Pp 215-222 in Shoreline Protection: Proceedings of a conference organised by the Institution of Civil Engineers and held at the University of Southampton on 14-15 September 1982. Telford, London.

Hutchinson, J.N., Bromhead, E.N. and Lupini, J.F. (1980). Additional observations on the Folkestone Warren landslides. Quarterly Journal of Engineering Geology, vol 13, pp 1-31.

Hutchinson, J.N., Chandler, M.P. and Bromhead, E.N. (1981). Cliff recession on the Isle of Wight S W Coast. 10th International Conference of Soil Mechanics and Foundation Engineering, Stockholm, vol 3, pp 429-434.

Hvorslev, M.J. (1951). Time lag and soil permeability in groundwater observations. U.S. Corps of Engineers, Waterways Experimental Station, Bull. No. 36. Vicksburg, Mississippi.

Ibbitt, R.P. (1972). Effects of random data errors on the parameter values for a conceptual model. Water Resources Research, vol 8, pp 70-78.

Ibbitt, R.P. and O'Donnell, T. (1971). Fitting methods for conceptual catchment models. Journal of the Hydraulics Division, Proceedings of the American Society of Civil Engineers, vol 97, pp 1331-1342.

Institute of Hydrology (1979). Neutron Probe System IH II: Instruction Manual. Natural Environment Research Council.

Johnson, N.L. (1949). Systems of frequency curves generated by methods of translation. Biometrika, vol 36 , pp 149-176.

Johnston, P.R. and Pilgrim, D.H. (1976). Parameter optimization for watershed models. Water Resources Research, vol 12, pp 477-486.

Keating, T. (1984). Recharge into a shingle beach. Journal of Hydrology, vol 72, pp 187-194.

Keen, D.H. (1980). The environment of deposition of the South Hampshire Plateau Gravels. Proceedings of the Hampshire Field Club and Archaeological Society, vol 36, pp 15-24.

Kilbourn, P.C.R. (1971). Further studies of the Barton Clay coastal exposure at Highcliffe, Hampshire. M.Sc. dissertation, University of Southampton.

Kishihara, N. and Gregory, S. (1982). Probable rainfall estimates and the problems of outliers. Journal of Hydrology, vol 58, pp 341-356.

Kitching, R., Shearer, T.R. and Shedlock, S.L. (1977). Recharge to Bunter Sandstone determined from lysimeters. Journal of Hydrology, vol 33, pp 207-232.

Kottegoda, N.T. (1980). Stochastic water resources technology. Macmillan, London.

Kottegoda , N.T. and Horder, M.A. (1980). Daily flow model based on rainfall occurrences using pulses and a transfer function. Journal of Hydrology, vol 47, pp 215-234.

Kuczera, G. (1982). On the relationship between the reliability of parameter estimates and hydrologic time series data used in calibration. Water Resources Research, vol 18, pp 146-154.

Lafleur,J. and Lefebvre, G. (1980). Groundwater regime associated with slope stability in Champlain clay deposits. Canadian Geotechnical Journal, vol 17, pp 44-53.

Lal, R. (1974). The effect of soil texture and density on the Neutron and Density Probe calibration for some tropical soils. Soil Science, vol 117, pp 183-190.

Leach, B. and Herbert, R. (1982). The genesis of a numerical model for the study of the hydrogeology of a steep hillside in Hong Kong. Quarterly Journal of Engineering Geology, vol 15, pp 243-259.

Linsley, R.K., Jr., Kohler, M.A., and Paulhus, J.L.H. (1975). Hydrology for engineers (2nd edition). McGraw-Hill, London.

Lloyd, J.W., Drennan, D.S.H. and Bennell, B.M.U. (1966). A ground water recharge study in north eastern Jordan. Proceedings of the Institution of Civil Engineers, vol 35, pp 615-631.

Long, I.F. and French, B.K. (1967). Measurements of soil moisture in the field by neutron moderation. Journal of Soil Science, vol 18, pp 149-166.

Luebs, R.E., Brown, M.J. and Laag, A.E. (1968). Determining water content of different soils by the neutron method. Soil Science, vol 106, pp 207-212.

Lumb, P. (1975). Slope failures in Hong Kong. Quarterly Journal of Engineering Geology, vol 8, pp 31-65.

Maasland, M. (1959). Water table fluctuations induced by intermittent recharge. Journal of Geophysical Research, vol 64, pp 549-559.

Mein, R.G. and Brown, B.M. (1978). Sensitivity of optimised parameters in watershed models. Water Resources Research, vol 14, pp 299-303.

Melville, R.V. and Freshney, E.C. (1982). The Hampshire Basin and adjoining areas, British regional geology (4th edition). HMSO, London.

Mercer, J.W. and Faust, C.R. (1980). Ground-water modelling: mathematical models. Ground Water, vol 18, pp 212-227.

Meteorological Office (1962). Hygrometric tables for use with Stevenson Screen readings in degrees Fahrenheit, Part 1. HMSO, London.

Meteorological Office (1963). Estimation of standard period averages for stations with incomplete data. Hydrological Memoranda No.5.

Ministry of Agriculture, Fisheries and Food (1967). Potential transpiration. Technical Bulletin No 16. HMSO, London.

Mockridge, R.G. (1983). Highcliffe Cliffs - the maintenance of coastal slopes. Pp 235-242 in Shoreline Protection: Proceedings of a conference organised by the Institution of Civil Engineers and held at the University of Southampton on 14-15 September 1982. Telford, London.

Muir-Wood, A.M. (1967). Coastal Stabilisation at Barton-on-Sea. Civil Engineering and Public Works Review, vol 62, pp 1401-1402.

Muir-Wood, A.M. (1971). Engineering aspects of coastal landslides. Proceedings of the Institution of Civil Engineers, vol 50, pp 257-276.

Nash, J.E. (1957). The form of the instantaneous unit hydrograph. International Association of Scientific Hydrology, General Assembly, Toronto. Publication No 45, vol 3, pp 114-121.

Nash, J.E. (1960). A unit hydrograph study, with particular reference to British catchments. Proceedings of the Institution of Civil Engineers, vol 17, pp 249-282.

Nash, J.E. and Sutcliffe, J.V. (1970). River flow forecasting through conceptual models. Part 1 - A discussion of principles. Journal of Hydrology, vol 10, pp 282-290.

Nwankwor, G.I., Cherry, J.A. and Gillham, R.W. (1984). A comparative study of specific yield determinations for a shallow sand aquifer. Ground Water, vol 22, pp 764-772.

Penman, H.L. (1948). Natural evaporation from open water, bare soil and grass. Proceedings of the Royal Society of London, Series A, vol 193, pp 120-145.

Penman, H.L. (1949). The dependence of transpiration on weather and soil conditions. Journal of Soil Science, vol 1, pp 74-89.

Penman, H.L. (1963). Vegetation and hydrology. Technical Communication No 53, Commonwealth Bureau of Soils, Commonwealth Agricultural Bureau, Farnham Royal, England.

Pettijohn, F.J., Potter, P.E. and Siever, R. (1972). Sand and Sandstone. Springer-Verlag, New York.

Pirt, J. and Bramley, E.A. (1985). The application of simple moisture accounting models to ungauged catchments. Journal of the Institution of Water Engineers, vol 39, pp 169-177.

Plumb, A. (1984). Locked characteristics in sand lenses in the Hampshire Plateau Gravel. B.Sc. dissertation, Department of Civil Engineering, Univeristy of Southampton.

Poreh, M. and Mechrez, E. (1984). The combined effect of wind and topography on rainfall distribution. Journal of Hydrology, vol 72, pp 1-23.

Premchitt, J., Brand, E.W. and Phillipson, H.B. (1986). Landslides caused by rapid groundwater changes. Pp 87-94 in "Groundwater in Engineering Geology" (ed. by J.C. Cripps, F.G. Bell, M.G. Culshaw). Geological Society, Engineering Geology Special Publication No 3.

Prickett, T.A. (1979). Ground-water computer models - state of the art. Ground Water, vol 17, pp 167-173.

Rasmussen, K.R. and Halgreen, C. (1978). Some errors in precipitation measurements. Nordic Hydrology, vol 9, pp 145-160.

Rehm, B.W., Moran, S.R. and Groenewold, G.H. (1982). Natural groundwater recharge in an upland area of Central North Dakota, U.S.A. Journal of Hydrology, vol 59, pp 293-314.

Rennolls, K., Carnell, R. and Tee, V. (1980). A descriptive model of the relationship between rainfall and soil water table. Journal of Hydrology, vol 47, pp 103-114.

Robinson, A.C. and Rodda, J.C. (1969). Rain, wind and the aerodynamic characteristics of rain-gauges. Meteorological Magazine, vol 98, pp 113-120.

Rodda, J.C. (1967a). The systematic error in rainfall measurement. Journal of the Institution of Water Engineers, vol 21, pp 173-177.

Rodda, J.C. (1967b). A country-wide study of intense rainfall for the United Kingdom. Journal of Hydrology, vol 5, pp 58-69.

Rodda, J.C. and Sheckley, A.V. (1978). Water resources and climatic change. Journal of the Institution of Water Engineers, vol 32, pp 76-83.

Rushton, K.R. and Rathod, K.S. (1979). Modelling rapid flow in aquifers. Ground Water, vol 17, pp 351-358.

Rushton, K.R. and Redshaw, S.C. (1979). Seepage and groundwater flow. Wiley, Chichester.

Rushton, K.R. and Tomlinson, L.M. (1980). Aquifer response to forecasting inputs. Journal of Hydrology, vol 48, pp 167-183.

Rushton, K.R. and Ward, C. (1979). The estimation of groundwater recharge. Journal of Hydrology, vol 41, pp 345-361.

Sällfors, G.B. and Svensson, C. (1984). Prediction of maximum ground water pressure. Proceedings of the 4th International Symposium on Landslides, Toronto, Canada. Vol 1, pp 437-440.

Sangrey, D.A. (1982). Evaluation of landslide properties. In "Application of Walls to Landslide Control Problems" (ed. by R.B. Reeves). American Society of Civil Engineers.

Sangrey, D.A., Harrop-Williams, K.O. and Kleiber, J.A. (1984). Predicting ground water response to precipitation. Journal of the Geotechnical Engineering Division, Proceedings of the American Society of Civil Engineers, vol 110, pp 957-975.

Sharma, T.C. (1985). Stochastic models applied to evaluating hydrologic changes. Journal of Hydrology, vol 78, pp 61-81.

Sharon, D. (1980). The distribution of hydrologically effective rainfall incident on sloping ground. Journal of Hydrology, vol 46, pp 165-188.

Shaw, E.M. (1983). Hydrology in Practice. Van Nostrand Reinhold(UK), Wokingham.

Sidle, R.C. and Swanston, D.N. (1982). Analysis of a small debris slide in coastal Alaska. Canadian Geotechnical Journal, vol 19, pp 167-174.

Singh, R. (1968). Double-mass analysis on the computer. Journal of the Hydraulics Division, Proceedings of the American Society of Civil Engineers, vol 94, no HY1, pp 139-142.

Skempton, A.W. and Hutchinson, J.N. (1969). Stability of natural slopes and embankment foundations. Proceedings of the 7th International Conference on Soil Mechanics and Foundation Engineering, Mexico, State of the Art, pp 291-340.

Smith, D.B., Wearn, P.L., Richards, H.J. and Rowe, P.C. (1970). Water movement in the unsaturated zone of high and low permeability strata by measuring natural Tritium. Pp 73-87 in "Symposium on the use of isotopes in hydrology", International Atomic Energy Authority, Vienna.

Smith, K. (1964). A long-period assessment of the Penman and Thornthwaite Potential Evapotranspiration Formulae. Journal of Hydrology, vol 2, pp 277-290.

Sophocleous, M. and Perry, C.A. (1985). Experimental studies in natural groundwater-recharge dynamics: The analysis of observed recharge events. Journal of Hydrology, vol 81, pp 297-332.

Sorooshian, S. and Dracup, J.A. (1980). Stochastic parameter estimation procedures for hydrologic rainfall-runoff models: correlated and heteroscedastic error cases. Water Resources Research, vol 16, pp 430-442.

Srikanthan, R. and McMahon, T.A. (1983). Stochastic simulation of evaporation data for Australia. Nordic Hydrology, vol 14, pp 207-228.

Steenhuis, T.S., Jackson, C.D., Kung, S.K.J. and Brutsaert, W. (1985). Measurement of groundwater recharge on Eastern Long Island, New York, U.S.A. Journal of Hydrology, vol 79, pp 145-171.

Sterrett, R.J. and Edil, T.B. (1982). Groundwater flow systems and stability of a slope. Ground Water, vol 20, pp 5-11.

Stigter, C.J. (1980). Assessment of the quality of generalized wind functions in Penman's equations. Journal of Hydrology, vol 45, pp 321-331.

Stopher, H.E. and Wise, E.B. (1966). Coast erosion problems in Christchurch Bay. Journal of the Institution of Municipal Engineers. Vol 93, pp 328-332.

Thompson, N., Barrie, I.A. and Ayles, M. (1981). The Meteorological Office Rainfall and Evaporation Calculation System: MORECS (July 1981). Hydrological Memorandum No 45, Met 08 (Hydrometeorological Services). HMSO.

Thomson, D.H. (1921). Hydrological conditions in the Chalk at Compton, W. Sussex. Transactions of the Institution of Water Engineers, vol 26, pp 228-251.

Thomson, D.H. (1931). Hydrological conditions in the Chalk at Compton, W. Sussex. (Second paper). Transactions of the Institution of Water Engineers, vol 36, pp 176-195.

Thomson, R.I. (1983). Sub-surface investigations on the cliff top at Naish Farm, Highcliffe. Progress Report to SERC, June 1983. Department of Civil Engineering, University of Southampton.

Thomson, R.I. (1986a). Periodic surveying of instrumentation used to gather hydrological information at Naish Farm, Highcliffe. Data Report No 1986/1, May 1986. Dept. of Civil Engineering, University of Southampton.

Thomson, R.I. (1986b). Piezometric measurements at Naish Farm, Highcliffe. Data Report No 1986/2, June 1986. Department of Civil Engineering, University of Southampton.

Thomson, R.I. (1986c). Soil moisture measurements at Naish Farm, Highcliffe, using a neutron probe. Data Report No 1986/3, July 1986. Department of Civil Engineering, University of Southampton.

Thornthwaite, C.W. (1948). An approach towards a rational classification of climate. Geographical Review, vol 38, pp 55-94.

Todd, D.K. (1959). Ground Water Hydrology. Wiley, London.

Turk, L.J. (1975). Diurnal fluctuations of water tables induced by atmospheric pressure changes. Journal of Hydrology, vol 26, pp 1-16.

Vachaud, G., Royer, J.M. and Cooper, J.D. (1977). Comparison of methods of calibration of a Neutron Probe by gravimetry or neutron-capture model. Journal of Hydrology, vol 34, pp 343-356.

Vaughan, P.R. and Walbancke, H.J. (1973). Pore pressure changes and the delayed failure of cutting slopes in overconsolidated clay. Géotechnique, vol 23, pp 531-539.

Viswanathan, M.N. (1983). The rainfall/water-table level relationship of an unconfined aquifer. Ground Water, vol 21, pp 49-56.

Wellings, S.R. (1984). Recharge of the upper chalk aquifer at a site in Hampshire, England. 1. Water balance and unsaturated flow. Journal of Hydrology, vol 69, pp 259-273.

West, H.D. (1985). Laboratory tests for seepage studies on the Naish Farm cliff slopes, at Highcliffe, Hampshire. B.Sc. dissertation, Department of Civil Engineering, University of Southampton.

Whipkey, R.Z. (1965). Subsurface stormflow from forested slopes. Bulletin of the International Association of Scientific Hydrology, vol 10, pp 74-85.

White, W.N. (1932). A method of estimating groundwater supplies based on discharge by plants and evaporation from soil. U.S. Geological Survey Water Supply Paper 659, Washington, D.C., pp 1-105.

Yevjevich, V. and Dyer, T.G.J. (1983). Basic structure of daily precipitation series. Journal of Hydrology, vol 64, pp 49-67.

Zanger, de, F.A.P. (1981). Exceptional groundwater level fluctuations at the Dutch island of Schiermonnikoog. Nordic Hydrology, vol 12, pp 111-118.

Zucker, M.B., Remson, I., Ebert, J. and Aguado, E. (1973). Hydrologic studies using the Boussinesq equation with a recharge term. Water Resources Research, vol 9, pp 586-592.

APPENDICES

APPENDIX A

Geophysical Survey Method

Contents

A.1 Introduction

The geophysical method used was an electrical resistivity method which is well suited to applications where there are only a few horizontal layers (as at Naish Farm). With this method depths of investigation can go down to 1km or more (Griffiths and King, 1981). However, the practical constraints of surface obstacles (e.g. buildings, roads) and geological complexity (lateral inhomogeneity) can severely limit the depth of investigation possible. This was particularly true at Naish Farm. The severest constraint was that the survey had to be done in between holiday chalets. However, the depth of interest was shallow enough for the survey to be practical. The chalet constaint also limited the total coverage of the area of interest, creating gaps where there were chalets.

A.2 Basic Principles

A.2.1 Electrical Measurements

The electrical resistivity method of subsurface investigation passes a current into the ground by conduction from electrodes. Any subsurface variation in resistivity alters the current flow in the soil which affects the distribution of electric potential at the ground surface. From this, information can be inferred about any subsurface layers or bodies. In this study it is the variation in depth to the Barton Clay (BC) which is of interest. A difference in the depth to the BC will cause a difference in the distribution of electric potential at the ground surface. By passing a current into the ground via two electrodes and monitoring the potential drop via two more electrodes, and using an appropriate expression for uniform ground, the value of resistivity of the ground can be determined. In non-uniform ground the same expression is used but the value calculated is termed the apparent

resistivity. It is the variation of this quantity with changes in electrode positioning (both spatially and relative to one another) that allows deductions to be made about the subsurface.

A.2.2 Electrical Resistivity of Soils

Current flow in soils takes place mainly through the groundwater present in pores and fissures. Clay is an exception to this in that conduction also takes place by way of weakly bonded surface ions. There are also some metallic ores which are conducting. Apart from these exceptions, therefore, soil resistivity is a function of water filled porosity. The resistivity of a deposit may not be spatially or temporally constant as its moisture content will vary in space (lateral inhomogeneity) and time (surface deposits influenced by variations in meteorological conditions).

A.2.3 Apparent Resistivity

Many different types of electrode configeration have been used in the past. The configeration known as the Wenner array is shown in the diagram below:

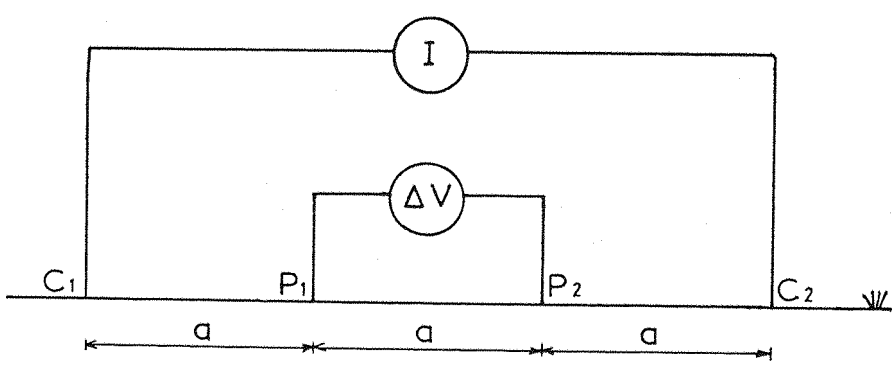

The four electrodes are placed in a line equidistant apart. The outer two electrodes pass a current through the ground and the inner two are used to measure the potential drop between them.

The equipment used was an ABM Terrameter. It compares the voltage drop across the potential electrodes with that across a potentiometer. The resistance, R, on the potentiometer was varied until the two potential drops were the same so that the resistance between the potential electrodes was equal to R. The apparent resistivity, ρ_a , of the mid point of the array is then given by the expression:

$$\rho_a = 2.\pi .a.R \qquad (A.1)$$

A.2.4 Layer Depth from Apparent Resistivity Measurements

In this study it is the layering of the soil that is of interest, i.e. the variation of resistivity with depth. To investigate this, a set of measurements are made using the same mid point (station) but with increasing electrode separation. The results are plotted as a resistivity curve of apparent resistivity versus electrode separation on log-log paper. For small electrode spacings the apparent resistivity is mainly determined by the resistivity of the Plateau Gravel (PG). As the electrode spacing is increased, the apparent resistivity is increasingly influenced by the resistivity of the BC. Thus, the resistivity curve will give an indication of the depth to the BC. To do this the curve is compared (fitted) with theoretical curves. These are based on the theory of infinitely horizontal layered soils of laterally constant resistivity. By curve matching, the resistivities of the PG and BC as well as the thickness of the PG can be determined.

A.2.5 Limitations of Curve Matching

It is theoretically possible to give a unique solution for a resistivity curve representing any number of layers of differing thicknesses and resistivities. However, the more layers there are, the more difficult is the interpretation due to several solutions giving similar resistivity curves. Also, departures

of the ground from the ideal model introduce ambiguities. The ground may not be horizontally layered; individual layers may vary in thickness and resistivity even over quite short distances; a layer may be very thin, or of intermediate resistivity compared to its two adjacent layers, such that it has little effect on the shape of the resistivity curve; the resistivity contrast between two layers may be very small. Borehole control can sort out a lot of these difficulties. But even with borehole control there are interpretation difficulties, which limit the application of this method to situations where there are only a very few layers of well marked contrasting resistivity.

A.2.6 Constant Separation Traverse

The method of increasing the electrode separation and analysing the variation in measured apparent resistivity is known as depth sounding. An alternative method of investigating subsurface variation is to study the spatial variation of apparent resistivity whilst using a constant electrode separation. This is known as a constant separation traverse. Spatial variation in apparent resistivity is then affected by lateral inhomogeneity of layer resistivity, layer thickness, and any geological change. The method is commonly used to detect the latter effect. In the absence of any geological change or marked spatial variation in layer resistivity the method can also be used to measure layer thickness. To do this the apparent resistivity is related to layer thickness as analysed by depth sounding. If the correlation and sensitivity of the relationship are good, then the method can be used.

A.2.7 Grid Spacing

The advantage of using a constant separation traverse is that

it is quick, and so enables a large number of stations to be used. To survey the topography of the irregular PG/BC unconformity a grid of stations is required. The density of the grid is influenced by the extent of the grid, the time available (number of stations possible), and on what horizontal scale is a variation in topography of interest (i.e. are trends in topography of interest or local variations such as buried channels). The quantitative interpretation of results makes use of plane layer theory. Therefore, the results will be meaningless unless the horizontal scale of the unconformity topography is several times that of its depth. The survey of the cliff face shows this to be the case, except for where involutions and frost wedges occur. However, these latter effects are isolated and not of interest in this survey. It is the presence of trends and buried channels in the level of the top of the BC that are of interest. A suggested minimum distance between stations equal to the depth of the unconformity is suggested by Griffiths and King (1981).

A.3 Geophysical Survey Method Used

A.3.1 Summary

To summarize the method used to survey the thickness of the PG: an electrical resistivity survey was carried out using a constant separation traverse at an electrode spacing of 6m and a Wenner electrode configeration orientated in a direction 1½ deg clockwise of the W - E direction. The grid spacing was 5 m near the cliff edge and 10 m further away. There now follows an explanation of these decisions.

A.3.2 Resistivity Method

An electrical resistivity method was used because the survey area had only two layers, viz. PG and BC for which the ground surface

and PG/BC unconformity surface (as observed at the cliff face) were near horizontal. The survey was carried out in the summer when the gravels were expected to be dry so that there would be a large resistivity contrast between the PG and BC. The depth of the unconformity was small enough for practical spread lengths to be possible despite surface obstacles.

A.3.3 Electrode Configeration

A Wenner electrode configuration was used, partly due to custom, and partly to the fact that the effects of local lateral inhomogeneities are to some extent smoothed out by this method measuring large potential differences.

A.3.4 Constant Separation Traverse

A constant separation traverse was used with a 6 m electrode separation, as there was a good, sensitive correlation between gravel depth and apparent resistivity. This made it possible to obtain a large amount of data. If depth sounding alone had been used, the amount of data obtained would have been limited, because depth sounding takes more time, and because the presence of chalets and roads made it impractical to have long spreads over large parts of the study area. Even using the constant separation traverse, surface obstacles still left gaps in the grid, but they were not as great as they would have been with depth sounding. The choice of 6 m for the separation was a compromise between being large enough to give a good sensitive correlation, and small enough to maximise the number of readings possible in between the chalets.

A.3.5 Grid Orientation

The orientation of the grid was chosen with one axis along a line, which ran through the two main fixed reference points used

for the EDM survey work on the undercliff. This base line was roughly parallel to the cliff edge which made it easier to set out the grid. The orientation of the array for the constant separation traverse was parallel to the base line, because firstly, this made setting out easier, and secondly, it enabled readings to be made close to the cliff edge.

A.3.6 Grid Spacing

Whilst both channels and trends in the level of the top of the BC are of interest over the whole area, the presence of channels is of particular interest near the cliff face. Therefore, the grid spacing used near the cliff face was smaller than that used further inland. Griffiths and King (1981) have suggested a minimum grid spacing equal to the depth of interest. As the maximum anticipated depth of PG was 5 m this was taken for the grid spacing for up to 50 m from the cliff face. Further away from the cliff face the grid spacing was expanded to 10 m.

APPENDIX B

Computation of the Penman Equation for Potential Evaporation

The Penman equation may be written as:

$$E = \frac{\Delta / \gamma}{\Delta / \gamma + 1} \cdot R_A \cdot (1-r).(a_1 + a_2 \cdot n/N)$$

$$+ \frac{\Delta / \gamma}{\Delta / \gamma + 1} \cdot a_3 \cdot \sigma \cdot T_a^4 \cdot (a_4 - a_5 \cdot \sqrt{e_d}) \cdot (a_6 + a_7 \cdot n/N)$$

$$- \frac{1}{\Delta / \gamma + 1} \cdot a_8 \cdot (a_9 + a_{10} \cdot h) \cdot (a_{11} + a_{12} \cdot u) \cdot (e_a - e_d)$$

(B.1)

The parameters $a_1, \ldots, a_{12}$, r are specified in the main text. Their values depend on the type of surface and the version of the formula used. The Stefan-Boltzman constant, σ, is taken to be 2.01×10^{-9} mm of evaporation/day/$^{\circ}K^4$. The function $(a_9 + a_{10} \cdot h)$ accounts for the effect of the altitude, h (m O.D.), of the station.

The computation of equation B.1 was done by computer. Daily values of the variables, Δ / γ, R_A, n/N, T_a, e_a, e_d, u were calculated and averaged over monthly and 7 day periods. The average values were then used to solve equation B.1. The procedure for calculating the variables is given below. The equations are from Chidley and Pike (1970) except where indicated.

Wind Speed, u

This is measured daily in km/day as a daily average. The result is converted to miles/day for use in equation B.1.

Temperature, T_a

The dry bulb temperature measured daily at 0900 GMT is used. The temperature is measured in degrees Celsius and then converted to degrees Kelvin for use in equation B.1 by adding 273.16.

Sunshine ratio, n/N

The number of hours of bright sunshine, n, is measured daily at Hurn Airport. The theoretical maximum duration of sunshine, N(hrs), is given by:

$$N = \frac{24}{\pi} \cdot \cos^{-1}(-\tan d \cdot \tan L) + 0.22 \qquad (B.2)$$

where N is the length of time between when the edge of the sun's disc appears and disappears below the horizon. The figure 0.22 allows for atmospheric refraction and for the edge, and not the centre, of the sun's disc being above the horizon. d is the sun's declination in radians. This varies between plus and minus ($23\frac{1}{2} \cdot 2\pi / 360$). A value of zero is arbitrarily assumed for the 21st March each year. L is the latitude of the location in radians. This is ($50.65 \times 2\pi / 360$) North for Naish Farm.

Incoming Short wave radiation above the atmosphere, R_A

The theoretical daily total expressed in mm of evaporation is

$$R_A = \frac{14.9158}{S^2} \cdot \left[\begin{array}{l} \cos^{-1}(-\tan d \cdot \tan L) \cdot \sin L \cdot \sin d \\ + \cos L \cdot \cos d \cdot \sin \left[\cos^{-1}(-\tan d \cdot \tan L) \right] \end{array} \right] \qquad (B.3)$$

where S is the sun's radius vector for which monthly average values are used (see table B.1 for values). The values have been obtained by:

i) Solving equation B.3 for ($R_A . S^2$) for each day. The values are summed to give monthly totals;

ii) Using tables in Shaw (1983), which have been extracted from MAFF (1967), monthly average values of R_A are obtained;

iii) The result of i is divided by that of ii to give an average value of S^2 for each month.

Saturation Vapour Pressure, e_a

The saturation vapour pressure in mb at a dry bulb temperature of T_a (^oC) is found from:

$$SVP(T_a) = \exp\left[54.878919 - \frac{6790.4985}{(T_a+273.16)} - 5.02808 \log_e(T_a+273.16) \right] \quad (B.4)$$

This is converted to mm of mercury for use in equation B.1 thus:

$$e_a = \frac{760}{1013} \cdot SVP(T_a) \quad (B.5)$$

Actual Vapour Pressure, e_d

The actual vapour pressure in mb (VP) is calculated from the Regnault formula as given in Meteorological Office (1962) thus:

$$VP = SVP(T_W) - 1.8 \times 0.444(T_a - T_W) \text{ for } T_W \geq 0^oC \quad (B.6)$$

or

$$VP = SVP(T_W) - 1.8 \times 0.4 \ (T_a - T_W) \text{ for } T_W < 0^oC \quad (B.7)$$

where T_W is the wet bulb temperature; the factor 1.8 is used to convert the wet bulb depression, $(T_a - T_W)$, from ^oC to ^oF; $SVP(T_W)$ is found using equation B.4 with T_W substituted for T_a. VP is converted to mm of mercury for use in equation B.1 thus:

$$e_d = \frac{760}{1013} \cdot VP \quad (B.8)$$

Weighting, Δ / γ

The constant of the wet and dry bulb psychrometer equation, γ, is taken to be 0·66mb/^{o}C. The slope of the saturation vapour pressure curve, Δ (mb/^{o}C), is:

$$\Delta = \frac{SVP(T_a)}{(T_a+273.16)} \cdot \left[\frac{6790.498}{(T_a+273.16)} - 5.02808 \right] \qquad (B.9)$$

Table B.1 Values of S^2 used in equation B.3

Month	S^2
January	0.9446
February	0.9255
March	0.9609
April	0.9926
May	1.0085
June	1.0260
July	1.0178
August	1.0108
September	0.9836
October	0.9282
November	0.9045
December	0.9459

APPENDIX C

Requirements of the Weather Station Site

The requirements of the weather station site were:

i) to be close to the study area;

ii) the instrumentation should not be oversheltered. Maximum advised shelter for a rain gauge is given by Shaw (1983), figure 3.6. This requires a clear area between chalets and caravans;

iii) the instrumentation should not be overexposed;

iv) to allow for chalets and caravans being moved. The weather station had to be sited where there was little risk of this.

Requirements ii and iv limit the number of possible sites to clear areas relatively near the cliff edge. Unfortunately, to some extent, this violates requirement iii; exposure may be altered due to slumping activity; and spatial variations of meteorological measurements may be significantly affected by the cliff edge. Thus, siting the weather station too near the cliff edge may not properly represent the cliff top climate. In the end, the weather station was sited 40 to 50 m from the cliff which was considered to be adequate to be representative of the cliff top.

APPENDIX D

Analysis of Homogeneity of Rainfall and PE Data

A detailed description of these tests is given by Buishand (1982)

Let MSS_i = mean rainfall (or PE) of surrounding stations for month i.

NF_i = rainfall (or PE) at Naish Farm for month i.

$Y_i = NF_i - MSS_i$.

The Y_i's are assumed to be independent and normally distributed. The statistics given here check the significance of a sudden change in the mean value.

Let $D_y^2 = \dfrac{\sum_{i=1}^{n} (Y_i - \bar{Y})^2}{n}$

$S_o^* = 0$; $S_k^* = \sum_{i=1}^{k} (Y_i - \bar{Y})$, k=1,2,...,n

$S_k^{**} = S_k^* / D_y$, k = 0,...,n

$Q = \max_{0 \leq k \leq n} / S_k^{**} /$

$R = \max_{0 \leq k \leq n} / S_k^{**} / - \min_{0 \leq k \leq n} / S_k^{**} /$

$Z_k^* = [\, k(n-k) \,]^{-\frac{1}{2}} \cdot S_k^*$, k=1,...,n-1

$Z_k^{**} = Z_k^* / D_y$

$U = \dfrac{1}{n(n+1)} \cdot \sum_{k=1}^{n-1} (S_k^{**})^2$

$A = \sum_{k=1}^{n-1} (Z_k^{**})^2$

The statistics used are: $Q/\sqrt{n}$; $R/\sqrt{n}$; U ; A.

The results are tabulated below. The figure in brackets is the value for the 95 per cent confidence level.

	$Q/\sqrt{n}$	$R/\sqrt{n}$	U	A
PE[1] (n=18)	1.11 (1.20)	1.61 (1.40)	.342 (.440)	2.026 (2.42)
Rainfall[1] (n=25)	1.228 (1.23)	1.228 (1.465)	.327 (.446)	1.852 (2.43)
Rainfall[2] (n=20)	0.836 (1.22)	1.022 (1.43)	.170 (.447)	0.212 (2.44)

Table Notes:

1. Using Hurn Airport as the mean of the surrounding stations.
2. Hurn Airport, Everton, Freshwater and Christchurch are the surrounding stations.
3. If the data is homogeneous there is a 95 per cent probability of the value in the table being less than the value in brackets.

APPENDIX E

The Modelling of Daily Rainfall

Daily rainfall models are usually of the type described by Shaw (1983, pp 395-8). Kottegoda and Horder (1980) and Buishand (1978) are examples of their application. Yevjevich and Dyer (1983) showed that the properties of daily rainfall vary seasonally. This is not surprising as weather type varies with the time of year. Allowing for seasonality increases the number of parameters necessary to model daily rainfall. Thus, modelling here is based on the four seasons and not a shorter (e.g. monthly) basis. The seasons are defined (Shaw, 1983, p. 396) as:

Spring	:	March, April, May
Summer	:	June, July, August
Autumn	:	September, October, November
Winter	:	December, January, February

The modelling of rainfall for each season is a two stage process. The first stage is to determine the number of days in each wet and dry spell (a wet day is one on which rainfall exceeds a selected threshold value). There are two approaches. The first is to fit separate independent probability distributions to the observed lengths of wet and dry spells. The second approach is to use Markov chains. A Markov chain relates the probability of occurence of an event (wet or dry day) to the state of the previous k days (k is the order of the process). Which approach is used, depends on the number of parameters needed to achieve a reasonable fit to the data. A Markov process is the simpler to use, but high order models need a large number of parameters (2^k). The parameters of a first and second order Markov process are given in table E.1. If a Markov model of third order, or higher, is necessary, the first approach is likely to be better as it is more parsimonious of parameters. However, as the need for an

accurate model is not so great for a groundwater study, a first or second order Markov process should be adequate. The number of wet days in a month is related to the monthly rainfall as shown by figure E.1. The relationship is not strong enough to show significant seasonal variation. If monthly rainfall has already been generated, the total number of wet days in the month should first be predicted from a suitable relationship which includes a random component (to account for the scatter shown by figure E.1). Necessary adjustment should then be made to the pattern of wet and dry days obtained by one of the above approaches.

The second stage is to determine the rainfall amounts on wet days. The simplest approach is to assume that the rainfall amounts for each wet day are independent and identically distributed. More complicated approaches allow for serial correlation, or for different frequency distributions depending on the state (wet or dry) of the previous and next days. The simplest approach is investigated here. The skew and kurtosis for each season for Hurn Airport and Naish Farm are given in table E.2 and plotted on figure E.2. Autumn, Winter and Spring have similar values whereas for Summer they are much higher. The purpose of figure E.2 is to identify the type of frequency distribution that should fit the data. Skew and Kurtosis vary depending on location, season, threshold value, and the data sample (e.g. 2 or 5 year sample in the case of Hurn Airport). However, these variations do not affect the choice of the type of distribution using figure E.2. The log-normal and Pearson Type III distributions are obviously inadequate. Figure E.2 shows that the Johnson S_B frequency distribution should fit the data.

The Johnson (1949) system of frequency curves are based on transformations of variables, such that the transformed variables may be considered to have a normal distribution. The Johnson S_B system of frequency curves is based on the transformation:

$$Z = \gamma + \delta \cdot \log\left[\frac{X - \xi}{\xi + \lambda - X}\right] \qquad (\xi < X < \xi + \lambda)$$

where X is the value of rainfall; Z is normally distributed with zero mean and unit variance; γ, δ, ξ, λ are parameters. The parameters ξ and λ define the end points, and if their values are known, then the parameters γ and δ may be estimated by the method of moments thus :

$$\hat{\gamma} = - \frac{\bar{Y}}{S_y} \quad , \text{ and } \quad \hat{\delta} = \frac{1}{S_y}$$

where $Y = \log \left[\frac{X - \xi}{\xi + \lambda - X} \right]$; $\bar{Y}$ and S_y are the mean and standard deviation of Y. However, the values of ξ and λ are not known. They have been estimated by successive trial and error. To compare the fit of each trial, the χ^2 goodness-of-fit test has been used (Chatfield (1983), pp 148-155). Final results are given in table E.2. It can be seen that the Johnson S_B type distribution fits all seasonal data. Not shown is the fact that the distribution could not be adequately fitted to data for the whole year for either weather station. Distribution parameters were fitted to the 2 year study period so as to establish seasonal relationships between the two weather stations.

The minimum and maximum values of the distribution have no physical justification and serve only to achieve an adequate fit to the data. Rainfall may occur outside these limits. Whereas rainfall below the lower limit is insignificant, this is not so for rainfall above the upper limit. Also, there is insufficient data to attach any confidence in the frequency distribution adequately fitting high rainfall values below the maximum. Therefore, for rainfall generation, the frequency distributions should only be used with probabilities of non-exceedance up to, say .95. Extreme value analysis should be applied to higher values. Even with long rainfall records, the accuracy of extreme rainfall estimates is not good (Bell, 1969). Problems in making frequency estimates of extreme rainfall are described in Rodda (1967b) and Kishihara and Gregory (1982). However, as an example, estimates of rainfall

amounts for given return periods have been obtained from the Meteorological Office. These estimates make no seasonal distinction (high rainfall is more likely in Summer and Autumn than in Winter and Spring), and are therefore only a rough guide for any given season. The probabilities of non-exceedance are shown in table E.3, and have been calculated assuming that, for all seasons, a given rainfall has the same return period. As the expected number of wet days varies between seasons, the calculated probabilities of non-exceedance also vary.

Table E.1 Parameters of a First and Second Order Markov Process for the 5 year Data Period of Hurn Airport

First Order

		Season and Final State							
		Spring		Summer		Autumn		Winter	
		D	W	D	W	D	W	D	W
Initial State	D	.74	.26	.78	.22	.70	.30	.72	.28
	W	.41	.59	.42	.58	.36	.64	.39	.61

Second Order

		Season and Final State							
		Spring		Summer		Autumn		Winter	
		D	W	D	W	D	W	D	W
Initial State	DD	.78	.22	.80	.20	.70	.30	.76	.24
	DW	.42	.58	.42	.58	.23	.77	.36	.64
	WD	.64	.36	.68	.32	.69	.31	.63	.37
	WW	.41	.59	.42	.58	.43	.57	.40	.60

Note: the state of day is denoted by D (dry) or W (wet), e.g. for an initial state of DW, the two preceding days were a dry day followed by a wet day.

Table E.2 Parameters of a Johnson S_B Distribution fitted to Daily Rainfall

Weather Station /Data Period	Season	Number of Wet Days	Skew	Kurtosis	Parameters				D Test Statistic
					ξ	λ	γ	δ	
Hurn Airport	Spring	179	1.361	4.911	.55	24.5	1.3159	.6628	6.56
1.8.80 to	Summer	159	3.285	14.597	.05	57.0	1.9823	.5580	7.14
31.7.85	Autumn	208	1.620	5.777	.65	34.4	1.2961	.5453	10.34
AB	Winter	190	1.503	4.840	.45	27.6	1.2945	.6284	5.03
Hurn Airport	Spring	84	1.529	5.148	.15	25.9	1.3049	.5365	4.40
23.9.82 to	Summer	44	3.998	18.392	.05	57.0	2.0750	.5355	1.52
9.10.84	Autumn	91	1.521	5.049	.75	33.3	1.2762	.5552	2.41
C	Winter	81	1.105	3.093	.55	24.5	1.0894	.5918	1.42
Naish Farm	Spring	81	1.707	5.586	.15	25.9	1.2727	.5212	3.08
23.9.82 to	Summer	37	3.473	16.168	.05	57.0	2.0900	.5704	1.72
9.10.84	Autumn	82	1.716	6.236	.75	31.3	1.2917	.6261	4.04
AC	Winter	79	1.450	4.797	.55	21.5	1.1448	.6295	4.37

Notes:

A. The skew and kurtosis of the data are plotted in figure E.2.

B. The number of degrees-of-freedom for the goodness-of-fit test is 5.

C. The number of degrees-of-freedom for the goodness-of-fit test is 2.

D. The fit is considered adequate if the test statistic is not significant at the 5 per cent level, i.e. for:

5 degrees-of-freedom, test statistic < 11.07
and 2 degrees-of-freedom, test statistic < 5.99

Table E.3 Extreme Values of Daily Rainfall

Season	Wet Days (1)	Probability of non-exceedance for given rainfall					$R_{.95}$ (mm) (2)
		26.5 mm	33.0 mm	39.1 mm	46.2 mm	53.6 mm	
Spring	179	.9860	.9930	.9965	.9986	.9993	15.8
Summer	159	.9843	.9921	.9961	.9984	.9992	20.2
Autumn	208	.9880	.9940	.9970	.9988	.9994	23.2
Winter	190	.9868	.9934	.9967	.9987	.9993	18.0

Notes:
1. This is the number of wet days in the 5 year data period.
2. $R_{.95}$ is the rainfall amount with a probability of non-exceedance of 0.95.

Figure E.1

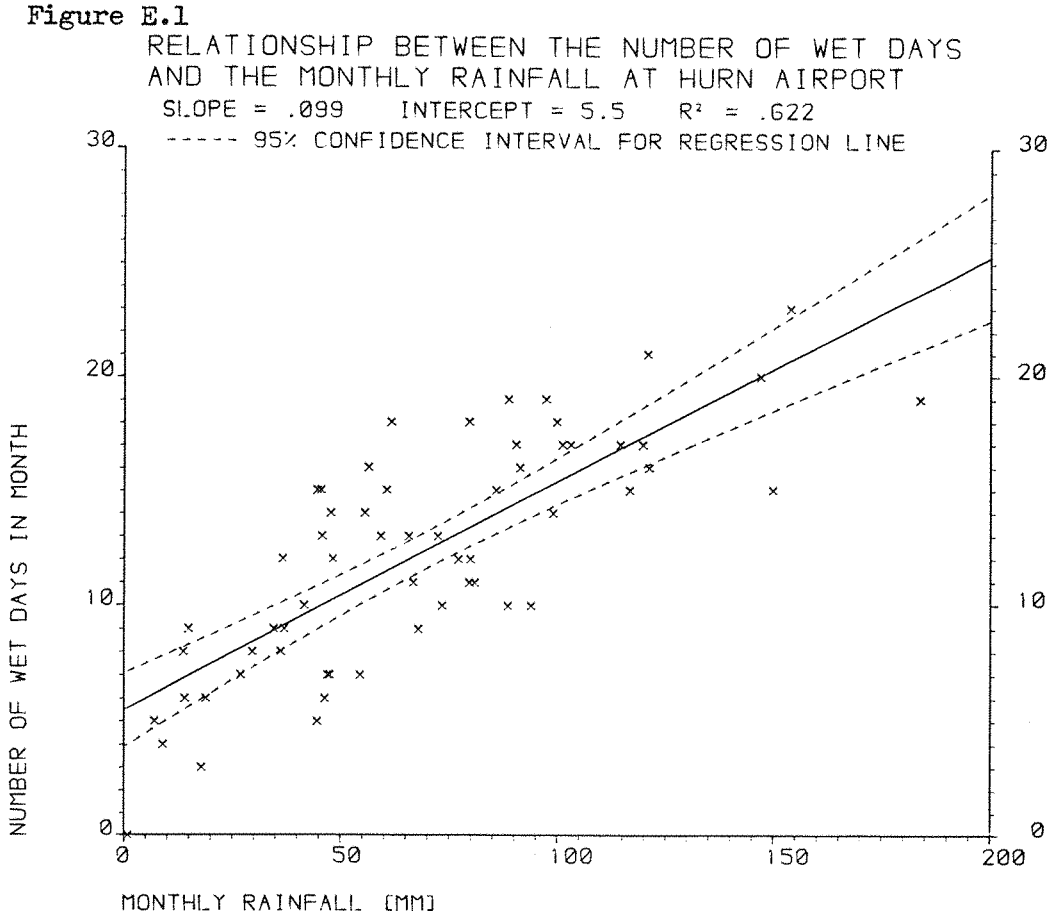

Figure E.2

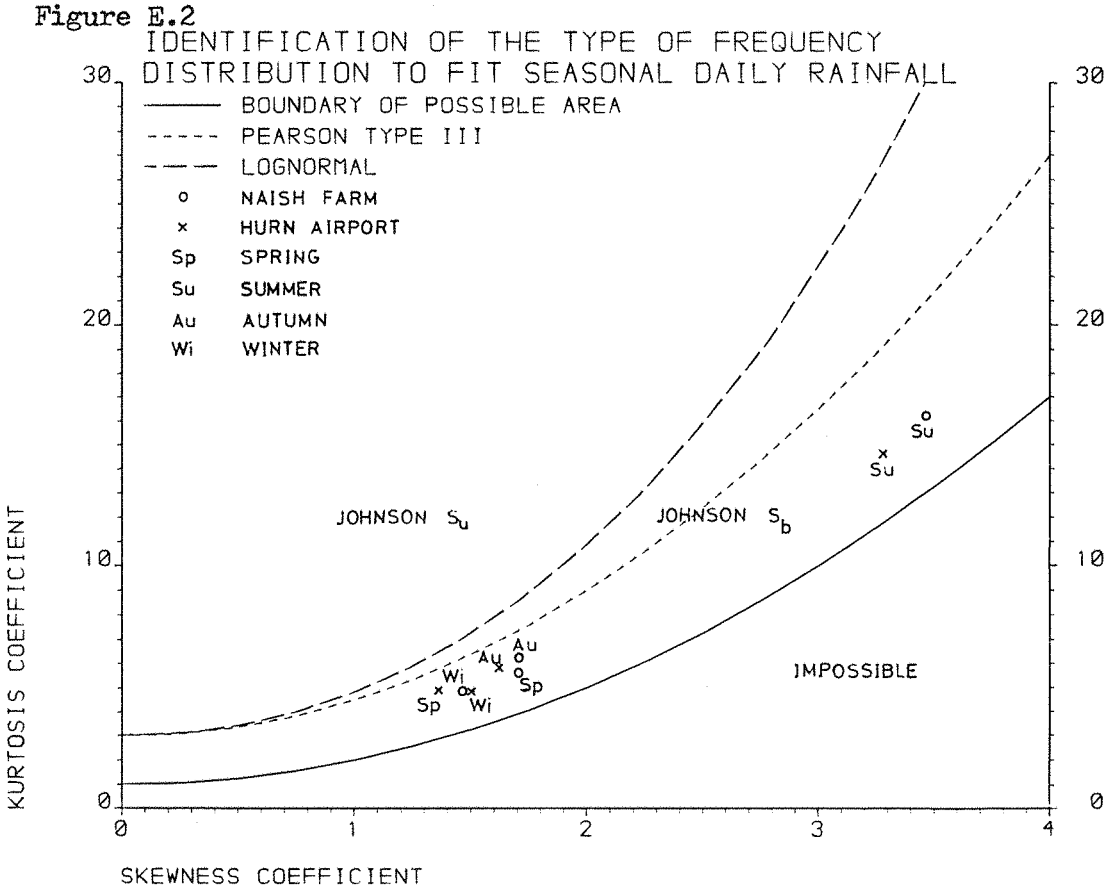

APPENDIX F

Determination of Plateau Gravel Permeability

Measurements of permeability were made on disturbed samples by West (1985). A constant head apparatus was used with material less than 6.3 mm in diameter. The particle size distribution of the PG used is shown in figure F.1. Sample PG(2) includes material greater than 6.3 mm. Sample PG(1) is sample PG(2) sieved to remove particle sizes greater than 6.3mm. Permeability varies with bulk density. The in situ density was not attainable. The permeability at the in situ density is determined here, by extrapolation on figure F.2, to be 1.5×10^{-5} m/s (1.3 m/day) for a PG sand lens, and 2.8×10^{-5} m/s (2.4 m/day) for the PG(1) sample. To calculate the permeability of the PG(2) sample, use is made of Hazen's formula:

$$K = A.d_{10}^2 \qquad (F.1)$$

where K is permeability,

d_{10} is the particle size at which 10 per cent by weight of the soil particles are finer,

A is a coefficient.

The value of d_{10} for sample PG(1) is .117 mm. For an in situ bulk density of 2.02 Mg/m^3, this gives a value of A of 2×10^{-3}. The value of A is assumed to be constant at the same bulk density for both samples PG(1) and PG(2). The value of d_{10} for sample PG(2) is .245 mm. Thus, the permeability of sample PG(2) at the in situ bulk density of 2.02 Mg/m^3 is 1.2×10^{-4} m/s (10.4 m/day). Equation F.1 is similarly used at other densities to obtain the relation for PG(2) shown in figure F.3. This shows that the results compare favourably with those of a similar soil type given in figure 2.8 of Cedergren (1977), although the PG samples are markedly less sensitive to changes in bulk density.

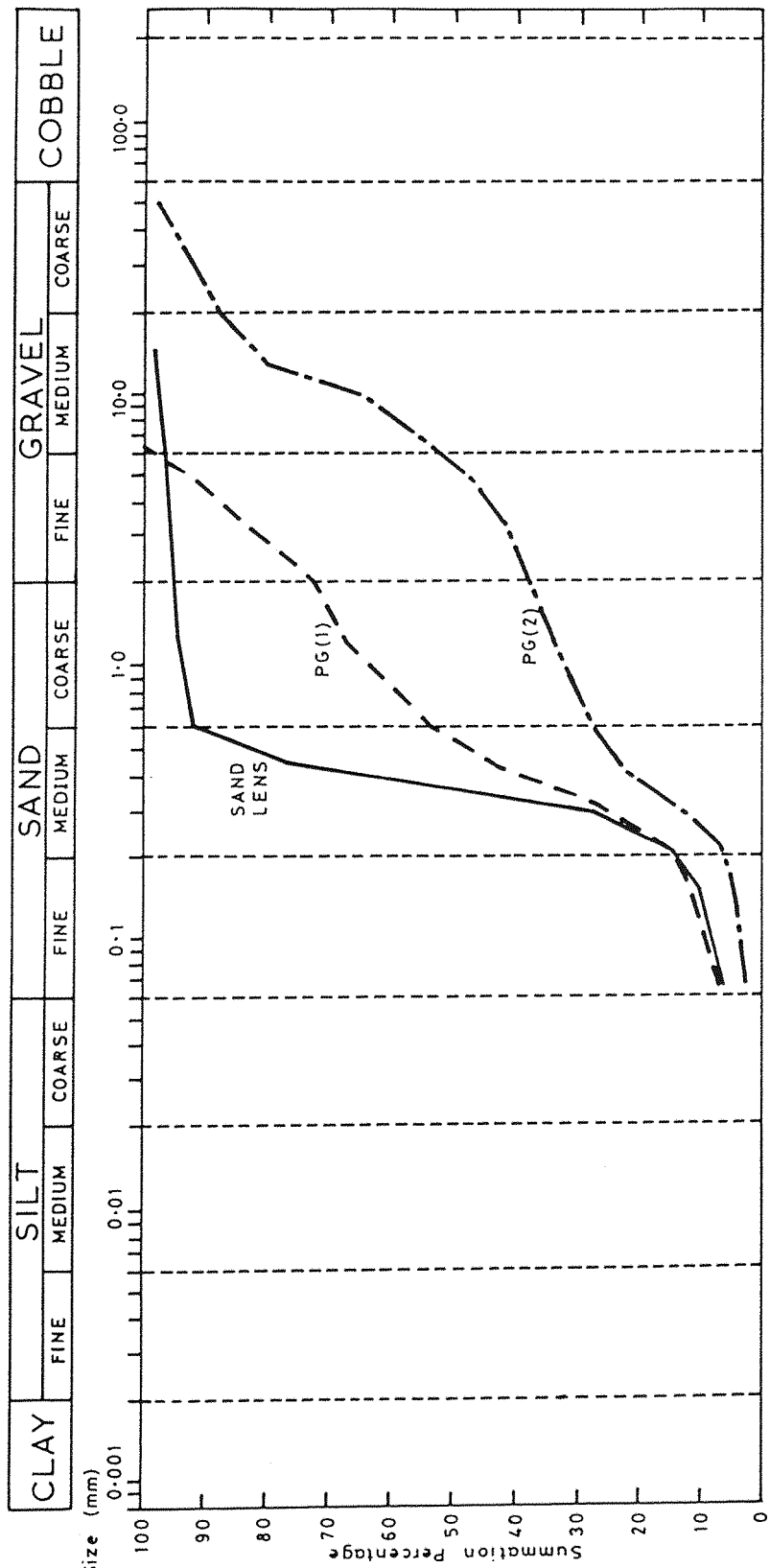

Figure F.1 Particle size distributions of the Plateau Gravel samples.

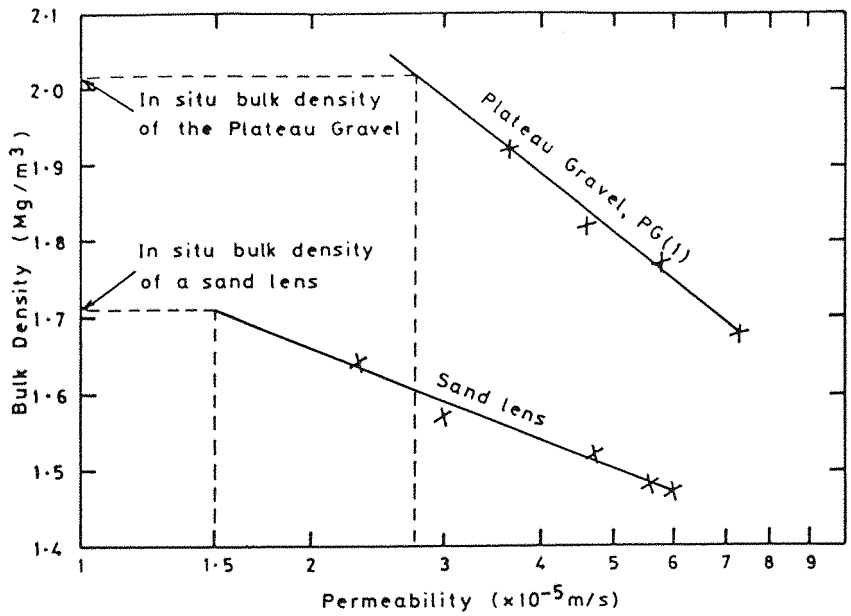

Figure F.2 Relation between permeability and bulk density. PG(1) does not include material greater than 6.3 mm.

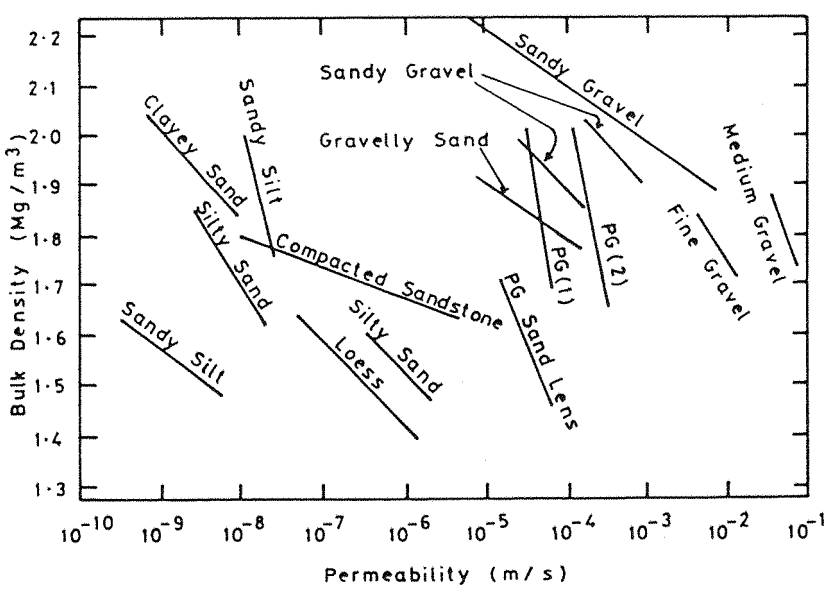

Figure F.3 Relation between permeability and soil type and bulk density. This is based on figure 2.8 in Cedergren (1977) with the results for the Plateau Gravel included. PG(2) includes material greater than 6.3 mm whereas PG(1) does not. The curve for PG(2)is produced from the curve for PG(1) and using Hazen's formula.

APPENDIX G

Mathematical Summary of the Calculation of Effective Rainfall
(Model I, figure 5.2)

DETENTION = P-RUNOFF

(i) For flux control, i.e. DETENTION $\geqslant$ PE

AE = PE

INFILTRATION = DETENTION - PE

ER_1 = A.INFILTRATION, where A is a parameter

INSTORE = INFILTRATION - ER_1

If INSTORE $\leqslant$ SMD_{old}

then SMD_{new} = SMD_{old} - INSTORE

and ER_2 = 0

$ER = ER_1 + ER_2$ = A.(P-RUNOFF-PE)

If INSTORE > SMD_{old}

then SMD_{new} = 0

and ER_2 = INSTORE - SMD_{old}

$ER = ER_1 + ER_2$ = P-RUNOFF-PE-SMD_{old}

(ii) For profile control, i.e. DETENTION < PE

E_1 = DETENTION

INFILTRATION = 0

ER = 0

INSTORE = 0

If PE - E_1 $\leqslant$ C - SMD_{old}

then SMD_{new} = SMD_{old} + (PE-E_1)

If $PE - E_1 > C - SMD_{old}$ and $SMD_{old} < C$

then $SMD'_{new} = C + 0.1[(PE-E_1)-(C-SMD_{old})]$

If $SMD_{old} \geqslant C$

then $SMD'_{new} = SMD_{old} + 0.1(PE-E_1)$

If $SMD'_{new} > D$

then $SMD_{new} = D$

If $SMD'_{new} \leqslant D$

then $SMD_{new} = SMD'_{new}$

$E_2 = \Delta S = SMD_{new} - SMD_{old}$

$AE = E_1 + E_2 = P\text{-}RUNOFF+SMD_{new}- SMD_{old}$

SMD_{old} and SMD_{new} are the SMD's at the start and end of the time step.

APPENDIX H

Calculation of the Total Recharge for the n^{th} Time Step
(Model II, figure 5.2)

The outflow response from a single reservoir having received an instantaneous unit input is:

$$q = \frac{1}{K} \cdot e^{-t/K} \qquad (H.1)$$

where q is the instantaneous outflow at time t after the input, and K is a decay constant. Assuming proportionality:

$$q = \frac{ER}{K} \cdot e^{-t/K} \qquad (H.2)$$

where q is now the instantaneous recharge and ER is the instantaneous input. ER is the effective rainfall, displaced in time by DELAY time steps (see figure 5.2). The effective rainfall is assumed, in this analysis, to occur instantaneously at the start of the time step to which it refers. Therefore, the instantaneous input in equation H.2, which occurs at time t = 0, is the effective rainfall calculated for the time step t = -DELAY to t = -DELAY+1. Integrating equation H.2 gives the total output for any one time step as:

$$Q = \int_{t}^{t+1} \frac{ER}{K} \cdot e^{-t/K} \cdot dt = -ER \left[e^{-t/K} \right]_{t}^{t+1}$$

$$= ER \cdot e^{-t/K} \cdot (1 - e^{-1/K}) \qquad (H.3)$$

Let ${}_jQ_i$ be the output for the i^{th} time step since the j^{th} input.

Let ${}_{j\text{-DELAY}}ER$ be the j^{th} input. Equation H.3 gives the recharge due to the j^{th} input as:

$$\text{For } t = 0 \qquad {}_jQ_1 = {}_{j\text{-DELAY}}ER \cdot (1 - e^{-1/K})$$

For $t = 1$

$$ {}_jQ_2 = {}_{j\text{-}DELAY}ER \cdot e^{-1/K} \cdot (1 - e^{-1/K}) $$
$$ = e^{-1/K} \cdot {}_jQ_1 $$

For $t = i$

$$ {}_jQ_{i+1} = {}_{j\text{-}DELAY}ER \cdot e^{-i/K} \cdot (1 - e^{-1/K}) $$
$$ = e^{-1/K} \cdot {}_jQ_i $$

For $t = i + 1$

$$ {}_jQ_{i+2} = {}_{j\text{-}DELAY}ER \cdot e^{-(i+1)/K} \cdot (1-e^{-1/K}) $$
$$ = e^{-1/K} \cdot {}_jQ_{i+1} $$

In general, for $i = 1$, ${}_jQ_i = {}_{j\text{-}DELAY}ER \cdot (1-e^{-1/K})$

for $i \geqslant 2$, ${}_jQ_i = e^{-1/K} \cdot {}_jQ_{i-1}$ (H.4)

Assuming superposition, the total groundwater recharge for the n^{th} time step is the sum of the groundwater recharges for that time step due to all the previous individual inputs of effective rainfall. This is given by :

$$ RECHARGE_n = \sum_{j=1}^{n} {}_jQ_{n-j+1} \qquad (H.5) $$

Substituting equations H.4 for terms in equation H.5 gives :

$$ RECHARGE_1 = {}_{1\text{-}DELAY}ER \cdot (1 - e^{-1/K}) $$

$$ RECHARGE_2 = e^{-1/K} \cdot {}_1Q_1 + {}_{2\text{-}DELAY}ER \cdot (1 - e^{-1/K}) $$

$$RECHARGE_3 = e^{-1/K} \cdot {}_1Q_2 + e^{-1/K} \cdot {}_2Q_1 + {}_{3\text{-DELAY}}ER \cdot (1 - e^{-1/K})$$

$$RECHARGE_n = e^{-1/K} \cdot {}_1Q_{n-1} + e^{-1/K} \cdot {}_2Q_{n-2} + e^{1/K} \cdot {}_3Q_{n-3} + \ldots.$$

$$\ldots. + e^{-1/K} \cdot {}_jQ_{n-j} + \ldots. + e^{-1/K} \cdot {}_{n-1}Q_1$$

$$+ {}_{n\text{-DELAY}}ER \cdot (1 - e^{-1/K})$$

$$= e^{-1/K} \cdot \left[\sum_{j=1}^{n-1} {}_jQ_{n-j} \right] + {}_{n\text{-DELAY}}ER \cdot (1 - e^{-1/K})$$

$$= e^{-1/K} \cdot RECHARGE_{n-1} + {}_{n\text{-DELAY}}ER \cdot (1 - e^{-1/K})$$

(H.6)(=5.4 in chapter 5)

Thus, the groundwater recharge for any given time step is the weighted average of the effective rainfall of DELAY time steps before and the previous time step's recharge. The relative weighting is determined by the parameter, K. The model uses equation H.6 for the calculation of recharge, with $RECHARGE_{n-1} = 0$ for $n = 1$ and at the start of groundwater level prediction $n \geq 5K$.

APPENDIX I

Sensitivity Analysis of the Optimal Parameter Solutions given in Table 6.4

Parameters are perturbed individually whilst holding the other parameters at the optimal values given in table 6.4. RUNOFF* and SY* are exceptions to this, as they allow for the inter-dependence between RUNOFF and SY.

V is the value of the perturbed parameter.

Δ is the reduction in the value of the objective function (for the calibration period 1st November 1982 to 12th January 1984) as a result of the change in the parameter value.

S_1 is a finite difference approximation of the second derivative of the relationship between the values of the objective function and the perturbed parameter. It is a measure of the parameter sensitivity or peakness of the relationship.

S_2 is a non-dimensionalised form of S_1

Mathematically:

$$S_1 = \left(\frac{\Delta_1}{(V_1 - V_0)} - \frac{\Delta_2}{(V_2 - V_0)} \right) \Big/ \left(\frac{V_1 - V_2}{2} \right)$$

and $$S_2 = \frac{V_0^2}{\text{CORREL}} \cdot S_1$$

where subscripts: 0 is for the optimal parameter value
1 is for the high parameter value
2 is for the low parameter value

CORREL is the value of the objective function.

Table I.1 Results for P61

Parameter	V	Δ	S_1	S_2
A	.362 .21	.005 .005	1.81	.14
C	32.6 20.5	.005 .005	2.9×10^{-4}	.20
SY	.0509 .0457	.005 .005	1488	3.8
SY*	.060 .041	.005 .005	116	0.30
RUNOFF	-.033 -.073	.005 .005	26	6.9×10^{-2}
RUNOFF*	.012 0 -.137	.005 .0032 .005	1.9	5.0×10^{-3}
K	3.2 1.15	.005 .005	9.7×10^{-3}	5.5×10^{-2}
DELAY	2 0	.0183 .0038	2.2×10^{-2}	2.4×10^{-2}

Table I.2 Results for P62

Parameter	V	Δ	S_1	S_2
A	.275 .211	.005 .005	9.8	.61
C	75.3 38.1	.005 .005	3.0×10^{-5}	.088
SY	.061 .0532	.005 .005	658	2.23
SY*	.0695 .049	.005 .005	100	.34
RUNOFF	-.089 -.014	.005 .005	7.1	1.9×10^{-2}
RUNOFF*	.043 0 -.161	.005 .0016 .005	.97	2.5×10^{-3}
K	6.7 3.3	.005 .005	3.6×10^{-3}	8.2×10^{-2}
DELAY	3 1	.0060 .0045	1.0×10^{-2}	4.4×10^{-2}

Table I.3 Results for P63

Parameter	V	Δ	S_1	S_2
A	.394 .207	.005 .005	1.2	.13
C	76.6 41.6	.005 .005	3.5×10^{-5}	.15
SY	.0955 .0867	.005 .005	517	4.3
SY*	.102 .0835	.005 .005	121	1.0
RUNOFF	.033 -.02	.005 .005	14	1.5×10^{-3}
RUNOFF*	.057 0 -.071	.005 .0001 .005	2.6	2.7×10^{-4}
K	6.1 2.4	.005 .005	3.0×10^{-3}	4.7×10^{-2}
DELAY	2 0	.0020 .0042	6.2×10^{-3}	6.3×10^{-3}

Table I.4 Results for P64

Parameter	V	Δ	S_1	S_2
A	.436 .27	.005 .005	1.7	.18
C	81.7 51.0	.005 .005	4.3×10^{-5}	.18
SY	.0826 .0708	.005 .005	288	1.7
SY*	.101 .06	.005 .005	25	.15
RUNOFF	-.07 -.14	.005 .005	8.3	8.5×10^{-2}
RUNOFF*	.005 0 -.245	.005 .0045 .005	.66	6.7×10^{-3}
K	2.8 0.45	.005 .005	7.3×10^{-3}	1.7×10^{-2}
DELAY	2 0	.0107 .0065	1.7×10^{-2}	1.8×10^{-2}

APPENDIX J

Estimation of the Position of the Groundwater Divide in the Plateau Gravel

Lateral groundwater flow in the Plateau Gravel (PG) is either toward the cliff face or Chewton Bunny. In order to calculate the flow to the cliff face, the position of the groundwater divide needs to be estimated. To do this, it is assumed that the PG/Barton Clay (BC) unconformity is horizontal and does not undulate. It is also assumed that the groundwater flow direction is perpendicular to the outlet boundary (cliff face or Chewton Bunny). If it is further assumed that the recharge is areally constant, and that the outflow at the two boundaries (cliff face and Chewton Bunny)are the same, then the groundwater divide is equidistant (along the flow lines) from the two boundaries. This equidistance may be estimated from maps. However, errors occur because it is not possible to accurately determine the outflow boundary along Chewton Bunny. This is because the unconformity slopes downwards as it approaches Chewton Bunny. Also, because of this, the position of the boundary along Chewton Bunny may vary with groundwater level. Thus, using the equidistance approach to accurately estimate the position of the groundwater divide is not easy.

To improve the estimate, existing groundwater level data is used and fitted to an equation describing the position of the groundwater table. Maasland (1959) examined the situation shown in figure J.1. The aquifer is unconfined and lies on an impervious layer down to which there are parallel flat drains (perpendicular to the paper). Steady state conditions (of recharge and groundwater level) are assumed. The position of the groundwater table in figure J.1 is given by:

$$z^n = h_1^n + B \cdot (L-x) \cdot x \qquad (J.1)$$

where $n = 1$ when $h_m \ll h_1 \ll L$

$n = 2$ when $h_1 \ll h_m \ll L$

B is a function of the recharge rate P.

Equation J.1 is of the general form:

$$z^n = a_o + a_1.x + a_2.x^2 \qquad (J.2)$$

The PG is analogous to figure J.1. The impervious layer is the BC. The cliff face and Chewton Bunny are the drains. The section line is along a flow line which bends at the groundwater divide. The maximum groundwater table level is at the groundwater divide. However, the BC is not impervious. If the leakage were uniform, this would only affect the value of B. However, the leakage is not uniform, and is shown in chapter 7 to increase with increasing proximity to the cliff face. The effect of this is to increase the curvature of the groundwater table (i.e. to increase the value of n). Leakage also causes the groundwater table at low groundwater levels to dip below the PG/BC unconformity at an unknown distance short of the cliff face. This situation is depicted in figure J.2. The value of h_1 is taken to be zero and the position of the origin is unknown. At high groundwater levels, the groundwater table intersects the cliff face at some distance above the unconformity. It is assumed that this represents the value of h_1, although the flow system is not exactly the same as assumed in figure J.1. (In reality the drains in figure J.1 would also have seepage faces, and the value of h_1 would be the depth of water in the drains plus a correction to allow for the seepage face.) Thus, at high groundwater levels, the value of h_1 is unknown and the position of the origin is at the cliff face.

Groundwater level data for the PG was used to solve equation J.2, with n, a_1, a_2, and either a_0 or the position of the origin unknown. Four equations are needed to solve the four unknowns. These are provided by four groundwater level observations.

Equation J.2 applies steady state conditions, which is far from the case for PG. Also, heterogeneity causes variable aquifer response to rainfall. This leads to a wide scatter in the results when using equation J.2 to find the position of the groundwater divide. The worse violations were screened by only using the groundwater level readings when:

i) the groundwater table is falling;
ii) the slope of the groundwater table is increasing toward the cliff face.

The first criterion is based on the assumption that the rate of movement of the groundwater table is relatively small (compared to when groundwater levels are rising) and is reasonably constant throughout the aquifer. Thus, it is assumed that this is when steady state conditions are least violated. The second criterion is a mathematical requirement of equation J.1.

The positions of the four groundwater level measurements (x_1, x_2, x_3, x_4) may be expressed with reference to just one of them by introducing the known constants K_1, K_2, K_3, K_4 (the distances between groundwater level measurements) such that:

$$\left.\begin{aligned} x_1 &= x_1 + K_1 \\ x_2 &= x_1 + K_2 \\ x_3 &= x_1 + K_3 \\ x_4 &= x_1 + K_4 \end{aligned}\right\} \quad (J.3)$$

K_1 is zero and the value of x_1 locates the co-ordinate system ($z = 0$ is arbitrarily fixed at 28.17 m O.D.). The groundwater levels at x_1, x_2, x_3, x_4 are z_1, z_2, z_3, z_4 respectively. Substituting equations J.3 into equation J.2 gives:

$$z_1^n = a_0 + a_1 \cdot x_1 + a_2 \cdot x_1^2 \quad (J.4)$$

$$z_2^n = a_0 + a_1 (x_1 + K_2) + a_2 (x_1 + K_2)^2 \qquad (J.5)$$

$$z_3^n = a_0 + a_1 (x_1 + K_3) + a_2 (x_1 + K_3)^2 \qquad (J.6)$$

$$z_4^n = a_0 + a_1 (x_1 + K_4) + a_2 (x_1 + K_4)^2 \qquad (J.7)$$

Rearranging equation J.4 gives:

$$a_1 = \frac{z_1^n - a_0}{x_1} - a_2 . x_1 \qquad (J.8)$$

Substituting equation J.8 into equation J.5 and rearranging gives:

$$a_2 = \frac{z_2^n - a_0}{K_2(x_1+K_2)} - \frac{z_1^n - a_0}{x_1 . K_2} \qquad (J.9)$$

Substituting equations J.8 and J.9 into equation J.6 and rearranging gives:

$$\left[z_1^n - z_3^n + \frac{K_3}{K_2} (z_2^n - z_1^n) \right] . x_1^2$$

$$+ \left[K_2(z_1^n - z_3^n) + \frac{K_3^2}{K_2} (z_2^n - z_1^n) \right] . x_1$$

$$+ K_3 (K_2 - K_3) (z_1^n - a_0)$$

$$= 0 \qquad (J.10)$$

The procedure is to first assign a value to n and assume a_0 to be zero. Then equation J.10 is solved to find x_1. It is a quadratic equation, such that there are two solutions for x_1 as the groundwater table dips below the unconformity in two places (near the cliff face and Chewton Bunny). Only the solution with the origin near the cliff face is used. Equation

J.9 then gives a_2 and equation J.8 gives a_1. The values of a_1, a_2, x_1 and n are then substituted into equation J.7 to obtain an estimate of z_4. The above procedure is repeated with different values of n, until the estimated value of z_4 is less than .005 m from the observed value of z_4.

If the value of x_1 is greater than the value of F (the distance between the cliff face and the location of the groundwater level measurement, z_1), then it is assumed equal to F (i.e. the origin to be at the cliff face) and a_0 to take some positive value. The above procedure is repeated except that equation J.10 is used to solve for a_0.

The slope of the groundwater table at the groundwater divide is zero. Therefore, to find the position of the groundwater divide (x_d), equation J.2 is differentiated, equated to zero, and rearranged to give:

$$x_d = - \frac{a_1}{2.a_2} \qquad (J.11)$$

The distance from the cliff face (G) is calculated using equation J.12.

$$G = x_d - x_1 + F \qquad (J.12)$$

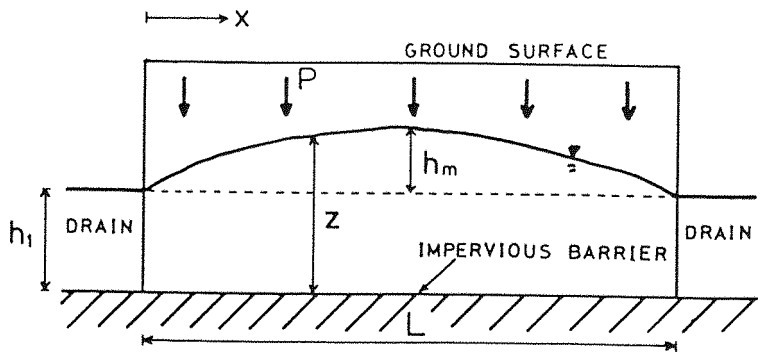

Figure J.1 Groundwater flow over a horizontal impervious barrier (after Maasland, 1959). Steady state conditions assumed with constant recharge rate, P.

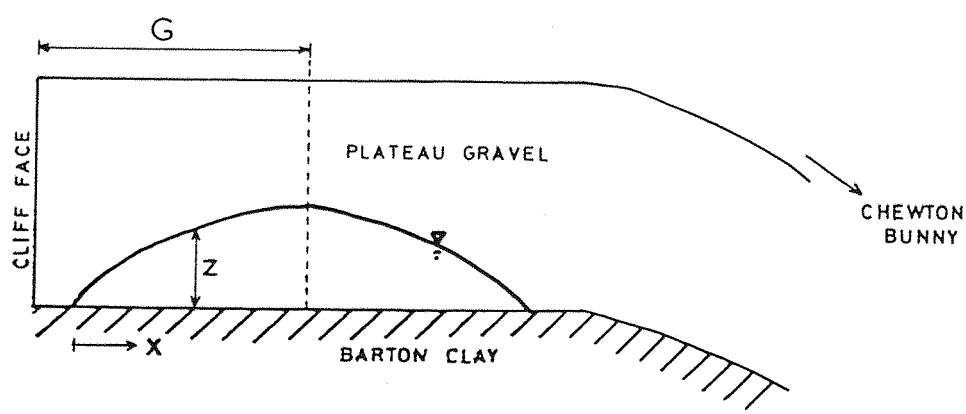

Figure J.2 Groundwater flow in the Plateau Gravel. Not to scale.